2018-08-16

Integrated Analysis of miRNA/mRNA Expression in the Neurocircuitry Underlying Nicotine Dependence

Alison P. Casserly
University of Massachusetts Medical School

INTEGRATED ANALYSIS OF miRNA/mRNA EXPRESSION IN THE NEUROCIRCUITRY UNDERLYING NICOTINE DEPENDENCE

A Dissertation Presented

By

ALISON P. CASSERLY

Submitted to the Faculty of the

University of Massachusetts Graduate School of Biomedical Sciences, Worcester

in partial fulfillment of the requirements for the degree of

DOCTOR OF PHILOSOPHY

AUGUST 16, 2018

M.D./Ph.D PROGRAM IN BIOMEDICAL SCIENCES

INTEGRATED ANALYSIS OF miRNA/mRNA EXPRESSION IN THE NEUROCIRCUITRY UNDERLYING NICOTINE DEPENDENCE

A Dissertation Presented By

ALISON P. CASSERLY

This work was undertaken in the Graduate School of Biomedical Sciences

M.D./Ph.D. Program

Under the Mentorship of

_____
Paul D. Gardner, Ph.D., Thesis Advisor

_____
Kensuke Futai, Ph.D., Member of Committee

_____
John Landers, Ph.D., Member of Committee

_____
David Weaver, Ph.D. Member of Committee

_____
Elizabeth M. Byrnes, Ph.D., External Member of Committee

_____
Haley Melikian, Ph.D., Chair of Committee

_____
Mary Ellen Lane, Ph.D.,
Dean of the Graduate School of Biomedical Sciences

August 16, 2018

This dissertation is dedicated to my amazing husband Mario, my beloved son Malcolm, and my supportive parents Sue and Jim. Without their love and patience, this work would not have been possible.

"It always helps to have people we love beside us when we have to do difficult things in life." – Mister Rodgers

ACKNOWLEDGEMENTS

“I wish there was a way to know you’re in the good old days, before you’ve actually left them.” – Andy Bernard “The Office”

I would first like to thank my graduate advisor, Dr. Paul D. Gardner. Although I might have reminded you almost daily of my excitement to get back to medical school, working with you for the past six years has been a real pleasure. Although my PhD work wasn’t as smooth as I had hoped, in the end, you helped me to produce a vast amount of data I can be proud of and learn innumerable lessons that I will carry with me throughout my career. Thank you for never letting me take the easy way out of any obstacle. Thank you for telling me I shouldn’t be panicking (daily). Thank you for letting me barge into your office whether you liked it or not. Thank you for letting me email you strings of deluded emails; it has been a lesson in professionalism. Thank you for nurturing my habit for swearing; also a lesson in professionalism. Thank you for always reminding me to always put my family and health first. Also, thank you for putting a screwdriver through my MacBook and letting my use my fellowship to get a new one. Thank you in advance for the glowing letters of recommendation. Finally, thank you for waiting to permanently injure yourself until I defend, despite your best efforts to do so. You are the best boss I have ever had, and I’m glad you are also my friend.

I would next like to thank Dr. Andrew R. Tapper, the other half of the Tardner Lab leadership. Your advice has been invaluable during my thesis work. I hope to have absorbed at least an ounce of your ability to strategically approach experiments, grants/fellowships, and manuscripts.

I am very grateful to my thesis committee members, Drs. Phil Zamore, Fen-Biao Gao, Joel Richter, and Haley Melikian. Their insights and advice were instrumental to the progression of my graduate studies. Their constructive criticisms provided both concrete suggestion and motivation, helping me to produce a body of quality work. I extend a special thanks to Dr. Phil Zamore, who served as chair of both my qualifying exam and thesis research advisory committee (TRAC), and Dr. Haley Melikian, a member of my TRAC and the chair of my dissertation exam committee.

I would like to extend my sincere gratitude to our collaborators Zhiping Weng and Junko Tsuji. Without their contribution, the bioinformatic analyses would have been an impossible feat. I want to extend a special thank you to Junko for continuing to work with me even after she left UMass for another full time job. I would also like to thank Alper Kucukural for patiently assisting me with use of the cluster and uploading of my data to the NCBI GEO. I would also like to thank Phil Zamore and Jennifer Broderick for guidance in the use of their small RNA library protocol.

My training and the success of my project would not have been possible without the support and guidance of all of my fellow lab members. I would like to specifically thank Susanna Molas, Ciearra Smith, and Rubing Zhao-Shea for their contributions to my project. I would like to thank Anthony Sacino for making the lab run smoothly, and also exposing himself to toxic chemicals on my behalf while I was pregnant. I would specifically like to acknowledge Ciearra, my lone graduate student partner in the Gardner lab. Her hard work, comradery and healthy venting sessions made even the hard times in lab fun. Finally, I would like to extend a special thank you to Rubing for her expertise and willingness to train me in seemingly every laboratory technique, her friendship, and her beautiful watercolor paintings. I would also like to acknowledge former lab members, Melissa Derner, Liwang Liu, Jennifer Ngolab, Xueyan Pang, and Lindsey Soll for their assistance, advice, and friendship. Each of you has made my arduous graduate studies a happy journey.

I would like to thank the M.D./Ph.D Program and Drs. Gyongyi Szabo and Silvia Corvera for their advising and leadership. I would like to specially thank Anne Michelson, the program administrator. Without her the program would not function, and I would never hand my forms in on time. I would like to thank my fellow M.D./Ph.D. students for their emotional support, late night study sessions and friendship. You all made this epically long training program pass a bit faster and made it a lot more enjoyable. I've loved seeing how we have all grown up since we started this program together way back in 2010.

Finally I would like to thank my friends and family. To Beth, Brooke, and all the Holy Cross ladies – You kept me grounded and were the best cheering section a girl could hope for. To my parents, Sue and Jim – Thank you for always supporting me in every way. You gave my work ethic, put me through college, and are the best grandparents. Thanks for never letting me stay home sick from school…ever. To my husband, Mario - Thank you for all you do to afford me the opportunity of fulfilling my dreams as a “professional student.” You never let me give up. Your patience and unwavering support amazes me every day. And thanks for being the perfect dad to our meatball.

ABSTRACT

Nicotine dependence is responsible for perpetuating the adverse health effects due to tobacco use, the leading cause of preventable death worldwide. Nicotine is an agonist for nicotinic acetylcholine receptors, which are enriched in the mesocorticolimbic and habenulo-interpeduncular circuitries, underlying nicotine reward and withdrawal, respectively. Drugs of abuse, including nicotine, induce stable neuroadaptations, requiring protein synthesis through regulation of transcription factors, epigenetic mechanisms, and non-coding RNAs. It also been shown that miRNAs in brain are regulated by nicotine and that miRNA dysregulation contributes to brain dysfunction, including drug addiction. While much is known about the neurocircuitry responsible for the behaviors associated with nicotine reward or withdrawal, the underlying molecular mechanisms of how these changes in behavior are induced are less clear.

Using miRNA-/mRNA-Seq, we demonstrate that there are widespread changes in both miRNA and mRNA expression in brain regions comprising the mesocorticolimbic circuit after chronic nicotine treatment, and the habenulo-interpeduncular circuit during acute nicotine withdrawal. Conserved, differentially expressed miRNAs were predicted to target inversely regulated mRNAs. We determined that expression of miR-106b-5p is up-regulated and *Profilin 2* (*Pfn2*), an actin-binding protein enriched in the brain, is down-regulated in the interpeduncular nucleus (IPN) during acute nicotine withdrawal. Further we show

that miR-106b-5p represses *Pfn2* expression. We demonstrate that knockdown of *Pfn2* in the IPN is sufficient to induce anxiety, a symptom of withdrawal. This novel role of *Pfn2* in nicotine withdrawal-associated anxiety is a prime example of this dataset's utility, allowing for the identification of a multitude of miRNAs/mRNA which may participate in the molecular mechanisms underlying the neuroadaptations of nicotine dependence.

TABLE OF CONTENTS

List of Tables

List of Figures

List of Abbreviations

aVTA	Anterior ventral tegmental area
BP	Biological process
bp	Base pair
CC	Cellular compartment
cDNA	Complementary DNA
CREB	cAMP response element binding protein
CRF	Corticotropin releasing factor
DAergic	Dopaminergic
DE	Differential expression/differentially expressed
DSM-V	Diagnostic and Statistical Manual of Mental Disorders (5th Edition)
EPM	Elevated plus maze
FBS	Fetal bovine serum
fr	Fasciculus retroflexus
GABA	Gamma-aminobutyric acid
GluR	Glutamate receptor
GO	Gene ontology
IPN	Interpeduncular nucleus
LCM	Laser capture microdissection
LDTg	Lateral dorsal tegmental area
LHb	Lateral habenula
MBT	Marble burying test
MF	Molecular function
MHb	Medial habenula
miRNA	MicroRNA
mRNA	Messenger RNA
MRE	MicroRNA response element
MSN	Medium spiny neurons
NAc	Nucleus accumbens
nAChR	Nicotinic acetylcholine receptors
NAWD	Acute nicotine withdrawal
Nic	Nicotine
NLWD	Long nicotine withdrawal
nt	Nucleotide
PFC	Prefrontal cortex
pVTA	Posterior ventral tegmental area
RISC	RNA-induced silencing complex
RMTg	Rostromedial tegmentum
RNA	Ribonucleic acid
RPM	Reads per million

RTI	RNA Therapeutics Institute
RT-qPCR	Quantitative reverse transcription polymerase chain reaction
Seq	Sequencing
SHS	Second-hand smoke
TA	Tartaric acid
TAL	Tartaric acid, long treatment
TBE	Tris/Borate/EDTA buffer
TM	Transmembrane
TPM	Transcripts per million
UMMS	University of Massachusetts Medical School
UTR	Untranslated region
VTA	Ventral tegmental area
WT	Wild-type

Copyrighted Materials

Portions of some chapters of this dissertation have appeared in:

Casserly AP, Tsuji J, Zhao-Shea R, Smith CB, Molas S, Tapper AR, Weng Z, Gardner PD. Integrated miRNA-/mRNA-Seq of the Habenulo-Interpeduncular Circuit Reveals a Novel Role for Profilin 2 in Nicotine Withdrawal-Associated Anxiety. Biological Psychiatry. *In Review*.

Contributions of authors are addressed at the beginning of each chapter.

List of Data Files

For the IPN, NAc, and MHb raw sequencing data, mapping statistics, expression matrices, and differential expression analysis tables are publically available on NCBI, GEO accession number GSE117069.

Mapping statistics, expression matrices and differential expression analyses tables for the VTA have been deposited on Dropbox and can be found using the following link:
https://www.dropbox.com/sh/ifhbbt67lpp5w9n/AAC7kCXEUFJAEnPVa2Pu07n_a?dl=0

CHAPTER 1

Introduction

1.A. Nicotine Dependence and Current Therapeutics

Prevalence and Mortality of Tobacco Use

Globally, tobacco use remains a prevalent health problem with more than 900 million daily smokers of all ages (Peacock et al. 2018). It is estimated that 15.2% of adults are daily smokers worldwide (Peacock et al. 2018). Smoking is the leading cause of preventable death and tobacco has the highest rate of age-standardized substance-attributable mortality, responsible for 110 per 100,000 deaths (Peacock et al. 2018). It is estimated tobacco-related illnesses are responsible for 6 million deaths annually (WHO 2012).

Smoking (including second hand smoke exposure) is the leading risk factor for disease burden in North America and Western Europe (Lim et al. 2012). It is estimated smoking shortens life expectancy by 10 years compared to those that have never smoked (Jha et al. 2013). The death rate for smokers aged 25-79 is about three times that of people that have never smoked, and this increased mortality is largely a result of neoplastic, respiratory and vascular diseases (Jha et al. 2013). In addition to lung cancer, development of other cancers including liver, colorectal, prostate, breast has been attributed to smoking (USDHHS 2014). Respiratory illnesses caused by smoking include chronic obstructive pulmonary disease, asthma, and increased susceptibility to respiratory infections such as tuberculosis (USDHHS 2014). Cigarette smoking increases the risk of vascular disease, including events such as myocardial

infarction (fatal and non-fatal) and stroke (Jha 2009). In fact, cardiovascular disease is the leading cause of death attributable to smoking, accounting for 1.5 million annual deaths worldwide (Jha 2009).

In addition to the direct exposure to smokers, non-smokers in the population are exposed to the toxic chemicals in second-hand smoke (SHS). In fact, 43% of the population has detectable levels of cotinine, a biomarker of tobacco exposure, in their blood (Pirkle et al. 2006) and SHS is estimated to contribute to over 53,000 deaths in the United States annually (Jacobs et al. 2013). Second-hand smoke increases the risk of tobacco-related cancers and other diseases in non-smokers (USDHHS 2006). For example, it is estimated that the risk of stroke is increased 20-30% in non-smokers exposed to second-hand smoke (Malek et al. 2015). In addition, second-hand smoke puts children at increased risk for sudden infant death syndrome, acute respiratory infections, and asthma (USDHHS 2006).

On top of the disease burden and lost years of human life, smoking and tobacco-related illnesses have a significant economic impact. Some estimate that $170 billion is spent on health care costs associated with diseases caused by smoking in the United States each year (Xu et al. 2015). In addition to the direct healthcare costs, the negative health effects of smoking result in lost productivity. For instance, it is estimated that there is $151 billion in lost productivity in the United States when only the years of productive life lost due to premature smoking-related deaths are considered (Ekpu and Brown 2015). If other factors

such as disability leaves and sick days were considered, the economic toll of smoking would certainly be even larger.

The Cycle of Nicotine Addiction

Despite the adverse health and financial consequences of tobacco use, daily smokers find cessation difficult, even when motivated to quit. This is because smokers become addicted to nicotine, a tertiary alkaloid present in tobacco (Russell 1971, Dani and Balfour 2011). Smokers often attempt to quit multiple times with a low probability of success (Peacock et al. 2014). This can best be explained by thinking of nicotine addiction as a chronically relapsing disorder (Koob and Le Moal 2008) (Figure 1.1).

In general, the rewarding properties of intoxication dominate the early stages of drug addiction (Koob and Le Moal 2008). Patients report that tobacco use results in various positive symptoms such as pleasure, relaxation, improved mood, arousal, improvement in attention and memory, and appetite suppression (Benowitz 1999, Benowitz 2010). The rewarding or motivating properties of nicotine are also evidenced by behavioral experiments in rodents. For example, mice and rats will self-administer nicotine intravenously (Corrigall and Coen 1989, Fowler and Kenny 2011) and condition a place preference to nicotine injection (Risinger and Oakes 1995, Le Foll and Goldberg 2005, Grabus et al. 2006), and these behavioral paradigms continue to be used to study mechanisms of nicotine addiction.

The repeated exposure to drugs, including nicotine, leads to the development of tolerance. The DSM-V defines tolerance as “a need for markedly increased amounts of the substance to achieve intoxication or desired effect” and “a markedly diminished effect with continued used of the same amount of the substance.” Rodents display tolerance to nicotine in locomotor activity, analgesia, and body temperature assays (Collins et al. 1988, Grabus et al. 2005). Once dependent on a drug, abstinence during a voluntary attempt to quit or involuntary inaccessibility to the drug induces a withdrawal state marked by negative somatic and affective signs (Koob and Le Moal 2008). The somatic, or physical, symptoms associated with nicotine withdrawal include bradycardia, gastrointestinal upset, and increased appetite (Jackson et al. 2015). The affective, or emotional, symptoms include anxiety, depression, dysphoria, irritability, difficulty concentrating, and craving (Hughes 2007, Jackson et al. 2015). Symptoms peak within the first week and are generally estimated to last for 2-4 weeks (Hughes 2007). In order to relieve these negative symptoms, many smokers will often relapse and resume tobacco use. For example, one study showed that in a group of female smokers, craving and withdrawal symptoms increase 2-5 days prior to relapse and drop over the course of 2 days subsequent to relapse, suggesting that escalation of withdrawal symptoms contribute to relapse (Allen et al. 2008). Despite the unpleasantness of the somatic symptoms, it is the affective symptoms that dominate the preoccupation with drug seeking and relapse (Hughes 2007, Piper et al. 2011, Aguirre et al.

2015). Taken together, while the rewarding properties of nicotine dominate initial drug-taking, avoidance of the negative affective symptoms experienced during withdrawal promote relapse and the habitual use of a tobacco (Allen et al. 2008, Koob and Le Moal 2008).

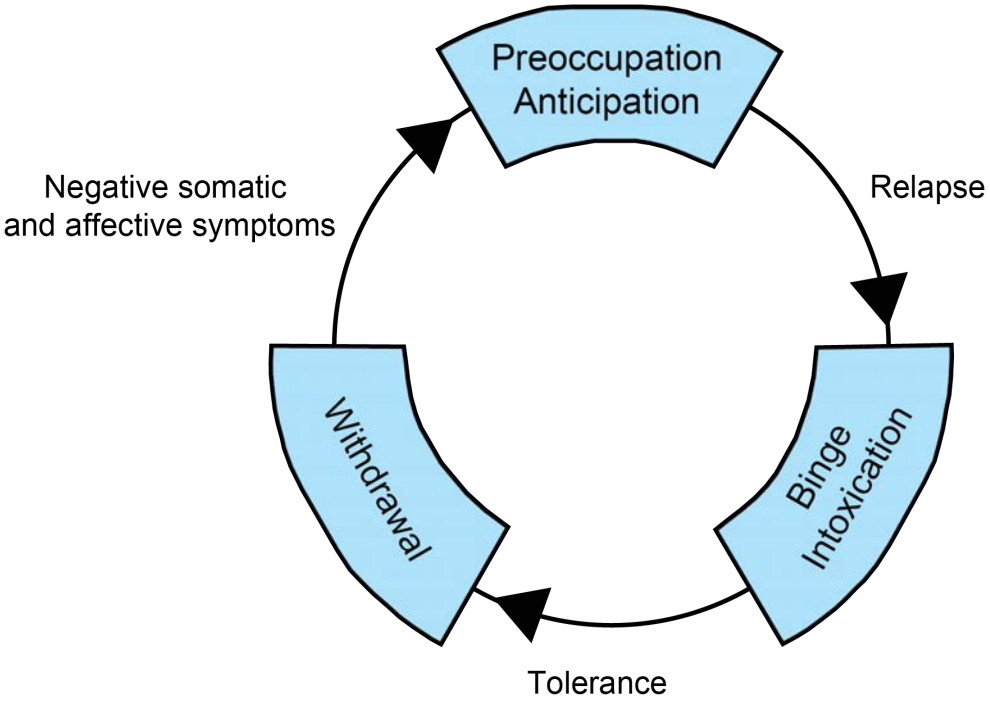

Figure 1.1. The cycle of addiction. Addiction is chronically relapsing disorder that occurs in three main stages: 1. Binge/intoxication, 2. Withdrawal, 3. Preoccupation/Anticipation. Adapted from Koob and Le Moal (Koob and Le Moal 2008).

Current Therapeutics For Smoking Cessation

Various studies conclude that smokers have a low probability of successful cessation. The CDC found that according to the 2015 National Health Interview Survey of adult smokers, 68% want to quit, 55.4% made an attempt within the past year, and only 7.4% have recently quit (Babb et al. 2017). Similarly, a study done in 1996 in the United Kingdom found that 31% of smokers will make an attempt to quit and only 29% of those who made a quit attempt (or ~10% of all smokers) remained abstinent for at least 3 months (West et al. 2001). There are great health benefits to smoking cessation and it is estimated that quitting by age 40 reduces the risk of death associated with continued smoking by 90% (Jha et al. 2013).

The few pharmacological cessation aids currently available have limited efficacy. One of the mainstays of smoking cessation is nicotine replacement therapy via patch or chewing gum. Meta-analysis indicates that only 27% of smokers are able to remain abstinent for at least 6 months while using a nicotine patch, compared to 13% in a placebo patch control group (Fiore et al. 1994). Nicotine replacement does not represent a long-term maintenance treatment option, as they are not efficacious beyond 24 weeks of use (Prochaska 2015). In recent years, electronic cigarettes (e-cigarettes) which allow for the inhalation of aerosol containing nicotine without the tobacco smoke have become popular, especially in adolescents (CDC 2013). Studies on the use of e-cigarettes as an effective method of nicotine replacement therapy are inconclusive due to the

poor quality of currently available data (Malas et al. 2016). In fact, e-cigarette use in youth aged 12-17 actually increases the chances of smoking traditional tobacco cigarettes in the future (Watkins et al. 2018).

The most commonly used non-nicotine pharmaceutical smoking cessation aids are bupropion and varenicline. Bupropion is an anti-depressant that exerts its effects by inhibiting norepinephrine and dopamine reuptake (Stahl et al. 2004). In addition to its anti-depressant effects, bupropion also acts as an antagonist for specific subtypes of nicotinic acetylcholine receptors (nAChRs), making it useful in the treatment of nicotine addiction (Slemmer et al. 2000). However, studies show that only about 20% of smokers remain abstinent for one year with the sustained-release bupropion (bupropion-SR) at various doses (Hurt et al. 1997), and this success rate is only marginally increased to about 30% by the addition of behavioral counseling (Swan et al. 2003). Varenicline is a partial agonist for the high affinity α4β2-contiaining nAChRs (Mihalak et al. 2006). In randomized control trials, varenicline has been shown to be more effective than bupropion-SR (Jorenby et al. 2006). However, still only 23% of patients on varenicline remain abstinent at one year compared to 14.6% taking bupropion and 10.3% in the placebo group (Jorenby et al. 2006). It is clear that these treatments increase the success rate of quitting compared to those attempting without the use of smoking cessation aids, but the overall success rates remain low regardless of the treatment choice. Without the development of new effective treatments

smokers will continue to struggle with cessation and a continued rise in tobacco-related deaths is anticipated (WHO 2012).

Interestingly, nicotine is often abused in conjunction with other substances, including alcohol (Falk et al. 2006, Cross et al. 2017). Continued cigarette smoking or initiation of smoking is associated with increased odds of substance use disorder relapse (Weinberger et al. 2017). Combining effective smoking cessation with the treatment of simultaneously occurring substance abuse disorders may be important for improving the chances of successful long-term outcomes for patients suffering from multiple addictions.

1.B. Neuronal Nicotinic Acetylcholine Receptors (nAChRs)

Structure of nAChRs

Nicotine is an agonist for nicotinic acetylcholine receptors (nAChRs), ligand-gated ion channels endogenously bound and activated by acetylcholine (Dani and De Biasi 2001, Benowitz 2009). Neuronal nAChRs are pentamers assembled from various combinations of transmembrane subunits arranged around a central, water-filled pore (Cooper et al. 1991, Dani and Bertrand 2007, Albuquerque et al. 2009). To date, eleven subunits, α2-α7, α9, α10 (encoded by genes *Chrna2-7*, *Chrna9*, *Chrna10*) and β2-β4 (*Chrnb2-4*), have been identified in mammalian neuronal nAChRs (Albuquerque et al. 2009). Each subunit contains four transmembrane (TM) domains, with the second TM domain lining the central pore, and extracellular N- and C-terminus domains (Albuquerque et al.

2009). The N-terminus of α subunits contains a cysteine loop, formed by two cysteines separated by 13 amino acids, which participates in agonist binding (Albuquerque et al. 2009).

Receptors can be heteromeric, containing both α and β subunits, or homomeric, the most common being α7 (Hurst et al. 2013). Different subunit combinations confer different affinities and functionalities to the receptor. For example, nAChRs containing α4 and β2 subunits (designated α4β2* to indicate that other subunits may be present) have relatively high affinity for nicotine compared to low-affinity homomeric α7 nAChRs (Dani and Bertrand 2007, Albuquerque et al. 2009). nAChR subunits are differentially expressed throughout the mammalian brain, with α4, β2, and α7 subunits showing the widest distribution and highest density of expression overall (Fowler et al. 2008). The heterogeneous distribution of nAChR subtypes throughout the brain modulates the activity of specific regions and circuits, contributing to their functions.

Function of nAChRs

When activated by ligand, nAChRs allow the influx of monovalent and divalent cations (Na^+, K^+, and Ca^{2+}) (Galzi et al. 1992, Dani and Bertrand 2007). This influx of cations then can enhance the Ca^{2+}-induced Ca^{2+} influx by activation of voltage-gated Ca^{2+} channels in the presynaptic terminal (Tredway et al. 1999, Dani and Bertrand 2007, Albuquerque et al. 2009). In mammals, neuronal

nAChRs of the central nervous system are located at pre-synaptic, pre-terminal, and extra-synaptic locations, and the intracellular Ca^{2+} signal resulting from their activation induces the release of neurotransmitters including dopamine, GABA, glutamate, and norepinephrine depending on the type of neuron on which they are located (Lena and Changeux 1997, Guo et al. 1998, Salminen et al. 2004, Azam et al. 2010, Garduno et al. 2012, Wang et al. 2014).

In addition to the increased release of neurotransmitters, the increased intracellular Ca^{2+} is an activator of other downstream effectors, including Ca^{2+}-dependent kinases and transcription factors. For example, nicotine is thought to regulate the phosphorylation of extracellular-regulated protein kinase (ERK) signaling proteins and the transcription factor cAMP response element binding protein (CREB), contributing to the mechanisms underlying neuroplasticity associated with nicotine dependence (Brunzell et al. 2003, Brunzell et al. 2009).

I.C. The Neurocircuitry of Nicotine Reward

The Mesocorticolimbic Pathway

The mesocorticolimbic dopamine pathway constitutes the brain circuitry responsible for the positive emotions and goal-directed motivations of rewarding stimuli, including pyschostimulant drugs of abuse (Koob and Volkow 2010, De Biasi and Dani 2011). The most important connections consist of dopaminergic (DAergic) neurons originating from the ventral tegmental area (VTA) and

projecting to the nucleus accumbens (NAc) and prefrontal cortex (PFC) (De Biasi and Dani 2011, Pistillo et al. 2015) (Figure 1.2). In general, the rewarding properties of addictive drugs, including nicotine, result from their ability to increase extra-cellular DA in the nucleus accumbens (NAc), located in the ventral striatum. (Di Chiara and Imperato 1988, Pontieri et al. 1996). Specifically, nicotine activates neurons within the VTA via nAChRs, stimulating increased release of DA within the NAc (Corrigall et al. 1994, Sombers et al. 2009, De Biasi and Dani 2011). Demonstrating the essential role of this circuit in nicotine reinforcement, lesioning of the NAc or blockade of nAChRs in the VTA reduces nicotine self-administration (Corrigall et al. 1992, Corrigall et al. 1994). Importantly, the mesocorticolimbic reward pathway is conserved among humans and rodents (Figure 1.2), and activation of this circuit is likely responsible for the initiation of addiction (Laviolette and van der Kooy 2004).

While this work will focus on the mesocorticolimbic DAergic reward pathway, it is important to note that this is not the only DAergic circuit contributing to behaviors associated with drug addiction. For instance, the dorsal striatum (caudate nucleus and putamen) is proposed to contribute to the compulsive drug-seeking exhibited in advanced addiction through its role in habit formation and storage of information about fixed action patterns (Gerdeman et al. 2003). The medium spiny neurons (MSNs) and interneurons of the dorsal striatum receive strong DAergic input from another midbrain region, the substantia nigra pars compacta (Lovinger 2010). High frequency stimulation of glutamatergic synapses

onto neurons in the dorsal striatum results in long-term depression (LTD), increasing extracellular dopamine and activating cholinergic interneurons (Partridge et al. 2002). Furthermore, activation of nAChRs expressed on the dopaminergic terminals in the dorsal striatum plays a role in the induction of LTD, and these mechanisms of synaptic plasticity may contribute to the formation of habits associated with nicotine addiction (Partridge et al. 2002).

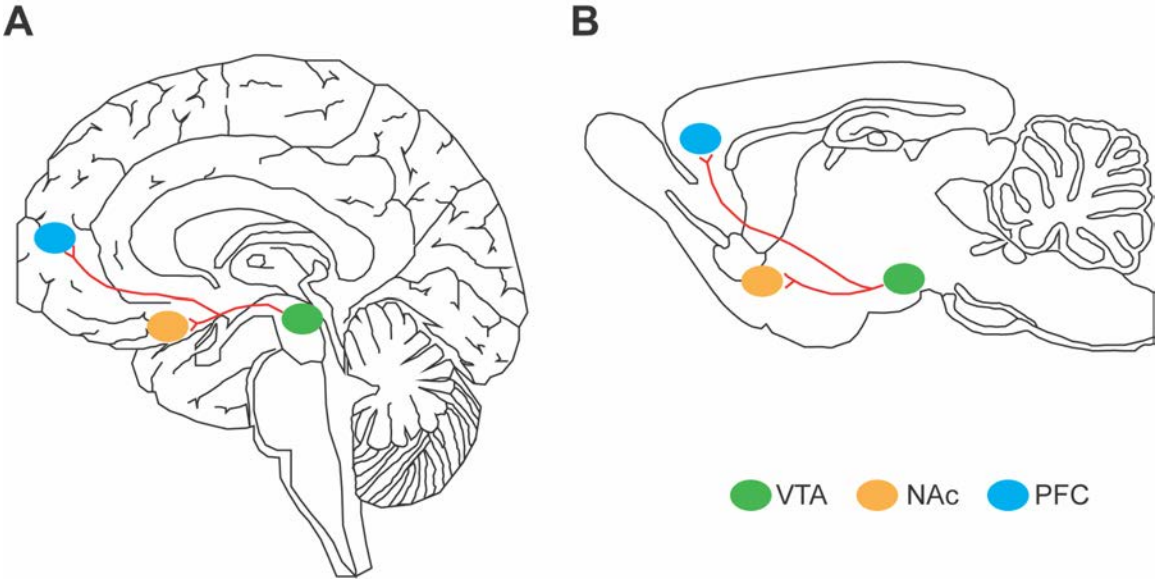

Figure 1.2. The mesocorticolimbic pathway. A sagittal representation of the reward circuit, consisting of dopaminergic neurons projecting from the VTA (green) to the NAc (orange) and the PFC (blue). This circuitry is conserved in humans **(A)** and rodents **(B)**. Abbreviations: VTA: Ventral tegmental area, NAc: Nucleus accumbens, PFC: Prefrontal cortex. Adapted from Laviolette and van der Kooy (Laviolette and van der Kooy 2004).

The Nucleus Accumbens (NAc)

The NAc is a bilateral nucleus residing in the ventral striatum, long considered a major center responsible for motivation and reward, including the effects of drugs of abuse (Salgado and Kaplitt 2015). The NAc is composed of about 90% GABAergic projection medium spiny neurons (MSNs) (Tepper and Bolam 2004, Sesack and Grace 2010). The remaining populations of neurons represent GABAergic and tonically active cholinergic interneurons (Tepper and Bolam 2004, Pistillo et al. 2015).

The NAc can be anatomically divided into two main sub-regions, the shell and the core, which also display differences in their afferent and efferent connections (Zahm and Brog 1992). There is a body of evidence indicating the shell is more important than the core for the rewarding and motivational properties of drugs, including nicotine (Ikemoto 2007). For example, rats will self-administer agonists for DA D1 and D2 receptors in the NAc shell but not the core (Ikemoto et al. 1997). Furthermore, microinfusion of DA receptor antagonists or lesions of DAergic terminals in the NAc shell disrupt conditioned place preference to nicotine and other drugs (Sellings and Clarke 2003, Fenu et al. 2006, Spina et al. 2006). However, the core also contributes to cue-conditioned motivated behaviors, including those in the context of drug addiction (Sesack and Grace 2010).

The main modulatory afferents to the NAc are DAergic inputs originating from the VTA, which is the central component of the reward circuit mediating

behavioral responses to natural rewards and drugs of abuse (Sesack and Grace 2010, De Biasi and Dani 2011). In addition to the DAergic input received from the VTA, the NAc receives excitatory glutamatergic afferents from limbic brain regions, including the PFC, basolateral amygdala, and the ventral subiculum of the hippocampus (Sesack and Grace 2010). These inputs likely contribute to goal-directed behaviors and positive reinforcement learning, providing executive control, affective motivation, and contextual information, respectively (Kalivas et al. 2005, Ambroggi et al. 2008, Gruber et al. 2009, Sesack and Grace 2010, Britt and Bonci 2013). The NAc also receives glutamatergic afferents from various thalamic subregions which may contribute to arousal and attention to rewarding stimuli (Smith et al. 2004).

The major efferent projections of the NAc include the substantia nigra, (through the ventral pallidum and the subthalamic nucleus), the VTA, hypothalamus, and brainstem (Sesack and Grace 2010, Pistillo et al. 2015). This reciprocal connection with the VTA allows the limbic regions to influence the activity of the basal ganglia controlling motor-related functions (Sesack and Grace 2010).

The Ventral Tegmental Area (VTA)

The VTA is a bilateral region of heterogeneous cellularity located in the ventral midbrain (Pistillo et al. 2015). Approximately 60% of the cells in the VTA are DAergic projection neurons (Pistillo et al. 2015). These DAergic neurons

exhibit a tonic firing pattern during resting conditions and display phasic burst firing in response to a rewarding experience (Schultz 1986). The phasic burst firing is capable of releasing more DA in projection areas (Schultz 1986, Pignatelli and Bonci 2015) and is sufficient to condition a place preference (Tsai et al. 2009).

The VTA can be subdivided into anatomical sub-regions, including the anterior and posterior regions (aVTA and pVTA, respectively). The aVTA and pVTA respond differently to drugs of abuse, including nicotine, opiates, and alcohol (Ikemoto et al. 2006, Ericson et al. 2008, Shabat-Simon et al. 2008, Zhao-Shea et al. 2011). For instance, rats self-administer nicotine into the pVTA, but not the aVTA (Ikemoto et al. 2006). DAergic neurons within the aVTA and pVTA differ in size distribution, density, and expression of nAChR subtypes (Zhao-Shea et al. 2011). Importantly, nicotine directly and preferentially activates DA neurons in the pVTA through its action on α4α6* nAChRs (Zhao-Shea et al. 2011). The efferent and afferent connection of the aVTA and the pVTA also differ. The aVTA projects to the NAc lateral shell and core, while the pVTA projects to the NAc medial shell and core, PFC and basolateral amygdala (Ikemoto 2007, Pistillo et al. 2015). These differences between the pVTA and aVTA may account for the differences in behavioral responses to nicotine.

Neurons releasing the inhibitory neurotransmitter GABA are also present in the VTA, representing 20-40% of the neurons in this region (Lammel et al. 2014). Both GABAergic projection neurons and interneurons are present and

enriched in the pVTA (Pistillo et al. 2015). A portion of these GABAergic neurons project to other brain regions including the PFC, NAc and lateral habenula (LHb) (Taylor et al. 2014, Pistillo et al. 2015). In fact, the majority of VTA projections to the PFC derive from GABAergic neurons (Carr and Sesack 2000). However, the majority of GABAergic neurons in the VTA are interneurons, synapsing with DAergic neurons within the VTA and tonically inhibiting their activity. *In vitro* studies suggested that nicotine exposure desensitizes nAChRs on these GABAergic interneurons, disinhibiting the activity of the DAergic VTA neurons (Mansvelder et al. 2002). Further supporting the prevailing 'disinhibition' hypothesis, *in vivo* activation of the GABAergic neurons in the VTA using optogenetics suppressed activity of neighboring DAergic neurons and disrupted reward behavior (van Zessen et al. 2012). In fact, optogenetic stimulation of GABAergic neurons in the VTA is sufficient to drive conditioned place aversion (Tan et al. 2012). However, additional *in vivo* studies have found that concerted activation of GABAergic neurons within the VTA are necessary for the induction of burst firing in the DAergic neurons important for reward behaviors (Tolu et al. 2013). Additionally, functional up-regulation of α4* nAChRs in GABAergic neurons within the VTA is sufficient to increase sensitivity to nicotine reward (Ngolab et al. 2015). Taken together, these data support a complex regulatory role of GABAergic neurons in the modulation of VTA DAergic transmission and its importance for nicotine reward.

Finally, there is a small population (~2-9%) of glutamatergic, non-DAergic, non-GABAergic neurons in the VTA (Nair-Roberts et al. 2008, Taylor et al. 2014, Pistillo et al. 2015). Additionally, a subpopulation of VTA DAergic neurons also express glutamate transporters and release glutamate in the NAc and PFC (Chuhma et al. 2004, Kawano et al. 2006, Gorelova et al. 2012).

The VTA receives input from throughout the CNS (Pistillo et al. 2015). Afferents from the striatum, including the NAc, directly project to both the DAergic and GABAergic neurons within the VTA (Watabe-Uchida et al. 2012). Forebrain areas projecting to the VTA include medial and lateral preoptic areas, LHb, medial and lateral hypothalamus, and the medial septum (Geisler et al. 2007, Watabe-Uchida et al. 2012). Ascending brainstem projections originate in regions including the pedunculopontine and laterodorsal tegmental (LDTg) nuclei and median raphe (Geisler et al. 2007, Watabe-Uchida et al. 2012). Glutamatergic afferents have been detected projecting from all regions except the NAc and the septum (Geisler et al. 2007). The cholinergic input to VTA DAergic neurons largely originates from the LDTg (Oakman et al. 1995, Omelchenko and Sesack 2006). These glutamatergic and cholinergic afferents modulate the activity of the VTA. Release of glutamate and acetylcholine from various afferents has been shown to activate the DAergic neurons within the VTA, modulating reward behaviors. For example, stimulation of LDTg neurons releases glutamate and ACh, activating DAergic VTA neurons that project to the NAc and inducing a conditioned place preference (Lammel et al. 2014). Finally, the aVTA receives

GABAergic inputs from the rostromedial tegmentum (RMTg) (Pistillo et al. 2015). The RMTg sends GABAergic projections to DAergic neurons in the VTA, inhibiting their activity and playing a role in aversive behaviors (Jhou et al. 2009, Barrot et al. 2012).

While traditionally considered a reward center, the VTA also has an important role in the affective symptoms of nicotine withdrawal. It is theorized that withdrawal from drugs induces an over-activation of the stress circuitry of the brain (Koob and Volkow 2010). DAergic neurons in the VTA also express corticotrophin-releasing factor (CRF), a prominent stress modulator (Grieder et al. 2014). DAergic neurons from the VTA expressing CRF project to the interpeduncular nucleus (IPN), and increased CRF signaling within the IPN triggers anxiety during nicotine withdrawal (Zhao-Shea et al. 2015, Molas et al. 2017).

nAChRs in the Mesocorticolimbic Pathway

Nicotine modulates the activity of neurons within the mesocorticolimbic reward pathway through interaction with nAChRs. The soma and dendrites of DAergic neurons in the VTA predominantly express α4β2* (with or without α5) and α4α6β2* nAChRs (Klink et al. 2001, Champtiaux et al. 2003, Gotti et al. 2010). GABAergic interneurons and terminals in the VTA also express α4β2* and α6β2* nAChR subtypes and their activation promotes the release of GABA (Klink et al. 2001, Pistillo et al. 2015). In the NAc, no functional nAChRs have been

detected in MSNs (Pisani et al. 2007). Striatal DAergic terminals express β2* nAChRs, allowing for cholinergic interneurons to regulate the probability of DA release in the NAc (Cachope et al. 2012, Threlfell et al. 2012). Additionally, GABA release by interneurons or projection neurons in the striatum is modulated predominantly by α4β2* nAChR receptors (Grilli et al. 2009, Pistillo et al. 2015).

Genetically modified mouse models provide evidence that different nAChR subunits play distinct roles in nicotine reward-associated behaviors. For example, β2, α4, or α6 nAChR subunit knockout (KO) mice do not systemically self-administer nicotine, and this behavior is rescued when the subunit was re-expressing in the VTA (Pons et al. 2008). However, α7-KO mice did not affect systemic nicotine self-administration, suggesting that α4β2* and α6β2*, but not α7, nAChRs are necessary and sufficient for nicotine self-administration (Pons et al. 2008). Further supporting the necessary role of β2* nAChRs in nicotine reward, β2 KO mice also do not condition a place preference to nicotine, while α7 KO mice do not show any deficit in this behavior (Walters et al. 2006). In addition, mice expressing hypersensitive α4* nAChRs condition a place to concentrations of nicotine 50-fold lower than WT mice (Tapper et al. 2004). Taken together, the heterogeneous expression of nAChR subunits and their distinct roles in nicotine reward behaviors illustrates the role of nAChRs in modulating the activity of the mesocorticolimbic reward circuit. Yet, there is still much to be elucidated about the up-stream regulators and down-stream effectors of nAChR expression and activity during nicotine exposure and reward.

I.D. The Neurocircuitry Of Nicotine Withdrawal

The Habenulo-Interpeduncular Pathway

The habenulo-interpeduncular circuit consists of neurons projecting from the medial habenula (MHb) to the interpeduncular nucleus (IPN) via the fasciculus retroflexus (Fr) (Antolin-Fontes et al. 2015, Molas et al. 2017) (Figure 1.3A). This circuit modulates basal negative emotional responses and is essential for nicotine withdrawal-induced anxiety (Molas et al. 2017). Both the MHb and IPN are enriched in nicotinic acetylcholine receptors and withdrawal symptoms can be precipitated by blockade of these receptors via microinfusion of mecamylamine, a non-selective nicotinic antagonist, into either region of nicotine dependent mice (Salas et al. 2009, Zhao-Shea et al. 2015). Pharmacological and optogenetic studies have shown that glutamatergic stimulation from the MHb activates specific sub-regions of the IPN, resulting in the somatic and affective symptoms of nicotine withdrawal (Zhao-Shea et al. 2013, Zhao-Shea et al. 2015). Specifically, GABAergic neurons in the IPN are activated during precipitated nicotine withdrawal and optogenetic activation of the GABAergic neurons in the IPN is sufficient to induce somatic withdrawal signs (Zhao-Shea et al. 2013). Pharmacologic blockade of the excitatory glutamatergic inputs to the IPN via infusion of the NMDA antagonist AP5 is sufficient to alleviate somatic and affective signs of precipitated withdrawal (Zhao-Shea et al. 2013, Zhao-Shea et al. 2015). Finally, optogenetic silencing of the

cholinergic/glutamatergic MHb-IPN inputs alleviates nicotine withdrawal-associated anxiety (Zhao-Shea et al. 2015). Overall, these studies show that glutamatergic inputs from the MHb activate GABAergic neurons in the IPN, inducing somatic and affective withdrawal symptoms in nicotine dependent mice.

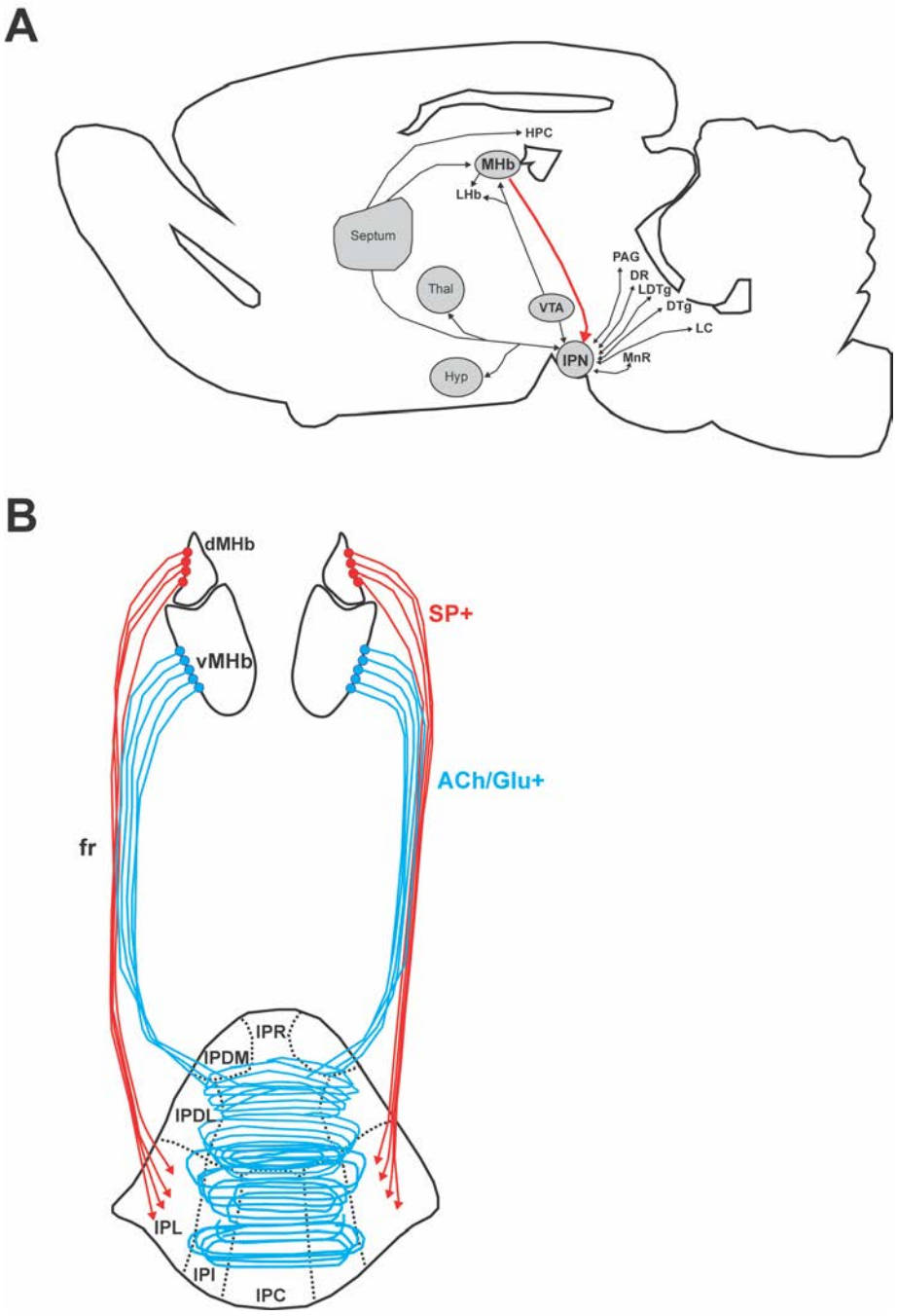

Figure 1.3. The habenulo-interpeduncular pathway. (A) A sagittal representation of the mouse habenulo-interpeduncular withdrawal circuit, consisting primarily of neurons projecting from the MHb to the IPN (red arrow). Abbreviations: DR: dorsal raphe, DTg: dorsal tegmental nuclei, HPC: hippocampus, Hyp: Hypothalamus, IPN: interpeduncular nucleus, LHb: lateral habenula, LC: locus coeruleus, LDTg: laterodorsal tegmental nuclei, MHb: medial

habenula, MnR: median raphe, PAG: periaqueductal grey, Thal: Thalamus, VTA: ventral tegmental area, Adapted from Antolin-Fontes et al. (Antolin-Fontes et al. 2015) and Molas et al. (Molas et al. 2017) **(B)** A coronal representation of the mouse habenulo-interpeduncular microcircuit. Substance P neurons (red) project from the dMHb to the IPL and ACh/Glu+ neurons (blue) project from the vMHb to the central IPN along the fasciculus retroflexus (fr). Abbreviations: dMHb: Dorsal medial habenula, IPDL: Dorsolateral IPN, IPDM: Dorsomedial IPN, IPI: Intermediate IPN, IPL: Lateral IPN, IPR: Rostral IPN, vMHb: Ventral medial habenula. Adapted from Molas et al. (Molas et al. 2017).

The Medial Habenula (MHb)

The habenula is a broadly conserved bilateral structure residing on the dorsomedial surface of the caudal thalamus that can be further subdivided into the medial and lateral habenula (MHb and LHb, respectively) (Hikosaka 2010). While the LHb projects densely to the RMTg inhibiting the firing of midbrain DA neurons (Jhou et al. 2009, Picciotto and Kenny 2013), the MHb projects almost exclusively to the IPN via the Fr (Hikosaka 2010) The medial habenula can be subdivided into the dorsal (dMHb) and ventral (vMHb) sub-regions, differentiated by neuron type, source of afferent projections and pattern of efferent projections to the IPN (Qin and Luo 2009, Molas et al. 2017). Afferents from the bed nucleus of the anterior commissure project to the dMHb while the vMHb receives glutamatergic and cholinergic input from the triangular septum (Qin and Luo 2009, Yamaguchi et al. 2013). The dMHb sends substance P fibers to the ipsilateral lateral portions of the IPN, while the cholinergic and/or glutamatergic neurons project from the vMHb to the central portion of the IPN (Molas et al. 2017) (Figure 1.3B). There is also evidence for unidirectional afferents from the MHb to the LHb, suggesting that the MHb may regulate the activity of the LHb (Sutherland 1982, Kim and Chang 2005), representing indirect intersection with the activity of the VTA.

The Interpeduncular Nucleus (IPN)

The IPN is a single midline nucleus in the posterior midbrain that lies ventral to the VTA (Klemm 2004). The IPN can be further subdivided into four paired (dorsolateral [IPDL], dorsomedial [IPDM], intermediate [IPI], and lateral [IPL]) and three unpaired (apical [IPA], central [IPC], and rostral [IPR]) sub-regions based on neuron type, afferents, and efferents (Hamill and Lenn 1984, Antolin-Fontes et al. 2015, Molas et al. 2017) (Figure 1.3B).

As discussed above, the major inputs to the IPN come from the MHb (Figure 1.3). Additional sources of neural projections include forebrain nuclei and midbrain nuclei (Antolin-Fontes et al. 2015) (Figure 1.3A). Forebrain nuclei afferents originate from regions such as the septum, ventral thalamus, and hypothalamus (Contestabile and Flumerfelt 1981, Jennes 1987, Villalobos and Ferssiwi 1987, Vertes and Fass 1988, Moore et al. 2000, Antolin-Fontes et al. 2015). Midbrain nuclei projections to the IPN include the dorsal tegmental nuclei (DTg), LDTg, dorsal (DR) and median raphe (MnR), periaqueductal gray, and locus coeruleus (Hamill and Jacobowitz 1984, Satoh and Fibiger 1986, Cornwall et al. 1990, Antolin-Fontes et al. 2015). As previously discussed, the VTA also projects to the IPI and modulates activity of the IPN through CRF signaling (Zhao-Shea et al. 2015).

IPN is composed predominantly of densely populated GABAergic neurons (Kawaja et al. 1989). The IPN sends efferent projections primarily to the MnR, DR, DTg and LDTg (Hamill and Lenn 1984, Groenewegen et al. 1986). The IPN

also sends efferent projections to regions including the septum, hypothalamus, thalamus, and hippocampus (Hamill and Lenn 1984, Vertes and Fass 1988, Antolin-Fontes et al. 2015).

Different sub-regions within the IPN mediate different aspects of nicotine withdrawal behaviors. The activation of the IPR during nicotine withdrawal triggers somatic withdrawal signs (Zhao-Shea et al. 2013). The IPI is activated during nicotine withdrawal, in part by CRF signaling from the VTA, inducing increased anxiety (Zhao-Shea et al. 2015). Additionally, through the complicated network of direct and indirect efferent and afferents, the MHb-IPN is interconnected with the classical anxiety circuitry, including the amygdala and bed nucleus of the stria terminalis (BNST), modulating negative emotions and anxiety (Molas et al. 2017).

nAChRs in the Habenulo-interpeduncular Pathway

The mHb and IPN exhibit the highest [$^{+}$H]-nicotine binding in the brain, suggesting high levels of nAChR expression in these regions (Marks et al. 1998). The MHb and IPN are enriched in nAChRs containing α5, α3, and β4 subunits, which are expressed by the *CHRNA5-A3-B2* gene cluster (Picciotto and Kenny 2013, Lassi et al. 2016). Interestingly, genome-wide association studies have identified associations between *CHRNA5-A3-B2* gene cluster and the risk of nicotine addiction and the heaviness of smoking habit (Saccone et al. 2007, Thorgeirsson et al. 2008). This enrichment of nAChR subunits in the withdrawal

circuit is supported by single-cell RT-PCR and electrophysiological experiments suggesting that ~90-100% of MHb neurons express the α3, α4, α5, β2, and β4 nAChR subunits (Sheffield et al. 2000). Additionally, ~40% of neurons in the MHb express α6, α7, and β3 nAChR subunits (Sheffield et al. 2000).

Genetic mouse models with various nAChR subunits knocked out shed light on the roles of specific nAChR subtypes in nicotine aversion and withdrawal. Mice lacking the α5 subunit display increased nicotine intake in a self-administration paradigm. When α5 is re-expressed in the MHb, nicotine self-administration returns to the level of a WT mouse, indicating α5* nAChRs participate in an inhibitory motivational signal that acts to limit nicotine intake (Fowler et al. 2011). Studies suggest that the different nAChR subtypes are responsible for the somatic and affective signs observed during nicotine withdrawal. For example, somatic signs observed during withdrawal precipitated with non-selective nAChR antagonist mecamylamine are decreased in α2 KO, α5 KO, α7 KO, and β4 KO mice (Salas et al. 2004, Jackson et al. 2008, Salas et al. 2009). β2 KO mice do not exhibit affective withdrawal signs such as anxiety or conditioned place aversion (Jackson et al. 2008). While much of the focus has been on determining the expression patterns and behavioral consequences of nAChR subtypes in the MHb-IPN axis, there remains much to be elucidated concerning the up-stream regulators and down-stream effectors activated by these nAChRs and their roles in nicotine withdrawal.

I.E. Neuroadaptations of Nicotine Dependence

nAChRs and Nicotine Dependence

The neurocircuitry controlling the behaviors associated with nicotine reward and withdrawal are well defined, but the cellular mechanisms underlying these behavioral changes are less clear. The most extensively studied phenomenon is the up-regulation of nAChRs after chronic nicotine exposure. It is well established that nAChRs, predominantly α4β2*, are up-regulated in the brain following chronic exposure to cigarette smoke or nicotine in both rodents and humans (Schwartz and Kellar 1983, Benwell et al. 1988, Yates et al. 1995, Flores et al. 1997, Nguyen et al. 2003). While not completely understood, it has been suggested that nicotine-induced up-regulation of nAChRs is thought to contribute to nicotine dependence by altering the neural network, possibly resulting in altered sensitivity to nicotine (Govind et al. 2009). When chronically stimulated by nicotine, nAChRs enter a deep state of desensitization, which may contribute to acute tolerance and promote nAChR up-regulation (Dani and De Biasi 2001).

In the mesocorticolimbic reward circuitry, desensitization of α4β2* nAChRs on GABAergic neurons of the VTA disinhibits DAergic projections to the NAc, leading to rewarding behaviors (Mansvelder et al. 2002, van Zessen et al. 2012). Additionally, chronic nicotine exposure leads to up-regulation of α4β2* nAChRs primarily on GABAergic neurons (Nashmi and Lester 2007). The restoration of nAChR function during nicotine abstinence leads to amplified

GABAergic activity by endogenous ACh, possibly contributing to nicotine withdrawal symptoms (Pistillo et al. 2015). Other studies have found that repeated nicotine exposure and withdrawal leads to increased density of nAChRs in the striatum and enhanced nicotine-conditioned placed preference in mice (Hilario et al. 2012).

In the habenulo-interpeduncular withdrawal circuit, chronic nicotine functionally up-regulates α6/α4* nAChRs in the cholinergic/glutamatergic neurons in the vMHb (Shih et al. 2015, Pang et al. 2016). During nicotine abstinence, this up-regulation of nAChRs in the MHb presumably results in increased cholinergic activation of glutamatergic neurons projecting to the IPN, inducing withdrawal-associated symptoms including anxiety (Pang et al. 2016, Molas et al. 2017).

The current prevailing hypothesis is that nAChR up-regulation results from post-transcriptional mechanisms including slowed rate of cell surface turn over, increased rate of subunit maturation and assembly, blockage of subunit degradation, changes in receptor stoichiometry, and changes in the conformation of nAChRs (Govind et al. 2009). It is generally accepted that nAChR up-regulation is not a result of an increase in transcription, as *in situ* hybridization experiments have indicated no increase in mRNA encoding nAChR subunits, including α4 and β2, in the brains of mice exposed to nicotine for 10 days (Marks et al. 1992). However, conflicting evidence from our laboratory showed there was an up-regulation of the *Chnrb2* transcript in the VTA of WT mice after

chronic nicotine treatment via osmotic minipump (Hogan et al. 2014). In light of this conflicting evidence, there is much yet to be elucidated concerning the complex mechanisms underlying the nicotine-mediated up-regulation of nAChRs in a subtype and sub-region specific manner.

Nicotine-induced Neuroadaptations and Transcriptional Regulation

Neuroplasticity describes the brain's ability to remodel the structural and functional connections in response to stimuli, from the level of the synapse to the circuit (Korpi et al. 2015). In general, chronic exposure to drugs of abuse induces stable neuroadaptations underlying the compulsion for continued drug use and susceptibility to relapse. These neuroadaptations are evidenced by many examples of drug-evoked long term potentiation and depression, strengthening and weakening synapses in the VTA and NAc (Madsen et al. 2012). These long-lasting changes in the addicted brain's function are thought to require alterations of gene expression and *de novo* protein synthesis through regulation of transcription factors, epigenetic mechanisms, and non-coding RNAs (Robison and Nestler 2011, Madsen et al. 2012).

Research has predominantly focused on the nicotine-induced nAChR up-regulation and its effects on nicotine reward and withdrawal behaviors, but other targets with a variety of regulatory functions at the synapse are also subject to regulation by nicotine. For example, expression of glutamatergic receptors (GluRs) is altered in a region-specific manner following chronic nicotine treatment

and withdrawal (Pistillo et al. 2016). These effects are long lasting, especially in the midbrain (Pistillo et al. 2016). Chronic nicotine exposure also increases the levels of high-affinity DA D2 receptors (Novak et al. 2010) and regulates of synaptic scaffolding proteins (Rezvani et al. 2007). Overall, nicotine employs a multitude of mechanisms to modify the synapse, possibly underlying the behaviors associated with nicotine reward and withdrawal.

Several studies have revealed that nicotine induces changes in the expression and activity of transcription factors. Most notably, levels of CREB and phosphorylated CREB, a constitutively expressed transcription factor, are altered in brain regions of the mesocorticolimbic pathway in mice exposed to nicotine and withdrawal (Pandey et al. 2001, Brunzell et al. 2003). Furthermore, activation of CREB in the NAc shell is required for the formation of a nicotine conditioned place preference (Brunzell et al. 2009). The Fos family of immediate early genes, including c-Fos and FosB, represents additional examples of transcription factors regulated by nicotine treatment or withdrawal (Marttila et al. 2006). Nicotine's regulation of the levels and activity state of transcription factors allows for widespread downstream regulation of the transcriptome in response to the nicotine stimulus, contributing to neuroadaptations at the synapse.

There is a limited body of work examining transcriptome-wide expression changes in the brain following nicotine exposure and withdrawal. Most studies employ microarrays to measure gene expression in various brain regions. Neural focused microarrays showed that specific regions of the rat mesolimbic circuit,

including the PFC, NAc, VTA, and amygdala, exhibit divergent transcriptional responses to chronically self-administered nicotine (Konu et al. 2001). Similarly, microarrays identified 4.1-14.3% of genes were modulated in the PFC, NAc, VTA, amygdala, and hippocampus of C57BL/6J mice receiving nicotine in their drinking water for two weeks (Wang et al. 2008). Interestingly, only a small number of genes were altered in more than one brain region, suggesting changes in transcription occur in a brain-region specific manner (Wang et al. 2008). Alterations in transcription also follow distinct time-courses, over the course of hours following a single sub-cutaneous nicotine injection (Chen et al. 2007) and days/weeks of continued nicotine injections (Li et al. 2004).

While the majority of studies investigate transcriptome-wide expression changes in specific regions of the brain, one study used single cell RNA-seq to investigate differential gene expression in specific neuron-subtypes. Nicotine induces differential expression of 129 genes in DAergic neurons of the substantia nigra pars compacta as determined by single cell RNA-Seq, many of which were related to the ubiquitin-proteosome pathway, cell cycle regulation, chromatin modification, DNA binding and regulation of transcription, and RNA processing (Henley et al. 2013). In addition, DAergic and GABAergic neurons have distinct transcriptome phenotypes in response to nicotine exposure (Henley et al. 2013).

Several studies have investigated the transcriptional effects of various modes of nicotine exposure on brain regions of the mesocorticolimbic reward pathway, but relatively little is known about alterations in gene expression at the

mRNA level within the MHb-IPN withdrawal axis in response to nicotine exposure. One study measured differential expression by microarray, finding that 615 mRNAs in the habenula were altered by self-administration of nicotine (Lee et al. 2015). However, the effect of withdrawal on the transcription of mRNAs in this circuit has not been pursued.

I.F. MicroRNA (miRNA) Biogenesis and Function

Canonical Biogenesis of miRNAs

miRNAs are non-coding RNA molecules ~22 nucleotides in length that direct Argonaute silencing complexes to repress the expression of mRNA targets by promoting mRNA decay or translational repression (Bartel 2018) (Figure 1.4). miRNA genes may be intergenic or reside in introns, using the same or distinct promoter of their host gene (Ozsolak et al. 2008). Primary transcripts, called pri-miRNAs, are transcribed from miRNA genes by RNA polymerase II (Lee et al. 2004) and form a hairpin structure. Drosha, a nuclear RNAse III endonuclease, forms the Microprocessor complex with two molecules of DGCR8 (DiGeorge syndrome critical region 8), a cofactor that possess two double-stranded RNA-binding domains (Han et al. 2004, Nguyen et al. 2015). The Microprocessor cleaves pri-miRNAs ~11 nucleotides away from the ssRNA-dsRNA ‘basal’ junction (Han et al. 2006). This cleavage generates ~60 nucleotide pre-miRNA

hairpin molecules with a 2 nucleotide 3'-overhang (Lee et al. 2003). Importantly, this cleavage defines the terminus of a miRNA, and thus its specificity (Ha and Kim 2014). The pre-miRNA is then exported to the cytoplasm by Exportin 5 (Xpo5) (Yi et al. 2003) where it is further processed by Dicer, an RNAse III endonuclease. Dicer cuts both RNA strands by the loop of the pre-miRNA leaving another 2 nucleotide 3'-overhang and generating the miRNA duplex (Bartel 2018). To achieve precise cleavage of ~22 nucleotide dsRNAs, it is hypothesized that Dicer acts as a 'molecular ruler' (Ha and Kim 2014). A PAZ (PIWI-AGO-ZWILLE) domain binds to the 5'-terminus of the pre-miRNA and Dicer's catalytic center, separated by a helical domain, cleaves the pre-miRNA at a fixed distance near the loop (Macrae et al. 2006, Park et al. 2011). The miRNA duplex is loaded into the AGO protein to form a RNA-induced silencing complex (RISC), and the passenger miRNA* is expelled and degraded (Kawamata and Tomari 2010), leaving the targeting guide strand. In principle, either strand may be loaded as the guide strand, so strand selection must be tightly regulated. The thermodynamic stability and sequence bias at the 5'-terminus of the miRNA duplex is thought to regulate guide strand selection (Schwarz et al. 2003, Hu et al. 2009, Meijer et al. 2014).

Biogenesis of miRNAs can be regulated at each step. Nuclear control points include pri-miRNA transcription by RNA Pol II and the localization, stability, and affinity of the Drosha/DGCR8 Microprocessor (Ha and Kim 2014). In the cytoplasm, miRNA biogenesis may be regulated at the level of Dicer processing,

AGO proteins and other members of the RISC, and miRNA stability/decay (Krol et al. 2010, Ha and Kim 2014).

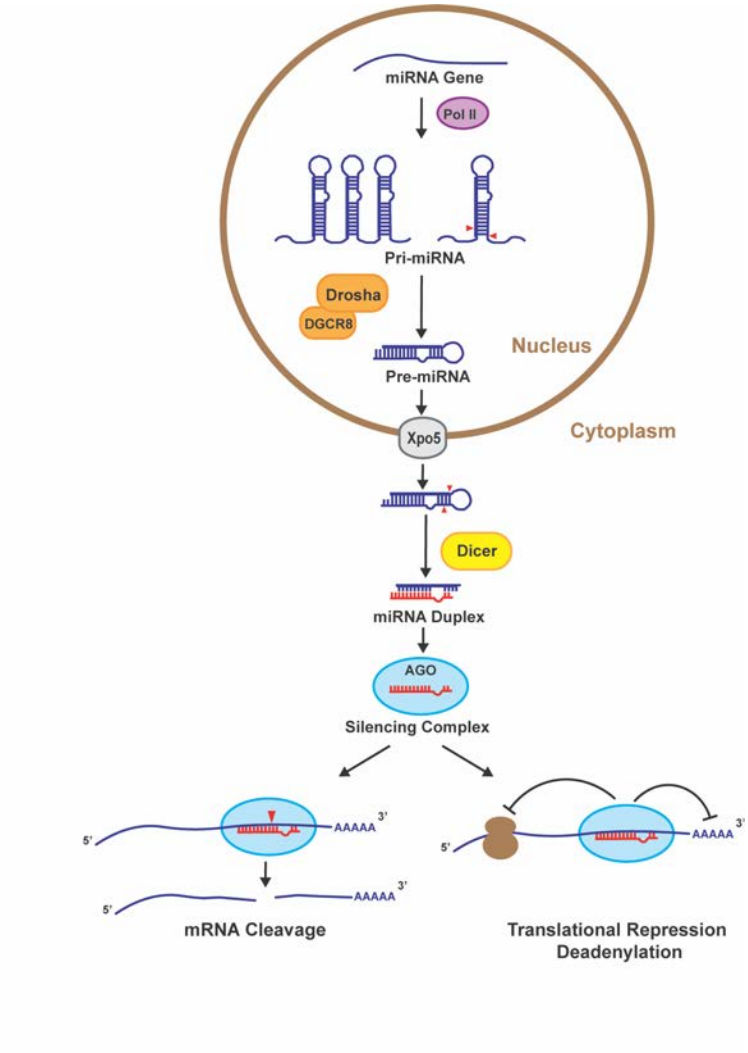

Figure 1.4. miRNA biogenesis. Pri-miRNAs are transcribed by RNA polymerase II (Pol II) in the nucleus and processed by Drosha/DGCR8 to generate pre-miRNAs with a stem-loop structure and a 2 nt 3´overhang. Pre-miRNAs leave the nucleus via exportin 5 (Xpo5) and are cleaved by Dicer in the cytoplasm to form a miRNA duplex. The miRNA guide strand is loaded into the Argonaute (AGO) silencing complex and directs repression of its mRNA target by cleavage, translational repression, or mRNA deadenylation. Adapted from Bartel (Bartel 2018) and O'Carrol and Schaefer (O'Carroll and Schaefer 2013).

miRNA Function

miRNAs repress expression of their targets through cleavage, deadenylation, or translational repression (Figure 1.4). Microarray and proteomic analysis has determined that the repression of mRNAs and protein by miRNAs is typically mild, with *in vitro* over-expression of miRNAs rarely inducing repression greater than 2- or 4-fold, respectively (Lim et al. 2005, Selbach et al. 2008). miRNAs direct cleavage of their target mRNA transcripts when base-pairing is extensive, however this mechanism of silencing has been reported in a few select cases in humans and mammals (Bartel 2018).

In mammals, the most dominant mechanisms of miRNA repression are mRNA destabilization and decay (Guo et al. 2010, Eichhorn et al. 2014). GW182 proteins (also known as TNRC6 proteins) co-assemble with AGO proteins in the RISC and are required for miRNA-mediated gene silencing (Jonas and Izaurralde 2015). GW182 proteins within the RISC recruit PAN2-PAN3 and CCR4-NOT deadenylation complexes to mRNA targets which shortens the Poly(A) tail and fates the mRNA for degradation (Braun et al. 2011, Chekulaeva et al. 2011, Fabian et al. 2011, Wilczynska and Bushell 2015, Bartel 2018).

miRNAs also act to repress the translation of their targets (Wilczynska and Bushell 2015, Bartel 2018). Translational repression by miRNAs is thought to occur through inhibition of the initiation step (Pillai et al. 2005, Mathonnet et al. 2007). The miRNA-RISC prevents recruitment of the pre-initiation complex by blocking the assembly of the eukaryotic translation initiation factor (eIF4F)

complex, interfering with recognition of the 5'-cap (Mathonnet et al. 2007, Fukaya et al. 2014). The RNA helicase activity of the eIF4F complex is thought to participate in initiation by unwinding the 5′-UTR into a conformation amenable to the binding of the pre-initiation complex (Fukaya et al. 2014). Also, in addition to their above roles in mRNA deadenylation, recruitment of GW182 and its downstream effector CCR4-NOT by the RISC is also thought to decrease the efficiency of translation (Wilczynska and Bushell 2015, Bartel 2018). This occurs via the recruitment of DEAD-box RNA helicase (DDX6), a known inhibitor of translation (Mathys et al. 2014).

miRNA Targets And Target Prediction

Despite repressing the expression of their targets by a small amount, miRNAs play an important role in the regulation of cellular functions and are predicted to regulate more than half of the human genome (Ameres and Zamore 2013). Each miRNA is predicted to target multiple, distinct mRNA transcripts (Lim et al. 2005). Conversely, a single mRNA transcript may be targeted by multiple miRNAs (Peter 2010). It is the mechanisms by which miRNAs target mRNAs that impart them with this expansive regulatory potential.

miRNAs recognize their mRNA targets through imperfect base-pairing of the miRNA seed region (nucleotides 2-7) with miRNA response elements (MREs) within the 3′-UTR of mRNAs (Lewis et al. 2003, Bartel 2009). In addition to the 6 nucleotide seed, canonical MREs also have an additional base pairing at

nucleotide 8 and/or an adenosine (A) at nucleotide 1 (Bennett et al. 2003) (Figure 1.5). Seed type efficacy is ranked from highest to lowest: 8mer > 7mer-m8 > 7mer-A1 (Grimson et al. 2007). Effective non-canonical sites, involving extensive base pairing to the 3'-end of the miRNA do exist, however, they are very rare for conserved miRNA families in mammals (Friedman et al. 2009). In fact, miRNAs will bind to non-canonical sites, however, novel non-canonical sites identified in high throughput CLIP and other biochemical studies conveyed no detectable repression in target mRNA or protein levels (Agarwal et al. 2015).

Figure 1.5. Canonical miRNA response elements (MREs). All canonical seed types base pair with nucleotides 2-7 of the miRNA. 7mer-A1 sites have an additional adenosine at position 1. 7mer-m8 sites have an additional seed match at position 8. 8mer sites contain both the adenosine at position 1 and the additional base pairing at position 8. Adapted from Bartel (Bartel 2009).

In addition to the base pairing of 7-8 nucleotides in the miRNA seed region to the MREs within the 3′-UTR of mRNAs, elements of the UTR context can also influence miRNA targeting (Bartel 2009). Position within the 3′-UTR can influence the effectiveness of a MRE. For example, more effective and preferentially conserved sites occur at least 15 nucleotides past the stop codon (Grimson et al. 2007). Additionally, sites occurring near either end of the 3′-UTR have improved efficacy (Grimson et al. 2007). Finally, occurrence of 2 MREs in close proximity to each other can act synergistically, improving their efficacy (Grimson et al. 2007).

In an effort to aid in target prediction, several computational algorithms, including TargetScan, have been developed. TargetScan v7.0 predicts miRNA targets based on seed pairing and ranks them based on a context++ score to predict their efficiency. The context++ takes into account a total of 14 features which include 3′-UTR target-site abundance, predicted thermodynamic stability of seed pairing, identity of nucleotides at position 8 and 1, 3′ supplementary pairing, predicted structural accessibility, distance from the stop codon or polyadenylation site, lengths of the open reading frame (ORF) and 3′-UTR, and site conservation (Agarwal et al. 2015). Broadly conserved miRNAs have more conserved targets than miRNAs conserved only in mammals (Friedman et al. 2009). Importantly, this version of TargetScan ranks predictions by probability of preferential site conservation (P_{CT}) (Friedman et al. 2009, Agarwal et al. 2015).

1.G. The Role Of miRNAs In Nicotine Dependence

Neuronal miRNAs

Regulation of gene expression by miRNAs contributes to neuronal development and normal brain function (Im and Kenny 2012). Approximately 50% of all miRNAs are expressed in the mammalian brain (O'Carroll and Schaefer 2013). The brain's miRNAs are regulated temporally, with varying levels of expression throughout development (Krichevsky et al. 2003, Landgraf et al. 2007). miRNAs display brain region-specific expression profiles (Landgraf et al. 2007, Bak et al. 2008, He et al. 2012). The spatial patterns of miRNA expression in the central nervous system (CNS) contribute to its complex, heterogeneous cell-type composition. In addition to the brain region-specificity of miRNA expression, different neuronal subtypes also display distinct miRNA expression profiles (He et al. 2012). Finally, miRNAs are differentially expressed among intraneuronal compartments, and are enriched in the dendritic spines and axon terminals of the synapse (Lugli et al. 2008, Natera-Naranjo et al. 2010, O'Carroll and Schaefer 2013). Also, synaptic expression of miRNAs is regulated by neuronal activity (Eacker et al. 2011, Siegel et al. 2011, Pichardo-Casas et al. 2012). This spatial and activity-dependent regulation of miRNAs suggests that miRNAs contribute to the mechanisms underlying neuroadaptations at the synapse.

Dysregulation of miRNAs in the brain have been shown to contribute to neurodevelopmental and neuropsychiatric disorders, including drug addiction (Im and Kenny 2012). For example, miR-212 expression is up-regulated in the dorsal striatum of rats self-administering cocaine (Hollander et al. 2010). Interestingly, miR-212 expression in the striatum decreases sensitivity to the motivational properties of cocaine, suggesting a miRNA can influence vulnerability to cocaine addiction (Hollander et al. 2010). Other drugs of abuse such as amphetamine, opioids, and alcohol also induce changes in miRNA expression in various cell types (Zheng et al. 2010, Lewohl et al. 2011, Lippi et al. 2011, Balaraman et al. 2012, Im and Kenny 2012). There are several studies suggesting nicotine regulates miRNA expression, however, little is known about the role of miRNAs in the mechanisms underlying nicotine dependence and withdrawal.

Regulation of miRNAs by Nicotine

Nicotine and tobacco smoke has been shown to regulate miRNA expression, contributing to various disease processes associated with smoking. Various *in vitro* studies identify miRNAs that are regulated by nicotine. For example, in canine atrial fibroblasts, nicotine down-regulates miR-133 and miR-590 (Shan et al. 2009). The de-repression of their targets, transforming growth factors, contributes to a profibrotic state associated with tobacco abuse (Shan et al. 2009). Nicotine up-regulates miR-21 in an esophageal carcinoma cell line, EC9706, contributing to the dysregulation of the epithelial to mesenchymal

transition observed in tumorigenesis in humans with esophageal cancer (Zhang et al. 2014). Use of microarray found that miR-140* was increased in undifferentiated rat adrenal pheochromocytoma PC12 cells exposed to nicotine (Huang and Li 2009). *In vitro*, this miRNA down-regulates *dynamin 1* (*dnm1*), a regulator of synaptic endocytosis, suggesting a role for a miRNA in nicotine-induced synaptic plasticity (Huang and Li 2009).

In vivo, exposure to cigarette smoke alters the expression of miRNAs in the lungs of mice and rats (Izzotti et al. 2009, Izzotti et al. 2011). In humans, expression of 43 miRNAs were significantly up-regulated in the plasma of cigarette smokers as compared to non-smokers (Takahashi et al. 2013). Interestingly, they found that quitting smoking returned miRNA plasma expression to levels observed in non-smokers (Takahashi et al. 2013).

Limited studies have examined the regulation of miRNAs by nicotine in specific regions of the mammalian brain (Lippi et al. 2011, Hogan et al. 2014, Lee et al. 2015). Previously, we showed that the expression of miRNAs predicted to target MREs within the 3′-UTRs of nAChR transcripts was altered after chronic nicotine treatment in whole brain or a specific brain region (Hogan et al. 2014). For example, miR-542-3p was down-regulated in the VTA of mice chronically exposed to nicotine, while expression of the β2 nAChR subunit, a predicted target, was up-regulated (Hogan et al. 2014). When specifically considering the withdrawal circuitry, the expression of many miRNAs and mRNAs is altered in the medial habenula of mice self-administering nicotine (Lee et al. 2015).

However, the targets of these miRNAs and their functions in the context of nicotine dependence have not been confirmed. Currently, there remain no reports analyzing the differential expression of miRNAs and mRNAs during nicotine withdrawal in brain regions comprising the MHb-IPN axis using Next Generation sequencing.

1.H. Thesis Overview

The goal of this work is to understand regulation of the miRNA and mRNA transcriptome in the mesocorticolimbic and habenulo-interpeduncular circuits during nicotine dependence and its contribution to the affective symptoms of nicotine withdrawal. This thesis explores multiple stages of nicotine dependence, including chronic exposure and both acute and prolonged withdrawal states, using Next Generation sequencing. This dataset reveals differential expression of mRNA transcripts that reflect both alterations in the activity of the reward and withdrawal circuitry and possible mechanisms underlying the neuroadaptations associated with nicotine dependence. In addition, integrated miRNA/mRNA differential expression analysis identified a multitude of genes regulated by chronic nicotine treatment and acute nicotine withdrawal that were predicted targets of inversely regulated miRNAs.

The brain region-specific analysis of mRNA expression identified a plethora of differentially expressed genes during acute nicotine withdrawal. To

demonstrate the utility of these differential expression and target prediction analyses, I further explored the role of one of these genes in nicotine withdrawal-associated anxiety behavior. *Profilin 2* (*Pfn2*), a regulator of actin dynamics, was down-regulated in the IPN during acute nicotine withdrawal and its expression is repressed by an inversely regulated miRNA, miRNA-106b-5p. Further, I show that knockdown of *Pfn2* in the IPN of WT mice is sufficient to induce anxiety, mimicking behaviors observed in acute nicotine withdrawal.

This work serves as a strong example of the value of this large data set in the identification of novel roles for genes previously not considered in the mechanisms of nicotine dependence. This large dataset contributes to a greater understanding of the neuroadaptations underlying nicotine dependence, beyond the well-studied functional up-regulation of nAChRs. Identification of novel regulatory mechanisms is essential for the design of more efficacious smoking cessation strategies to combat the affective symptoms of withdrawal, such as anxiety.

Chapter 2

Integrated miRNA-/mRNA-Seq Analysis of the Mesocorticolimbic Reward Circuit During Chronic Nicotine Treatment and Withdrawal

Contributions:
Elevated plus maze and marble burying tests were performed by Rubing Zhao-Shea.
Bioinformatic analysis related to mapping, differential expression, and gene ontology was performed by Junko Tsuji.
Small RNA-Seq library synthesis protocol was courtesy of the Zamore Lab.
Paul Gardner assisted with experimental design.
I performed experimental design, library synthesis, sequencing, and data interpretation.

2.A. Introduction

Tobacco use is a prevalent health problem worldwide, with more than 900 million daily smokers (Peacock et al. 2018) and an estimated 6 million deaths due to tobacco-related illnesses annually (WHO 2012). The few pharmacological cessation aids currently available have limited efficacy (Jorenby et al. 2006, Cinciripini et al. 2013, Koegelenberg et al. 2014, Kotz et al. 2014), and without the intervention of new effective treatments, tobacco-related mortality is anticipated to rise to 8 million deaths per year (WHO 2012).

The addictive component of tobacco is nicotine, a tertiary alkaloid that is an agonist of nicotinic acetylcholine receptors (nAChRs), ligand-gated ion channels endogenously activated by acetylcholine (Albuquerque et al. 2009). nAChRs are enriched in the mesolimbic and habenulo-interpeduncular circuitries underlying nicotine reward and withdrawal, respectively (Dani and De Biasi 2013, Picciotto and Mineur 2014, Molas et al. 2017). Cessation of nicotine induces a withdrawal syndrome consisting of negative somatic, affective and cognitive symptoms. Affective symptoms primarily include depressed mood, irritability, craving and anxiety (Hughes 2007, Jackson et al. 2015). While the rewarding properties of nicotine dominate initial drug-taking, it is largely avoidance of affective withdrawal symptoms that promotes relapse and habitual use (Allen et al. 2008, Koob and Le Moal 2008).

The mesocorticolimbic reward pathway is composed mainly of DAergic neurons projecting from the VTA to the NAc and PFC (De Biasi and Dani 2011, Pistillo et al. 2015). The positive and motivational emotions associated with nicotine exposure result from activation of neurons in the VTA, inducing them to release increased levels of DA in the NAc (Schultz 1986, Tsai et al. 2009, Pignatelli and Bonci 2015). Exposure to nicotine induces neuroadaptations that alter the function of this circuit, influencing the sensitivity to the rewarding effects of nicotine and contributing to the emergence of a withdrawal syndrome during abstinence. For example, chronic nicotine exposure up-regulates and desensitizes nAChRs on the GABAergic interneurons within the VTA, disinhibiting the activity of DAergic projections to the NAc (Mansvelder et al. 2002, van Zessen et al. 2012). However, when nicotine is withdrawn activity of these GABAergic neurons is amplified by endogenous cholinergic signaling, inhibiting DA output from the VTA (Pistillo et al. 2015). It is thought that this alteration of signaling within the reward circuit contributes to induction of withdrawal symptoms. The VTA may further contribute to the development of withdrawal by direct stimulation of the IPN, a prominent withdrawal and anxiety center, via corticotrophin releasing factor (CRF) signaling (Zhao-Shea et al. 2015).

While much is known about the neurocircuitry responsible for nicotine reward and withdrawal-associated behaviors, the molecular mechanisms underlying the induction of these behavioral alterations are less clear. Chronic drug exposure induces stable neuroadaptations underlying the compulsion for

continued use and susceptibility to relapse. These long-lasting changes in the function of the addicted brain are thought to require alterations of gene expression through regulation of transcription factors, epigenetic mechanisms, and non-coding RNAs (Robison and Nestler 2011, Madsen et al. 2012).

microRNAs (miRNAs) are non-coding RNA molecules ~22 nucleotides in length that repress the expression of mRNA targets by promoting mRNA decay or translational repression (Bartel 2018). miRNAs recognize their targets through imperfect base-pairing of the seed region (nucleotides 2-7) with miRNA response elements (MREs) within the 3′-untranslated regions (UTRs) of mRNAs (Lewis et al. 2003, Bartel 2009). Tobacco smoke and nicotine have been shown to regulate the expression of miRNAs in various cell lines, organisms, and tissues (Izzotti et al. 2009, Shan et al. 2009, Izzotti et al. 2011, Takahashi et al. 2013, Hogan et al. 2014, Zhang et al. 2014).

Dysregulation of miRNAs in the brain have been shown to contribute to neurodevelopmental and neuropsychiatric disorders, including drug addiction (Hollander et al. 2010, Im and Kenny 2012). However, little is known about the role of miRNAs in the mechanisms underlying nicotine dependence and withdrawal. Few studies have examined the regulation of miRNAs by nicotine in specific regions of the mammalian brain (Lippi et al. 2011, Hogan et al. 2014, Lee et al. 2015). Previously, we showed that the expression of miRNAs predicted to target MREs within the 3′-UTRs of nAChRs was altered after chronic nicotine treatment in whole brain or a specific brain region (Hogan et al. 2014). Nicotine

has been reported to regulate miRNAs and mRNAs in the MHb, with microarrays detecting expression changes in mice self-administering nicotine (Lee et al. 2015). However, the targets of these miRNAs and their functions in the context of nicotine dependence have not been elucidated.

Using integrated miRNA- and mRNA-Seq, we asked whether there are changes in miRNA and mRNA expression in the NAc and VTA during chronic nicotine treatment and acute withdrawal. We conclude that these sequencing datasets represent a valuable resource, aiding the identification of a plethora of miRNAs/mRNAs playing a role(s) in the molecular mechanisms underlying the neuroadaptations of nicotine dependence.

2.B. Materials and Methods

Animals and Drug Treatment

All experiments were conducted in accordance with the guidelines for care and use of laboratory animals provided by the National Research Council as well as with an approved animal protocol (Protocol A-1788, PI: Andrew Tapper) from the Institutional Animal Care and Use Committee of the University of Massachusetts Medical School (UMMS). Wild-type (WT) male C57BL/6J mice (The Jackson Laboratory) were group-housed in a 12-h light/dark cycle (lights

ON at 7 A.M.) with food and water provided *ad libitum*. At 6 weeks of age, mice were treated with nicotine tartrate (200 µg/ml nicotine base) or equivalent tartaric acid in their drinking water with saccharine (3 g/L) to make the solutions more palatable. After 6 weeks, mice in the withdrawal groups were spontaneously withdrawn from nicotine by replacement of their nicotine bottles with tartaric acid solution. After a 48-hour or 4-week withdrawal period, mice were tested in behavioral assays or sacrificed for tissue collection.

Behavioral Assays

All behavioral testing was performed during the light phase in dim white light after habituation to the testing room (≥ 30 min). On the first test day, mice underwent the marble burying test (MBT) followed by the elevated plus maze (EPM).

MBT. For 2 days prior to testing, mice were habituated to individual standard mouse cages, filled 5-6 cm with bedding material, for approximately 1 hour per day. On the test day, 15 sterilized 1.5-cm diameter glass marbles were placed in the cages, equally spaced in a 3 x 5 grid arrangement. Mice were placed in the test cage for 30 min. then returned to their home cage. The number of marbles buried at least 75% with bedding were counted by an experimenter blinded to the treatment groups.

EPM. Testing was performed on a sanitized, black Plexiglas apparatus consisting of 2 open (30 x 5 x 0.25 cm) and 2 closed arms with high walls (30 x 5

x 15 cm), arranged in a perpendicular arrangement, 45 cm above the floor. Mice were placed individually in the junction (5 x 5 cm) facing the open arms and allowed to freely explore the maze for 5 min. Time spent in each arm and the number of arm entries was recorded by MED-PC IV software (MED Associates, Inc.).

Tissue Collection and RNA Isolation

Fresh frozen brains were sliced ~1 mm thick and brain regions were dissected using a circular tissue punch. The NAc and midbrain (enriched in VTA) were dissected by bilateral 1 mm diameter and 0.75 mm diameter circular tissue punches, respectively. Punches were expelled into lysis buffer (miRVana miRNA isolation kit, Ambion, AM1560). Punches from 4 brains were combined for each sample intended for sequencing experiments. Unless otherwise stated, total RNA was isolated using the miRVana kit according to manufacturer's instructions. Total RNA concentration and A260/280 were assessed using a NanoDrop2000 (ThermoFisher Scientific).

Small RNA Sequencing and Analysis

Total RNA (approximately 2-9 µg, A260/280 > 1.8) was separated on a 15% polyacrylamide, 7M urea, 1X TBE gel. Small RNA (18-30 nucleotides) was excised and eluted from the gel. Libraries were synthesized using a modified protocol for Illumina TruSeq Small RNA Cloning (April 2014,

www.zamorelab.umassmed.edu/protocols/). Small RNA was ligated to 3' and 5' adapters and cDNA was reverse transcribed by AMV Reverse Transcriptase (NEB, M0277S). The cDNA libraries were amplified by Accuprime *Pfx* DNA Polymerase (Invitrogen, 12344-024) for 18 PCR cycles using a common primer and a primer containing a 6-nucleotide barcoding index. The libraries were gel-purified on a 2.5% Low-Range Ultra Agarose (BioRad, 1613106) 1X TBE gel and eluted using a QIAquick Gel Extraction kit (Qiagen, 28704). Library sizes and quality were assessed by Fragment Analyzer (Advanced Analytical, AATI). Library concentrations were determined using KAPA Library Quantification Kits (KAPA Biosystems).

Table 2.1. Oligo sequences for miRNA-Seq library synthesis

Oligo	**Sequence (5'-3')**
3' Adapter	rApp/nnntggaattctcgggtgccaagg/ddC/
5' Adapter	guucagaguucuacaguccgacgauc
RT primer	ccttggcacccgagaattcca
PCR forward primer	aatgatacggcgaccaccgagatctacacgttcagagttctacagtccga
PCR index primers (Barcode)	
Index Primer 1	caagcagaagacggcatacgagatcgtgatgtgactggagttccttggcacccgagaattcca
Index Primer 2	caagcagaagacggcatacgagatacatcggtgactggagttccttggcacccgagaattcca
Index Primer 3	caagcagaagacggcatacgagatgcctaagtgactggagttccttggcacccgagaattcca
Index Primer 4	caagcagaagacggcatacgagattggtcagtgactggagttccttggcacccgagaattcca
Index Primer 5	caagcagaagacggcatacgagatcactgtgtgactggagttccttggcacccgagaattcca
Index Primer 6	caagcagaagacggcatacgagatattggcgtgactggagttccttggcacccgagaattcca
Index Primer 7	caagcagaagacggcatacgagatgatctggtgactggagttccttggcacccgagaattcca
Index Primer 8	caagcagaagacggcatacgagattcaagtgtgactggagttccttggcacccgagaattcca
Index Primer 9	caagcagaagacggcatacgagatctgatcgtgactggagttccttggcacccgagaattcca
Index Primer 10	caagcagaagacggcatacgagataagctagtgactggagttccttggcacccgagaattcca
Index Primer 11	caagcagaagacggcatacgagatgtagccgtgactggagttccttggcacccgagaattcca
Index Primer 12	caagcagaagacggcatacgagattacaaggtgactggagttccttggcacccgagaattcca
Index Primer 14	caagcagaagacggcatacgagatggaactgtgactggagttccttggcacccgagaattcca
Index Primer 15	caagcagaagacggcatacgagattgacatgtgactggagttccttggcacccgagaattcca
Index Primer 16	caagcagaagacggcatacgagatggacggtgactggagttccttggcacccgagaattcca

Libraries were pooled and single-end (75 cycles) sequencing was performed on a NextSeq500 (Illumina) in the RNA Therapeutics Institute (RTI) at the UMMS. Reads passing a quality filter of 80% Q30 were used for analysis. The 3'-adapter sequence was removed using Cutadapt (version 1.11) with '–overlap' option 7 bp. Reads between 15-27 nucleotides long were mapped to the UCSC mouse reference genome (mm10) using Bowtie (version 1.1.2) allowing for no mismatches. miRNA reads ±5 nucleotides from the mature, annotated 5' start position were counted. Reads mapping to multiple locations on a single mature miRNA were recorded as a single count, and reads mapped to multiple mature miRNAs were apportioned by the number of the aligned mature miRNAs. Samples with greater than 1 million mappable reads were used in differential expression (DE) analysis. Samples were normalized using RUV-Seq (Risso et al. 2014), removing 3-4 factors of variance. DE was analyzed using DESeq2 (Love et al. 2014). In each condition, miRNAs with 0 reads per million (RPM) in more than half the samples were omitted.

mRNA Sequencing and Analysis

RNA > 30 nucleotides long was eluted from the same 15% polyacrylamide, 7M urea, 1X TBE gel as the small RNA. Approximately 0.5-1.5 µg of RNA were used to synthesize sequencing libraries using the TruSeq Stranded mRNA Library Prep kit (Illumina, RS-122-2101/2) according to manufacturer's instructions. Libraries were gel-purified on 2% Low-Range Ultra Agarose 1X TBE

gels and eluted using a QIAquick Gel Extraction kit. As in miRNA library synthesis, mRNA library sizes and quality were assessed by Fragment Analyzer and library concentrations were determined using KAPA Library Quantification Kits.

Paired-end (76 cycles x 2) sequencing was performed on a NextSeq500 in the RTI at the UMMS. Reads were mapped to the UCSC mouse reference genome (mm10) using STAR (version 2.5.3a) and the mapped reads were quantified with RSEM (version 1.3.0). RNA-seq libraries with > 30 million mappable reads were used in DE analysis. (Table S2) Samples were normalized using RUV-Seq (version 1.8.0) (Risso et al. 2014) removing unwanted variables including batch effects. DE analysis was performed using DESeq2 (version 1.14.1) (Love et al. 2014). In each condition, mRNAs with 0 transcripts per million (TPM) in more than half the samples were omitted. Genome Ontology (GO) term enrichment for biological processes, molecular function, and cellular component was performed on the DE mRNAs using GOseq (version 1.28.0) (Young et al. 2010). REVIGO was used to reduce GO terms by combining and removing closely related terms (Supek et al. 2011). To provide a well-balanced representation of reduced GO terms, a *simRel* cutoff of 0.4 was used (Schlicker et al. 2006).

Target Prediction Analysis

TargetScan Mouse 7.1 (http://www.targetscan.org/mmu_71/) was used to identify differentially expressed miRNAs that are predicted to target sites within the 3′-UTR of inversely differentially expressed mRNAs. Analysis was limited to miRNAs conserved in vertebrates and mammals, differentially expressed with an FDR < 0.01. Only mRNAs with an FDR < 0.01 and fold change > 2, were considered for target prediction.

2.C. Results

Acute nicotine withdrawal induces anxiety.

To assess the validity of our drug treatment paradigm, anxiety was measured using the MBT and EPM. Mice were treated with nicotine (Nic) or tartaric acid (TA) control solutions in their drinking water for 6 weeks. To induce spontaneous nicotine withdrawal, nicotine solution bottles were replaced with TA for 48 hours prior to measurement of anxiety behaviors (Figure 2.1A). Mice in acute nicotine withdrawal (NAWD) buried significantly more marbles than TA controls, indicating increased anxiety (Figure 2.1B). Further indicating an anxious phenotype, NAWD mice also spent significantly less time in the open arm of the EPM (Figure 2.1C). Importantly, there was no significant difference in the number

of total arm entries, indicating there was no effect of acute nicotine withdrawal on locomotor activity confounding these results (Figure 2.1D).

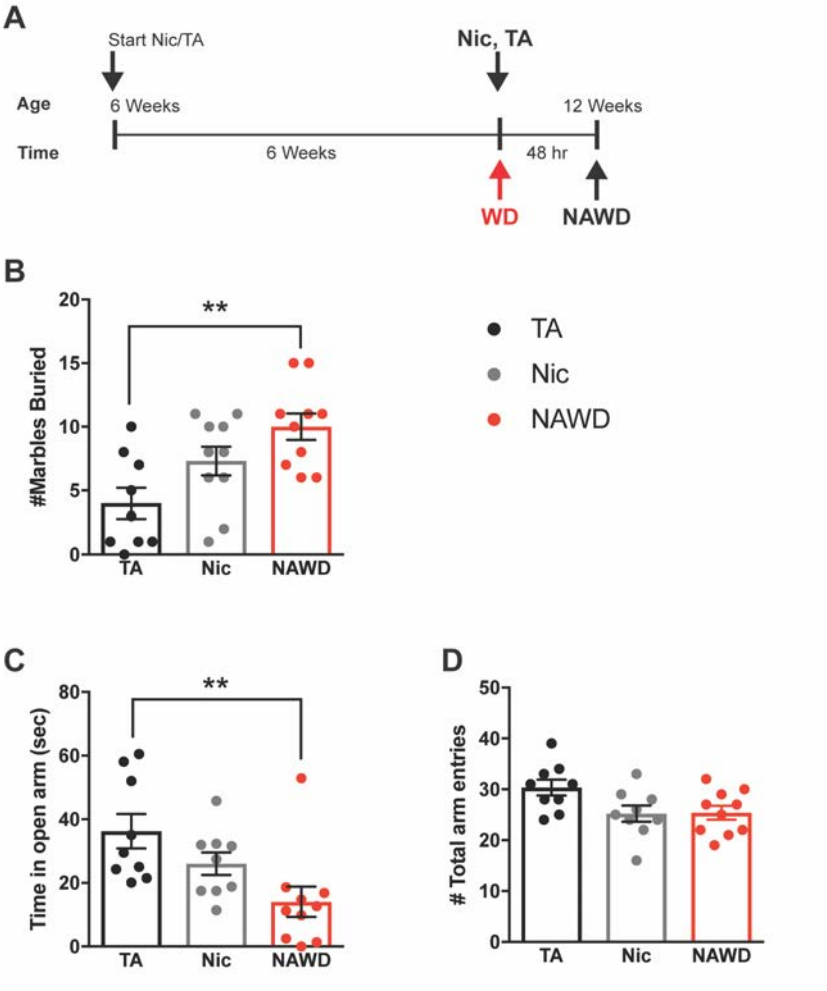

Figure 2.1. NAWD-treated mice display increased anxiety. Anxiety was assayed by the MBT and EPM to compare mice treated with nicotine (Nic, open bars) or acute nicotine withdrawal (NAWD, gray bars) to TA controls (filled bars). (A) Schematic of nicotine and acute (48-hr) withdrawal treatment. (B) The number of marbles buried in 30 min. Statistical analysis by one-way ANOVA ($F_{2,26}$ = 6.974, P = 0.0038) with the Bonferroni's multiple comparison post-test found there are significantly more marbles buried only by NAWD mice compared to TA controls. (**) P < 0.01, n = 9-10. (C) Time spent in open arms of the elevated plus maze in 5 min as described in the Methods and Materials. Statistical analysis by one-way ANOVA ($F_{2,25}$ = 5.77, P = 0.0087) with Bonferroni's post-test found only NAWD spend significantly less time in the open arm compared to TA controls. (**) P < 0.01, n = 9-10. (D) The number of total arm entries in the elevated plus maze in 5 min. Statistical analysis by one-way ANOVA (F2,25 = 3.672, P = 0.04) with Bonferroni's multiple comparisons post-test found there was no significant effect on locomotor activity between any group.

Differential expression of miRNAs in the NAc and midbrain during chronic nicotine treatment and acute withdrawal.

To assess the regulation of miRNAs and mRNAs by chronic nicotine treatment and acute withdrawal in the mesocorticolimbic reward circuitry, we sequenced and performed differential expression analysis of RNAs isolated from the NAc and midbrain.

Mice treated chronically with nicotine display limited significant (FDR < 0.01) changes in miRNA expression in both the NAc and the midbrain, compared to nicotine-naïve mice. In the NAc, expression of only 12 total miRNAs was significantly altered in Nic mice compared to TA controls, 11 being up-regulated (Figures 2.2A and 2.3). Chronic nicotine treatment induces modest changes in miRNA expression, with fold changes no more than ~1.5. None of these miRNAs are similarly differentially expressed when NAWD mice are compared to TA controls, suggesting all of these miRNAs return to baseline expression levels after an acute 48-hour withdrawal.

In the midbrain, there are only 3 miRNAs significantly differentially expressed in Nic mice compared to TA controls, all of them up-regulated (Figures 2.2C and 2.4). As in the NAc, the limited Nic-induced changes in miRNA expression level are modest, not exceeding an increase of 30%. Two of these miRNAs, miR-129-1-3p and miR-129-2-3p, are members of the same family. As in the NAc, none of the miRNAs altered by nicotine exposure are similarly altered

when NAWD mice are compared to TA controls, suggesting their expression levels return to baseline within 48 hours after nicotine treatment is ceased.

After a short, 48-hr withdrawal from nicotine, there are only 2 miRNAs significantly down-regulated in the NAc when comparing NAWD mice to TA controls (Figures 2.2E and 2.3). As indicated above, neither of these miRNAs was significantly differentially expressed in Nic mice, indicating that their down-regulation is not an effect of the initial nicotine treatment itself. Additionally, both of these miRNAs, miR-5121 and miR-3473b, are similarly down-regulated when NAWD mice are compared to either TA- or Nic-treated mice (Figure 2.2I), further suggesting that altered expression is solely an effect of nicotine withdrawal.

In contrast to the limited regulation of miRNAs in the NAc, acute nicotine withdrawal evoked differential expression of 59 miRNAs in the midbrain (FDR < 0.01). Thirty-eight miRNAs are up-regulated and 21 miRNAs are down-regulated when NAWD mice are compared to TA controls (Figures 2.2G and 2.4). As in the NAc, none of these miRNAs were significantly differentially expressed in Nic mice, indicating that their differential expression is not a consequence of the initial nicotine treatment itself. Further, a subset of 18 miRNAs in the midbrain are significantly and similarly up- or down-regulated when NAWD mice are compared to either the TA- or Nic-treated group (Figure 2.2K), suggesting that their differential expression is an effect solely of withdrawal and chronic nicotine treatment itself does not induce their regulation.

The identity of the miRNAs regulated by nicotine treatment and withdrawal in the NAc and midbrain were compared. Interestingly, no miRNAs were similarly differentially expressed in both the NAc and the midbrain of Nic or NAWD mice compared to nicotine-naïve controls.

Differential expression of mRNAs in the NAc and midbrain during chronic nicotine treatment and acute withdrawal.

Chronic nicotine treatment induces widespread changes in mRNA expression in the both the NAc and midbrain. To focus on mRNAs that are robustly differentially expressed, only mRNAs that are up- or down-regulated with a fold change of at least 2 are discussed. In the NAc, there are a total of 852 genes significantly differentially expressed (FDR < 0.01) with fold changes > 2 in Nic compared to TA mice (Figures 2.2B and 2.5). The majority of these genes are repressed by nicotine, with 648 down-regulated and 204 up-regulated. Of these genes only 25 are similarly differentially expressed in NAWD mice compared to TA controls (Figure 2.7A), indicating the majority of transcriptional changes return to control levels 48 hours after nicotine treatment has ceased.

In the midbrain, there are a total of 547 genes significantly differentially expressed with a fold change > 2 in Nic compared to TA mice (Figures 2.2D and 2.6). In contrast to the NAc, the expression of the majority of these genes is enhanced, with 520 up-regulated and 27 down-regulated. Of these genes, 505

remain similarly differentially expressed 48 hours after nicotine is withdrawn, comparing NAWD to TA mice (Figure 2.7B).

In the NAc, there are relatively few mRNAs regulated during acute nicotine withdrawal. There are only 32 total mRNAs significantly differentially expressed with a fold change > 2 when NAWD mice are compared to TA controls (Figure 2.2F). However, as stated above, 25 (~78%) of these were regulated in a similar manner after nicotine treatment alone. Additionally, if nicotine withdrawal were the sole stimulus for a transcriptional change, it would follow that the expression of that mRNA should be similarly altered when NAWD are compared to TA or nicotine-treated mice. There are no mRNAs that are similarly altered when NAWD are compared to either TA or Nic mice (Figures 2.2J and 2.7A). This would suggest that the initial chronic nicotine treatment itself is largely responsible for the limited transcriptional changes observed in the NAc during acute nicotine withdrawal.

The midbrain, unlike the NAc, displays widespread transcriptional changes during acute nicotine withdrawal. When NAWD mice are compared to TA controls, there are a total of 1674 mRNAs significantly differentially expressed with a fold change > 2 in the midbrain (Figure 2.2H). The vast majority of genes were up-regulated, with only 144 exhibiting down-regulation during acute withdrawal. As previously discussed, 505 of these genes were differentially expressed after nicotine treatment alone (Figure 2.7B). Furthermore, only 30 of these genes are similarly differentially expressed when NAWD mice are

compared to TA or Nic mice (Figures 2.2L and 2.7B). All together, this suggests that the initial chronic nicotine treatment itself induces the majority of the mRNA regulation observed in the midbrain during acute nicotine withdrawal.

The identity of mRNAs regulated by nicotine treatment and withdrawal were compared between the NAc and midbrain. There is only a single mRNA similarly regulated by chronic nicotine treatment in these brain regions. *Histidine decarboxylase* (*Hdc*) was up-regulated in both the NAc and the midbrain of Nic mice compared to TA controls. However, the expression of many mRNAs was oppositely regulated in Nic mice. There were 110 mRNAs that were repressed in the NAc and up-regulated in the midbrain after chronic nicotine treatment. Only one mRNA*, Kelch like family member 4 (Klhl4)*, was oppositely regulated, being up-regulated in the NAc and down-regulated in the midbrain. During acute withdrawal, there is only one mRNA, *Gm1821*, similarly down-regulated in both the NAc and midbrain. Additionally, a limited number of mRNAs are oppositely regulated during acute withdrawal, with 16 being repressed in the NAc and up-regulated in the midbrain in NAWD mice compared to TA controls.

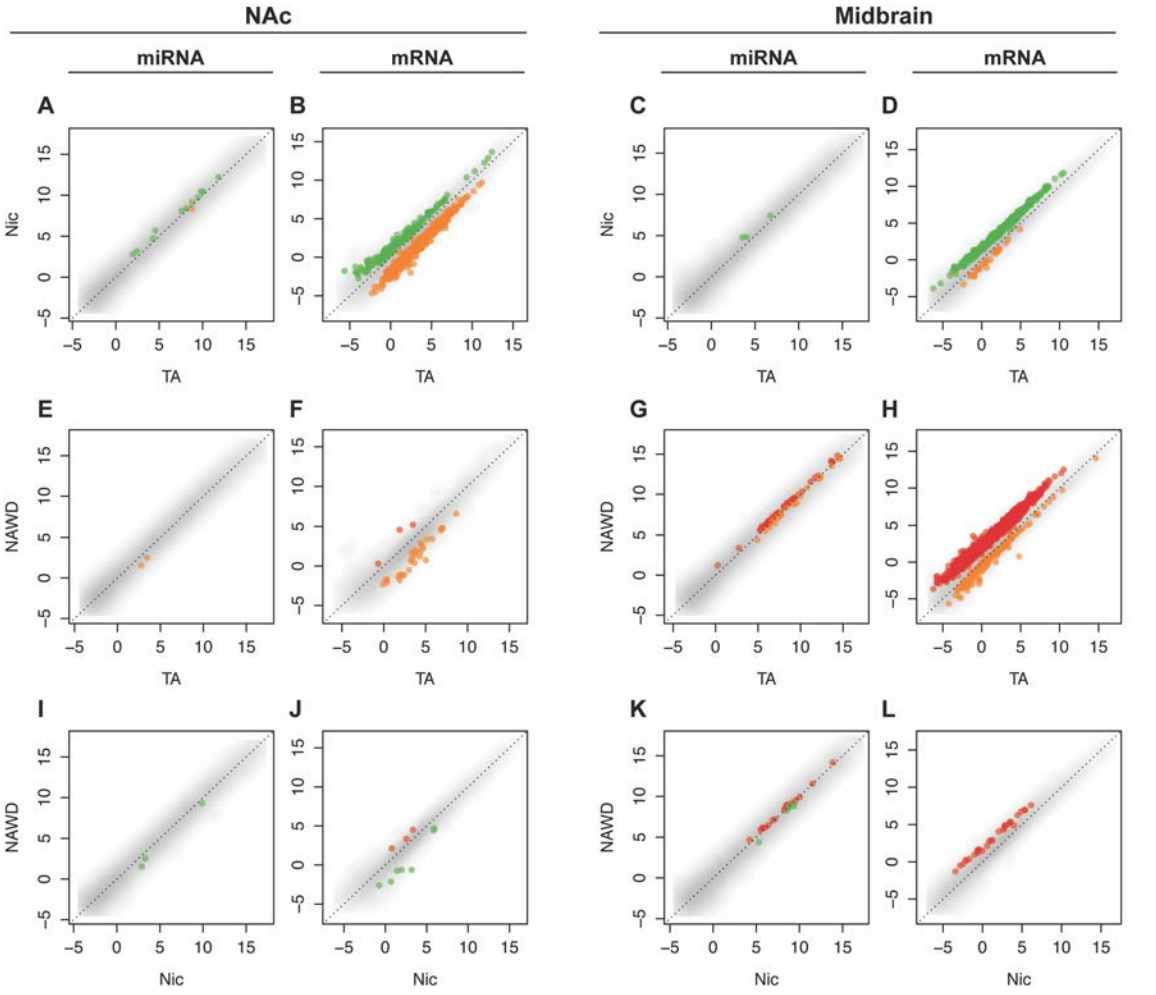

Figure 2.2. Differential expression of miRNAs/mRNAs within the NAc and midbrain during nicotine treatment and acute withdrawal. Scatter plots display differential expression of miRNAs or mRNAs in the NAc (A-B, E-F, I-J) and midbrain (C-D, G-H, K-L) measured by deep sequencing. RNAs isolated from tissue punches of nicotine-treated (Nic, A-D) and acute withdrawal (NAWD, E-H) mice are compared to TA-treated controls. NAWD mice were also compared to Nic mice (I-L). Each dot represents an individual miRNA or mRNA plotted as $\log_2$(RPM) or $\log_2$(TPM), respectively. All miRNAs with a FDR < 0.01 and mRNAs with FDR < 0.01 and FC > 2 are highlighted in color. Orange dots are up-regulated in TA, green dots are up-regulated in Nic, and red dots are up-regulated in NAWD in each comparison. Only miRNAs with RPM > 0 and mRNAs with TPM > 0 in at least half of the replicates in each treatment group are shown. n = 4-5, with each library synthesized using pooled RNA from 4 mice.

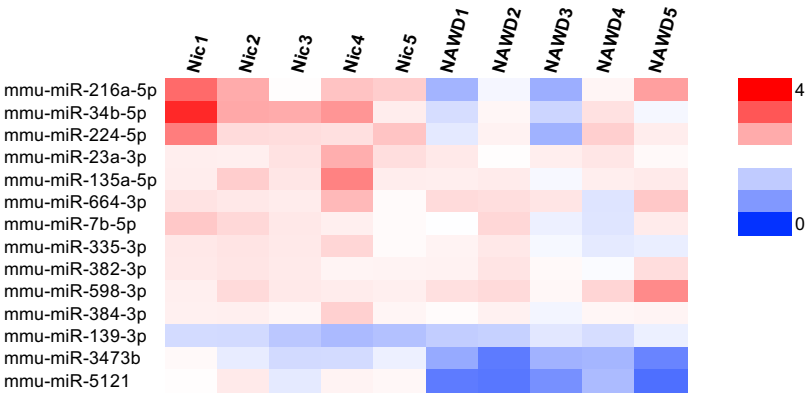

Figure 2.3. Relative expression heatmap of miRNAs altered in the NAc during nicotine treatment and withdrawal. Heat map displaying miRNAs that are significantly differentially expressed in the NAc during chronic nicotine treatment or withdrawal compared to TA controls (left). Each column represents an individual biological replicate of mice treated chronically with nicotine (Nic) or acute nicotine withdrawal (NAWD). Each replicate contained RNA pooled from 4 mice. The colors represent fold change, calculated as read per million (RPM) normalized to the average RPM of the TA control group. Red represents up-regulation and blue represents down-regulation.

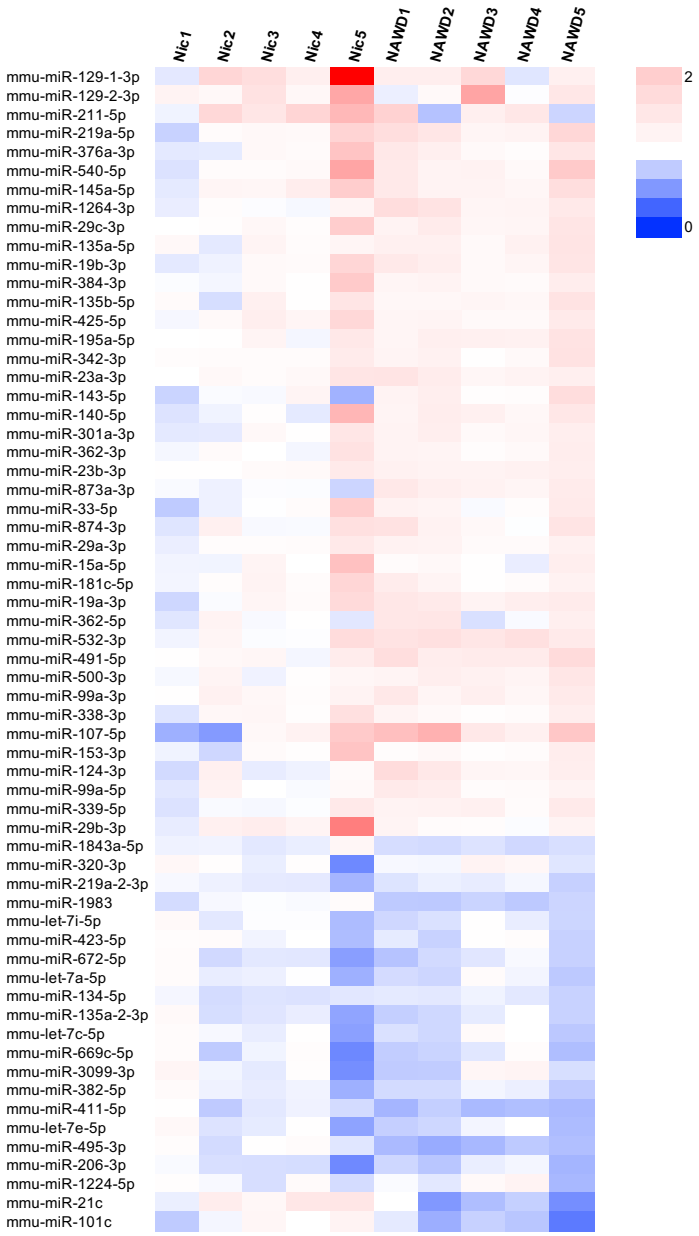

Figure 2.4. Relative expression heatmap of miRNAs altered in the midbrain during nicotine treatment and withdrawal. Heat map displaying miRNAs that are significantly differentially expressed in midbrain punches enriched for the VTA during chronic nicotine treatment or withdrawal compared to TA controls (left). Each column represents an individual biological replicate of mice treated chronically with nicotine (Nic) or acute nicotine withdrawal (NAWD). Each replicate contained RNA pooled from 4 mice. The colors represent fold change, calculated as read per million (RPM) normalized to the average RPM of the TA control group. Red represents up-regulation and blue represents down-regulation.

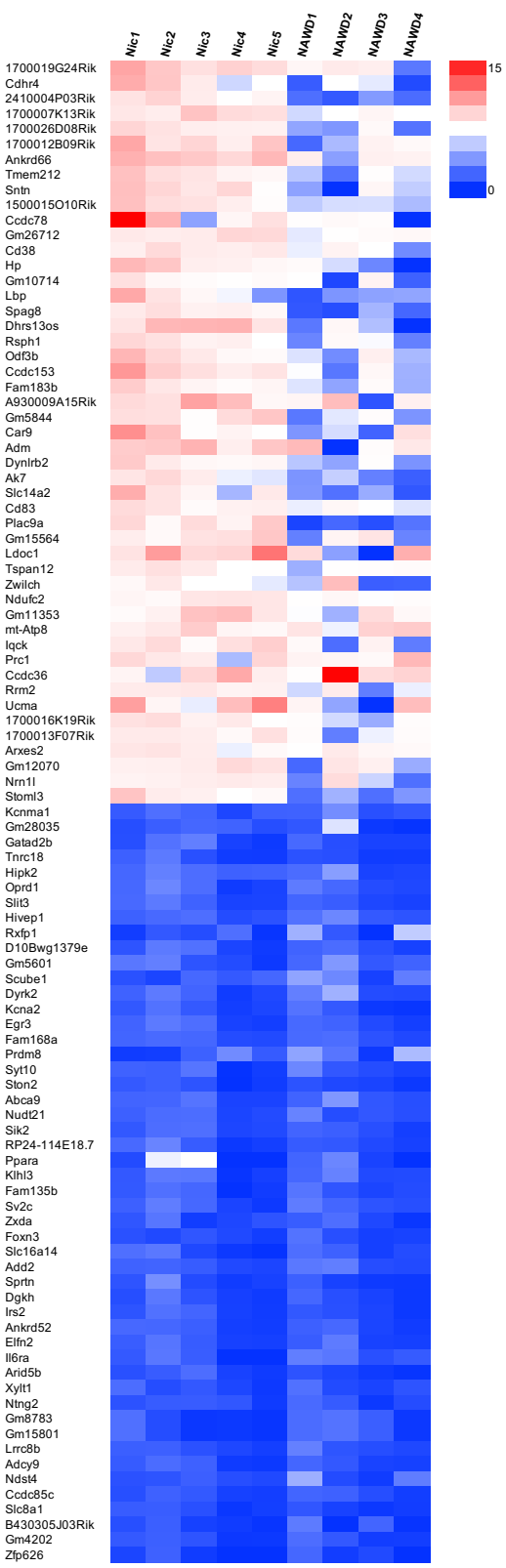

Figure 2.5. Relative expression heatmap of mRNAs altered in the NAc during chronic nicotine treatment. Heat map displaying the 50 most up-regulated and 50 most down-regulated mRNAs in the NAc during chronic nicotine treatment relative to TA controls (left). Each column represents an individual biological replicate of mice treated chronically with nicotine (Nic) or acute nicotine withdrawal (NAWD). Each replicate contained RNA pooled from 4 mice. The colors represent fold change, calculated as transcript per million (TPM) normalized to the average TPM of the TA control group. Red represents up-regulation and blue represents down-regulation. Only mRNAs with TPM > 0 in more than half of the replicates were included.

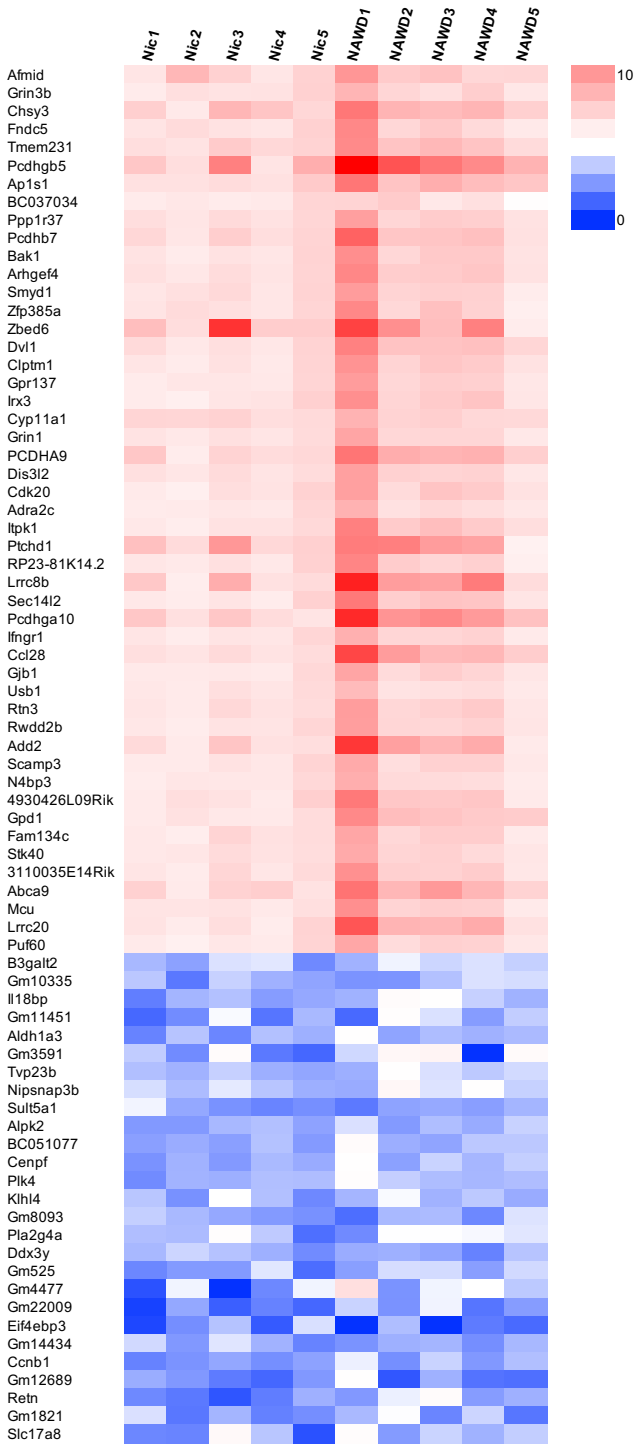

Figure 2.6. Relative expression heatmap of mRNAs altered in the midbrain during chronic nicotine treatment. Heat map displaying the 50 most up-regulated and all significantly down-regulated mRNAs in midbrain punches enriched for VTA during chronic nicotine treatment relative to TA controls (left). Each column represents an individual biological replicate of mice treated chronically with nicotine (Nic) or acute nicotine withdrawal (NAWD). Each replicate contained RNA pooled from 4 mice. The colors represent fold change, calculated as transcript per million (TPM) normalized to the average TPM of the TA control group. Red represents up-regulation and blue represents down-regulation. Only mRNAs with TPM > 0 in more than half of the replicates were included.

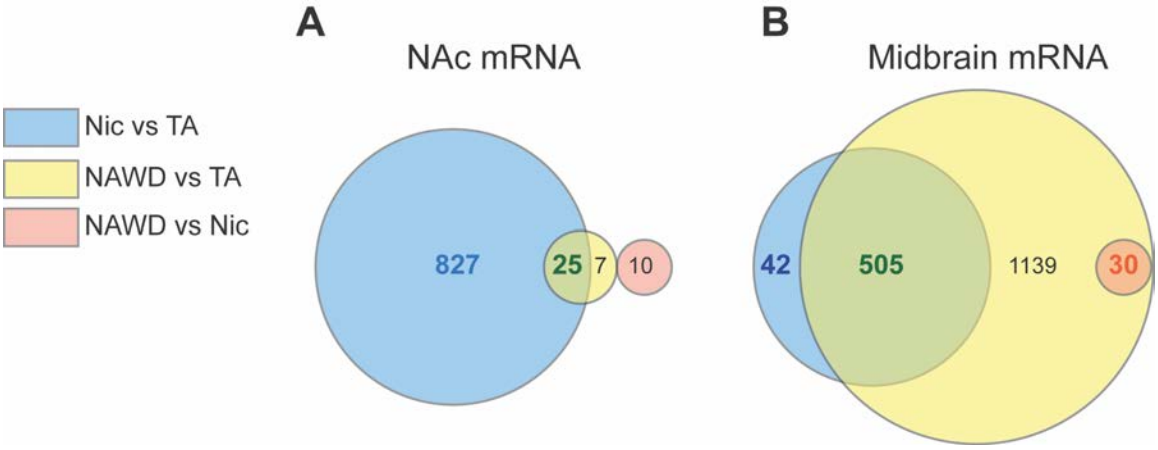

Figure 2.7. Overlap of similarly differentially expressed mRNAs between treatment conditions in the NAc and midbrain. Venn diagrams showing numbers of differentially expressed mRNAs (FDR < 0.01, FC > 2) in the NAc (A) and midbrain (B) in each treatment condition, designated by color. Regions where the circles overlap indicate that the transcripts are similarly up- or down-regulated in both conditions. Numbers indicate the number of mRNAs represented.

Nicotine withdrawal-associated anxiety persists for at least 4 weeks.

To test the hypothesis that nicotine withdrawal-associated anxiety is persistent over a prolonged period of time, mice were treated with chronic nicotine in their drinking water for 6 weeks then withdrawn for 4 weeks. After 4 weeks of abstinence, anxiety was assayed by the MBT and EPM comparing long withdrawal (NLWD) mice to age matched controls (TAL) (Figure 2.8A).

There is a trend (P = 0.0984) for NLWD mice to bury more marbles than TAL controls, but the MBT does not indicate a significant effect of prolonged nicotine withdrawal on anxiety (Figure 2.8B). However, NLWD mice spend significantly less time in the open arms of the EPM compared to TAL mice, indicating NLWD mice are more anxious (Figure 2.8C). There is no effect of long nicotine withdrawal on the total number of arm entries, suggesting there is no confounding effect of long withdrawal on the locomotor activity (Figure 2.8D).

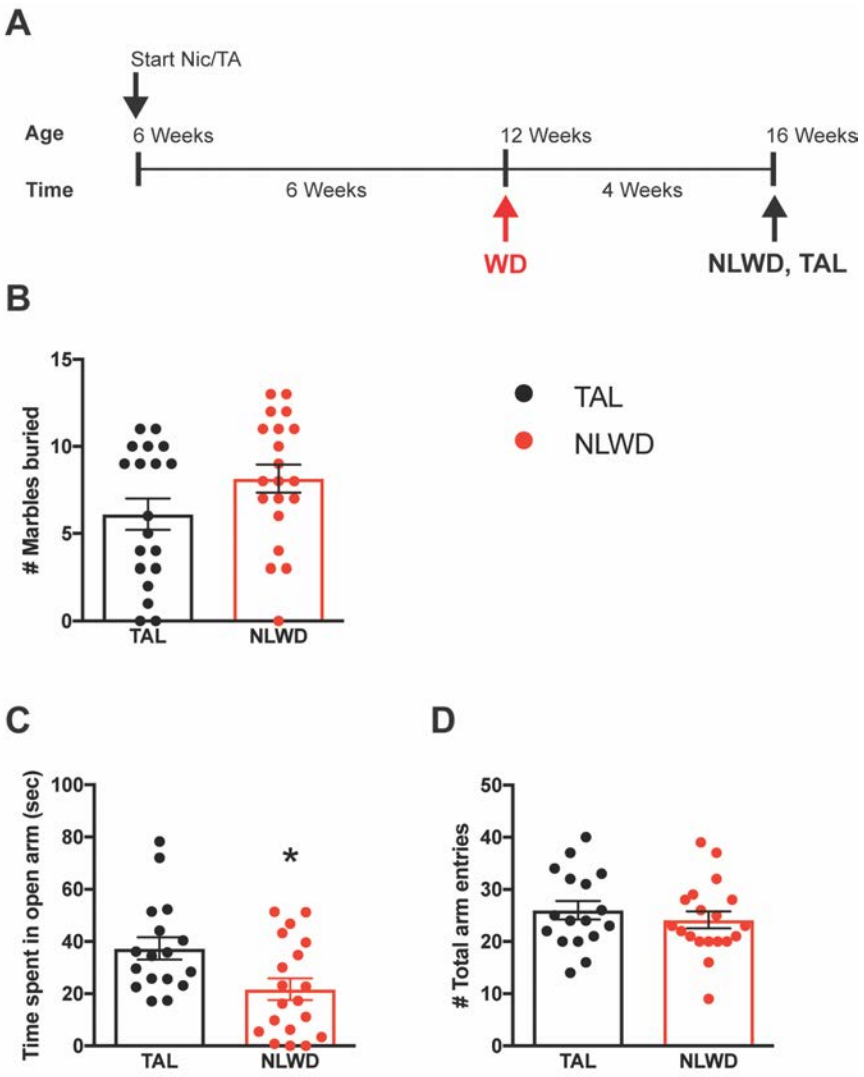

Figure 2.8. Withdrawal-associated anxiety persists for at least 4 weeks. Anxiety was assayed by the MBT and EPM to compare mice after a long (4-week) withdrawal from nicotine treatment (NLWD, empty bars) to age-matched, TA controls (TAL, filled bars). (A) Schematic of NLWD treatment and age-matched TAL controls. (B) The number of marbles buried in 30 min. Statistical analysis by unpaired, two-tailed *t*-test (t_{37} = 1.695, P = 0.0984) found the there is no significant effect of long nicotine withdrawal on the number of marbles buried, n = 19-20. (C) Time spent in open arms of the EPM in 5 min. Statistical analysis by unpaired, two-tailed *t*-test (t_{34} = 2.602, P = 0.0136) determined NLWD spent significantly less time in the open arm compared to controls. (*) P < 0.05, n = 17-19. (D) The number of total arm entries in the EPM in 5 min. Statistical analysis by unpaired, two-tailed *t*-test (t_{34} = 0.7664, P = 0.4487) found there was no significant effect on locomotor activity. n = 17-19.

Differential expression of miRNA/mRNAs in the NAc and VTA after prolonged nicotine withdrawal.

In the NAc, there are a limited number of miRNAs significantly differentially expressed after a prolonged nicotine withdrawal compared to age-matched controls. Only 16 miRNAs were significantly differentially expressed in NLWD mice compared to TAL controls, with 10 up-regulated and 6 down-regulated (Figure 2.9A). These miRNAs displayed only small alterations in expression, with no changes in relative expression exceeding 30%. Additionally, none of these were similarly regulated at the acute withdrawal time point, comparing NAWD to TA controls. Strikingly, there are no miRNAs significantly altered after a prolonged withdrawal in the midbrain (Figure 2.9C).

There are 40 mRNAs differentially expressed with fold changes > 2 in the NAc of NLWD mice compared to TAL controls, with 14 up-regulated and 26 down-regulated (Figure 2.9B). In the midbrain, there is only a single mRNA, Gm9531, that is significantly down-regulated (Figure 2.9D). In either region, none of the transcripts altered after a long withdrawal are similarly differentially expressed during acute withdrawal.

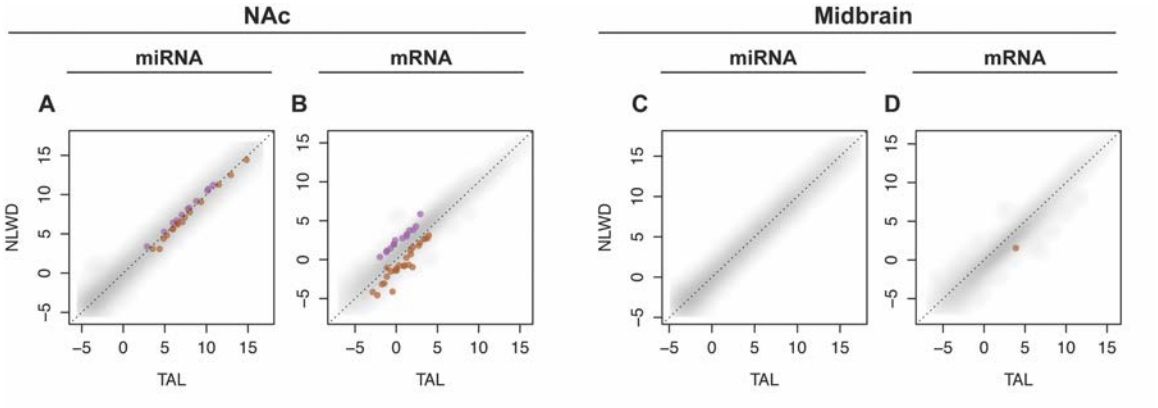

Figure 2.9. Differential expression of miRNAs and mRNAs in the NAc and midbrain of NLWD- and TAL-treated mice. Scatter plots display differential expression of miRNAs or mRNAs in the NAc (A, B) and VTA (C, D) measured by deep sequencing. miRNAs (A, C) and mRNAs (B, D) isolated from mice after a long (4-week) withdrawal from nicotine (NLWD) are compared to age-matched TA-treated controls (TAL). Each dot represents an individual miRNA or mRNA plotted as $\log_2$(RPM) and $\log_2$(TPM), respectively. miRNAs (FDR < 0.01) and mRNAs (FDR < 0.01, FC >2) that are up-regulated (purple) and down-regulated (brown) in NLWD mice are highlighted. All miRNAs have RPM > 0 and all mRNAs have TPM > 0 in more than half of the replicates in each treatment group. n = 5, with each library synthesized using pooled RNA from 4 mice.

Gene ontology (GO) analysis of differentially expressed mRNAs in the NAc and midbrain

Gene ontology (GO) analysis was performed on differentially expressed mRNAs for all treatment groups in the NAc and midbrain. Comprehensive heat maps display all of the reduced GO terms with significant enrichment for up- and down-regulated genes in each brain region (Figures 2.11-2.16). To describe differential expression in the NAc and midbrain after chronic nicotine treatment, I have highlighted selected GO terms describing cellular compartments (CC, Figure 2.10A), molecular functions (MF, Figure 2.10B), and biological processes (BP, Figure 2.10C) that were significantly enriched for up- or down-regulated genes.

GO analysis of genes differentially expressed in the NAc after chronic nicotine treatment determined there was significant enrichment of terms related to neuronal structures and functions. In the CC analysis, there was significant enrichment of up-regulated genes related to the vesicle and myelin sheath and down-regulated genes related to the neuron, neuron projections, and the synapse. MF analysis determined there was significant enrichment of down-regulated genes related to ion channel binding, glutamate receptor binding, and α-adrenergic receptor activity. BP analysis revealed there was significant over-representation of down-regulated genes related to GO terms including regulation of synapse structure or activity, cell projection organization, cell communication, and regulation of neurotransmitter levels. The NAc of Nic mice also exhibited an

overrepresentation of up-regulated genes related to the mitochondria/energetics and the ribosome.

In general, the midbrain exhibited GO enrichment pattern opposite to the NAc after chronic nicotine treatment. Specifically, while GO terms related to the neuron were enriched in down-regulated genes in the NAc, the midbrain shows an overrepresentation of up-regulated genes in CC, MF, and BP terms related to the neuron, neuron projection, synapses, receptor binding. There is also an enrichment of down-regulated genes related to mitochondria, metabolism, and the ribosome in the midbrain of Nic mice.

GO analysis also determined there was an opposite enrichment pattern of additional MF terms related to binding in the NAc and midbrain during chronic nicotine treatment. For instance, there is an overrepresentation of genes involved in the binding of chromatin, proteins, kinases, transcription factors, and cytoskeleton proteins that are down-regulated in the NAc and up-regulated in the midbrain.

Finally, in the NAc and the midbrain there is an enrichment of both up- and down-regulated genes related to heterocyclic compound binding and metabolism during chronic nicotine treatment.

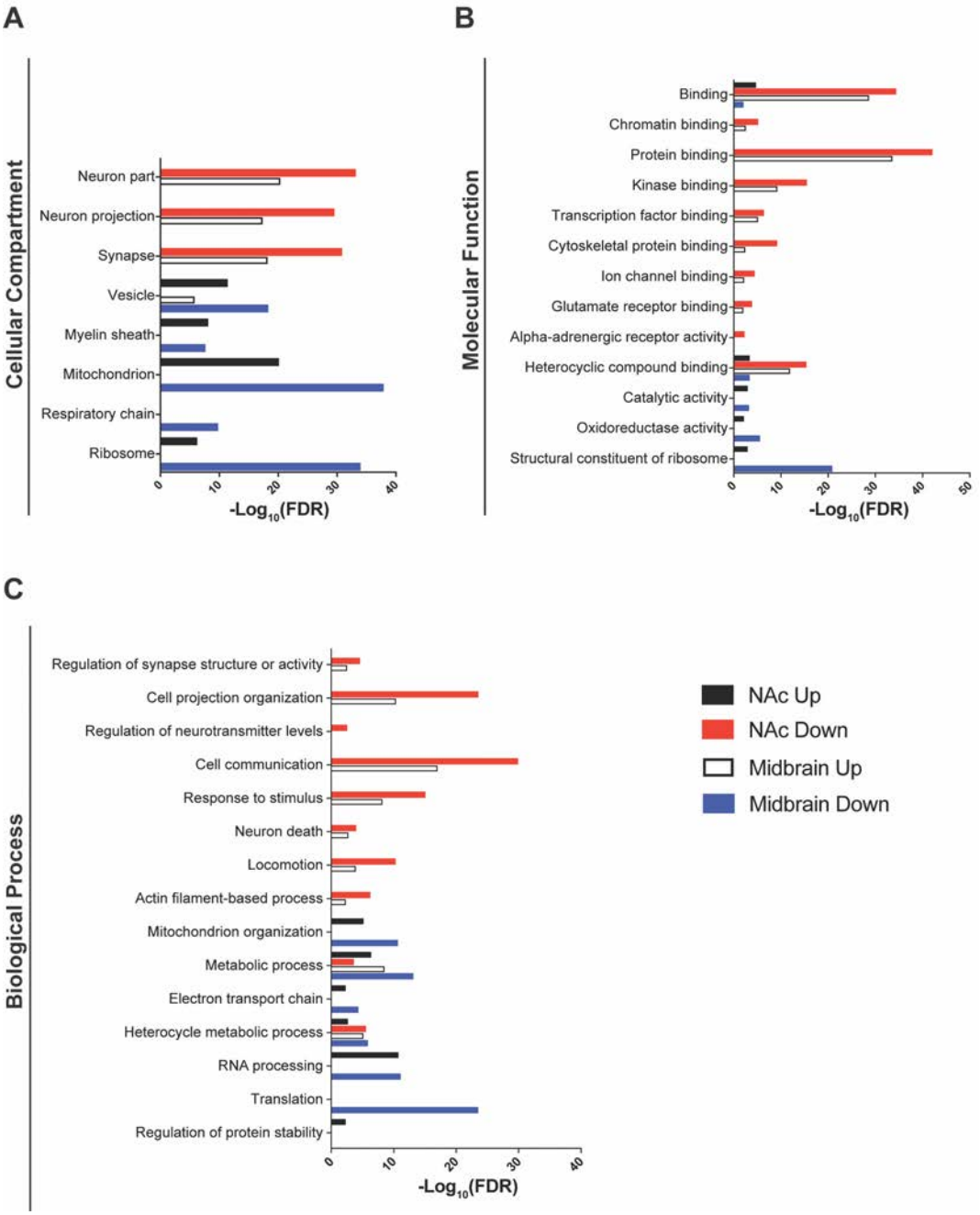

Figure 2.10. Genes differentially expressed in the NAc and midbrain during chronic nicotine treatment are overrepresented in gene ontology terms related to the synaptic transmission, neuronal morphology, energetics, and translation. The vertical axes define the selected GO terms describing the cellular compartment (A), molecular function (B), or biological process (C). The horizontal axis plots the significance of enrichment of the GO term, plotted as $-Log_{10}(FDR)$.

Because there are so few genes differentially expressed during acute nicotine withdrawal in the NAc, there was no significant enrichment of any GO terms in CC, MF, or BP analysis. In the midbrain, analysis of CC, MF, and BP GO terms exhibit an enrichment pattern that largely overlaps with that observed in the midbrain after chronic nicotine treatment alone (Figures 2.11-2.16).

After a prolonged withdrawal, NLWD mice display an enrichment of up-regulated genes related neuronal GO terms in the NAc. This includes CC terms describing the neuron part, neuron projection, synapse, and vesicles. Significantly enriched BP terms include cell communication, cell projection communication and neuron development. There was no significant enrichment of down-regulated genes in any GO term.

Figure 2.11. Enrichment of cellular compartments with genes up-regulated in the NAc and midbrain. Heat map of the significance of enrichment of reduced GO terms describing the cellular compartment with up-regulated mRNAs

in the NAc and midbrain punches enriched in VTA. Each column is designated a specific brain region and treatment comparison (bottom). Each row is designated a GO term (right) reduced with a sim_{Rel} cut off of 0.4 as described in the Methods and Materials. The number of terms combined within the single GO term, *rf*, is indicated by the green color gradient (left). The color gradient of the box (red) indicates the significance of enrichment as $-\log_{10}(\text{FDR})$.

Figure 2.12. Enrichment of molecular functions with genes up-regulated in the NAc and midbrain. Heat map of the significance of enrichment of reduced GO terms describing the cellular compartment with up-regulated mRNAs in the NAc and midbrain punches enriched in VTA. Each column is designated a specific brain region and treatment comparison (bottom). Each row is designated a GO term (right) reduced with a sim_{Rel} cut off of 0.4 as described in the Methods and Materials. The number of terms combined within the single GO term, *rf*, is indicated by the green color gradient (left). The color gradient of the box (red) indicates the significance of enrichment as $-\log_{10}$(FDR).

Figure 2.13. Enrichment of biological processes with genes up-regulated in the NAc and midbrain. Heat map of the significance of enrichment of reduced

GO terms describing the cellular compartment with up-regulated mRNAs in the NAc and midbrain punches enriched in VTA. Each column is designated a specific brain region and treatment comparison (bottom). Each row is designated a GO term (right) reduced with a sim_{Rel} cut off of 0.4 as described in the Methods and Materials. The number of terms combined within the single GO term, *rf*, is indicated by the green color gradient (left). The color gradient of the box (red) indicates the significance of enrichment as $-Log_{10}$(FDR).

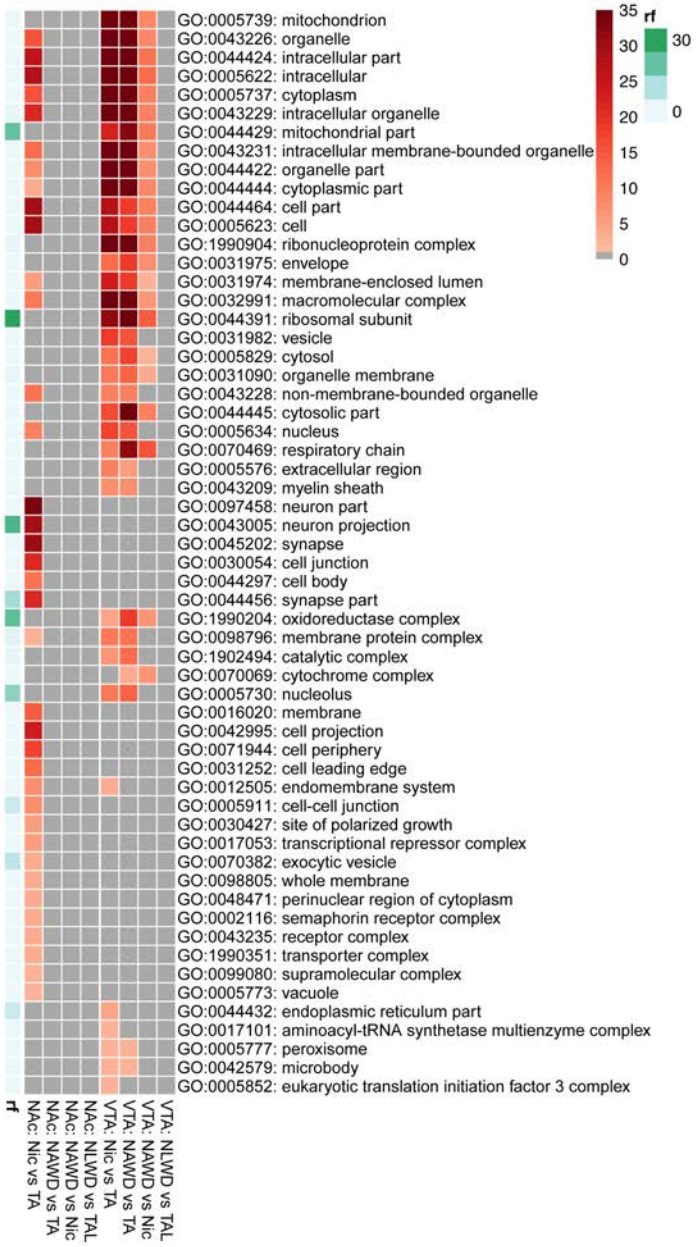

Figure 2.14. Enrichment of cellular compartments with genes down-regulated in the NAc and midbrain. Heat map of the significance of enrichment of reduced GO terms describing the cellular compartment with down-regulated mRNAs in the NAc and midbrain. Each column is designated a specific brain region and treatment comparison (bottom). Each row is designated a GO term (right) reduced with a sim_{Rel} cut off of 0.4 as described in the Methods and Materials. The number of terms combined within the single GO term, *rf*, is indicated by the green color gradient (left). The color gradient of the box (red) indicates the significance of enrichment as $-Log_{10}$(FDR).

Figure 2.15. Enrichment of molecular functions with genes down-regulated in the NAc and midbrain. Heat map of the significance of enrichment of reduced GO terms describing the cellular compartment with down-regulated mRNAs in the NAc and midbrain punches enriched in VTA. Each column is designated a specific brain region and treatment comparison (bottom). Each row is designated a GO term (right) reduced with a sim_{Rel} cut off of 0.4 as described in the Methods and Materials. The number of terms combined within the single GO term, *rf*, is indicated by the green color gradient (left). The color gradient of the box (red) indicates the significance of enrichment as $-Log_{10}$(FDR).

Figure 2.16. Enrichment of biological processes with genes down-regulated in the NAc and midbrain. Heat map of the significance of enrichment of

reduced GO terms describing the cellular compartment with down-regulated mRNAs in the NAc and midbrain punches enriched in VTA. Each column is designated a specific brain region and treatment comparison (bottom). Each row is designated a GO term (right) reduced with a sim_{Rel} cut off of 0.4 as described in the Methods and Materials. The number of terms combined within the single GO term, *rf*, is indicated by the green color gradient (left). The color gradient of the box (red) indicates the significance of enrichment as $-\log_{10}$(FDR).

Target prediction of miRNAs differentially expressed in the NAc

Because miRNAs are traditionally considered to be repressors of gene expression, Targetscan Mouse 7.1 was used to predict MREs within the 3′-UTR of differentially expressed mRNAs for inversely regulated miRNAs. Due to the fact that conservation of MREs increases the likelihood of biological function, only miRNAs and MREs conserved in vertebrates or mammals were considered in target prediction analysis.

In the NAc, miRNAs that are differentially expressed during chronic nicotine treatment are predicted to target reciprocally expressed mRNAs. Of the miRNAs regulated by chronic nicotine treatment in the NAc, only 8 are conserved, all of which were up-regulated. Targetscan Mouse 7.1 determined that each of these 8 miRNAs targeted at least one of 204 down-regulated mRNAs at conserved MREs (Table 2.2). Of these 204 predicted mRNA targets, 81 contain multiple MREs for a single or different miRNAs. Additionally, only 10 of these predicted targets remain differentially expressed during acute nicotine withdrawal (Table 2.2, green).

None of the three miRNAs regulated in the NAc of NAWD compared to TA or Nic mice were conserved in vertebrates or mammals. Because there were no conserved miRNAs that were differentially expressed during acute nicotine withdrawal, target prediction analysis was not performed.

All 16 miRNAs that were differentially expressed in the NAc of NLWD mice compared to TAL controls are conserved in vertebrates and mammals. However,

only one, miR-22-3p, was predicted to target a single conserved MRE within the 3′-UTR of an anti-correlated gene, *Synaptotagmin like 4* (*Sytl4*) (Table 2.3).

Table 2.2. Target prediction of miRNAs differentially expressed in the NAc after chronic nicotine exposure (Nic) compared to TA controls. mRNAs similarly differentially expressed in NAWD compared to TA mice are highlighted in green.

mRNA	mRNA FC	mRNA FDR	miRNA	miRNA FC	miRNA FDR	Seed Type	Position in 3′-UTR
Slc8a1	0.203	4.55E-15	miR-34b-5p	1.465	3.47E-03	7mer-m8	14840-14846
			miR-23a-3p	1.382	6.75E-06	7mer-m8	14104-14110
			miR-135a-5p	1.366	1.06E-03	8mer	12878-12885
			miR-135a-5p	1.366	1.06E-03	7mer-A1	14659-14665
			miR-384-3p	1.203	9.74E-03	7mer-A1	10334-10340
Adcy9	0.237	1.28E-11	miR-7b-5p	1.304	6.75E-03	8mer	804-811
			miR-7b-5p	1.304	6.75E-03	8mer	1731-1738
Xylt1	0.250	4.28E-09	miR-34b-5p	1.465	3.47E-03	7mer-m8	488-494
			miR-224-5p	1.437	3.04E-03	7mer-m8	5031-5037
Arid5b	0.250	1.11E-09	miR-135a-5p	1.366	1.06E-03	7mer-m8	1890-1898
Il6ra	0.255	9.50E-07	miR-23a-3p	1.382	6.75E-06	8mer	543-550
			miR-382-3p	1.260	6.66E-04	7mer-m8	548-554
Elfn2	0.255	3.34E-12	miR-7b-5p	1.304	6.75E-03	8mer	815-822
Ankrd52	0.256	2.20E-11	miR-216a-5p	1.485	2.10E-03	7mer-m8	2254-2260
			miR-34b-5p	1.465	3.47E-03	8mer	2936-2943
			miR-23a-3p	1.382	6.75E-06	7mer-m8	1983-1989
Irs2	0.256	9.31E-11	miR-135a-5p	1.366	1.06E-03	7mer-A1	2288-2294
			miR-7b-5p	1.304	6.75E-03	7mer-m8	1478-1484
			miR-7b-5p	1.304	6.75E-03	8mer	2170-2177
Dgkh	0.260	1.95E-09	miR-135a-5p	1.366	1.06E-03	7mer-m8	246-252
Add2	0.270	9.69E-14	miR-34b-5p	1.465	3.47E-03	7mer-m8	252-258
			miR-23a-3p	1.382	6.75E-06	8mer	3421-3428
			miR-7b-5p	1.304	6.75E-03	7mer-m8	5178-5184
Foxn3	0.272	6.52E-10	miR-34b-5p	1.465	3.47E-03	7mer-A1	5886-5892
			miR-135a-5p	1.366	1.06E-03	8mer	236-243
			miR-135a-5p	1.366	1.06E-03	8mer	798-805
			miR-7b-5p	1.304	6.75E-03	8mer	6142-6149
			miR-384-3p	1.203	9.74E-03	8mer	1845-1852
Fam135b	0.284	1.30E-06	miR-224-5p	1.437	3.04E-03	8mer	618-625
			miR-384-3p	1.203	9.74E-03	7mer-A1	1059-1065
			miR-384-3p	1.203	9.74E-03	8mer	1074-1081
Fam168a	0.299	2.19E-10	miR-7b-5p	1.304	6.75E-03	8mer	5368-5375
Egr3	0.299	1.30E-09	miR-216a-5p	1.485	2.10E-03	8mer	1342-1349
			miR-23a-3p	1.382	6.75E-06	7mer-m8	2007-2013
			miR-23a-3p	1.382	6.75E-06	7mer-A1	2280-2286
			miR-7b-5p	1.304	6.75E-03	8mer	711-718
			miR-382-3p	1.260	6.66E-04	8mer	2328-2335
Kcna2	0.300	4.42E-07	miR-34b-5p	1.465	3.47E-03	7mer-m8	9136-9142
			miR-224-5p	1.437	3.04E-03	7mer-m8	131-137
Dyrk2	0.302	3.18E-10	miR-23a-3p	1.382	6.75E-06	7mer-A1	3713-3719
D10Bwg1379e	0.308	1.27E-07	miR-135a-5p	1.366	1.06E-03	7mer-A1	7367-7373
Hivep1	0.312	1.71E-10	miR-382-3p	1.260	6.66E-04	8mer	3430-3437
Hipk2	0.313	2.48E-09	miR-23a-3p	1.382	6.75E-06	8mer	7721-7728
Tnrc18	0.314	1.09E-08	miR-224-5p	1.437	3.04E-03	7mer-m8	512-518
Gatad2b	0.314	2.90E-07	miR-216a-5p	1.485	2.10E-03	8mer	2375-2382
			miR-34b-5p	1.465	3.47E-03	7mer-m8	3859-3865
			miR-7b-5p	1.304	6.75E-03	7mer-A1	2193-2199
Kcnma1	0.315	1.14E-09	miR-224-5p	1.437	3.04E-03	7mer-m8	206-212
			miR-382-3p	1.260	6.66E-04	7mer-m8	550-556
Kif3b	0.326	2.62E-10	miR-135a-5p	1.366	1.06E-03	8mer	2900-2907
Ppargc1b	0.330	1.40E-10	miR-34b-5p	1.465	3.47E-03	8mer	291-298
			miR-135a-5p	1.366	1.06E-03	8mer	4787-4794
Glg1	0.333	1.57E-12	miR-216a-5p	1.485	2.10E-03	7mer-m8	4508-4514
			miR-7b-5p	1.304	6.75E-03	7mer-m8	1617-1623
			miR-7b-5p	1.304	6.75E-03	7mer-m8	1837-1843

Bcl9l	0.336	1.70E-08	miR-23a-3p	1.382	6.75E-06	7mer-A1	2001-2007
			miR-135a-5p	1.366	1.06E-03	8mer	1328-1335
Lcor	0.344	6.84E-05	miR-224-5p	1.437	3.04E-03	7mer-m8	6991-6997
			miR-384-3p	1.203	9.74E-03	8mer	6632-6639
Atp8b2	0.350	2.14E-09	miR-224-5p	1.437	3.04E-03	7mer-m8	481-487
Lemd3	0.350	3.93E-11	miR-23a-3p	1.382	6.75E-06	8mer	360-367
			miR-7b-5p	1.304	6.75E-03	7mer-m8	60-66
Shank1	0.354	1.39E-09	miR-135a-5p	1.366	1.06E-03	7mer-A1	319-325
			miR-7b-5p	1.304	6.75E-03	8mer	2547-2554
Pxdn	0.357	4.80E-09	miR-23a-3p	1.382	6.75E-06	8mer	646-653
Nrg1	0.359	3.78E-06	miR-135a-5p	1.366	1.06E-03	8mer	4253-4260
Ankrd50	0.361	5.69E-09	miR-23a-3p	1.382	6.75E-06	8mer	1644-1651
Slfn5	0.361	4.42E-04	miR-135a-5p	1.366	1.06E-03	8mer	2678-2685
Plce1	0.368	3.20E-09	miR-382-3p	1.260	6.66E-04	7mer-m8	873-879
Slc6a17	0.368	1.50E-09	miR-34b-5p	1.465	3.47E-03	7mer-m8	1001-1007
Adam23	0.368	4.60E-10	miR-23a-3p	1.382	6.75E-06	8mer	1260-1267
Dio2	0.369	3.31E-07	miR-382-3p	1.260	6.66E-04	8mer	4557-4564
G3bp2	0.371	6.08E-09	miR-23a-3p	1.382	6.75E-06	7mer-m8	78-84
			miR-23a-3p	1.382	6.75E-06	7mer-A1	110-116
			miR-7b-5p	1.304	6.75E-03	8mer	1796-1803
Kcnb1	0.372	6.08E-09	miR-23a-3p	1.382	6.75E-06	8mer	2246-2253
			miR-135a-5p	1.366	1.06E-03	7mer-A1	2406-2412
			miR-135a-5p	1.366	1.06E-03	7mer-m8	7998-8004
			miR-135a-5p	1.366	1.06E-03	7mer-A1	8047-8053
			miR-7b-5p	1.304	6.75E-03	7mer-m8	1451-1457
			miR-7b-5p	1.304	6.75E-03	7mer-m8	1689-1695
Fndc3a	0.372	1.77E-09	miR-34b-5p	1.465	3.47E-03	7mer-A1	1332-1338
Slitrk5	0.373	2.28E-09	miR-216a-5p	1.485	2.10E-03	7mer-A1	408-414
			miR-224-5p	1.437	3.04E-03	7mer-m8	276-282
Hecw2	0.375	2.98E-09	miR-34b-5p	1.465	3.47E-03	7mer-A1	237-243
Shc3	0.375	7.03E-08	miR-224-5p	1.437	3.04E-03	7mer-A1	7481-7487
			miR-384-3p	1.203	9.74E-03	8mer	4484-4491
Dusp8	0.376	5.31E-08	miR-135a-5p	1.366	1.06E-03	8mer	500-507
Elmsan1	0.376	9.13E-08	miR-34b-5p	1.465	3.47E-03	7mer-m8	2952-2958
Kcnq5	0.377	1.46E-08	miR-224-5p	1.437	3.04E-03	8mer	572-579
			miR-135a-5p	1.366	1.06E-03	7mer-A1	37-43
			miR-135a-5p	1.366	1.06E-03	7mer-m8	2812-2818
			miR-384-3p	1.203	9.74E-03	8mer	1110-1117
Ddx17	0.378	3.60E-07	miR-34b-5p	1.465	3.47E-03	8mer	145-152
Zcchc14	0.379	1.78E-09	miR-135a-5p	1.366	1.06E-03	7mer-m8	38-44
Frrs1l	0.382	4.75E-09	miR-216a-5p	1.485	2.10E-03	8mer	5517-5524
Hcn4	0.382	1.28E-03	miR-7b-5p	1.304	6.75E-03	7mer-A1	2335-2341
Setd1b	0.383	3.11E-08	miR-23a-3p	1.382	6.75E-06	8mer	437-444
Fam120a	0.384	7.67E-11	miR-7b-5p	1.304	6.75E-03	7mer-A1	861-867
Taf4a	0.387	2.04E-07	miR-135a-5p	1.366	1.06E-03	8mer	265-272
Slmap	0.387	2.03E-09	miR-216a-5p	1.485	2.10E-03	7mer-m8	227-233
			miR-224-5p	1.437	3.04E-03	7mer-m8	621-627
			miR-224-5p	1.437	3.04E-03	7mer-A1	928-934
			miR-23a-3p	1.382	6.75E-06	7mer-m8	618-624
Zdhhc23	0.388	6.18E-05	miR-34b-5p	1.465	3.04E-03	8mer	3056-3063
			miR-135a-5p	1.366	1.06E-03	7mer-A1	3285-3291
Cdh4	0.388	4.06E-09	miR-34b-5p	1.465	3.47E-03	8mer	2316-2323
Slc9a1	0.389	1.11E-07	miR-23a-3p	1.382	6.75E-06	7mer-m8	1356-1362
Wipf1	0.389	1.78E-09	miR-382-3p	1.260	6.66E-04	8mer	2786-2793
Ndst1	0.390	4.94E-10	miR-34b-5p	1.465	3.47E-03	8mer	701-708
			miR-34b-5p	1.465	3.47E-03	7mer-A1	1614-1620
			miR-34b-5p	1.465	3.47E-03	7mer-m8	1798-1804
			miR-23a-3p	1.382	6.75E-06	8mer	1552-1559
Cdkl1	0.391	2.29E-06	miR-135a-5p	1.366	1.06E-03	8mer	3019-3026
Kcnc3	0.392	3.04E-06	miR-135a-5p	1.366	1.06E-03	7mer-A1	261-267
Myrip	0.392	2.99E-08	miR-34b-5p	1.465	3.47E-03	7mer-m8	29-35
Fndc3b	0.392	3.71E-08	miR-34b-5p	1.465	3.47E-03	7mer-A1	3011-3017
			miR-384-3p	1.203	9.74E-03	7mer-m8	164-170
Dhcr24	0.392	2.28E-11	miR-7b-5p	1.304	6.75E-03	8mer	1917-1924

Col4a1	0.394	1.21E-10	miR-23a-3p	1.382	6.75E-06	8mer	792-799
Sptbn2	0.395	4.10E-10	miR-34b-5p	1.465	3.47E-03	7mer-A1	45-51
Pcdh1	0.395	7.72E-10	miR-34b-5p	1.465	3.47E-03	7mer-m8	1916-1922
			miR-7b-5p	1.304	6.75E-03	7mer-m8	2981-2987
			miR-382-3p	1.260	6.66E-04	7mer-m8	1054-1060
Dido1	0.396	1.48E-08	miR-224-5p	1.437	3.04E-03	8mer	2668-2675
Cacul1	0.396	3.32E-08	miR-23a-3p	1.382	6.75E-06	7mer-m8	3395-3401
Cdk13	0.398	3.56E-08	miR-23a-3p	1.382	6.75E-06	7mer-m8	2686-2692
Zc3h12c	0.401	1.52E-07	miR-23a-3p	1.382	6.75E-06	7mer-A1	121-127
Ambra1	0.401	1.34E-07	miR-23a-3p	1.382	6.75E-06	7mer-m8	902-908
			miR-7b-5p	1.304	6.75E-03	8mer	342-349
Sik1	0.403	5.26E-08	miR-23a-3p	1.382	6.75E-06	7mer-A1	95-101
Gucy1a2	0.403	3.55E-04	miR-135a-5p	1.366	1.06E-03	7mer-m8	5092-5098
Syngap1	0.403	1.08E-07	miR-384-3p	1.203	9.74E-03	8mer	901-908
Otud7a	0.403	8.43E-11	miR-34b-5p	1.465	3.47E-03	7mer-m8	605-611
			miR-7b-5p	1.304	6.75E-03	7mer-A1	346-352
			miR-384-3p	1.203	9.74E-03	7mer-A1	159-165
Shank3	0.403	1.06E-07	miR-34b-5p	1.465	3.47E-03	8mer	540-547
			miR-7b-5p	1.304	6.75E-03	8mer	520-527
Tex2	0.404	6.04E-09	miR-135a-5p	1.366	1.06E-03	7mer-A1	580-586
Satb1	0.405	2.14E-09	miR-34b-5p	1.465	3.47E-03	7mer-m8	554-560
			miR-23a-3p	1.382	6.75E-06	8mer	655-662
			miR-23a-3p	1.382	6.75E-06	8mer	992-999
			miR-23a-3p	1.382	6.75E-06	7mer-A1	1263-1269
			miR-7b-5p	1.304	6.75E-03	7mer-m8	1021-1027
Vti1a	0.408	1.71E-07	miR-7b-5p	1.304	6.75E-03	8mer	3584-3591
Jph1	0.411	9.13E-09	miR-23a-3p	1.382	6.75E-06	7mer-m8	122-128
Fam168b	0.411	1.52E-09	miR-7b-5p	1.304	6.75E-03	8mer	3955-3962
			miR-382-3p	1.260	6.66E-04	7mer-A1	241-247
Ccdc171	0.413	8.48E-04	miR-23a-3p	1.382	6.75E-06	7mer-m8	562-568
			miR-135a-5p	1.366	1.06E-03	7mer-m8	290-296
Klf12	0.414	3.66E-03	miR-34b-5p	1.465	3.47E-03	7mer-m8	3964-3970
			miR-7b-5p	1.304	6.75E-03	8mer	3933-3940
			miR-382-3p	1.260	6.66E-04	8mer	3456-3463
Grin2a	0.414	3.77E-03	miR-7b-5p	1.304	6.75E-03	7mer-A1	155-161
Zfp281	0.415	8.03E-11	miR-34b-5p	1.465	3.47E-03	8mer	56-63
			miR-382-3p	1.260	6.66E-04	8mer	735-742
Plec	0.417	1.59E-09	miR-7b-5p	1.304	6.75E-03	7mer-m8	113-119
Rasal2	0.417	7.24E-08	miR-135a-5p	1.366	1.06E-03	7mer-m8	915-921
			miR-135a-5p	1.366	1.06E-03	8mer	5315-5322
Cpeb2	0.417	5.57E-09	miR-34b-5p	1.465	3.47E-03	7mer-A1	703-709
			miR-23a-3p	1.382	6.75E-06	8mer	718-725
			miR-7b-5p	1.304	6.75E-03	7mer-A1	3631-3637
Kcnd3	0.417	7.05E-08	miR-34b-5p	1.465	3.47E-03	8mer	824-831
Tbck	0.418	1.17E-03	miR-34b-5p	1.465	3.47E-03	8mer	230-237
Hs6st3	0.418	6.02E-03	miR-23a-3p	1.382	6.75E-06	7mer-A1	6614-6620
			miR-382-3p	1.260	6.66E-04	7mer-A1	6581-6587
Cbfa2t3	0.419	5.72E-06	miR-34b-5p	1.465	3.47E-03	8mer	892-899
			miR-23a-3p	1.382	6.75E-06	8mer	1879-1886
Ccnd1	0.419	2.76E-10	miR-34b-5p	1.465	3.47E-03	7mer-A1	1856-1862
			miR-23a-3p	1.382	6.75E-06	7mer-m8	1948-1954
Zbtb16	0.420	1.14E-04	miR-23a-3p	1.382	6.75E-06	8mer	2446-2453
			miR-23a-3p	1.382	6.75E-06	8mer	2810-2817
Chsy3	0.420	2.43E-10	miR-23a-3p	1.382	6.75E-06	7mer-m8	407-413
			miR-7b-5p	1.304	6.75E-03	8mer	165-172
Adarb1	0.420	8.52E-08	miR-384-3p	1.203	9.74E-03	7mer-m8	414-420
Syde2	0.421	7.26E-07	miR-224-5p	1.437	3.04E-03	8mer	862-869
Nacc1	0.423	1.35E-08	miR-216a-5p	1.485	2.10E-03	7mer-m8	2461-2467
			miR-23a-3p	1.382	6.75E-06	8mer	2506-2513
Map3k5	0.423	7.20E-09	miR-23a-3p	1.382	6.75E-06	7mer-m8	397-403
Cxcl12	0.423	5.99E-08	miR-135a-5p	1.366	1.06E-03	7mer-A1	1241-1247
Trove2	0.424	9.86E-08	miR-7b-5p	1.304	6.75E-03	8mer	6403-6410
Pvrl1	0.424	2.98E-09	miR-135a-5p	1.366	1.06E-03	7mer-m8	1831-1837
Pou3f3	0.424	6.50E-07	miR-34b-5p	1.465	3.47E-03	7mer-A1	1214-1220

			miR-135a-5p	1.366	1.06E-03	8mer	6036-6043
			miR-384-3p	1.203	9.74E-03	8mer	5126-5133
Scn2b	0.425	4.33E-08	miR-34b-5p	1.465	3.47E-03	7mer-m8	1079-1085
			miR-34b-5p	1.465	3.47E-03	7mer-A1	1991-1997
			miR-34b-5p	1.465	3.47E-03	8mer	2005-2012
			miR-135a-5p	1.366	1.06E-03	8mer	1650-1657
			miR-7b-5p	1.304	6.75E-03	7mer-m8	3381-3387
Crtc1	0.426	5.67E-07	miR-34b-5p	1.465	3.47E-03	7mer-m8	445-451
Gadl1	0.427	8.44E-03	miR-384-3p	1.203	9.74E-03	7mer-A1	103-109
Smad7	0.427	5.54E-08	miR-216a-5p	1.485	2.10E-03	7mer-m8	1280-1286
Slit1	0.427	5.94E-11	miR-23a-3p	1.382	6.75E-06	7mer-A1	3614-3620
			miR-7b-5p	1.304	6.75E-03	8mer	3607-3614
Asap2	0.429	4.52E-06	miR-384-3p	1.203	9.74E-03	8mer	1849-1856
Soga1	0.429	2.96E-06	miR-34b-5p	1.465	3.47E-03	8mer	106-113
Fbxl14	0.429	2.76E-06	miR-23a-3p	1.382	6.75E-06	7mer-m8	1759-1765
Sdk1	0.429	9.66E-07	miR-135a-5p	1.366	1.06E-03	8mer	2087-2094
Agap2	0.431	1.11E-07	miR-34b-5p	1.465	3.47E-03	7mer-m8	518-524
Diras1	0.432	3.07E-08	miR-7b-5p	1.304	6.75E-03	7mer-m8	2200-2206
Palld	0.432	4.81E-03	miR-23a-3p	1.382	6.75E-06	7mer-m8	1742-1748
Satb2	0.434	5.34E-03	miR-34b-5p	1.465	3.47E-03	8mer	674-681
			miR-34b-5p	1.465	3.47E-03	8mer	2412-2419
			miR-23a-3p	1.382	6.75E-06	8mer	2651-2658
Eif4ebp2	0.434	3.04E-06	miR-23a-3p	1.382	6.75E-06	8mer	1832-1839
			miR-7b-5p	1.304	6.75E-03	7mer-A1	1277-1283
Gprin3	0.435	8.38E-04	miR-382-3p	1.260	6.66E-04	8mer	1459-1466
Phlpp1	0.435	3.17E-10	miR-224-5p	1.437	3.04E-03	8mer	486-493
			miR-382-3p	1.260	6.66E-04	7mer-A1	289-295
Papln	0.440	2.31E-04	miR-382-3p	1.260	6.66E-04	7mer-A1	2720-2726
Actn1	0.440	5.81E-06	miR-384-3p	1.203	9.74E-03	7mer-A1	372-378
Scn3b	0.441	4.40E-07	miR-224-5p	1.437	3.04E-03	7mer-m8	80-86
Pip4k2b	0.442	2.64E-07	miR-224-5p	1.437	3.04E-03	7mer-m8	3522-3528
			miR-23a-3p	1.382	6.75E-06	8mer	3461-3468
Tcf20	0.442	3.11E-08	miR-23a-3p	1.382	6.75E-06	8mer	467-474
			miR-382-3p	1.260	6.66E-04	7mer-m8	674-680
Adcy1	0.443	3.91E-07	miR-23a-3p	1.382	6.75E-06	8mer	8686-8693
			miR-135a-5p	1.366	1.06E-03	7mer-A1	3106-3112
Nipal3	0.448	4.16E-08	miR-7b-5p	1.304	6.75E-03	7mer-m8	377-383
			miR-7b-5p	1.304	6.75E-03	7mer-m8	2981-2987
Foxk1	0.448	3.41E-07	miR-23a-3p	1.382	6.75E-06	7mer-m8	5065-5071
			miR-382-3p	1.260	6.66E-04	8mer	4702-4709
Smad4	0.450	1.96E-08	miR-34b-5p	1.465	3.47E-03	7mer-m8	2499-2505
			miR-224-5p	1.437	3.04E-03	7mer-m8	993-999
			miR-224-5p	1.437	3.04E-03	7mer-m8	1136-1142
			miR-135a-5p	1.366	1.06E-03	7mer-A1	2094-2100
Csnk1a1	0.450	7.12E-07	miR-135a-5p	1.366	1.06E-03	7mer-m8	1174-1180
Ksr1	0.452	1.12E-09	miR-7b-5p	1.304	6.75E-03	8mer	2597-2604
			miR-23a-3p	1.382	6.75E-06	7mer-m8	2541-2547
Zbtb14	0.453	7.39E-07	miR-224-5p	1.437	3.04E-03	8mer	429-436
Ubr4	0.453	6.52E-08	miR-224-5p	1.437	3.04E-03	7mer-A1	282-288
			miR-135a-5p	1.366	1.06E-03	7mer-m8	200-206
H6pd	0.454	3.95E-06	miR-7b-5p	1.304	6.75E-03	8mer	4083-4090
Trio	0.454	7.79E-08	miR-135a-5p	1.366	1.06E-03	7mer-A1	1508-1514
Adcy8	0.455	3.12E-08	miR-23a-3p	1.382	6.75E-06	8mer	920-927
Btbd7	0.456	1.35E-03	miR-23a-3p	1.382	6.75E-06	8mer	2513-2520
Tns1	0.456	7.21E-08	miR-382-3p	1.260	6.66E-04	7mer-A1	4276-4282
Ppp1r9b	0.458	1.28E-06	miR-216a-5p	1.485	2.10E-03	7mer-m8	431-437
			miR-34b-5p	1.465	3.47E-03	7mer-A1	303-309
			miR-135a-5p	1.366	1.06E-03	7mer-A1	736-742
Fzd5	0.459	2.86E-06	miR-216a-5p	1.485	2.10E-03	7mer-A1	4176-4182
			miR-224-5p	1.437	3.04E-03	7mer-m8	3710-3716
			miR-23a-3p	1.382	6.75E-06	8mer	451-458
			miR-7b-5p	1.304	6.75E-03	7mer-m8	2054-2060
			miR-384-3p	1.203	9.74E-03	7mer-m8	3172-3178
Tob2	0.460	1.92E-05	miR-34b-5p	1.465	3.47E-03	8mer	1398-1405

Nfic	0.460	5.14E-06	miR-7b-5p	1.304	6.75E-03	8mer	2498-2505
Ddn	0.462	1.97E-08	miR-34b-5p	1.465	3.47E-03	8mer	1062-1069
Ntn1	0.463	1.45E-08	miR-34b-5p	1.465	3.47E-03	8mer	579-586
			miR-34b-5p	1.465	3.47E-03	8mer	1561-1568
Stxbp5l	0.463	1.42E-03	miR-384-3p	1.203	9.74E-03	8mer	5545-5552
Mtcl1	0.463	5.37E-07	miR-34b-5p	1.465	3.47E-03	7mer-m8	123-129
			miR-384-3p	1.203	9.74E-03	8mer	1319-1326
Fndc5	0.463	2.98E-09	miR-224-5p	1.437	3.04E-03	7mer-m8	1931-1937
			miR-135a-5p	1.366	1.06E-03	7mer-m8	1751-1757
Cadm3	0.463	2.42E-07	miR-23a-3p	1.382	6.75E-06	8mer	1066-1073
			miR-135a-5p	1.366	1.06E-03	8mer	1985-1992
			miR-7b-5p	1.304	6.75E-03	7mer-m8	1575-1581
			miR-7b-5p	1.304	6.75E-03	7mer-A1	1791-1797
Arid1a	0.464	2.97E-07	miR-216a-5p	1.485	2.10E-03	7mer-m8	1146-1152
Map3k3	0.465	6.96E-07	miR-23a-3p	1.382	6.75E-06	7mer-m8	1432-1438
Zfp318	0.465	2.64E-07	miR-34b-5p	1.465	3.47E-03	7mer-m8	4925-4931
Slc16a6	0.466	5.46E-05	miR-135a-5p	1.366	1.06E-03	7mer-A1	1807-1813
Rab5b	0.467	1.20E-06	miR-135a-5p	1.366	1.06E-03	7mer-m8	1597-1603
Oxsr1	0.467	6.75E-07	miR-34b-5p	1.465	3.47E-03	7mer-A1	78-84
Tmem164	0.469	6.42E-06	miR-34b-5p	1.465	3.47E-03	8mer	477-484
Cic	0.469	9.56E-07	miR-216a-5p	1.485	2.10E-03	7mer-A1	589-595
			miR-135a-5p	1.366	1.06E-03	7mer-m8	114-120
Thrb	0.470	1.10E-06	miR-135a-5p	1.366	1.06E-03	8mer	1506-1513
Shisa7	0.470	1.03E-05	miR-34b-5p	1.465	3.47E-03	7mer-m8	2639-2645
			miR-34b-5p	1.465	3.47E-03	7mer-m8	2852-2858
			miR-135a-5p	1.366	1.06E-03	7mer-m8	609-615
			miR-135a-5p	1.366	1.06E-03	8mer	3680-3687
Cacnb1	0.470	2.56E-06	miR-34b-5p	1.465	3.47E-03	7mer-m8	1259-1265
Ankhd1	0.470	2.84E-07	miR-23a-3p	1.382	6.75E-06	8mer	405-412
Camsap2	0.471	1.52E-09	miR-23a-3p	1.382	6.75E-06	7mer-A1	2004-2010
			miR-382-3p	1.260	6.66E-04	7mer-m8	1163-1169
Myo1c	0.472	1.00E-07	miR-216a-5p	1.485	2.10E-03	7mer-m8	296-302
			miR-34b-5p	1.465	3.47E-03	7mer-m8	869-875
			miR-135a-5p	1.366	1.06E-03	7mer-m8	337-343
			miR-384-3p	1.203	9.74E-03	7mer-A1	316-322
Pik3r2	0.472	7.72E-10	miR-135a-5p	1.366	1.06E-03	8mer	145-152
Klf3	0.473	8.53E-06	miR-23a-3p	1.382	6.75E-06	8mer	238-245
			miR-23a-3p	1.382	6.75E-06	7mer-A1	3570-3576
			miR-135a-5p	1.366	1.06E-03	7mer-m8	3261-3267
Pacsin1	0.473	9.29E-07	miR-7b-5p	1.304	6.75E-03	8mer	460-467
Cmip	0.475	7.10E-07	miR-23a-3p	1.382	6.75E-06	7mer-A1	2078-2084
Nacc2	0.476	1.14E-06	miR-23a-3p	1.382	6.75E-06	7mer-m8	69-75
			miR-23a-3p	1.382	6.75E-06	7mer-m8	118-124
			miR-23a-3p	1.382	6.75E-06	8mer	2379-2386
Nrxn2	0.477	5.48E-08	miR-34b-5p	1.465	3.47E-03	8mer	20-27
Lnx2	0.477	1.72E-06	miR-384-3p	1.203	9.74E-03	7mer-A1	649-655
Enah	0.477	7.46E-07	miR-224-5p	1.437	3.04E-03	7mer-m8	1013-1019
			miR-224-5p	1.437	3.04E-03	8mer	9295-9302
			miR-7b-5p	1.304	6.75E-03	7mer-m8	433-439
			miR-382-3p	1.260	6.66E-04	8mer	568-575
			miR-384-3p	1.203	9.74E-03	8mer	1611-1618
Nfix	0.478	7.38E-07	miR-23a-3p	1.382	6.75E-06	7mer-A1	3949-3955
Slc24a4	0.478	1.12E-06	miR-216a-5p	1.485	2.10E-03	7mer-m8	5651-5657
Arid1b	0.478	1.49E-07	miR-382-3p	1.260	6.66E-04	7mer-A1	582-588
Mlh3	0.479	7.19E-09	miR-7b-5p	1.304	6.75E-03	8mer	671-678
Map7d1	0.480	2.72E-09	miR-23a-3p	1.382	6.75E-06	7mer-A1	327-333
Ints1	0.481	4.64E-07	miR-382-3p	1.260	6.66E-04	7mer-A1	4861-4867
Spred2	0.482	7.65E-06	miR-382-3p	1.260	6.66E-04	7mer-m8	431-437
Hcn2	0.483	1.16E-07	miR-135a-5p	1.366	1.06E-03	8mer	85-92
Reln	0.484	1.39E-05	miR-34b-5p	1.465	3.47E-03	7mer-A1	778-784
Adra2a	0.485	5.78E-06	miR-23a-3p	1.382	6.75E-06	8mer	1343-1350
			miR-135a-5p	1.366	1.06E-03	7mer-m8	825-831
Rock1	0.486	2.69E-05	miR-34b-5p	1.465	3.47E-03	7mer-A1	984-990
			miR-135a-5p	1.366	1.06E-03	8mer	734-741

Lnpep	0.486	3.19E-03	miR-216a-5p	1.485	2.10E-03	7mer-m8	5637-5643
Fam53c	0.487	2.60E-06	miR-7b-5p	1.304	6.75E-03	8mer	1290-1297
Nlgn2	0.489	3.07E-06	miR-7b-5p	1.304	6.75E-03	8mer	1727-1734
Ism1	0.489	3.74E-05	miR-224-5p	1.437	3.04E-03	8mer	343-350
			miR-23a-3p	1.382	6.75E-06	7mer-m8	340-346
Prr12	0.489	5.10E-06	miR-384-3p	1.203	9.74E-03	7mer-A1	296-302
Hic1	0.490	1.04E-03	miR-23a-3p	1.382	6.75E-06	8mer	461-468
Clcn3	0.490	6.80E-09	miR-34b-5p	1.465	3.47E-03	8mer	1334-1341
			miR-23a-3p	1.382	6.75E-06	7mer-m8	839-845
			miR-23a-3p	1.382	6.75E-06	7mer-m8	1199-1205
			miR-135a-5p	1.366	1.06E-03	8mer	1825-1832
Hhip	0.491	3.02E-03	miR-7b-5p	1.304	6.75E-03	8mer	1621-1628
Ago1	0.491	7.26E-06	miR-135a-5p	1.366	1.06E-03	7mer-m8	1861-1867
			miR-7b-5p	1.304	6.75E-03	7mer-m8	707-713
Stox2	0.492	8.20E-07	miR-7b-5p	1.304	6.75E-03	7mer-m8	6297-6303
Kcnab3	0.494	1.21E-04	miR-135a-5p	1.366	1.06E-03	8mer	185-192
Fbxo11	0.494	1.08E-06	miR-384-3p	1.203	9.74E-03	7mer-m8	750-756
			miR-23a-3p	1.382	6.75E-06	7mer-m8	403-409
Zbtb46	0.494	2.99E-05	miR-135a-5p	1.366	1.06E-03	8mer	2820-2827
Ppfia3	0.496	2.42E-07	miR-7b-5p	1.304	6.75E-03	7mer-m8	353-359
Ncdn	0.496	4.83E-09	miR-34b-5p	1.465	3.47E-03	8mer	850-857
Trank1	0.497	4.98E-06	miR-34b-5p	1.465	3.47E-03	8mer	1021-1028
			miR-34b-5p	1.465	3.47E-03	8mer	1083-1090
			miR-23a-3p	1.382	6.75E-06	8mer	93-100
Bsn	0.498	7.99E-07	miR-135a-5p	1.366	1.06E-03	7mer-m8	773-779
			miR-135a-5p	1.366	1.06E-03	7mer-m8	1183-1189
Cacng7	0.498	4.73E-07	miR-7b-5p	1.304	6.75E-03	8mer	833-840
Calcrl	0.499	1.51E-04	miR-23a-3p	1.382	6.75E-06	8mer	2586-2593
Map1a	0.499	2.97E-07	miR-34b-5p	1.465	3.47E-03	7mer-m8	838-844
B4galt5	0.499	3.12E-05	miR-135a-5p	1.366	1.06E-03	7mer-m8	660-666
			miR-382-3p	1.260	6.66E-04	7mer-m8	2852-2858
Fam160a2	0.499	2.84E-07	miR-34b-5p	1.465	3.47E-03	7mer-A1	1635-1641

Table 2.3. Target prediction of miRNAs differentially expressed in the NAc after a prolonged nicotine withdrawal (NLWD) compared to age-matched controls (TAL).

mRNA	mRNA FC	mRNA FDR	miRNA	miRNA FC	miRNA FDR	Seed Type	Position in 3′-UTR
Sytl4	0.472	9.08E-04	miR-22-3p	1.195	3.10E-03	8mer	1421-1428

Target prediction of miRNAs differentially expressed in the midbrain

As for the NAc, TargetScan Mouse 7.1 was used to predict conserved MREs within the 3′-UTRs of differentially expressed mRNAs for inversely regulated and conserved miRNAs in the midbrain. All 3 miRNAs that are up-regulated in the midbrain during chronic nicotine treatment are broadly conserved among vertebrates. However, only one miRNA, miR-211-5p, is predicted to target a single conserved MRE in one inversely regulated gene, *B3galt2* which encodes β-1,3-galactosyltransferase (Table 2.4).

In the midbrain, of the miRNAs differentially expressed in NAWD mice compared to TA controls, 45 are conserved, with 31 up- and 14 down-regulated. TargetScan Mouse 7.1 predicted that 16 of the conserved miRNAs up-regulated during acute withdrawal target at least one of 13 down-regulated mRNAs at a conserved MRE within the 3′-UTR (Table 2.5). Twelve of the down-regulated mRNA targets that were predicted have multiple MREs, for a single or different miRNAs. All 14 conserved down-regulated miRNAs are predicted to target at least one of 367 up-regulated mRNAs (Table 2.5). One hundred and five (~28%) predicted target mRNAs are similarly differentially expressed in the in Nic-treated mice compared to controls (Table 2.5, green). Of these targets, only 7 (~2%) mRNAs are similarly up-regulated in NAWD mice compared to either TA or Nic (Table 2.5, orange). Multiple MREs, for a single or different miRNAs, are present in 186 (~51%) of the predicted targets.

There are no miRNAs differentially expressed after a long withdrawal from nicotine, hence no target prediction analysis was performed.

Table 2.4. Target prediction of miRNAs differentially expressed in the midbrain after chronic nicotine exposure (Nic) compared to TA controls.

mRNA	mRNA FC	mRNA FDR	miRNA	miRNA FC	miRNA FDR	Seed Type	Position in 3′-UTR
B3galt2	0.500	4.83E-06	miR-211-5p	1.288	6.75E-03	8mer	2918-2925

Table 2.5. Target prediction of miRNAs differentially expressed in the midbrain during acute nicotine withdrawal (NAWD) compared to TA controls. mRNAs similarly up- or down-regulated in Nic compared to TA mice are highlighted in green. mRNAs highlighted in orange are similarly differentially expressed in NAWD compared to Nic mice.

mRNA	mRNA FC	mRNA FDR	miRNA	miRNA FC	miRNA FDR	Seed Type	Position in 3′-UTR
TTC14	6.211	1.23E-07	miR-1224-5p	0.626	2.78E-06	8mer	670-677
			let-7e-5p	0.678	1.81E-04	7mer-A1	2550-2556
			let-7c-5p	0.725	2.96E-03	7mer-A1	2550-2556
			let-7a-5p	0.737	4.64E-03	7mer-A1	2550-2556
			let-7i-5p	0.754	2.96E-03	7mer-A1	2550-2556
			miR-219a-2-3p	0.777	9.18E-03	7mer-A1	493-499
Serpine1	5.870	4.74E-19	miR-134-5p	0.735	1.80E-04	8mer	345-352
Lrrc8b	5.185	4.39E-23	let-7e-5p	0.678	1.81E-04	7mer-m8	965-971
			let-7c-5p	0.725	2.96E-03	7mer-m8	965-971
			let-7a-5p	0.737	4.64E-03	7mer-m8	965-971
			let-7i-5p	0.754	2.96E-03	7mer-m8	965-971
Ccdc85c	4.785	7.98E-09	miR-411-5p	0.687	1.81E-04	7mer-m8	2702-2708
Slc16a14	4.742	1.53E-08	let-7e-5p	0.678	1.81E-04	8mer	38-45
			let-7c-5p	0.725	2.96E-03	8mer	38-45
			let-7a-5p	0.737	4.64E-03	8mer	38-45
			let-7i-5p	0.754	2.96E-03	8mer	38-45
BC037034	4.647	2.54E-22	miR-423-5p	0.746	7.22E-03	8mer	447-454
Ap1s1	4.569	7.84E-38	miR-206-3p	0.664	2.84E-04	7mer-m8	174-180
			let-7e-5p	0.678	1.81E-04	7mer-m8	428-434
			let-7c-5p	0.725	2.96E-03	7mer-m8	428-434
			let-7a-5p	0.737	4.64E-03	7mer-m8	428-434
			let-7i-5p	0.754	2.96E-03	7mer-m8	428-434
Lrrc20	4.498	1.99E-29	let-7e-5p	0.678	1.81E-04	7mer-m8	1046-1052
			let-7c-5p	0.725	2.96E-03	7mer-m8	1046-1052
			let-7a-5p	0.737	4.64E-03	7mer-m8	1046-1052
			let-7i-5p	0.754	2.96E-03	7mer-m8	1046-1052
Ccnd1	4.432	2.04E-33	miR-206-3p	0.664	2.84E-04	7mer-A1	911-917
			let-7e-5p	0.678	1.81E-04	7mer-A1	2003-2009
			let-7c-5p	0.725	2.96E-03	7mer-A1	2003-2009
			let-7a-5p	0.737	4.64E-03	7mer-A1	2003-2009
			let-7i-5p	0.754	2.96E-03	7mer-A1	2003-2009
Arid5b	4.313	2.86E-13	miR-320-3p	0.778	3.84E-03	7mer-m8	829-835
Ncdn	4.240	2.86E-66	miR-320-3p	0.778	3.84E-03	7mer-m8	110-116
Mex3d	4.138	9.98E-36	miR-320-3p	0.778	3.84E-03	8mer	142-149
Chsy3	4.103	5.74E-21	miR-495-3p	0.670	8.82E-05	7mer-m8	179-185
			let-7e-5p	0.678	1.81E-04	7mer-A1	40-46
			let-7c-5p	0.725	2.96E-03	7mer-A1	40-46
			let-7a-5p	0.737	4.64E-03	7mer-A1	40-46

			let-7i-5p	0.754	2.96E-03	7mer-A1	40-46
			miR-320-3p	0.778	3.84E-03	7mer-A1	763-769
Cdk20	4.044	9.55E-37	miR-21c	0.609	2.84E-04	7mer-m8	326-332
Tmem231	3.968	3.84E-32	let-7e-5p	0.678	1.81E-04	8mer	35-42
			let-7c-5p	0.725	2.96E-03	8mer	35-42
			let-7a-5p	0.737	4.64E-03	8mer	35-42
			let-7i-5p	0.754	2.96E-03	8mer	35-42
Lnx2	3.931	7.20E-27	miR-495-3p	0.670	8.82E-05	7mer-A1	1612-1618
Hnrnpul1	3.841	5.07E-32	miR-411-5p	0.687	1.81E-04	7mer-m8	391-397
Ppp1r9b	3.793	3.56E-27	miR-1224-5p	0.626	2.78E-06	8mer	57-64
Arl10	3.783	4.57E-19	miR-206-3p	0.664	2.84E-04	8mer	1225-1232
Arhgef4	3.782	4.41E-36	miR-219a-2-3p	0.777	9.18E-03	7mer-m8	1444-1450
Dcaf15	3.763	5.74E-35	let-7e-5p	0.678	1.81E-04	7mer-m8	31-37
			let-7c-5p	0.725	2.96E-03	7mer-m8	31-37
			let-7a-5p	0.737	4.64E-03	7mer-m8	31-37
			let-7i-5p	0.754	2.96E-03	7mer-m8	31-37
Ankrd52	3.665	6.81E-16	let-7e-5p	0.678	1.81E-04	7mer-A1	1419-1425
			let-7c-5p	0.725	2.96E-03	7mer-A1	1419-1425
			miR-134-5p	0.735	1.80E-04	7mer-m8	1050-1056
			let-7a-5p	0.737	4.64E-03	7mer-A1	1419-1425
			miR-423-5p	0.746	7.22E-03	7mer-m8	3202-3208
			let-7i-5p	0.754	2.96E-03	7mer-A1	1419-1425
			miR-219a-2-3p	0.777	9.18E-03	8mer	4839-4846
			miR-320-3p	0.778	3.84E-03	7mer-m8	1883-1889
			miR-320-3p	0.778	3.84E-03	7mer-m8	4289-4295
Gpr137	3.604	3.26E-32	let-7e-5p	0.678	1.81E-04	7mer-m8	253-259
			let-7c-5p	0.725	2.96E-03	7mer-m8	253-259
			let-7a-5p	0.737	4.64E-03	7mer-m8	253-259
			let-7i-5p	0.754	2.96E-03	7mer-m8	253-259
Frmd8	3.582	2.59E-36	miR-206-3p	0.664	2.84E-04	8mer	417-424
Bcl2l1	3.581	1.81E-13	miR-495-3p	0.670	8.82E-05	7mer-A1	1219-1225
			let-7e-5p	0.678	1.81E-04	8mer	947-954
			let-7c-5p	0.725	2.96E-03	8mer	947-954
			let-7a-5p	0.737	4.64E-03	8mer	947-954
			let-7i-5p	0.754	2.96E-03	8mer	947-954
4930426L09Rik	3.575	1.01E-11	miR-495-3p	0.670	8.82E-05	8mer	469-476
Slc8a1	3.564	8.40E-08	miR-206-3p	0.664	2.84E-04	8mer	1800-1807
			miR-495-3p	0.670	8.82E-05	7mer-A1	14884-14890
			miR-495-3p	0.670	8.82E-05	7mer-A1	15119-15125
Spred2	3.559	1.72E-27	miR-320-3p	0.778	3.84E-03	7mer-m8	2223-2229
Ankrd13c	3.549	2.11E-20	miR-206-3p	0.664	2.84E-04	7mer-A1	2055-2061
			miR-495-3p	0.670	8.82E-05	8mer	713-720
			miR-495-3p	0.670	8.82E-05	7mer-A1	1022-1028
			miR-382-5p	0.708	2.21E-05	7mer-m8	5264-5270
Ndrg2	3.548	3.74E-27	miR-382-5p	0.708	2.21E-05	7mer-m8	820-826
Irs2	3.526	3.33E-14	let-7e-5p	0.678	1.81E-04	8mer	475-482
			let-7c-5p	0.725	2.96E-03	8mer	475-482
			let-7a-5p	0.737	4.64E-03	8mer	475-482
			let-7i-5p	0.754	2.96E-03	8mer	475-482
Elfn2	3.526	3.33E-13	miR-423-5p	0.746	7.22E-03	7mer-m8	1246-1252
Palm2Akap2	3.506	7.01E-04	miR-320-3p	0.778	3.84E-03	7mer-A1	783-789
Gatad2b	3.482	1.11E-05	miR-21c	0.609	2.84E-04	8mer	3506-3513
			miR-21c	0.609	2.84E-04	8mer	5308-5315
Rgs16	3.467	1.51E-19	let-7e-5p	0.678	1.81E-04	7mer-m8	1405-1411
			let-7c-5p	0.725	2.96E-03	7mer-m8	1405-1411
			let-7a-5p	0.737	4.64E-03	7mer-m8	1405-1411
			let-7i-5p	0.754	2.96E-03	7mer-m8	1405-1411
Kcnc3	3.462	1.58E-15	let-7e-5p	0.678	1.81E-04	7mer-m8	1556-1562
			let-7c-5p	0.725	2.96E-03	7mer-m8	1556-1562
			let-7a-5p	0.737	4.64E-03	7mer-m8	1556-1562
			let-7i-5p	0.754	2.96E-03	7mer-m8	1556-1562
			miR-320-3p	0.778	3.84E-03	7mer-m8	2057-2063
Rasl10b	3.450	3.60E-33	let-7e-5p	0.678	1.81E-04	7mer-m8	1251-1257
			let-7c-5p	0.725	2.96E-03	7mer-m8	1251-1257
			let-7a-5p	0.737	4.64E-03	7mer-m8	1251-1257

			miR-423-5p	0.746	7.22E-03	8mer	747-754
			let-7i-5p	0.754	2.96E-03	7mer-m8	1251-1257
Dyrk2	3.419	3.36E-09	miR-495-3p	0.670	8.82E-05	7mer-A1	3887-3893
			let-7e-5p	0.678	1.81E-04	7mer-A1	3105-3111
			let-7c-5p	0.725	2.96E-03	7mer-A1	3105-3111
			let-7a-5p	0.737	4.64E-03	7mer-A1	3105-3111
			let-7i-5p	0.754	2.96E-03	7mer-A1	3105-3111
Adcy9	3.418	5.78E-10	let-7e-5p	0.678	1.81E-04	7mer-A1	2303-2309
			let-7c-5p	0.725	2.96E-03	7mer-A1	2303-2309
			let-7a-5p	0.737	4.64E-03	7mer-A1	2303-2309
			let-7i-5p	0.754	2.96E-03	7mer-A1	2303-2309
Ppm1f	3.388	1.89E-23	let-7e-5p	0.678	1.81E-04	8mer	2985-2992
			let-7c-5p	0.725	2.96E-03	8mer	2985-2992
			let-7a-5p	0.737	4.64E-03	8mer	2985-2992
			let-7i-5p	0.754	2.96E-03	8mer	2985-2992
			miR-320-3p	0.778	3.84E-03	7mer-m8	893-899
Src	3.382	1.86E-31	miR-206-3p	0.664	2.84E-04	8mer	1791-1798
Col1a2	3.379	1.44E-14	let-7e-5p	0.678	1.81E-04	8mer	415-422
			let-7c-5p	0.725	2.96E-03	8mer	415-422
			let-7a-5p	0.737	4.64E-03	8mer	415-422
			let-7i-5p	0.754	2.96E-03	8mer	415-422
Usp20	3.346	3.51E-25	miR-320-3p	0.778	3.84E-03	7mer-m8	281-287
H6pd	3.340	3.26E-15	miR-134-5p	0.735	1.80E-04	8mer	1968-1975
Pou3f1	3.337	3.99E-28	miR-495-3p	0.670	8.82E-05	8mer	1420-1427
Slc25a25	3.324	1.23E-30	miR-206-3p	0.664	2.84E-04	8mer	979-986
Tmem86a	3.267	4.98E-18	miR-1224-5p	0.626	2.78E-06	7mer-m8	1007-1013
Tcf20	3.262	1.39E-24	miR-206-3p	0.664	2.84E-04	8mer	915-922
			miR-219a-2-3p	0.777	9.18E-03	8mer	537-544
Dtx2	3.234	3.28E-17	let-7e-5p	0.678	1.81E-04	8mer	233-240
			let-7e-5p	0.678	1.81E-04	7mer-A1	341-347
			let-7c-5p	0.725	2.96E-03	8mer	233-240
			let-7c-5p	0.725	2.96E-03	7mer-A1	341-347
			let-7a-5p	0.737	4.64E-03	8mer	233-240
			let-7a-5p	0.737	4.64E-03	7mer-A1	341-347
			let-7i-5p	0.754	2.96E-03	8mer	233-240
			let-7i-5p	0.754	2.96E-03	7mer-A1	341-347
Dlg4	3.191	3.84E-32	miR-206-3p	0.664	2.84E-04	8mer	336-343
Camkv	3.174	3.17E-27	miR-495-3p	0.670	8.82E-05	8mer	1978-1985
Hp1bp3	3.172	1.40E-21	miR-206-3p	0.664	2.84E-04	7mer-A1	1193-1199
			miR-495-3p	0.670	8.82E-05	7mer-m8	1179-1185
Kcnk12	3.169	6.31E-15	miR-134-5p	0.735	1.80E-04	7mer-A1	501-507
Klhl24	3.164	4.83E-22	miR-219a-2-3p	0.777	9.18E-03	8mer	830-837
B430305J03Rik	3.151	4.62E-05	miR-134-5p	0.735	1.80E-04	7mer-m8	250-256
Pias4	3.136	1.82E-21	let-7e-5p	0.678	1.81E-04	7mer-m8	444-450
			let-7c-5p	0.725	2.96E-03	7mer-m8	444-450
			let-7a-5p	0.737	4.64E-03	7mer-m8	444-450
			let-7i-5p	0.754	2.96E-03	7mer-m8	444-450
			miR-219a-2-3p	0.777	9.18E-03	7mer-A1	459-465
Dazap1	3.126	1.46E-28	miR-320-3p	0.778	3.84E-03	8mer	210-217
B3glct	3.124	8.41E-14	miR-1224-5p	0.626	2.78E-06	8mer	2911-2918
Unc5a	3.093	4.06E-26	let-7e-5p	0.678	1.81E-04	7mer-m8	312-318
			let-7c-5p	0.725	2.96E-03	7mer-m8	312-318
			let-7a-5p	0.737	4.64E-03	7mer-m8	312-318
			let-7i-5p	0.754	2.96E-03	7mer-m8	312-318
Fndc3a	3.079	3.18E-18	miR-206-3p	0.664	2.84E-04	8mer	2039-2046
			let-7e-5p	0.678	1.81E-04	7mer-m8	505-511
			let-7e-5p	0.678	1.81E-04	7mer-A1	2024-2030
			let-7c-5p	0.725	2.96E-03	7mer-m8	505-511
			let-7c-5p	0.725	2.96E-03	7mer-A1	2024-2030
			let-7a-5p	0.737	4.64E-03	7mer-m8	505-511
			let-7a-5p	0.737	4.64E-03	7mer-A1	2024-2030
			let-7i-5p	0.754	2.96E-03	7mer-m8	505-511
			let-7i-5p	0.754	2.96E-03	7mer-A1	2024-2030
Smad6	3.068	1.30E-09	miR-134-5p	0.735	1.80E-04	7mer-m8	415-421
Fam168b	3.050	1.20E-19	miR-206-3p	0.664	2.84E-04	7mer-m8	2620-2626

			miR-134-5p	0.735	1.80E-04	7mer-m8	37-43
Bri3bp	3.043	8.56E-25	miR-206-3p	0.664	2.84E-04	7mer-m8	5496-5502
Ambra1	3.037	1.11E-14	miR-423-5p	0.746	7.22E-03	8mer	1019-1026
Klhl36	3.035	6.69E-23	miR-320-3p	0.778	3.84E-03	7mer-m8	62-68
Hip1r	3.033	4.69E-21	miR-320-3p	0.778	3.84E-03	8mer	2511-2518
Stk40	3.031	3.64E-21	miR-21c	0.609	2.84E-04	7mer-m8	393-399
			let-7e-5p	0.678	1.81E-04	7mer-m8	268-274
			let-7c-5p	0.725	2.96E-03	7mer-m8	268-274
			miR-134-5p	0.735	1.80E-04	7mer-A1	1908-1914
			let-7a-5p	0.737	4.64E-03	7mer-m8	268-274
			let-7i-5p	0.754	2.96E-03	7mer-m8	268-274
Dvl2	3.016	5.52E-18	miR-134-5p	0.735	1.80E-04	8mer	2497-2504
Hyal1	3.013	1.27E-06	miR-134-5p	0.735	1.80E-04	8mer	73-80
Numbl	3.000	1.01E-15	let-7e-5p	0.678	1.81E-04	7mer-A1	575-581
			let-7c-5p	0.725	2.96E-03	7mer-A1	575-581
			let-7a-5p	0.737	4.64E-03	7mer-A1	575-581
			miR-423-5p	0.746	7.22E-03	8mer	95-102
			let-7i-5p	0.754	2.96E-03	7mer-A1	575-581
Rnf39	2.995	6.84E-03	let-7e-5p	0.678	1.81E-04	7mer-m8	617-623
			let-7c-5p	0.725	2.96E-03	7mer-m8	617-623
			let-7a-5p	0.737	4.64E-03	7mer-m8	617-623
			let-7i-5p	0.754	2.96E-03	7mer-m8	617-623
Slitrk5	2.988	1.49E-16	miR-495-3p	0.670	8.82E-05	7mer-m8	437-443
			let-7e-5p	0.678	1.81E-04	7mer-m8	2273-2279
			let-7c-5p	0.725	2.96E-03	7mer-m8	2273-2279
			let-7a-5p	0.737	4.64E-03	7mer-m8	2273-2279
			let-7i-5p	0.754	2.96E-03	7mer-m8	2273-2279
Fbxl14	2.982	1.63E-13	let-7e-5p	0.678	1.81E-04	7mer-m8	690-696
			let-7c-5p	0.725	2.96E-03	7mer-m8	690-696
			let-7a-5p	0.737	4.64E-03	7mer-m8	690-696
			let-7i-5p	0.754	2.96E-03	7mer-m8	690-696
Gfod1	2.975	8.03E-12	let-7e-5p	0.678	1.81E-04	8mer	303-310
			let-7c-5p	0.725	2.96E-03	8mer	303-310
			let-7a-5p	0.737	4.64E-03	8mer	303-310
			let-7i-5p	0.754	2.96E-03	8mer	303-310
Ppara	2.975	2.21E-03	miR-21c	0.609	2.84E-04	8mer	571-578
			let-7e-5p	0.678	1.81E-04	7mer-A1	4391-4397
			let-7c-5p	0.725	2.96E-03	7mer-A1	4391-4397
			let-7a-5p	0.737	4.64E-03	7mer-A1	4391-4397
			let-7i-5p	0.754	2.96E-03	7mer-A1	4391-4397
Nacc1	2.974	1.70E-20	miR-423-5p	0.746	7.22E-03	7mer-m8	410-416
			miR-423-5p	0.746	7.22E-03	8mer	598-605
Tob2	2.956	4.32E-10	let-7e-5p	0.678	1.81E-04	7mer-m8	1435-1441
			let-7c-5p	0.725	2.96E-03	7mer-m8	1435-1441
			let-7a-5p	0.737	4.64E-03	7mer-m8	1435-1441
			let-7i-5p	0.754	2.96E-03	7mer-m8	1435-1441
Gas2l1	2.947	1.87E-20	miR-206-3p	0.664	2.84E-04	7mer-m8	151-157
Evx2	2.940	8.00E-04	miR-320-3p	0.778	3.84E-03	8mer	2289-2296
Calm3	2.898	8.84E-15	miR-495-3p	0.670	8.82E-05	7mer-m8	324-330
			miR-320-3p	0.778	3.84E-03	7mer-m8	1301-1307
Atp8b2	2.877	6.51E-11	miR-423-5p	0.746	7.22E-03	7mer-A1	393-399
Bhlhe41	2.867	4.99E-23	miR-495-3p	0.670	8.82E-05	7mer-m8	1087-1093
Nipal3	2.856	7.94E-18	miR-495-3p	0.670	8.82E-05	7mer-A1	3368-3374
Cdk13	2.853	8.29E-20	miR-382-5p	0.708	2.21E-05	8mer	1851-1858
			miR-320-3p	0.778	3.84E-03	8mer	103-110
			miR-320-3p	0.778	3.84E-03	7mer-A1	1947-1953
Cnksr3	2.852	4.58E-15	miR-134-5p	0.735	1.80E-04	7mer-A1	1074-1080
Hs6st3	2.846	7.12E-03	miR-320-3p	0.778	3.84E-03	8mer	1434-1441
Klf9	2.845	1.70E-20	let-7e-5p	0.678	1.81E-04	7mer-m8	2018-2024
			let-7c-5p	0.725	2.96E-03	7mer-m8	2018-2024
			let-7a-5p	0.737	4.64E-03	7mer-m8	2018-2024
			let-7i-5p	0.754	2.96E-03	7mer-m8	2018-2024
Xylt1	2.829	1.42E-04	miR-495-3p	0.670	8.82E-05	7mer-A1	5439-5445
			let-7e-5p	0.678	1.81E-04	8mer	4158-4165
			let-7c-5p	0.725	2.96E-03	8mer	4158-4165

			let-7a-5p	0.737	4.64E-03	8mer	4158-4165
			let-7i-5p	0.754	2.96E-03	8mer	4158-4165
Pcgf3	2.820	2.17E-11	let-7e-5p	0.678	1.81E-04	8mer	1621-1628
			let-7c-5p	0.725	2.96E-03	8mer	1621-1628
			let-7a-5p	0.737	4.64E-03	8mer	1621-1628
			let-7i-5p	0.754	2.96E-03	8mer	1621-1628
			miR-320-3p	0.778	3.84E-03	8mer	2492-2499
Map7d1	2.820	7.03E-35	miR-423-5p	0.746	7.22E-03	8mer	183-190
Grb2	2.818	1.28E-18	miR-320-3p	0.778	3.84E-03	7mer-m8	861-867
Kctd13	2.817	1.79E-26	miR-206-3p	0.664	2.84E-04	8mer	168-175
Zfp787	2.814	1.32E-28	miR-423-5p	0.746	7.22E-03	7mer-m8	29-35
Myrip	2.793	6.31E-15	let-7e-5p	0.678	1.81E-04	7mer-A1	162-168
			let-7c-5p	0.725	2.96E-03	7mer-A1	162-168
			let-7a-5p	0.737	4.64E-03	7mer-A1	162-168
			let-7i-5p	0.754	2.96E-03	7mer-A1	162-168
Lemd3	2.782	7.19E-17	miR-21c	0.609	2.84E-04	7mer-m8	625-631
Ddx19b	2.777	4.81E-15	let-7e-5p	0.678	1.81E-04	8mer	118-125
			miR-382-5p	0.708	2.21E-05	7mer-m8	191-197
			let-7c-5p	0.725	2.96E-03	8mer	118-125
			let-7a-5p	0.737	4.64E-03	8mer	118-125
			let-7i-5p	0.754	2.96E-03	8mer	118-125
Dusp8	2.769	1.89E-12	miR-21c	0.609	2.84E-04	8mer	1657-1664
Foxq1	2.765	1.34E-12	miR-320-3p	0.778	3.84E-03	8mer	627-634
Mycl	2.765	5.51E-17	miR-21c	0.609	2.84E-04	7mer-m8	1697-1703
			let-7e-5p	0.678	1.81E-04	7mer-A1	541-547
			let-7c-5p	0.725	2.96E-03	7mer-A1	541-547
			let-7a-5p	0.737	4.64E-03	7mer-A1	541-547
			let-7i-5p	0.754	2.96E-03	7mer-A1	541-547
Sfxn5	2.764	3.74E-14	miR-206-3p	0.664	2.84E-04	7mer-m8	2265-2271
Zfp281	2.763	6.75E-15	miR-206-3p	0.664	2.84E-04	7mer-A1	686-692
			miR-206-3p	0.664	2.84E-04	7mer-m8	5157-5163
			miR-495-3p	0.670	8.82E-05	7mer-A1	138-144
			miR-495-3p	0.670	8.82E-05	8mer	5079-5086
			let-7e-5p	0.678	1.81E-04	8mer	3451-3458
			let-7c-5p	0.725	2.96E-03	8mer	3451-3458
			let-7a-5p	0.737	4.64E-03	8mer	3451-3458
			let-7i-5p	0.754	2.96E-03	8mer	3451-3458
			miR-320-3p	0.778	3.84E-03	7mer-m8	648-654
			miR-320-3p	0.778	3.84E-03	7mer-A1	742-748
Ip6k3	2.753	2.11E-09	miR-495-3p	0.670	8.82E-05	7mer-A1	865-871
			miR-495-3p	0.670	8.82E-05	7mer-m8	924-930
Rbms1	2.752	5.07E-16	let-7e-5p	0.678	1.81E-04	8mer	1900-1907
			let-7c-5p	0.725	2.96E-03	8mer	1900-1907
			let-7a-5p	0.737	4.64E-03	8mer	1900-1907
			let-7i-5p	0.754	2.96E-03	8mer	1900-1907
Zfp503	2.752	7.68E-20	miR-495-3p	0.670	8.82E-05	8mer	582-589
			miR-219a-2-3p	0.777	9.18E-03	7mer-m8	738-744
Igf1r	2.747	7.22E-11	miR-495-3p	0.670	8.82E-05	7mer-A1	6977-6983
			let-7e-5p	0.678	1.81E-04	7mer-A1	112-118
			let-7e-5p	0.678	1.81E-04	8mer	2724-2731
			let-7e-5p	0.678	1.81E-04	7mer-m8	6830-6836
			let-7c-5p	0.725	2.96E-03	7mer-A1	112-118
			let-7c-5p	0.725	2.96E-03	8mer	2724-2731
			let-7c-5p	0.725	2.96E-03	7mer-m8	6830-6836
			let-7a-5p	0.737	4.64E-03	7mer-A1	112-118
			let-7a-5p	0.737	4.64E-03	8mer	2724-2731
			let-7a-5p	0.737	4.64E-03	7mer-m8	6830-6836
			let-7i-5p	0.754	2.96E-03	7mer-A1	112-118
			let-7i-5p	0.754	2.96E-03	8mer	2724-2731
			let-7i-5p	0.754	2.96E-03	7mer-m8	6830-6836
			miR-320-3p	0.778	3.84E-03	7mer-m8	208-214
			miR-320-3p	0.778	3.84E-03	7mer-A1	5931-5937
Tpcn1	2.741	2.95E-18	miR-495-3p	0.670	8.82E-05	7mer-A1	1886-1892
			miR-423-5p	0.746	7.22E-03	7mer-m8	1775-1781
Satb1	2.735	2.13E-16	miR-21c	0.609	2.84E-04	7mer-m8	941-947

			miR-495-3p	0.670	8.82E-05	8mer	459-466
			miR-495-3p	0.670	8.82E-05	7mer-A1	1127-1133
			miR-219a-2-3p	0.777	9.18E-03	7mer-A1	884-890
Rgmb	2.734	7.73E-15	miR-495-3p	0.670	8.82E-05	7mer-m8	2486-2492
Syt2	2.729	3.10E-15	let-7e-5p	0.678	1.81E-04	7mer-A1	90-96
			let-7c-5p	0.725	2.96E-03	7mer-A1	90-96
			let-7a-5p	0.737	4.64E-03	7mer-A1	90-96
			let-7i-5p	0.754	2.96E-03	7mer-A1	90-96
Crb2	2.727	3.55E-04	let-7e-5p	0.678	1.81E-04	8mer	700-707
			let-7c-5p	0.725	2.96E-03	8mer	700-707
			let-7a-5p	0.737	4.64E-03	8mer	700-707
			let-7i-5p	0.754	2.96E-03	8mer	700-707
Xpo7	2.727	2.16E-13	miR-320-3p	0.778	3.84E-03	7mer-A1	492-498
Dyrk1b	2.725	1.26E-14	miR-423-5p	0.746	7.22E-03	7mer-m8	19-25
Oprd1	2.724	3.04E-03	miR-423-5p	0.746	7.22E-03	7mer-m8	24-30
Pcdh1	2.722	4.69E-21	miR-495-3p	0.670	8.82E-05	7mer-m8	3968-3974
			miR-320-3p	0.778	3.84E-03	7mer-A1	4014-4020
Sass6	2.720	7.10E-10	let-7e-5p	0.678	1.81E-04	7mer-m8	1986-1992
			let-7c-5p	0.725	2.96E-03	7mer-m8	1986-1992
			let-7a-5p	0.737	4.64E-03	7mer-m8	1986-1992
			let-7i-5p	0.754	2.96E-03	7mer-m8	1986-1992
			miR-320-3p	0.778	3.84E-03	8mer	2730-2737
Nudt5	2.720	8.20E-16	miR-411-5p	0.687	1.81E-04	7mer-m8	2845-2851
Vgf	2.718	1.64E-21	miR-423-5p	0.746	7.22E-03	7mer-A1	458-464
Dpysl3	2.711	3.35E-16	let-7e-5p	0.678	1.81E-04	7mer-A1	2094-2100
			let-7c-5p	0.725	2.96E-03	7mer-A1	2094-2100
			let-7a-5p	0.737	4.64E-03	7mer-A1	2094-2100
			let-7i-5p	0.754	2.96E-03	7mer-A1	2094-2100
			miR-219a-2-3p	0.777	9.18E-03	8mer	2006-2013
			miR-320-3p	0.778	3.84E-03	7mer-A1	160-166
Dusp4	2.702	9.71E-07	let-7e-5p	0.678	1.81E-04	7mer-A1	278-284
			let-7c-5p	0.725	2.96E-03	7mer-A1	278-284
			let-7a-5p	0.737	4.64E-03	7mer-A1	278-284
			let-7i-5p	0.754	2.96E-03	7mer-A1	278-284
Nrxn2	2.689	4.34E-21	miR-495-3p	0.670	8.82E-05	7mer-A1	983-989
			miR-495-3p	0.670	8.82E-05	7mer-m8	1083-1089
Jup	2.686	2.40E-20	miR-320-3p	0.778	3.84E-03	7mer-A1	245-251
Wbp2	2.678	2.71E-21	miR-206-3p	0.664	2.84E-04	7mer-m8	424-430
Sdk1	2.674	2.46E-12	let-7e-5p	0.678	1.81E-04	7mer-m8	402-408
			let-7c-5p	0.725	2.96E-03	7mer-m8	402-408
			let-7a-5p	0.737	4.64E-03	7mer-m8	402-408
			let-7i-5p	0.754	2.96E-03	7mer-m8	402-408
			miR-320-3p	0.778	3.84E-03	7mer-m8	950-956
			miR-320-3p	0.778	3.84E-03	7mer-m8	1156-1162
Ralb	2.664	1.17E-19	let-7e-5p	0.678	1.81E-04	7mer-m8	997-1003
			let-7c-5p	0.725	2.96E-03	7mer-m8	997-1003
			let-7a-5p	0.737	4.64E-03	7mer-m8	997-1003
			let-7i-5p	0.754	2.96E-03	7mer-m8	997-1003
Zswim4	2.662	1.09E-17	let-7e-5p	0.678	1.81E-04	7mer-A1	513-519
			let-7c-5p	0.725	2.96E-03	7mer-A1	513-519
			let-7a-5p	0.737	4.64E-03	7mer-A1	513-519
			let-7i-5p	0.754	2.96E-03	7mer-A1	513-519
Syvn1	2.662	3.53E-21	miR-423-5p	0.746	7.22E-03	7mer-m8	311-317
Agap2	2.658	1.81E-20	miR-423-5p	0.746	7.22E-03	7mer-m8	989-995
Nedd4l	2.651	5.10E-16	miR-206-3p	0.664	2.84E-04	7mer-A1	4519-4525
			let-7e-5p	0.678	1.81E-04	7mer-m8	3550-3556
			let-7c-5p	0.725	2.96E-03	7mer-m8	3550-3556
			let-7a-5p	0.737	4.64E-03	7mer-m8	3550-3556
			let-7i-5p	0.754	2.96E-03	7mer-m8	3550-3556
Map1a	2.644	1.28E-17	miR-206-3p	0.664	2.84E-04	8mer	883-890
Pbx2	2.643	1.17E-14	let-7e-5p	0.678	1.81E-04	7mer-A1	452-458
			let-7e-5p	0.678	1.81E-04	7mer-m8	520-526
			let-7c-5p	0.725	2.96E-03	7mer-A1	452-458
			let-7c-5p	0.725	2.96E-03	7mer-m8	520-526
			let-7a-5p	0.737	4.64E-03	7mer-A1	452-458

			let-7a-5p	0.737	4.64E-03	7mer-m8	520-526
			let-7i-5p	0.754	2.96E-03	7mer-A1	452-458
			let-7i-5p	0.754	2.96E-03	7mer-m8	520-526
Ntn1	2.636	5.82E-14	let-7e-5p	0.678	1.81E-04	8mer	242-249
			let-7c-5p	0.725	2.96E-03	8mer	242-249
			let-7a-5p	0.737	4.64E-03	8mer	242-249
			let-7i-5p	0.754	2.96E-03	8mer	242-249
Prrc2a	2.635	1.84E-15	miR-495-3p	0.670	8.82E-05	8mer	347-354
C2cd4c	2.633	1.78E-13	miR-495-3p	0.670	8.82E-05	7mer-m8	1291-1297
Myl9	2.633	1.54E-03	miR-134-5p	0.735	1.80E-04	7mer-m8	37-43
Pard3	2.631	1.25E-13	miR-134-5p	0.735	1.80E-04	8mer	1075-1082
Mfsd12	2.630	5.45E-14	miR-423-5p	0.746	7.22E-03	7mer-m8	1163-1169
B3gnt7	2.624	3.60E-04	let-7e-5p	0.678	1.81E-04	8mer	576-583
			let-7c-5p	0.725	2.96E-03	8mer	576-583
			let-7a-5p	0.737	4.64E-03	8mer	576-583
			let-7i-5p	0.754	2.96E-03	8mer	576-583
Pag1	2.618	1.38E-11	miR-21c	0.609	2.84E-04	8mer	994-1001
			let-7e-5p	0.678	1.81E-04	8mer	5835-5842
			let-7c-5p	0.725	2.96E-03	8mer	5835-5842
			let-7a-5p	0.737	4.64E-03	8mer	5835-5842
			let-7i-5p	0.754	2.96E-03	8mer	5835-5842
Lhx4	2.618	3.33E-03	miR-495-3p	0.670	8.82E-05	7mer-m8	4111-4117
Pdgfa	2.608	4.11E-23	miR-206-3p	0.664	2.84E-04	7mer-m8	69-75
Ccdc71l	2.598	6.28E-18	let-7e-5p	0.678	1.81E-04	8mer	299-306
			let-7c-5p	0.725	2.96E-03	8mer	299-306
			let-7a-5p	0.737	4.64E-03	8mer	299-306
			let-7i-5p	0.754	2.96E-03	8mer	299-306
Tmx4	2.591	3.75E-13	let-7e-5p	0.678	1.81E-04	7mer-A1	3371-3377
			let-7c-5p	0.725	2.96E-03	7mer-A1	3371-3377
			let-7a-5p	0.737	4.64E-03	7mer-A1	3371-3377
			let-7i-5p	0.754	2.96E-03	7mer-A1	3371-3377
Ahdc1	2.591	1.58E-15	miR-423-5p	0.746	7.22E-03	7mer-m8	107-113
Xpnpep3	2.587	2.13E-08	miR-206-3p	0.664	2.84E-04	7mer-A1	241-247
			miR-495-3p	0.670	8.82E-05	7mer-A1	4403-4409
Zfp36l2	2.583	4.83E-22	miR-21c	0.609	2.84E-04	7mer-m8	487-493
			miR-206-3p	0.664	2.84E-04	7mer-A1	628-634
Kalrn	2.580	3.37E-14	miR-206-3p	0.664	2.84E-04	7mer-m8	647-653
Gorasp1	2.576	1.69E-16	miR-423-5p	0.746	7.22E-03	7mer-m8	1408-1414
Rffl	2.575	5.74E-19	miR-21c	0.609	2.84E-04	7mer-m8	2005-2011
			miR-495-3p	0.670	8.82E-05	7mer-A1	2140-2146
			let-7e-5p	0.678	1.81E-04	7mer-m8	1590-1596
			let-7c-5p	0.725	2.96E-03	7mer-m8	1590-1596
			let-7a-5p	0.737	4.64E-03	7mer-m8	1590-1596
			let-7i-5p	0.754	2.96E-03	7mer-m8	1590-1596
Mylk	2.573	2.23E-08	miR-206-3p	0.664	2.84E-04	8mer	1370-1377
Klhl3	2.566	2.02E-03	miR-382-5p	0.708	2.21E-05	7mer-m8	337-343
Gdnf	2.566	2.60E-03	miR-495-3p	0.670	8.82E-05	7mer-A1	1828-1834
Setd1b	2.563	9.74E-07	miR-21c	0.609	2.84E-04	7mer-m8	1012-1018
Tmem184b	2.558	5.86E-22	miR-134-5p	0.735	1.80E-04	7mer-A1	960-966
Otud7a	2.557	2.59E-17	let-7e-5p	0.678	1.81E-04	7mer-m8	652-658
			let-7c-5p	0.725	2.96E-03	7mer-m8	652-658
			let-7a-5p	0.737	4.64E-03	7mer-m8	652-658
			let-7i-5p	0.754	2.96E-03	7mer-m8	652-658
			miR-320-3p	0.778	3.84E-03	7mer-m8	1898-1904
Ptrf	2.553	2.88E-11	let-7e-5p	0.678	1.81E-04	8mer	2637-2644
			let-7c-5p	0.725	2.96E-03	8mer	2637-2644
			let-7a-5p	0.737	4.64E-03	8mer	2637-2644
			let-7i-5p	0.754	2.96E-03	8mer	2637-2644
Ehd1	2.547	4.49E-17	miR-21c	0.609	2.84E-04	8mer	665-672
Pgrmc2	2.533	8.59E-19	miR-21c	0.609	2.84E-04	7mer-m8	1133-1139
Crkl	2.529	3.39E-13	miR-320-3p	0.778	3.84E-03	7mer-m8	100-106
Mapk8ip3	2.519	1.29E-15	miR-320-3p	0.778	3.84E-03	7mer-m8	110-116
Ptprg	2.517	1.87E-17	miR-206-3p	0.664	2.84E-04	8mer	287-294
Smad7	2.509	2.51E-10	miR-21c	0.609	2.84E-04	8mer	1165-1172

Slc8a2	2.505	2.54E-19	miR-206-3p	0.664	2.84E-04	8mer	582-589
			let-7e-5p	0.678	1.81E-04	7mer-m8	609-615
			let-7c-5p	0.725	2.96E-03	7mer-m8	609-615
			let-7a-5p	0.737	4.64E-03	7mer-m8	609-615
			let-7i-5p	0.754	2.96E-03	7mer-m8	609-615
Zcchc14	2.500	2.28E-15	miR-495-3p	0.670	8.82E-05	7mer-A1	3485-3491
			miR-382-5p	0.708	2.21E-05	7mer-m8	746-752
			miR-382-5p	0.708	2.21E-05	7mer-m8	1687-1693
Gpr157	2.499	4.14E-09	let-7e-5p	0.678	1.81E-04	7mer-m8	141-147
			let-7c-5p	0.725	2.96E-03	7mer-m8	141-147
			let-7a-5p	0.737	4.64E-03	7mer-m8	141-147
			let-7i-5p	0.754	2.96E-03	7mer-m8	141-147
Slc12a9	2.497	9.93E-14	let-7e-5p	0.678	1.81E-04	8mer	267-274
			let-7c-5p	0.725	2.96E-03	8mer	267-274
			let-7a-5p	0.737	4.64E-03	8mer	267-274
			let-7i-5p	0.754	2.96E-03	8mer	267-274
Creb5	2.497	2.74E-03	miR-206-3p	0.664	2.84E-04	8mer	3758-3765
Cops7b	2.496	1.51E-11	miR-495-3p	0.670	8.82E-05	7mer-A1	1063-1069
			miR-423-5p	0.746	7.22E-03	7mer-A1	108-114
Epha4	2.495	3.77E-08	miR-21c	0.609	2.84E-04	8mer	2232-2239
			let-7e-5p	0.678	1.81E-04	7mer-A1	37-43
			let-7c-5p	0.725	2.96E-03	7mer-A1	37-43
			let-7a-5p	0.737	4.64E-03	7mer-A1	37-43
			let-7i-5p	0.754	2.96E-03	7mer-A1	37-43
Ssh1	2.488	1.35E-17	let-7e-5p	0.678	1.81E-04	7mer-m8	511-517
			let-7c-5p	0.725	2.96E-03	7mer-m8	511-517
			let-7a-5p	0.737	4.64E-03	7mer-m8	511-517
			let-7i-5p	0.754	2.96E-03	7mer-m8	511-517
Rasa1	2.478	3.12E-11	miR-21c	0.609	2.84E-04	7mer-A1	191-197
			miR-206-3p	0.664	2.84E-04	8mer	118-125
			miR-495-3p	0.670	8.82E-05	7mer-A1	689-695
			miR-320-3p	0.778	3.84E-03	8mer	620-627
C1galt1	2.478	8.06E-12	miR-206-3p	0.664	2.84E-04	8mer	91-98
			let-7e-5p	0.678	1.81E-04	8mer	1824-1831
			let-7c-5p	0.725	2.96E-03	8mer	1824-1831
			let-7a-5p	0.737	4.64E-03	8mer	1824-1831
			let-7i-5p	0.754	2.96E-03	8mer	1824-1831
Zfp180	2.454	1.45E-12	miR-495-3p	0.670	8.82E-05	8mer	1349-1356
Golga7	2.454	3.91E-17	let-7e-5p	0.678	1.81E-04	7mer-m8	70-76
			miR-495-3p	0.670	8.82E-05	7mer-A1	779-785
			let-7c-5p	0.725	2.96E-03	7mer-m8	70-76
			let-7a-5p	0.737	4.64E-03	7mer-m8	70-76
			let-7i-5p	0.754	2.96E-03	7mer-m8	70-76
Dnajb12	2.452	3.34E-14	miR-423-5p	0.746	7.22E-03	7mer-m8	2260-2266
Rmdn3	2.452	4.12E-11	miR-320-3p	0.778	3.84E-03	7mer-m8	580-586
Slc38a9	2.449	4.46E-13	let-7e-5p	0.678	1.81E-04	7mer-A1	426-432
			let-7c-5p	0.725	2.96E-03	7mer-A1	426-432
			let-7a-5p	0.737	4.64E-03	7mer-A1	426-432
			let-7i-5p	0.754	2.96E-03	7mer-A1	426-432
Dnal1	2.445	1.39E-11	let-7e-5p	0.678	1.81E-04	7mer-m8	3400-3406
			let-7c-5p	0.725	2.96E-03	7mer-m8	3400-3406
			let-7a-5p	0.737	4.64E-03	7mer-m8	3400-3406
			let-7i-5p	0.754	2.96E-03	7mer-m8	3400-3406
Scn4b	2.438	4.50E-08	let-7e-5p	0.678	1.81E-04	8mer	2190-2197
			let-7c-5p	0.725	2.96E-03	8mer	2190-2197
			let-7a-5p	0.737	4.64E-03	8mer	2190-2197
			let-7i-5p	0.754	2.96E-03	8mer	2190-2197
Slc45a4	2.436	1.11E-19	let-7e-5p	0.678	1.81E-04	7mer-m8	896-902
			miR-382-5p	0.708	2.21E-05	7mer-A1	4015-4021
			let-7c-5p	0.725	2.96E-03	7mer-m8	896-902
			let-7a-5p	0.737	4.64E-03	7mer-m8	896-902
			let-7i-5p	0.754	2.96E-03	7mer-m8	896-902
Col4a2	2.435	2.81E-12	let-7e-5p	0.678	1.81E-04	7mer-A1	235-241
			let-7c-5p	0.725	2.96E-03	7mer-A1	235-241
			let-7a-5p	0.737	4.64E-03	7mer-A1	235-241

			let-7i-5p	0.754	2.96E-03	7mer-A1	235-241
Carf	2.433	3.04E-13	miR-206-3p	0.664	2.84E-04	7mer-m8	2051-2057
Pcbp1	2.431	2.98E-22	miR-21c	0.609	2.84E-04	7mer-m8	192-198
Tmem198b	2.431	4.73E-15	let-7e-5p	0.678	1.81E-04	7mer-m8	205-211
			let-7e-5p	0.678	1.81E-04	7mer-m8	688-694
			let-7c-5p	0.725	2.96E-03	7mer-m8	205-211
			let-7c-5p	0.725	2.96E-03	7mer-m8	688-694
			let-7a-5p	0.737	4.64E-03	7mer-m8	205-211
			let-7a-5p	0.737	4.64E-03	7mer-m8	688-694
			let-7i-5p	0.754	2.96E-03	7mer-m8	205-211
			let-7i-5p	0.754	2.96E-03	7mer-m8	688-694
Hmga1	2.429	9.92E-12	let-7e-5p	0.678	1.81E-04	7mer-m8	801-807
			let-7c-5p	0.725	2.96E-03	7mer-m8	801-807
			let-7a-5p	0.737	4.64E-03	7mer-m8	801-807
			let-7i-5p	0.754	2.96E-03	7mer-m8	801-807
Cbfa2t3	2.426	7.46E-08	let-7e-5p	0.678	1.81E-04	7mer-m8	1388-1394
			let-7c-5p	0.725	2.96E-03	7mer-m8	1388-1394
			let-7a-5p	0.737	4.64E-03	7mer-m8	1388-1394
			let-7i-5p	0.754	2.96E-03	7mer-m8	1388-1394
Zbtb7b	2.424	1.21E-15	miR-206-3p	0.664	2.84E-04	7mer-A1	141-147
			miR-423-5p	0.746	7.22E-03	7mer-m8	500-506
Sik3	2.418	3.64E-18	miR-382-5p	0.708	2.21E-05	8mer	2071-2078
Nova2	2.412	6.66E-15	miR-219a-2-3p	0.777	9.18E-03	7mer-m8	2308-2314
Slmo2	2.411	3.00E-12	miR-495-3p	0.670	8.82E-05	7mer-A1	59-65
Lmtk3	2.409	4.54E-15	miR-382-5p	0.708	2.21E-05	7mer-m8	479-485
Ppp1r15b	2.409	6.00E-14	let-7e-5p	0.678	1.81E-04	8mer	2032-2039
			let-7c-5p	0.725	2.96E-03	8mer	2032-2039
			let-7a-5p	0.737	4.64E-03	8mer	2032-2039
			let-7i-5p	0.754	2.96E-03	8mer	2032-2039
Yy1	2.409	2.95E-07	let-7e-5p	0.678	1.81E-04	8mer	1085-1092
			let-7c-5p	0.725	2.96E-03	8mer	1085-1092
			let-7a-5p	0.737	4.64E-03	8mer	1085-1092
			let-7i-5p	0.754	2.96E-03	8mer	1085-1092
			miR-219a-2-3p	0.777	9.18E-03	8mer	258-265
Tbkbp1	2.407	4.50E-17	let-7e-5p	0.678	1.81E-04	8mer	975-982
			let-7c-5p	0.725	2.96E-03	8mer	975-982
			let-7a-5p	0.737	4.64E-03	8mer	975-982
			let-7i-5p	0.754	2.96E-03	8mer	975-982
AI606181	2.401	3.07E-13	let-7e-5p	0.678	1.81E-04	7mer-A1	1999-2005
			let-7c-5p	0.725	2.96E-03	7mer-A1	1999-2005
			let-7a-5p	0.737	4.64E-03	7mer-A1	1999-2005
			let-7i-5p	0.754	2.96E-03	7mer-A1	1999-2005
Lphn1	2.388	1.98E-13	miR-320-3p	0.778	3.84E-03	7mer-m8	1060-1066
Gas7	2.387	1.18E-14	let-7e-5p	0.678	1.81E-04	8mer	599-606
			let-7c-5p	0.725	2.96E-03	8mer	599-606
			let-7a-5p	0.737	4.64E-03	8mer	599-606
			let-7i-5p	0.754	2.96E-03	8mer	599-606
Fzd8	2.385	9.45E-11	miR-320-3p	0.778	3.84E-03	7mer-m8	1686-1692
Ndst1	2.382	6.28E-09	miR-206-3p	0.664	2.84E-04	7mer-A1	1873-1879
			miR-495-3p	0.670	8.82E-05	7mer-m8	1107-1113
			miR-134-5p	0.735	1.80E-04	8mer	1855-1862
			miR-423-5p	0.746	7.22E-03	7mer-A1	390-396
Kremen1	2.378	6.23E-13	let-7e-5p	0.678	1.81E-04	7mer-m8	2858-2864
			miR-495-3p	0.670	8.82E-05	7mer-A1	3296-3302
			let-7c-5p	0.725	2.96E-03	7mer-m8	2858-2864
			let-7a-5p	0.737	4.64E-03	7mer-m8	2858-2864
			let-7i-5p	0.754	2.96E-03	7mer-m8	2858-2864
Smad9	2.375	3.17E-12	miR-206-3p	0.664	2.84E-04	7mer-A1	2894-2900
			miR-495-3p	0.670	8.82E-05	7mer-m8	2611-2617
Ppp2r5e	2.355	3.97E-15	miR-134-5p	0.735	1.80E-04	8mer	1729-1736
Mllt3	2.354	5.10E-09	miR-320-3p	0.778	3.84E-03	8mer	132-139
Pea15a	2.352	2.27E-14	miR-206-3p	0.664	2.84E-04	7mer-m8	286-292
Rhob	2.348	7.44E-21	miR-21c	0.609	2.84E-04	7mer-m8	1317-1323
Mllt1	2.343	1.54E-13	miR-495-3p	0.670	8.82E-05	7mer-A1	1794-1800
Iglon5	2.338	3.83E-10	let-7e-5p	0.678	1.81E-04	7mer-A1	1386-1392

			let-7c-5p	0.725	2.96E-03	7mer-A1	1386-1392
			let-7a-5p	0.737	4.64E-03	7mer-A1	1386-1392
			let-7i-5p	0.754	2.96E-03	7mer-A1	1386-1392
Sp2	2.334	2.74E-13	miR-206-3p	0.664	2.84E-04	8mer	536-543
			miR-495-3p	0.670	8.82E-05	7mer-A1	1044-1050
Pten	2.333	1.02E-14	miR-495-3p	0.670	8.82E-05	7mer-A1	3214-3220
			miR-495-3p	0.670	8.82E-05	8mer	3225-3232
			miR-219a-2-3p	0.777	9.18E-03	7mer-m8	133-139
			miR-320-3p	0.778	3.84E-03	8mer	2806-2813
Gpx3	2.331	8.26E-10	miR-134-5p	0.735	1.80E-04	8mer	1116-1123
Zbtb4	2.331	4.65E-10	miR-206-3p	0.664	2.84E-04	8mer	443-450
Usp32	2.329	1.30E-09	let-7e-5p	0.678	1.81E-04	7mer-m8	438-444
			miR-495-3p	0.670	8.82E-05	8mer	1650-1657
			let-7c-5p	0.725	2.96E-03	7mer-m8	438-444
			let-7a-5p	0.737	4.64E-03	7mer-m8	438-444
			let-7i-5p	0.754	2.96E-03	7mer-m8	438-444
Med22	2.323	1.40E-17	miR-423-5p	0.746	7.22E-03	7mer-m8	2178-2184
Csnk1a1	2.323	1.20E-08	miR-495-3p	0.670	8.82E-05	7mer-A1	331-337
			miR-495-3p	0.670	8.82E-05	7mer-A1	1180-1186
Zxdb	2.322	2.65E-12	miR-206-3p	0.664	2.84E-04	8mer	1962-1969
Mnt	2.321	8.14E-19	let-7e-5p	0.678	1.81E-04	7mer-A1	1607-1613
			let-7c-5p	0.725	2.96E-03	7mer-A1	1607-1613
			let-7a-5p	0.737	4.64E-03	7mer-A1	1607-1613
			let-7i-5p	0.754	2.96E-03	7mer-A1	1607-1613
Slc25a22	2.315	2.71E-14	miR-206-3p	0.664	2.84E-04	7mer-m8	225-231
Agpat1	2.314	1.35E-16	miR-206-3p	0.664	2.84E-04	8mer	262-269
R3hdm2	2.312	4.23E-14	miR-495-3p	0.670	8.82E-05	7mer-m8	487-493
			miR-495-3p	0.670	8.82E-05	7mer-m8	586-592
			miR-495-3p	0.670	8.82E-05	7mer-m8	590-596
			miR-495-3p	0.670	8.82E-05	7mer-m8	594-600
Las1l	2.311	3.07E-11	miR-320-3p	0.778	3.84E-03	7mer-m8	112-118
Pdgfb	2.309	1.59E-15	let-7e-5p	0.678	1.81E-04	7mer-m8	641-647
			let-7c-5p	0.725	2.96E-03	7mer-m8	641-647
			let-7a-5p	0.737	4.64E-03	7mer-m8	641-647
			let-7i-5p	0.754	2.96E-03	7mer-m8	641-647
Cbln1	2.308	2.41E-10	miR-320-3p	0.778	3.84E-03	7mer-m8	845-851
Glyr1	2.306	1.81E-15	miR-219a-2-3p	0.777	9.18E-03	7mer-m8	1306-1312
Naa20	2.302	8.51E-08	miR-320-3p	0.778	3.84E-03	7mer-A1	365-371
Magix	2.298	5.94E-04	miR-134-5p	0.735	1.80E-04	7mer-m8	994-1000
Sez6l	2.296	5.03E-08	miR-21c	0.609	2.84E-04	7mer-A1	2782-2788
Otud5	2.296	4.19E-18	miR-206-3p	0.664	2.84E-04	7mer-A1	236-242
			let-7e-5p	0.678	1.81E-04	8mer	1921-1928
			let-7c-5p	0.725	2.96E-03	8mer	1921-1928
			let-7a-5p	0.737	4.64E-03	8mer	1921-1928
			let-7i-5p	0.754	2.96E-03	8mer	1921-1928
Rnf44	2.294	1.57E-13	let-7e-5p	0.678	1.81E-04	7mer-A1	2041-2047
			let-7c-5p	0.725	2.96E-03	7mer-A1	2041-2047
			let-7a-5p	0.737	4.64E-03	7mer-A1	2041-2047
			let-7i-5p	0.754	2.96E-03	7mer-A1	2041-2047
Rab22a	2.290	3.71E-10	miR-21c	0.609	2.84E-04	7mer-m8	2342-2348
Cadm3	2.290	6.00E-16	miR-423-5p	0.746	7.22E-03	8mer	844-851
			miR-423-5p	0.746	7.22E-03	8mer	1830-1837
Ncf2	2.288	6.28E-09	miR-206-3p	0.664	2.84E-04	8mer	1105-1112
Ift80	2.283	5.71E-10	miR-206-3p	0.664	2.84E-04	8mer	337-344
Zyg11b	2.282	2.28E-13	miR-411-5p	0.687	1.81E-04	7mer-m8	6286-6292
Rbfox2	2.282	7.71E-20	miR-1224-5p	0.626	2.78E-06	8mer	939-946
			let-7e-5p	0.678	1.81E-04	7mer-A1	128-134
			let-7c-5p	0.725	2.96E-03	7mer-A1	128-134
			let-7a-5p	0.737	4.64E-03	7mer-A1	128-134
			let-7i-5p	0.754	2.96E-03	7mer-A1	128-134
Ypel2	2.278	2.69E-10	miR-206-3p	0.664	2.84E-04	7mer-m8	1919-1925
Plec	2.273	1.42E-08	miR-423-5p	0.746	7.22E-03	8mer	1167-1174
Hoxd1	2.273	2.69E-05	let-7e-5p	0.678	1.81E-04	7mer-m8	492-498
			let-7c-5p	0.725	2.96E-03	7mer-m8	492-498

			let-7a-5p	0.737	4.64E-03	7mer-m8	492-498
			let-7i-5p	0.754	2.96E-03	7mer-m8	492-498
Limd2	2.263	8.80E-15	let-7e-5p	0.678	1.81E-04	7mer-m8	364-370
			miR-382-5p	0.708	2.21E-05	7mer-m8	2353-2359
			let-7c-5p	0.725	2.96E-03	7mer-m8	364-370
			let-7a-5p	0.737	4.64E-03	7mer-m8	364-370
			let-7i-5p	0.754	2.96E-03	7mer-m8	364-370
			miR-219a-2-3p	0.777	9.18E-03	8mer	2133-2140
Ulk1	2.262	1.57E-15	miR-320-3p	0.778	3.84E-03	7mer-m8	466-472
Mark2	2.262	3.58E-13	miR-423-5p	0.746	7.22E-03	7mer-m8	1605-1611
Pcdh9	2.261	2.97E-10	miR-495-3p	0.670	8.82E-05	8mer	1275-1282
Apba1	2.260	1.05E-08	let-7e-5p	0.678	1.81E-04	7mer-m8	3102-3108
			let-7c-5p	0.725	2.96E-03	7mer-m8	3102-3108
			let-7a-5p	0.737	4.64E-03	7mer-m8	3102-3108
			let-7i-5p	0.754	2.96E-03	7mer-m8	3102-3108
Xpo1	2.259	1.08E-09	miR-1224-5p	0.626	2.78E-06	7mer-A1	669-675
			miR-320-3p	0.778	3.84E-03	7mer-m8	656-662
Trove2	2.258	1.64E-12	let-7e-5p	0.678	1.81E-04	7mer-A1	2753-2759
			let-7c-5p	0.725	2.96E-03	7mer-A1	2753-2759
			let-7a-5p	0.737	4.64E-03	7mer-A1	2753-2759
			let-7i-5p	0.754	2.96E-03	7mer-A1	2753-2759
			miR-320-3p	0.778	3.84E-03	7mer-m8	566-572
B630019K06Rik	2.256	1.32E-14	miR-219a-2-3p	0.777	9.18E-03	8mer	223-230
Zfp36l1	2.255	1.70E-07	miR-206-3p	0.664	2.84E-04	7mer-A1	939-945
			miR-206-3p	0.664	2.84E-04	7mer-m8	1605-1611
Mmp14	2.254	1.74E-06	miR-495-3p	0.670	8.82E-05	7mer-A1	1615-1621
Lrfn4	2.248	2.61E-09	let-7e-5p	0.678	1.81E-04	7mer-A1	122-128
			let-7c-5p	0.725	2.96E-03	7mer-A1	122-128
			let-7a-5p	0.737	4.64E-03	7mer-A1	122-128
			let-7i-5p	0.754	2.96E-03	7mer-A1	122-128
Itga9	2.243	9.16E-11	miR-134-5p	0.735	1.80E-04	7mer-m8	3583-3589
Stim2	2.239	5.08E-11	miR-320-3p	0.778	3.84E-03	7mer-A1	321-327
			miR-411-5p	0.687	1.81E-04	7mer-m8	151-157
Mvb12b	2.238	1.41E-20	let-7e-5p	0.678	1.81E-04	7mer-A1	1268-1274
			miR-495-3p	0.670	8.82E-05	7mer-A1	3461-3467
			miR-495-3p	0.670	8.82E-05	7mer-m8	3475-3481
			let-7c-5p	0.725	2.96E-03	7mer-A1	1268-1274
			let-7a-5p	0.737	4.64E-03	7mer-A1	1268-1274
			let-7i-5p	0.754	2.96E-03	7mer-A1	1268-1274
Acsl6	2.238	1.77E-17	let-7e-5p	0.678	1.81E-04	8mer	406-413
			miR-495-3p	0.670	8.82E-05	7mer-A1	3475-3481
			let-7c-5p	0.725	2.96E-03	8mer	406-413
			let-7a-5p	0.737	4.64E-03	8mer	406-413
			let-7i-5p	0.754	2.96E-03	8mer	406-413
Cntfr	2.232	7.33E-15	miR-21c	0.609	2.84E-04	7mer-m8	406-412
Fam168a	2.230	1.31E-06	miR-206-3p	0.664	2.84E-04	8mer	1021-1028
			miR-206-3p	0.664	2.84E-04	8mer	4582-4589
			miR-134-5p	0.735	1.80E-04	7mer-A1	25-31
Ppp2r2c	2.229	3.04E-08	miR-320-3p	0.778	3.84E-03	7mer-m8	2400-2406
Arhgap23	2.226	5.35E-14	miR-206-3p	0.664	2.84E-04	7mer-A1	929-935
Cdc34	2.226	2.05E-07	let-7e-5p	0.678	1.81E-04	7mer-A1	31-37
			let-7e-5p	0.678	1.81E-04	8mer	68-75
			let-7c-5p	0.725	2.96E-03	7mer-A1	31-37
			let-7c-5p	0.725	2.96E-03	8mer	68-75
			let-7a-5p	0.737	4.64E-03	7mer-A1	31-37
			let-7a-5p	0.737	4.64E-03	8mer	68-75
			let-7i-5p	0.754	2.96E-03	7mer-A1	31-37
			let-7i-5p	0.754	2.96E-03	8mer	68-75
Ctif	2.223	6.55E-11	let-7e-5p	0.678	1.81E-04	7mer-m8	3824-3830
			let-7c-5p	0.725	2.96E-03	7mer-m8	3824-3830
			let-7a-5p	0.737	4.64E-03	7mer-m8	3824-3830
			let-7i-5p	0.754	2.96E-03	7mer-m8	3824-3830
Vangl2	2.219	1.54E-09	let-7e-5p	0.678	1.81E-04	7mer-A1	2107-2113
			let-7e-5p	0.678	1.81E-04	7mer-m8	2910-2916
			let-7c-5p	0.725	2.96E-03	7mer-A1	2107-2113

			let-7c-5p	0.725	2.96E-03	7mer-m8	2910-2916
			let-7a-5p	0.737	4.64E-03	7mer-A1	2107-2113
			let-7a-5p	0.737	4.64E-03	7mer-m8	2910-2916
			let-7i-5p	0.754	2.96E-03	7mer-A1	2107-2113
			let-7i-5p	0.754	2.96E-03	7mer-m8	2910-2916
Crk	2.218	2.92E-09	let-7e-5p	0.678	1.81E-04	7mer-A1	1544-1550
			let-7c-5p	0.725	2.96E-03	7mer-A1	1544-1550
			let-7a-5p	0.737	4.64E-03	7mer-A1	1544-1550
			let-7i-5p	0.754	2.96E-03	7mer-A1	1544-1550
			miR-320-3p	0.778	3.84E-03	7mer-m8	100-106
Usf2	2.214	1.74E-18	miR-423-5p	0.746	7.22E-03	7mer-m8	76-82
G3bp2	2.213	6.77E-07	miR-206-3p	0.664	2.84E-04	7mer-A1	920-926
Zfp217	2.211	1.85E-04	miR-206-3p	0.664	2.84E-04	7mer-A1	1909-1915
Khsrp	2.202	8.74E-13	miR-206-3p	0.664	2.84E-04	7mer-m8	1385-1391
			let-7e-5p	0.678	1.81E-04	8mer	502-509
			let-7c-5p	0.725	2.96E-03	8mer	502-509
			let-7a-5p	0.737	4.64E-03	8mer	502-509
			let-7i-5p	0.754	2.96E-03	8mer	502-509
Tom1l2	2.202	2.71E-09	miR-423-5p	0.746	7.22E-03	8mer	2562-2569
Kank4	2.201	7.37E-06	miR-206-3p	0.664	2.84E-04	7mer-m8	114-120
Ddn	2.201	4.78E-06	let-7e-5p	0.678	1.81E-04	7mer-m8	1391-1397
			let-7c-5p	0.725	2.96E-03	7mer-m8	1391-1397
			let-7a-5p	0.737	4.64E-03	7mer-m8	1391-1397
			let-7i-5p	0.754	2.96E-03	7mer-m8	1391-1397
Nfatc4	2.200	4.17E-03	miR-423-5p	0.746	7.22E-03	7mer-m8	703-709
Slc16a3	2.199	3.29E-13	miR-1224-5p	0.626	2.78E-06	8mer	1920-1927
			miR-206-3p	0.664	2.84E-04	7mer-A1	174-180
			miR-134-5p	0.735	1.80E-04	8mer	1314-1321
Gpc4	2.191	8.69E-07	let-7e-5p	0.678	1.81E-04	7mer-A1	2291-2297
			let-7c-5p	0.725	2.96E-03	7mer-A1	2291-2297
			let-7a-5p	0.737	4.64E-03	7mer-A1	2291-2297
			let-7i-5p	0.754	2.96E-03	7mer-A1	2291-2297
Fndc3b	2.189	8.67E-08	miR-1224-5p	0.626	2.78E-06	8mer	2682-2689
			miR-206-3p	0.664	2.84E-04	8mer	2915-2922
			let-7e-5p	0.678	1.81E-04	7mer-A1	1379-1385
			let-7e-5p	0.678	1.81E-04	7mer-A1	2897-2903
			let-7c-5p	0.725	2.96E-03	7mer-A1	1379-1385
			let-7c-5p	0.725	2.96E-03	7mer-A1	2897-2903
			let-7a-5p	0.737	4.64E-03	7mer-A1	1379-1385
			let-7a-5p	0.737	4.64E-03	7mer-A1	2897-2903
			let-7i-5p	0.754	2.96E-03	7mer-A1	1379-1385
			let-7i-5p	0.754	2.96E-03	7mer-A1	2897-2903
			miR-219a-2-3p	0.777	9.18E-03	7mer-m8	2866-2872
Amotl2	2.184	3.91E-12	miR-495-3p	0.670	8.82E-05	7mer-A1	1628-1634
			miR-382-5p	0.708	2.21E-05	8mer	1487-1494
Ephb4	2.183	8.90E-06	miR-423-5p	0.746	7.22E-03	7mer-m8	475-481
			miR-219a-2-3p	0.777	9.18E-03	7mer-m8	1412-1418
Cacng2	2.180	1.00E-14	miR-320-3p	0.778	3.84E-03	8mer	1419-1426
Atad2b	2.179	6.05E-03	miR-411-5p	0.687	1.81E-04	7mer-m8	3134-3140
Palm3	2.179	1.89E-05	let-7e-5p	0.678	1.81E-04	7mer-m8	41-47
			let-7c-5p	0.725	2.96E-03	7mer-m8	41-47
			let-7a-5p	0.737	4.64E-03	7mer-m8	41-47
			let-7i-5p	0.754	2.96E-03	7mer-m8	41-47
Zfp280b	2.172	6.28E-09	let-7e-5p	0.678	1.81E-04	8mer	2452-2459
			let-7c-5p	0.725	2.96E-03	8mer	2452-2459
			let-7a-5p	0.737	4.64E-03	8mer	2452-2459
			let-7i-5p	0.754	2.96E-03	8mer	2452-2459
Eaf1	2.172	4.45E-10	miR-206-3p	0.664	2.84E-04	8mer	2394-2401
Gse1	2.170	7.42E-11	miR-495-3p	0.670	8.82E-05	7mer-m8	787-793
			miR-495-3p	0.670	8.82E-05	7mer-m8	826-832
			miR-495-3p	0.670	8.82E-05	7mer-m8	830-836
1700017B05Rik	2.169	3.68E-08	let-7e-5p	0.678	1.81E-04	8mer	279-286
			let-7c-5p	0.725	2.96E-03	8mer	279-286
			let-7a-5p	0.737	4.64E-03	8mer	279-286
			let-7i-5p	0.754	2.96E-03	8mer	279-286

Kcnd3	2.165	9.79E-09	miR-206-3p	0.664	2.84E-04	8mer	4480-4487
Col3a1	2.163	1.37E-04	let-7e-5p	0.678	1.81E-04	8mer	403-410
			let-7c-5p	0.725	2.96E-03	8mer	403-410
			let-7a-5p	0.737	4.64E-03	8mer	403-410
			let-7i-5p	0.754	2.96E-03	8mer	403-410
Scube3	2.163	1.58E-05	let-7e-5p	0.678	1.81E-04	7mer-m8	897-903
			let-7c-5p	0.725	2.96E-03	7mer-m8	897-903
			let-7a-5p	0.737	4.64E-03	7mer-m8	897-903
			let-7i-5p	0.754	2.96E-03	7mer-m8	897-903
Mbtps2	2.163	4.85E-07	let-7e-5p	0.678	1.81E-04	7mer-m8	1373-1379
			let-7c-5p	0.725	2.96E-03	7mer-m8	1373-1379
			let-7a-5p	0.737	4.64E-03	7mer-m8	1373-1379
			let-7i-5p	0.754	2.96E-03	7mer-m8	1373-1379
Igfbp4	2.162	2.76E-07	miR-320-3p	0.778	3.84E-03	8mer	353-360
Prex1	2.162	5.74E-13	miR-206-3p	0.664	2.84E-04	8mer	397-404
			miR-411-5p	0.687	1.81E-04	7mer-A1	811-817
			miR-382-5p	0.708	2.21E-05	7mer-m8	796-802
Epha2	2.159	3.44E-03	miR-206-3p	0.664	2.84E-04	7mer-m8	645-651
Shank1	2.158	1.85E-08	miR-423-5p	0.746	7.22E-03	8mer	424-431
Zbtb6	2.157	1.00E-07	miR-206-3p	0.664	2.84E-04	7mer-m8	2845-2851
			miR-219a-2-3p	0.777	9.18E-03	8mer	427-434
Traf7	2.154	1.50E-11	miR-495-3p	0.670	8.82E-05	7mer-A1	1553-1559
Golga7b	2.153	7.05E-14	let-7e-5p	0.678	1.81E-04	8mer	1521-1528
			let-7c-5p	0.725	2.96E-03	8mer	1521-1528
			let-7a-5p	0.737	4.64E-03	8mer	1521-1528
			let-7i-5p	0.754	2.96E-03	8mer	1521-1528
Rimbp2	2.150	4.08E-07	miR-21c	0.609	2.84E-04	7mer-A1	60-66
Cd276	2.148	4.83E-06	let-7e-5p	0.678	1.81E-04	7mer-A1	1476-1482
			let-7c-5p	0.725	2.96E-03	7mer-A1	1476-1482
			let-7a-5p	0.737	4.64E-03	7mer-A1	1476-1482
			let-7i-5p	0.754	2.96E-03	7mer-A1	1476-1482
Chd4	2.147	1.86E-12	let-7e-5p	0.678	1.81E-04	7mer-m8	427-433
			let-7c-5p	0.725	2.96E-03	7mer-m8	427-433
			let-7a-5p	0.737	4.64E-03	7mer-m8	427-433
			let-7i-5p	0.754	2.96E-03	7mer-m8	427-433
Ets1	2.144	1.82E-07	miR-206-3p	0.664	2.84E-04	8mer	2885-2892
			miR-495-3p	0.670	8.82E-05	7mer-m8	648-654
			miR-495-3p	0.670	8.82E-05	7mer-m8	3268-3274
Mfrp	2.144	4.67E-05	miR-411-5p	0.687	1.81E-04	8mer	1738-1745
Atl3	2.141	1.06E-10	miR-320-3p	0.778	3.84E-03	7mer-m8	283-289
Jph1	2.140	9.74E-09	miR-21c	0.609	2.84E-04	7mer-m8	2236-2242
Eef2k	2.134	3.30E-11	let-7e-5p	0.678	1.81E-04	7mer-m8	638-644
			let-7c-5p	0.725	2.96E-03	7mer-m8	638-644
			let-7a-5p	0.737	4.64E-03	7mer-m8	638-644
			let-7i-5p	0.754	2.96E-03	7mer-m8	638-644
B930041F14Rik	2.134	1.60E-15	let-7e-5p	0.678	1.81E-04	7mer-m8	1228-1234
			let-7c-5p	0.725	2.96E-03	7mer-m8	1228-1234
			let-7a-5p	0.737	4.64E-03	7mer-m8	1228-1234
			let-7i-5p	0.754	2.96E-03	7mer-m8	1228-1234
Rai1	2.128	3.69E-10	miR-1224-5p	0.626	2.78E-06	7mer-m8	817-823
Fam155a	2.128	3.31E-15	miR-206-3p	0.664	2.84E-04	7mer-m8	1443-1449
			miR-320-3p	0.778	3.84E-03	7mer-m8	200-206
Dlgap4	2.120	4.00E-12	let-7e-5p	0.678	1.81E-04	8mer	1417-1424
			let-7c-5p	0.725	2.96E-03	8mer	1417-1424
			let-7a-5p	0.737	4.64E-03	8mer	1417-1424
			let-7i-5p	0.754	2.96E-03	8mer	1417-1424
Dlgap4	2.120	4.00E-12	miR-423-5p	0.746	7.22E-03	7mer-m8	1409-1415
Slmap	2.120	2.01E-10	miR-21c	0.609	2.84E-04	7mer-m8	916-922
Slit1	2.116	6.62E-14	miR-495-3p	0.670	8.82E-05	7mer-A1	3403-3409
Ell2	2.115	1.58E-08	miR-495-3p	0.670	8.82E-05	8mer	225-232
			miR-320-3p	0.778	3.84E-03	8mer	1059-1066
Fam117b	2.115	3.20E-09	miR-206-3p	0.664	2.84E-04	8mer	1131-1138
			miR-320-3p	0.778	3.84E-03	7mer-m8	512-518
Tmem64	2.114	9.62E-06	miR-320-3p	0.778	3.84E-03	7mer-A1	891-897

			miR-320-3p	0.778	3.84E-03	8mer	952-959
Ppargc1b	2.113	3.99E-04	miR-495-3p	0.670	8.82E-05	7mer-m8	5889-5895
			miR-495-3p	0.670	8.82E-05	7mer-m8	5893-5899
			miR-495-3p	0.670	8.82E-05	7mer-m8	5897-5903
			miR-495-3p	0.670	8.82E-05	7mer-m8	5901-5907
			let-7e-5p	0.678	1.81E-04	7mer-A1	24-30
			let-7e-5p	0.678	1.81E-04	7mer-A1	32-38
			let-7c-5p	0.725	2.96E-03	7mer-A1	24-30
			let-7c-5p	0.725	2.96E-03	7mer-A1	32-38
			let-7a-5p	0.737	4.64E-03	7mer-A1	24-30
			let-7a-5p	0.737	4.64E-03	7mer-A1	32-38
			let-7i-5p	0.754	2.96E-03	7mer-A1	24-30
			let-7i-5p	0.754	2.96E-03	7mer-A1	32-38
Adipor2	2.109	3.70E-03	let-7e-5p	0.678	1.81E-04	7mer-A1	182-188
			let-7c-5p	0.725	2.96E-03	7mer-A1	182-188
			let-7a-5p	0.737	4.64E-03	7mer-A1	182-188
			let-7i-5p	0.754	2.96E-03	7mer-A1	182-188
Rnf217	2.108	1.39E-07	let-7e-5p	0.678	1.81E-04	7mer-A1	9027-2033
			let-7c-5p	0.725	2.96E-03	7mer-A1	9027-2033
			let-7a-5p	0.737	4.64E-03	7mer-A1	9027-2033
			let-7i-5p	0.754	2.96E-03	7mer-A1	9027-2033
Sypl2	2.098	1.25E-03	miR-134-5p	0.735	1.80E-04	8mer	2662-2669
Shank3	2.091	2.11E-10	miR-423-5p	0.746	7.22E-03	8mer	534-541
Slc36a4	2.087	3.04E-10	miR-320-3p	0.778	3.84E-03	7mer-A1	1920-1926
Sox11	2.088	9.24E-09	miR-495-3p	0.670	8.82E-05	7mer-m8	6593-6599
Stk24	2.086	6.79E-09	let-7e-5p	0.678	1.81E-04	7mer-A1	670-676
			let-7c-5p	0.725	2.96E-03	7mer-A1	670-676
			let-7a-5p	0.737	4.64E-03	7mer-A1	670-676
			let-7i-5p	0.754	2.96E-03	7mer-A1	670-676
			miR-320-3p	0.778	3.84E-03	7mer-A1	797-803
Dpp3	2.086	8.12E-13	let-7e-5p	0.678	1.81E-04	8mer	111-118
			let-7c-5p	0.725	2.96E-03	8mer	111-118
			let-7a-5p	0.737	4.64E-03	8mer	111-118
			let-7i-5p	0.754	2.96E-03	8mer	111-118
Lrrc14	2.084	2.09E-13	miR-134-5p	0.735	1.80E-04	8mer	1638-1645
Hipk2	2.083	1.76E-07	let-7e-5p	0.678	1.81E-04	7mer-A1	7178-7184
			let-7c-5p	0.725	2.96E-03	7mer-A1	7178-7184
			let-7a-5p	0.737	4.64E-03	7mer-A1	7178-7184
			let-7i-5p	0.754	2.96E-03	7mer-A1	7178-7184
			miR-320-3p	0.778	3.84E-03	7mer-A1	6281-6287
			miR-320-3p	0.778	3.84E-03	7mer-A1	9410-9416
Efnb2	2.082	9.37E-07	miR-206-3p	0.664	2.84E-04	8mer	3086-3093
Nek9	2.081	7.86E-12	let-7e-5p	0.678	1.81E-04	7mer-A1	270-276
			let-7c-5p	0.725	2.96E-03	7mer-A1	270-276
			let-7a-5p	0.737	4.64E-03	7mer-A1	270-276
			let-7i-5p	0.754	2.96E-03	7mer-A1	270-276
Rbfox1	2.078	1.98E-08	miR-206-3p	0.664	2.84E-04	7mer-A1	718-724
			let-7e-5p	0.678	1.81E-04	7mer-A1	202-208
			let-7c-5p	0.725	2.96E-03	7mer-A1	202-208
			let-7a-5p	0.737	4.64E-03	7mer-A1	202-208
			let-7i-5p	0.754	2.96E-03	7mer-A1	202-208
Prrc1	2.075	5.37E-12	miR-206-3p	0.664	2.84E-04	7mer-A1	159-165
Jund	2.074	6.18E-06	miR-206-3p	0.664	2.84E-04	7mer-m8	469-475
Icmt	2.069	8.00E-09	miR-320-3p	0.778	3.84E-03	8mer	438-445
Metrn	2.064	2.16E-05	miR-423-5p	0.746	7.22E-03	7mer-m8	540-546
Fstl4	2.060	1.46E-03	let-7e-5p	0.678	1.81E-04	8mer	3391-3398
			let-7c-5p	0.725	2.96E-03	8mer	3391-3398
			let-7a-5p	0.737	4.64E-03	8mer	3391-3398
			let-7i-5p	0.754	2.96E-03	8mer	3391-3398
Mgat5	2.057	4.47E-11	miR-495-3p	0.670	8.82E-05	7mer-A1	3769-3775
			miR-206-3p	0.664	2.84E-04	8mer	4448-4455
Pbx3	2.056	3.03E-12	let-7e-5p	0.678	1.81E-04	7mer-A1	938-944
			let-7e-5p	0.678	1.81E-04	7mer-m8	1005-1011
			let-7c-5p	0.725	2.96E-03	7mer-A1	938-944
			let-7c-5p	0.725	2.96E-03	7mer-m8	1005-1011

			let-7a-5p	0.737	4.64E-03	7mer-A1	938-944
			let-7a-5p	0.737	4.64E-03	7mer-m8	1005-1011
			let-7i-5p	0.754	2.96E-03	7mer-A1	938-944
			let-7i-5p	0.754	2.96E-03	7mer-m8	1005-1011
			miR-320-3p	0.778	3.84E-03	8mer	218-225
			miR-320-3p	0.778	3.84E-03	8mer	929-936
2700081O15Rik	2.053	3.99E-09	miR-21c	0.609	2.84E-04	7mer-m8	102-1108
Adora1	2.052	8.05E-08	miR-423-5p	0.746	7.22E-03	7mer-m8	508-514
Mesdc1	2.048	5.01E-11	let-7e-5p	0.678	1.81E-04	7mer-A1	354-360
			let-7c-5p	0.725	2.96E-03	7mer-A1	354-360
			let-7a-5p	0.737	4.64E-03	7mer-A1	354-360
			let-7i-5p	0.754	2.96E-03	7mer-A1	354-360
Ttbk1	2.043	1.64E-11	miR-134-5p	0.735	1.80E-04	7mer-m8	2592-2598
Magi2	2.039	8.83E-14	miR-206-3p	0.664	2.84E-04	7mer-A1	2431-2437
			miR-134-5p	0.735	1.80E-04	7mer-A1	2517-2523
			miR-320-3p	0.778	3.84E-03	7mer-A1	783-789
Btbd11	2.037	1.03E-07	miR-495-3p	0.670	8.82E-05	8mer	1128-1135
Klf3	2.034	7.56E-05	miR-21c	0.609	2.84E-04	8mer	3478-3485
			miR-1224-5p	0.626	2.78E-06	7mer-m8	3674-3680
Shisa7	2.033	2.48E-06	miR-320-3p	0.778	3.84E-03	7mer-m8	3507-3513
Arf3	2.030	8.81E-12	miR-206-3p	0.664	2.84E-04	7mer-A1	227-233
			miR-206-3p	0.664	2.84E-04	7mer-m8	2398-2404
Ranbp9	2.028	1.35E-08	miR-495-3p	0.670	8.82E-05	7mer-m8	545-552
Sp9	2.023	5.34E-05	miR-495-3p	0.670	8.82E-05	7mer-m8	1360-1366
C77080	2.022	2.26E-07	miR-206-3p	0.664	2.84E-04	8mer	432-439
Mta3	2.021	6.20E-09	miR-495-3p	0.670	8.82E-05	7mer-m8	53-59
			miR-495-3p	0.670	8.82E-05	7mer-m8	57-63
Emilin2	2.020	1.39E-05	miR-320-3p	0.778	3.84E-03	7mer-A1	39-45
Egln2	2.019	3.56E-10	let-7e-5p	0.678	1.81E-04	7mer-A1	484-490
			let-7c-5p	0.725	2.96E-03	7mer-A1	484-490
			let-7a-5p	0.737	4.64E-03	7mer-A1	484-490
			let-7i-5p	0.754	2.96E-03	7mer-A1	484-490
Fbxo33	2.018	2.49E-07	miR-206-3p	0.664	2.84E-04	8mer	1156-1163
Mink1	2.018	1.17E-09	miR-495-3p	0.670	8.82E-05	7mer-A1	737-743
			miR-219a-2-3p	0.777	9.18E-03	8mer	750-757
Map4k4	2.018	8.77E-09	let-7e-5p	0.678	1.81E-04	8mer	976-983
			let-7c-5p	0.725	2.96E-03	8mer	976-983
			let-7a-5p	0.737	4.64E-03	8mer	976-983
			let-7i-5p	0.754	2.96E-03	8mer	976-983
Acvr1	2.017	1.12E-08	miR-382-5p	0.708	2.21E-05	7mer-m8	635-641
AI846148	2.016	8.48E-10	let-7e-5p	0.678	1.81E-04	7mer-m8	404-410
			let-7c-5p	0.725	2.96E-03	7mer-m8	404-410
			let-7a-5p	0.737	4.64E-03	7mer-m8	404-410
			let-7i-5p	0.754	2.96E-03	7mer-m8	404-410
Skida1	2.014	3.34E-06	miR-495-3p	0.670	8.82E-05	8mer	2936-2942
			let-7e-5p	0.678	1.81E-04	7mer-A1	318-324
			let-7c-5p	0.725	2.96E-03	7mer-A1	318-324
			let-7a-5p	0.737	4.64E-03	7mer-A1	318-324
			let-7i-5p	0.754	2.96E-03	7mer-A1	318-324
Tspan33	2.014	1.17E-10	miR-495-3p	0.670	8.82E-05	7mer-m8	906-912
Gsg1l	2.012	1.95E-09	let-7e-5p	0.678	1.81E-04	7mer-m8	1621-1627
			let-7c-5p	0.725	2.96E-03	7mer-m8	1621-1627
			let-7a-5p	0.737	4.64E-03	7mer-m8	1621-1627
			let-7i-5p	0.754	2.96E-03	7mer-m8	1621-1627
Bahd1	2.010	6.68E-09	miR-21c	0.609	2.84E-04	7mer-m8	1500-1506
			let-7e-5p	0.678	1.81E-04	7mer-A1	387-393
			let-7c-5p	0.725	2.96E-03	7mer-A1	387-393
			let-7a-5p	0.737	4.64E-03	7mer-A1	387-393
			let-7i-5p	0.754	2.96E-03	7mer-A1	387-393
			miR-320-3p	0.778	3.84E-03	8mer	381-388
Ephb2	2.007	2.89E-13	miR-495-3p	0.670	8.82E-05	7mer-m8	826-832
			miR-495-3p	0.670	8.82E-05	7mer-m8	895-901
Pptc7	2.007	1.70E-08	let-7e-5p	0.678	1.81E-04	7mer-A1	1355-1361
			let-7c-5p	0.725	2.96E-03	7mer-A1	1355-1361
			let-7a-5p	0.737	4.64E-03	7mer-A1	1355-1361

			let-7i-5p	0.754	2.96E-03	7mer-A1	1355-1361
Tsc22d4	2.006	1.32E-14	miR-320-3p	0.778	3.84E-03	7mer-A1	86-92
Tfip11	2.005	1.71E-11	miR-1224-5p	0.626	2.78E-06	7mer-m8	239-245
Bpnt1	2.005	1.74E-10	miR-206-3p	0.664	2.84E-04	7mer-m8	866-872
Cadm1	2.005	2.34E-08	miR-21c	0.609	2.84E-04	7mer-m8	2768-2774
Nacc2	2.005	3.93E-09	miR-495-3p	0.670	8.82E-05	7mer-m8	3667-3673
			miR-320-3p	0.778	3.84E-03	8mer	3536-3543
Etv5	2.005	3.38E-06	miR-134-5p	0.735	1.80E-04	8mer	622-629
Samd4	2.004	2.04E-11	miR-495-3p	0.670	8.82E-05	8mer	4126-4133
Osbpl7	2.002	1.73E-06	miR-206-3p	0.664	2.84E-04	8mer	818-825
Zbtb16	2.001	3.99E-03	let-7e-5p	0.678	1.81E-04	7mer-A1	1292-1298
			let-7e-5p	0.678	1.81E-04	7mer-m8	1874-1880
			let-7e-5p	0.678	1.81E-04	8mer	4746-4753
			let-7c-5p	0.725	2.96E-03	7mer-A1	1292-1298
			let-7c-5p	0.725	2.96E-03	7mer-m8	1874-1880
			let-7c-5p	0.725	2.96E-03	8mer	4746-4753
			let-7a-5p	0.737	4.64E-03	7mer-A1	1292-1298
			let-7a-5p	0.737	4.64E-03	7mer-m8	1874-1880
			let-7a-5p	0.737	4.64E-03	8mer	4746-4753
			miR-423-5p	0.746	7.22E-03	8mer	537-544
			let-7i-5p	0.754	2.96E-03	7mer-A1	1292-1298
			let-7i-5p	0.754	2.96E-03	7mer-m8	1874-1880
			let-7i-5p	0.754	2.96E-03	8mer	4746-4753
Spred3	2.001	1.67E-12	let-7e-5p	0.678	1.81E-04	7mer-m8	2235-2241
			let-7c-5p	0.725	2.96E-03	7mer-m8	2235-2241
			let-7a-5p	0.737	4.64E-03	7mer-m8	2235-2241
			let-7i-5p	0.754	2.96E-03	7mer-m8	2235-2241
Eme2	2.001	5.67E-11	miR-1224-5p	0.626	2.78E-06	7mer-m8	1731-1737
			miR-134-5p	0.735	1.80E-04	8mer	2270-2277
Zfp825	0.494	2.71E-03	miR-181c-5p	1.325	2.96E-03	8mer	155-162
			miR-181c-5p	1.325	2.96E-03	8mer	773-780
Pik3c2a	0.481	8.03E-07	miR-219a-5p	1.858	2.44E-10	7mer-m8	1390-1396
			miR-195a-5p	1.476	2.07E-04	7mer-A1	367-373
			miR-23a-3p	1.401	3.50E-04	7mer-m8	2726-2732
			miR-15a-5p	1.375	2.96E-03	7mer-A1	367-373
			miR-124-3p	1.335	8.42E-03	8mer	519-526
			miR-124-3p	1.335	8.42E-03	7mer-m8	1979-1985
			miR-124-3p	1.335	8.42E-03	7mer-A1	2467-2473
			miR-23b-3p	1.327	1.72E-03	7mer-m8	2726-2732
Gm6710	0.465	3.85E-07	miR-181c-5p	1.325	2.96E-03	8mer	71-78
Slc35a1	0.460	2.33E-06	miR-135a-5p	1.522	2.22E-05	7mer-m8	430-436
			miR-135b-5p	1.451	1.38E-04	7mer-m8	430-436
Tmed5	0.458	1.02E-08	miR-135a-5p	1.522	2.22E-05	8mer	1575-1582
			miR-135b-5p	1.451	1.38E-04	8mer	1575-1582
Gcnt1	0.452	8.58E-03	miR-23a-3p	1.401	3.50E-04	8mer	1353-1360
			miR-23b-3p	1.327	1.72E-03	8mer	1353-1360
A230046K03Rik	0.445	9.34E-11	miR-135a-5p	1.522	2.21E-05	8mer	648-655
			miR-135b-5p	1.451	1.38E-04	8mer	648-655
Crip3	0.443	7.44E-03	miR-195a-5p	1.476	2.07E-04	7mer-A1	16-22
			miR-15a-5p	1.375	2.96E-03	7mer-A1	16-22
Diap3	0.434	8.60E-05	miR-219a-5p	1.858	2.44E-10	8mer	819-826
			miR-301a-3p	1.389	7.38E-04	8mer	950-957
Gm14327	0.429	1.74E-10	miR-181c-5p	1.325	2.96E-03	8mer	1685-1692
			miR-181c-5p	1.325	2.96E-03	8mer	1769-1776
			miR-181c-5p	1.325	2.96E-03	8mer	1853-1860
			miR-181c-5p	1.325	2.96E-03	8mer	2020-2027
			miR-181c-5p	1.325	2.96E-03	8mer	2104-2111
			miR-181c-5p	1.325	2.96E-03	8mer	2187-2194
Gbp7	0.422	4.10E-04	miR-135a-5p	1.522	2.21E-05	7mer-m8	3356-3362
			miR-135b-5p	1.451	1.38E-04	7mer-m8	3356-3362
			miR-23a-3p	1.401	3.50E-04	8mer	3541-3548
			miR-23b-3p	1.327	1.72E-03	8mer	3541-3548
Ddx3y	0.414	3.41E-09	miR-19b-3p	1.524	2.21E-05	7mer-A1	1414-1420
			miR-19b-3p	1.524	2.21E-05	8mer	1747-1754
			miR-29c-3p	1.503	2.10E-05	7mer-A1	1346-1352

			miR-195a-5p	1.476	2.07E-04	8mer	1767-1774
			miR-19a-3p	1.384	2.96E-03	7mer-A1	1414-1420
			miR-19a-3p	1.384	2.96E-03	8mer	1747-1754
			miR-15a-5p	1.375	2.96E-03	8mer	1767-1774
			miR-124-3p	1.335	8.42E-03	7mer-m8	1284-1290
			miR-29a-3p	1.300	2.79E-03	7mer-A1	1346-1352
			miR-29b-3p	1.278	9.08E-03	7mer-A1	1346-1352
Gm12689	0.346	01.18E-04	miR-342-3p	1.506	2.70E-04	8mer	738-745
			miR-23a-3p	1.401	3.50E-04	8mer	421-428
			miR-23b-3p	1.327	1.72E-03	8mer	421-428

2.D. Discussion

Oral nicotine administration and spontaneous withdrawal is a valid model of acute and prolonged nicotine withdrawal-associated anxiety

We used a mouse model of oral nicotine administration and spontaneous withdrawal to determine transcriptome-wide changes in miRNA and mRNA expression. Our lab has previously published that treatment with oral nicotine at this dose (200 µg/ml) results in nicotine dependence and measurement of serum cotinine, a biomarker for nicotine exposure, is consistent with those observed in heavy smokers (Lawson et al. 1998, Zhao-Shea et al. 2015). We further confirmed this was a valid model of nicotine dependence and withdrawal by assessing anxiety, one of the most prominent affective symptoms of nicotine withdrawal, 48 hours after cessation of chronic oral nicotine treatment. Mice in acute withdrawal (NAWD) did indeed show increased anxiety, burying more marbles during the MBT and spending less time in the open arms of the EPM compared to TA controls. These results are consistent with previous data published by Zhao-Shea et al., showing 6-week treatment with 200 µg/ml nicotine drinking solution followed by precipitated or spontaneous (24-hr) withdrawal is sufficient to induce activation of the IPN and increase anxiety in the MBT and EPM (Zhao-Shea et al. 2013).

To determine the persistence of affective withdrawal symptoms, we also measured anxiety after a prolonged, 4-week withdrawal from a 6-week oral

nicotine treatment (NLWD). Interestingly, NLWD mice displayed increased anxiety in the EPM, but not the MBT. This is consistent with reports of human patients experiencing nicotine withdrawal, with affective symptoms peaking within the first week of withdrawal and lasting up to 2-4 weeks (Hughes 2007). In mice, somatic signs of withdrawal also peak within the first few days of withdrawal and then subside within a week (Damaj et al. 2003). Because the MBT uses a physical action (digging) as a measure of anxiety, there may be a contribution of physical discomfort and other somatic signs to the outcome of this test. This may explain why the anxious phenotype of NLWD mice as measured by the MBT is diminished to a non-statistically significant trend. Additionally, pharmacological assessment of the MBT suggests that this assay may be limited in its ability to evaluate anxiety. Diazepam, an anxiolytic, has been shown to decrease marble burying (Jimenez-Gomez et al. 2011). However, βCCM, a beta carboline known to be anxiogenic in rodents, is unable to increase marble burying in mice (Jimenez-Gomez et al. 2011). To confirm the anxious phenotype of NLWD mice observed in the EPM, at least one additional behavioral assay for anxiety, such as the open field test should be performed. The open field test may be provide more consistent results this assay has been used to detect anxiogenic effects during pharmacological testing (Prut and Belzung 2003).

Transcriptional Regulation of mRNAs in the Reward Circuitry by Nicotine Treatment and Withdrawal.

Transcriptome-wide expression changes in the mesocorticolimbic reward circuit induced by chronic nicotine treatment and withdrawal were measured by mRNA-Seq. Differential mRNA expression analysis identified an abundance of mRNAs significantly up- or down-regulated (FDR < 0.01) by nicotine treatment or withdrawal. To narrow our focus to mRNAs that undergo robust changes in expression, we considered only genes that exhibit fold changes > 2.

In the NAc, there were widespread alterations in mRNA expression during chronic nicotine treatment compared to TA controls. These changes in gene expression are likely reflective of the activation the mesocorticolimbic reward pathway in response to nicotine exposure. This is supported by the GO analysis which shows up- or down regulated genes are enriched in terms related to the structure and function of the synapse, vesicle, and neuron projections. In addition, there is an enrichment of up-regulated genes in terms related to the mitochondrion and ribosome. Alterations in the expression of genes related to metabolic processes and the mitochondrial respiratory chain are consistent with a previous reports looking at the regulation of RNA in neocortical neurons after chronic nicotine treatment (Yang et al. 2017). The regulation of genes related to mitochondrial and ribosomal function may reflect efforts to fulfill the increased demands for energy and protein products in activated neurons.

In contrast, there are very few alterations in gene expression in the NAc when mice in acute nicotine withdrawal were compared to TA controls. This would suggest that in the NAc, the majority of genes regulated by chronic nicotine exposure rapidly return to the expression levels observed in drug-naïve animals after nicotine cessation. However, there is a small subset of genes that remain similarly altered when Nic and NAWD are compared to TA controls. This suggests that this select group of genes is differentially expressed during chronic nicotine exposure and these changes in expression persist for at least 48 hours after nicotine is spontaneously withdrawn. If regulation of mRNA level was the consequence solely of nicotine withdrawal (Figure 2.13 orange), expression of a gene would be similarly altered when NAWD mice are compared to either TA- or Nic-treated mice. Because there is no commonality among the genes that are differentially expressed when NAWD mice are compared to TA or Nic, the initial nicotine exposure itself must have some contribution to all of the differential expression observed in acute nicotine withdrawal. The propensity for mRNA expression to rapidly return to control levels after nicotine exposure is ceased makes it unlikely that gene regulation at the transcript level in the NAc contributes to anxiety behaviors observed in acute nicotine withdrawal.

Chronic nicotine treatment also induces extensive changes in mRNA expression in the midbrain. In contrast to the NAc, there are few genes regulated in the midbrain only during chronic nicotine treatment, rapidly returning expression levels indistinguishable from drug-naïve animals during acute

withdrawal. The majority (~92%) of genes differentially expressed during chronic nicotine exposure are similarly altered in NAWD mice compared to TA controls. Hence, regulation of these mRNAs, representing ~30% of all genes differentially expressed during acute withdrawal, is initially a consequence of the chronic nicotine treatment, with the effect persisting for at least 48 hours after spontaneous withdrawal. Of the remaining mRNAs altered during acute nicotine withdrawal, a subset of only 30 mRNAs are similarly differentially expressed in NAWD compared to either TA or Nic mice. This indicates that only a small fraction (~2%) of all genes altered during acute withdrawal are up- or down-regulated solely after nicotine is withdrawn, with no effects of nicotine treatment contributing to their regulation. Stated another way, chronic nicotine treatment itself contributes at least partly to the regulation of the majority of mRNAs differentially expressed during acute nicotine withdrawal. This conclusion is further supported by the GO analysis. In the midbrain, the terms describing the CC, MF and BP that are significantly enriched in genes up- or down-regulated during nicotine treatment or acute withdrawal are largely the same. Similar to the NAc, nicotine (and withdrawal) responsive genes are overrepresented in GO terms that likely reflect neuroadaptations induced by the activation of the mesocorticolimbic circuit during nicotine treatment, including those related to the structure and function of the synapse, vesicle, and neuron projections.

While the majority of differentially expressed genes in both the NAc and midbrain are regulated as a consequence of nicotine exposure itself, the

persistence of these expression changes during acute nicotine withdrawal are only observed in midbrain punches, enriched for the VTA. Although traditionally thought of as part of the reward circuitry, the VTA is also interconnected with the habenulo-interpeduncular withdrawal circuitry and plays a role in nicotine withdrawal-associated anxiety (Zhao-Shea et al. 2015, Molas et al. 2017). In light of this dual role of the VTA, our results lead to the hypothesis that differential expression of mRNAs in the midbrain occurring after chronic nicotine exposure and acute withdrawal may be involved in the molecular mechanisms underlying nicotine withdrawal symptoms including anxiety. These genes and their neuronal functions should be the focus of future studies.

Although the NAc and midbrain both show widespread differential expression of genes induced by chronic nicotine treatment, only 1 is similarly regulated in both brain regions. Thus, expression in NAc and midbrain are regulated by nicotine in a brain-region specific manner. Further supporting this, GO analysis revealed that reciprocally regulated mRNAs in the NAc and midbrain were enriched in the same CC, BP, and MF terms. For example, GO terms related to neuron projections, the synapse, receptor binding, regulation of neurotransmitter levels, and cell-to-cell communication are significantly enriched in genes that are down-regulated in the NAc and up-regulated in the midbrain during chronic nicotine treatment. This inverse relationship reflects the brain-region specificity of neuroadaptative mechanisms induced by chronic nicotine exposure. Both brain regions show enrichment of CC, BP, and MF terms related

to heterocycle metabolism in up- and down-regulated genes. This may reflect the induction of compensatory mechanisms to metabolize nicotine, a heterocyclic compound.

Differential expression analysis identified only 40 mRNAs in the NAc and 1 mRNA in the midbrain that were uniquely altered after a prolonged nicotine withdrawal compared to age-matched TAL controls. This suggests their up- or down-regulation occurs over a longer time course (beyond the acute 48-hour time point) and persists for at least 4 weeks. Interestingly, synaptic depression in the NAc shell is observed in acute withdrawal (24hr) from cocaine, while potentiation is observed after a long (10-14 days) withdrawal (Kourrich et al. 2007). It is believed this effect is a function of time, as further work determined prolonged cocaine treatment in the absence of withdrawal also induced potentiation at the glutamatergic synapses of NAc MSNs (Dobi et al. 2011). Delayed sensitization of DA responses to nicotine has also been observed in the NAc. Exposure to nicotine 3 weeks prior was sufficient to enhance electrically evoked [^{3}H]DA release from the NAc in slice (Schoffelmeer et al. 2002). The differential expression observed in the NAc of NLWD mice may reflect this delayed sensitization to nicotine stimulation. Because mice remain anxious for 4 weeks after withdrawal, regulation of this limited group of genes may also contribute to the neuroadaptations underlying persistent anxiety induced by nicotine withdrawal and should be the subject of future studies.

Regulation of miRNAs and their targets in the reward circuitry during chronic nicotine treatment and withdrawal.

Integrated differential expression analysis of miRNA- and mRNA-Seq data was used in conjunction with TargetScan Mouse 7.1 to identify predicted targets of conserved miRNAs up- or down-regulated during nicotine treatment and acute withdrawal. Because miRNAs are traditionally negative regulators of gene expression (Bartel 2018), only inversely regulated mRNA targets were identified. Additionally, because conservation strengthens the validity of miRNA target prediction (Friedman et al. 2009), only conserved miRNAs and MREs were considered in this analysis.

Differential expression of miRNAs by chronic nicotine treatment and acute withdrawal in the NAc, follows the same pattern observed for the mRNAs. Generally, in the NAc, alterations in miRNA expression occur during chronic nicotine treatment and then rapidly return to control levels after nicotine is withdrawn. There are only 8 conserved miRNAs differentially expressed during nicotine treatment compared to TA controls. Despite their limited quantity, these miRNAs are predicted to target conserved MREs within the 3′-UTR of at least one of 204 inversely regulated mRNAs. This means that ~24% of all nicotine responsive mRNAs are predicted targets of anti-correlated, conserved miRNAs. Also, all but 10 of the predicted targets return to control expression levels during acute nicotine withdrawal, as observed for all of the miRNAs themselves. Each of the miRNAs differentially expressed in the NAc during nicotine treatment are up-

or down-regulated with small fold changes (FC > 1.5). However, the presence of more than one predicted MRE within the 3′-UTR of ~40% of the predicted mRNA targets increase the likelihood that miRNAs play a biologically important role in the regulation of mRNAs by chronic nicotine treatment in the NAc.

In contrast to the NAc, the midbrain has only 3 miRNAs differentially expressed by nicotine treatment. Furthermore, the expression of only one predicted mRNA target is anti-correlated. However, when NAWD mice are compared to TA controls, 54 conserved miRNAs are differentially expressed. Thirty of these miRNAs were predicted to target a conserved MRE within the 3′-UTR of at least one of 380 inversely regulated mRNAs. Again, all of the miRNAs are up- or down-regulated with modest fold changes (FC <2). However, about half of the mRNA targets contain multiple MREs for the same or distinct miRNAs, supporting the hypothesis that the limited number of modestly differentially expressed miRNAs contributes to the regulation of mRNAs in the midbrain during acute nicotine withdrawal.

Of the 380 predicted mRNAs predicted to be targets of inversely expressed miRNAs in NAWD mice compared to TA controls, 105 (~28%) are similarly differentially expressed during nicotine treatment alone. Additionally, only 7 (~2%) of the predicted mRNA targets are similarly differentially expressed in NAWD mice compared to either TA or Nic, meaning their regulation is in effect solely of withdrawal. This suggests that while miRNAs do not play a significant role in the initial regulation of genes in the midbrain by chronic nicotine treatment,

the induction of miRNAs observed during acute nicotine withdrawal contributes to the propensity of nicotine responsive genes to remain persistently differentially expressed during nicotine withdrawal.

Chapter 3

Integrated miRNA-/mRNA-Seq Analysis of the Habenulo-Interpeduncular Circuitry During Chronic Nicotine Treatment and Withdrawal

Contributions:
Bioinformatic analysis related to mapping, differential expression, and gene ontology was performed by Junko Tsuji.
Paul Gardner assisted with experimental design.
I was responsible for experimental design, library synthesis, sequencing, and data interpretation.

3.A. Introduction

Tobacco use is a prevalent health problem worldwide, with more than 900 million daily smokers (Peacock et al. 2018) and an estimated 6 million deaths due to tobacco-related illnesses annually (WHO 2012). The few pharmacological cessation aids currently available have limited efficacy (Jorenby et al. 2006, Cinciripini et al. 2013, Koegelenberg et al. 2014, Kotz et al. 2014), and without the intervention of new effective treatments, tobacco-related mortality is anticipated to rise to 8 million deaths per year (WHO 2012).

The addictive component of tobacco is nicotine, a tertiary alkaloid that is an agonist of nicotinic acetylcholine receptors (nAChRs), ligand-gated ion channels endogenously activated by acetylcholine (Albuquerque et al. 2009). nAChRs are enriched in the mesolimbic and habenulo-interpeduncular circuitries underlying nicotine reward and withdrawal, respectively (Dani and De Biasi 2013, Picciotto and Mineur 2014, Molas et al. 2017). Cessation of nicotine induces a withdrawal syndrome consisting of negative somatic, affective and cognitive symptoms. Affective symptoms primarily include depressed mood, irritability, craving and anxiety (Hughes 2007, Jackson et al. 2015). While the rewarding properties of nicotine dominate initial drug-taking, it is largely avoidance of affective withdrawal symptoms that promotes relapse and habitual use (Allen et al. 2008, Koob and Le Moal 2008).

The habenulo-interpeduncular withdrawal circuitry consists primarily of neurons projecting from the medial habenula (MHb), a paired epithalamic

nucleus, to the interpeduncular nucleus (IPN), a single symmetrical nucleus in the midbrain, via the fasciculus retroflexus (Antolin-Fontes et al. 2015, Molas et al. 2017). In mice experiencing spontaneous nicotine withdrawal, there is increased glutamate release from habenular axon terminals, activating GABAergic neurons in the IPN (Zhao-Shea et al. 2013). Activation of the IPN results in the increased somatic signs and anxiety observed during nicotine withdrawal (Zhao-Shea et al. 2013, Zhao-Shea et al. 2015). Optogenetic investigation of this circuit has revealed that silencing the MHb decreases activation of IPN neurons and decreases anxiety during nicotine withdrawal (Zhao-Shea et al. 2015).

While much is known about the neurocircuitry responsible for nicotine withdrawal-associated anxiety and somatic symptoms, the molecular mechanisms underlying the induction of these behavioral alterations are less clear. Chronic drug exposure induces stable neuroadaptations underlying the compulsion for continued use and susceptibility to relapse. These long-lasting changes in the addicted brain's function are thought to require alterations of gene expression through regulation of transcription factors, epigenetic mechanisms, and non-coding RNAs (Robison and Nestler 2011, Madsen et al. 2012).

microRNAs (miRNAs) are non-coding RNA molecules ~22 nucleotides in length that repress the expression of mRNA targets by promoting mRNA decay or translational repression (Bartel 2018). miRNAs recognize their targets through imperfect base-pairing of the seed region (nucleotides 2-7) with miRNA response

elements (MREs) within the 3′-UTRs of mRNAs (Lewis et al. 2003, Bartel 2009). Tobacco smoke and nicotine have been shown to regulate the expression of miRNAs in various cell lines, organisms, and tissues (Izzotti et al. 2009, Shan et al. 2009, Izzotti et al. 2011, Takahashi et al. 2013, Zhang et al. 2014) .

Dysregulation of miRNAs in the brain have been shown to contribute to neurodevelopmental and neuropsychiatric disorders, including drug addiction (Hollander et al. 2010, Im and Kenny 2012). However, little is known about the role of miRNAs in the mechanisms underlying nicotine dependence and withdrawal. Few studies have examined the regulation of miRNAs by nicotine in specific regions of the mammalian brain (Lippi et al. 2011, Hogan et al. 2014, Lee et al. 2015). Previously, we showed that the expression of miRNAs predicted to target MREs within the 3′-UTRs of nAChRs was altered after chronic nicotine treatment in whole brain or a specific brain region (Hogan et al. 2014). Nicotine has been reported to regulate miRNAs and mRNAs in the MHb, with microarrays detecting expression changes in mice self-administering nicotine (Lee et al. 2015). However, the targets of these miRNAs and their functions in the context of nicotine dependence have not been elucidated.

Using integrated miRNA- and mRNA-Seq, we asked whether there are changes in miRNA and mRNA expression in the MHb and IPN chronic nicotine treatment and during acute nicotine withdrawal. We hypothesize that use of these valuable sequencing datasets makes it possible to identify a multitude of

miRNAs/genes playing a role(s) in the molecular mechanisms underlying the neuroadaptations involved in nicotine dependence.

3.B. Materials and Methods

Materials and Methods are identical to those appearing in Chapter 2.B unless otherwise noted.

Tissue Collection and RNA Isolation

The same brains used for transcriptome analysis of the mesocorticolimbic pathway were used for these experiments. Fresh frozen brains were coronally sliced (~1 mm) and the MHb and IPN were dissected using a circular tissue punch. The MHb and IPN were each extracted using a single midline 0.75 mm diameter punch and expelled into lysis buffer (miRVANA Total RNA Isolation Kit). Each sample for sequencing consisted of punches from 4 brains combined. Additional mice were treated for RT-qPCR validation of the differential expression analysis, pooling tissue from 2 brains per sample. RNA isolation proceeded as described in in Chapter 2.B.

Quantitative Reverse Transcription-PCR (RT-qPCR)

RT-qPCR for miRNAs and mRNAs was performed as previously described (Hogan et al. 2014). RNA was reverse transcribed by MMLV-reverse transcriptase (ThermoFisher Cat. # 28025013 or AM2043) using random decamers or miRNA-specific primers according to the manufacturer's instruction. Quantitative PCR was performed on a Applied Biosystems 7500 Real-Time PCR System using TaqMan miRNA and gene expression assays (ThermoFisher) for miR-106b-5p (Assay ID 000442), *Pfn2* (Assay ID Mm01289572_m1), *Pfn1* (Assay ID Mm00726691_s1), *Atg7* (Assay ID Mm00512209_m1), *Arf5* (Assay ID Mm00500199_m1), *Bcl2l1* (Assay ID Mm00437783_m1), and *Eif5a* (Assay ID Mm01245535_m1). Reactions were performed in technical triplicates. Relative miRNA/gene expression was determined using the $2^{-\Delta\Delta Ct}$ method (Livak and Schmittgen 2001). miRNA and mRNA expression were normalized to snoRNA202 (Assay ID 001232) and β-glucuronidase (Assay ID Mm01197698_m1), respectively, unless otherwise noted.

3.C. Results

Differential expression of miRNAs and mRNAs in the MHb and IPN after chronic nicotine-treatment and acute withdrawal.

To determine the effect of chronic nicotine treatment and withdrawal on the miRNA and mRNA expression in the withdrawal circuit, we sequenced RNAs

isolated from the MHb and IPN and performed differential expression analysis. RNA for these sequencing libraries was extracted from tissue samples dissected from the same brains as those used to investigate regulation of transcripts in the mesocorticolimbic pathway described in Chapter 2.

In the withdrawal circuit, there were few miRNAs differentially expressed after chronic nicotine treatment. In the IPN, only 8 miRNAs were significantly altered when Nic mice are compared to TA controls (Figure 3.1A). The majority of these miRNAs were only modestly regulated, with only 2 exhibiting fold changes > 2. Seven miRNAs were down-regulated by nicotine treatment and all of these are persistently repressed after a 48-hr withdrawal, when NAWD mice are compared to TA controls (Figures 3.1E and 3.6A). In the MHb, there were only 6 differentially expressed miRNAs in Nic mice compared to TA controls (Figure 3.1C), all with fold changes < 2. Only 1 of these miRNAs remained similarly regulated after nicotine was discontinued, comparing NAWD- to TA-treated mice (Figures 3.1G and 3.6B).

However, after acute nicotine withdrawal, a multitude of miRNAs in the withdrawal circuit exhibit significant, albeit small, changes in expression level. In the IPN, there was a total of 87 miRNAs significantly differentially expressed in NAWD mice compared to TA controls (Figures 3.1E and 3.2), with only 11 being up- or down-regulated with a fold change > 2. The distribution between up- and down-regulated miRNAs is roughly equal, with 42 being enhanced and 45 repressed. Twenty-nine (~33%) of these miRNAs were similarly differentially

expressed when NAWD mice are compared to either TA or Nic mice (Figures 3.1I and 3.6A). This suggests that nicotine exposure itself had no effect on their expression and regulation of these miRNAs in the IPN is due entirely to withdrawal.

Similar to the IPN, there were 85 miRNAs differentially expressed in the MHb of mice in acute nicotine withdrawal compared to TA controls (Figures 3.1G and 3.3). The majority of these miRNAs are only modestly regulated, with only 2 miRNAs exhibiting fold changes > 2. Thirty-five and 50 of the miRNAs differentially expressed during acute nicotine withdrawal were up- and down-regulated, respectively. Forty miRNAs were similarly differentially expressed in NAWD mice when compared to either TA or Nic (Figures 3.1K and 3.6B). This suggests that regulation of almost half the miRNAs altered during acute nicotine withdrawal in the MHb is solely the result of withdrawal, with no contribution of the chronic nicotine treatment itself.

None of the miRNAs regulated by chronic nicotine treatment are differentially expressed in both the IPN and MHb, suggesting that nicotine-induced miRNA regulation in the MHb-IPN axis occurs in a brain-region specific manner. Of the miRNAs regulated during acute nicotine withdrawal compared to TA controls, only 16 miRNAs are similarly differentially expressed in both the IPN and MHb. This suggests that while there are some commonly regulated miRNAs in the withdrawal circuit, the majority of miRNA regulation during acute nicotine withdrawal also occurs in a brain region-specific manner.

In a pattern similar to miRNAs, there were few mRNAs significantly differentially expressed (with a fold change > 2) by chronic nicotine treatment in the IPN and MHb. In the IPN, there were only 4 differentially expressed mRNAs in Nic mice compared to TA controls (Figure 3.1B), all of them up-regulated. None of these mRNAs were similarly differentially expressed in NAWD mice compared to TA control, suggesting all of them returned to control expression levels within 48 hours of nicotine withdrawal (Figure 3.6C).

In the MHb, chronic nicotine treatment resulted in the differential expression of 26 mRNAs compared to TA controls (Figure 3.1D), with 18 up- and 8 down-regulated. Only 2 of these mRNAs are similarly differentially expressed in NAWD mice compared to TA controls, suggesting that the majority of mRNAs regulated during chronic nicotine rapidly return to baseline expression levels after nicotine is withdrawn (Figure 3.6D).

In contrast to chronic nicotine treatment alone, there are many mRNAs differentially expressed in the MHb-IPN axis during acute nicotine withdrawal. In the IPN, 335 genes were significantly differentially expressed with a fold change > 2 (Figures 3.1F and 3.4). The expression of the majority of these mRNAs is increased, with 292 up- and 43 down-regulated. Of these mRNAs, 303 (~90%) were similarly altered when NAWD mice are compared to either Nic or TA mice, suggesting their regulation was an effect of acute nicotine withdrawal and there was no effect of nicotine treatment alone (Figures 3.1J and 3.6C).

In the MHb, there were 154 mRNAs significantly differentially expressed with a fold change > 2 during acute nicotine withdrawal compared to TA controls. Almost all mRNAs were up-regulated in NAWD mice, with only 3 exhibiting down-regulation (Figures 3.1H and 3.5). Additionally, 122 (~79%) of genes regulated when NAWD is compared to TA are similarly up- or down-regulated when compared to Nic mice (Figures 3.1L and 3.6D). This indicates that the majority of genes are altered during acute withdrawal as a result of nicotine withdrawal, and chronic nicotine treatment itself does not contribute to their regulation.

To determine that brain region specificity of changes in gene expression during chronic nicotine treatment and withdrawal in the withdrawal circuitry, the identity of mRNAs up- or down-regulated in the IPN and MHb were compared. There were no mRNAs similarly differentially expressed (FDR 0.01, FC > 2) in both the IPN and MHb of Nic mice compared to TA controls. Additionally, there were no mRNAs differentially expressed in both brain regions of NAWD compared to TA mice. This suggests that mRNAs are regulated by chronic nicotine and withdrawal in a brain region specific manner in the MHb-IPN axis.

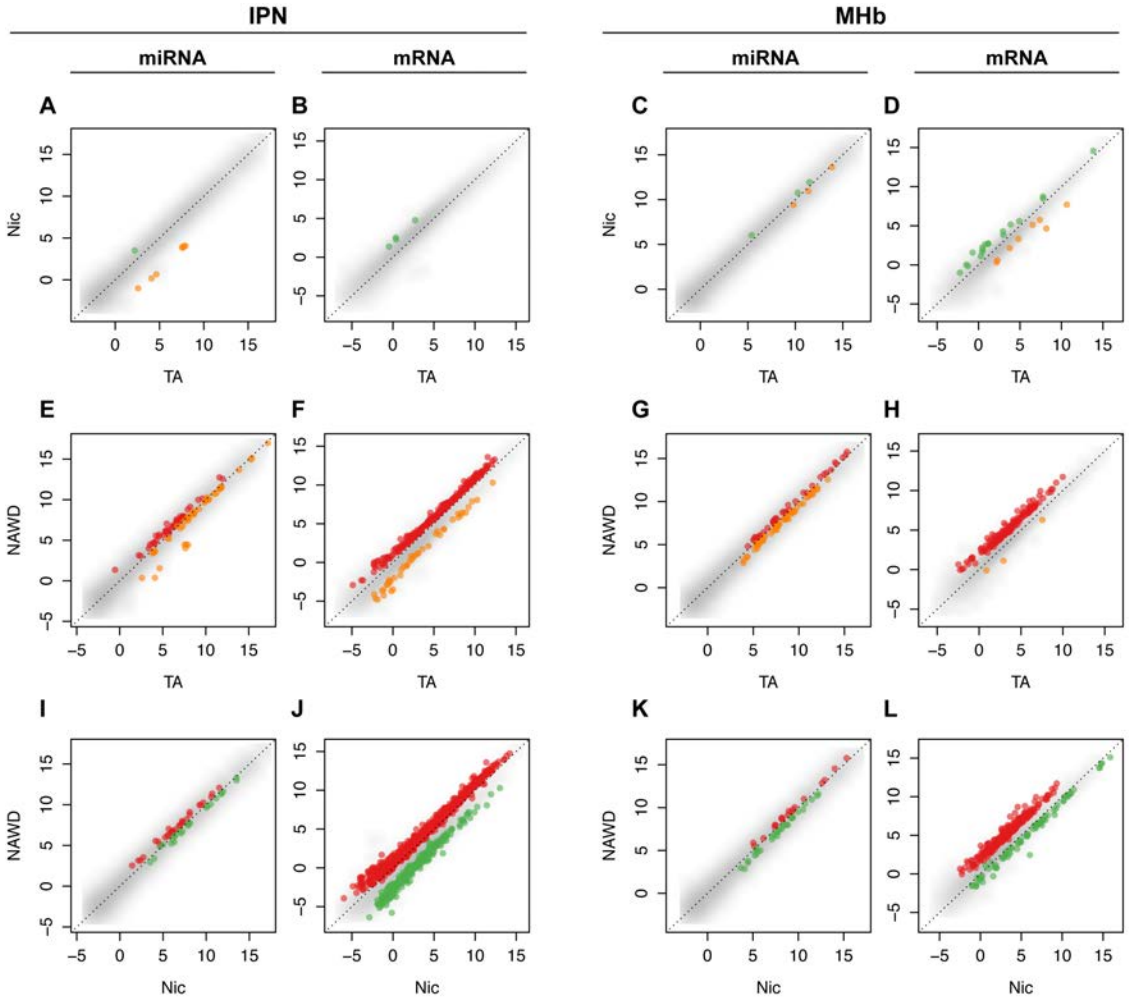

Figure 3.1. Differential expression of miRNAs and mRNAs within the MHb-IPN withdrawal axis during chronic nicotine treatment and acute withdrawal. Scatter plots display differential expression of miRNAs or mRNAs in the IPN (A-B, E-F, I-J) and MHb (C-D, G-H, K-L) measured by deep sequencing. RNAs isolated from tissue punches of nicotine-treated (Nic, A-D) and acute withdrawal (NAWD, E-H) mice are compared to TA-treated controls. NAWD mice were also compared to Nic mice (I-L). Each dot represents an individual miRNA or mRNA plotted as $\log_2$(RPM) or $\log_2$(TPM), respectively. All miRNAs with a FDR < 0.01 and mRNAs with FDR < 0.01 and FC > 2 are highlighted in color. Orange dots are up-regulated in TA, green dots are up-regulated in Nic, and red dots are up-regulated in NAWD in each comparison. Only miRNAs with RPM > 0 and mRNAs with TPM > 0 in at least half of the replicates in each treatment group are shown. n = 4-5, with each library synthesized using pooled RNA from 4 mice.

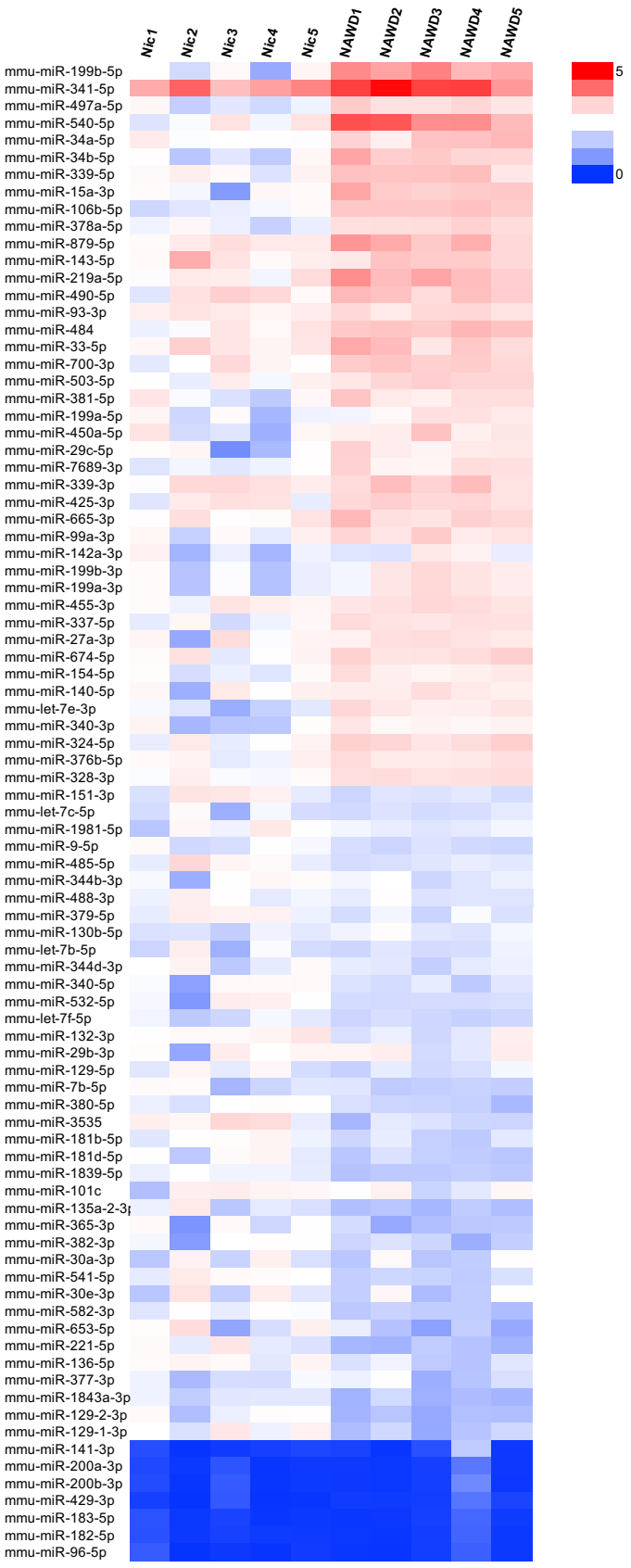

Figure 3.2. Relative expression heatmap of miRNAs differentially expressed in the IPN during acute nicotine withdrawal. Heat map displaying miRNAs that are significantly differentially expressed in the IPN during acute withdrawal compared to TA controls (left). Each column represents an individual biological replicate of mice treated chronically with nicotine (Nic) or acute nicotine withdrawal (NAWD). Each replicate contained RNA pooled from 4 mice. The colors represent fold change, calculated as read per million (RPM) normalized to the average RPM of the TA control group. Red represents up-regulation and blue represents down-regulation.

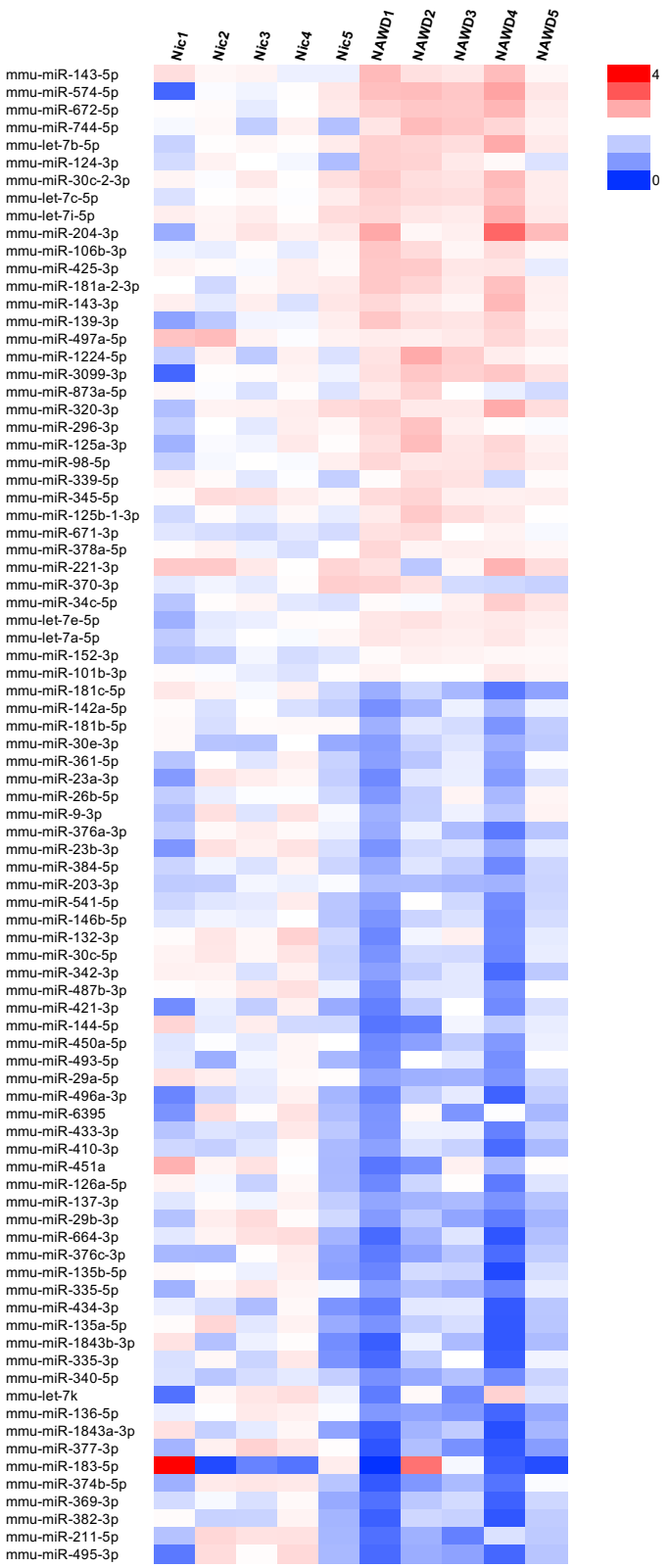

Figure 3.3. Relative expression heatmap of miRNAs differentially expressed in the MHb during acute nicotine withdrawal. Heat map displaying miRNAs that are significantly differentially expressed in the MHb during acute withdrawal compared to TA controls (left). Each column represents an individual biological replicate of mice treated chronically with nicotine (Nic) or acute nicotine withdrawal (NAWD). Each replicate contained RNA pooled from 4 mice. The colors represent fold change, calculated as read per million (RPM) normalized to the average RPM of the TA control group. Red represents up-regulation and blue represents down-regulation.

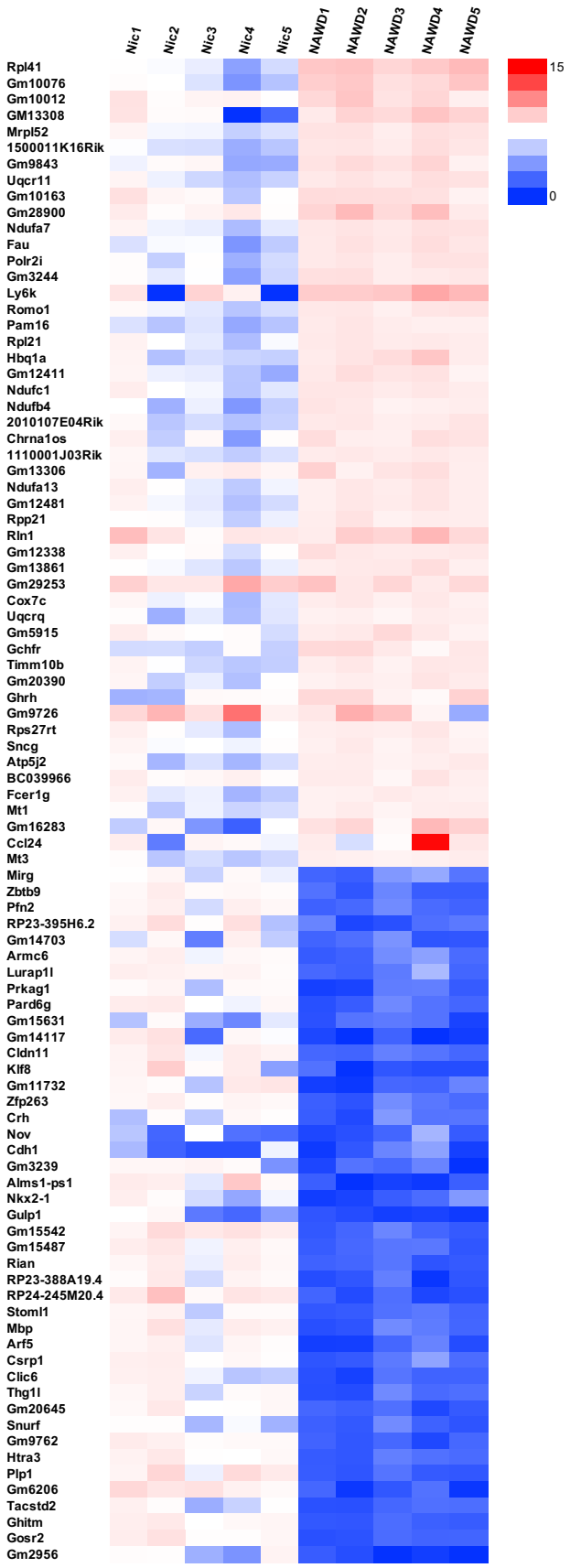

Figure 3.4. Relative expression heatmap of mRNAs differentially expressed in the IPN acute nicotine withdrawal. Heat map displaying the 50 most up-regulated and all down-regulated mRNAs in the NAc during acute nicotine withdrawal relative to TA controls (left). Each column represents an individual biological replicate of mice treated chronically with nicotine (Nic) or acute nicotine withdrawal (NAWD). Each replicate contained RNA pooled from 4 mice. The colors represent fold change, calculated as transcript per million (TPM) normalized to the average TPM of the TA control group. Red represents up-regulation and blue represents down-regulation. Only mRNAs with TPM > 0 in more than half of the replicates were included.

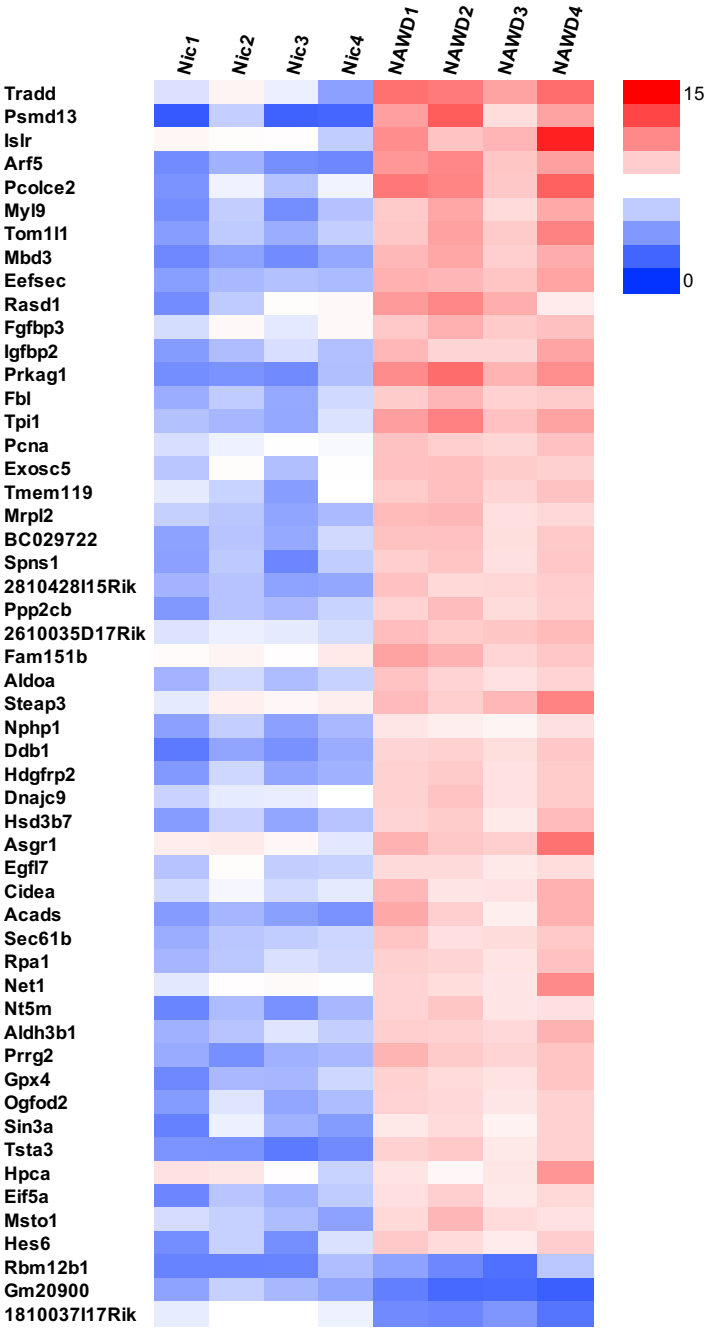

Figure 3.5. Relative expression heatmap of mRNAs differentially expressed in the MHb during acute nicotine withdrawal. Heat map displaying the 50 most up-regulated and all down-regulated mRNAs in the MHb during acute nicotine withdrawal relative to TA controls (left). Each column represents an individual biological replicate of mice treated chronically with nicotine (Nic) or acute nicotine withdrawal (NAWD). Each replicate contained RNA pooled from 4 mice. The colors represent fold change, calculated as transcript per million (TPM) normalized to the average TPM of the TA control group. Red represents up-regulation and blue represents down-regulation. Only mRNAs with TPM > 0 in more than half of the replicates were included.

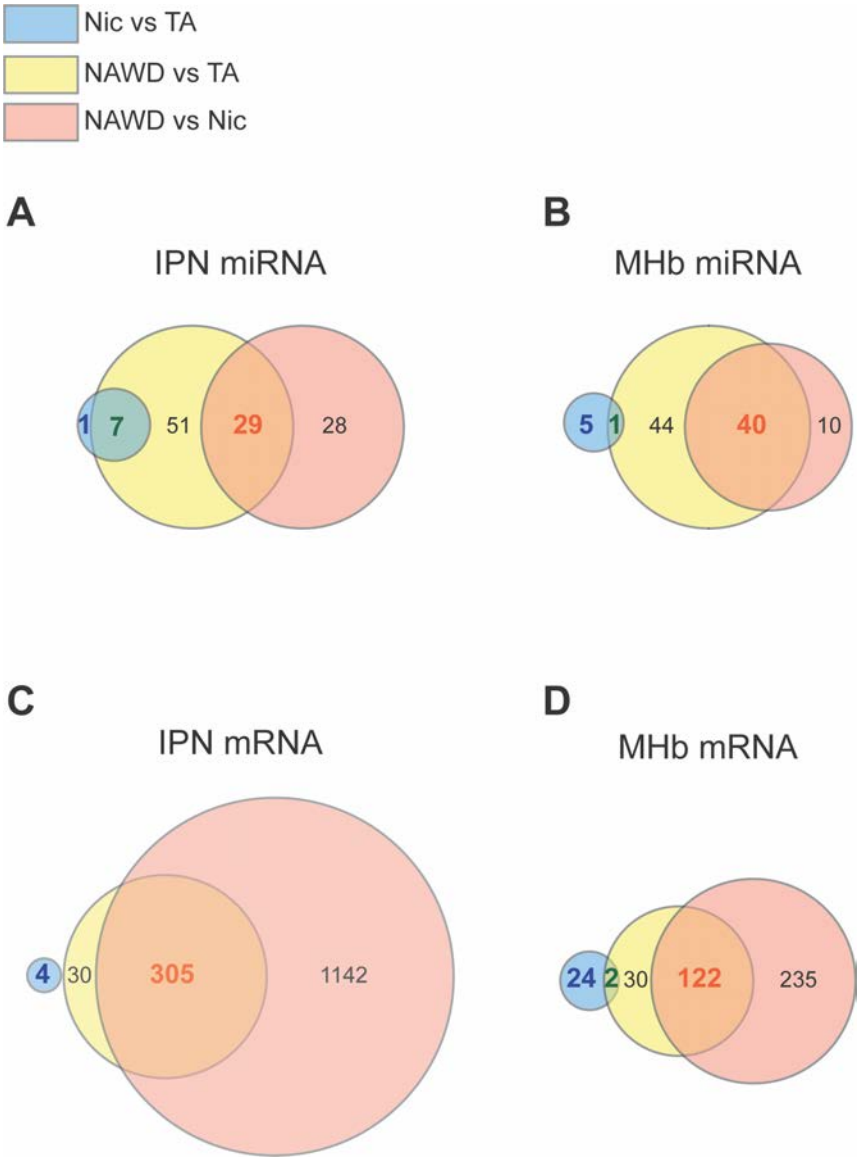

Figure 3.6. Overlap of similarly differentially expressed miRNAs and mRNAs between treatment conditions within the IPN and MHb. Venn diagrams showing numbers of differentially expressed miRNAs (FDR < 0.01) and mRNAs (FDR < 0.01, FC > 2) in the IPN (A,B) and MHb (C,D) in each treatment condition, designated by color. Regions where the circles overlap indicate that the transcripts are similarly up- or down-regulated in both conditions. Numbers indicate the number of miRNAs or mRNAs.

Differential expression of miRNAs/mRNAs in the MHb and IPN after prolonged nicotine withdrawal.

To determine the persistence of the alterations in miRNA and mRNA expression following acute nicotine withdrawal, another group of mice underwent a long (4-week) withdrawal after chronic nicotine treatment (NLWD). Interestingly, there were no significantly differentially expressed miRNAs in either the IPN or MHb of NLWD mice compared to age-matched TA-treated (TAL) controls (Figures 3.7A and 3.7C). Similarly, there are no mRNAs differentially expressed with a fold change > 2 in the MHb of NLWD mice compared to TAL controls (Figure 3.7D). In the IPN, 39 genes were differentially expressed after prolonged withdrawal (Figure 3.7B). However, none of these genes were also similarly regulated after acute withdrawal.

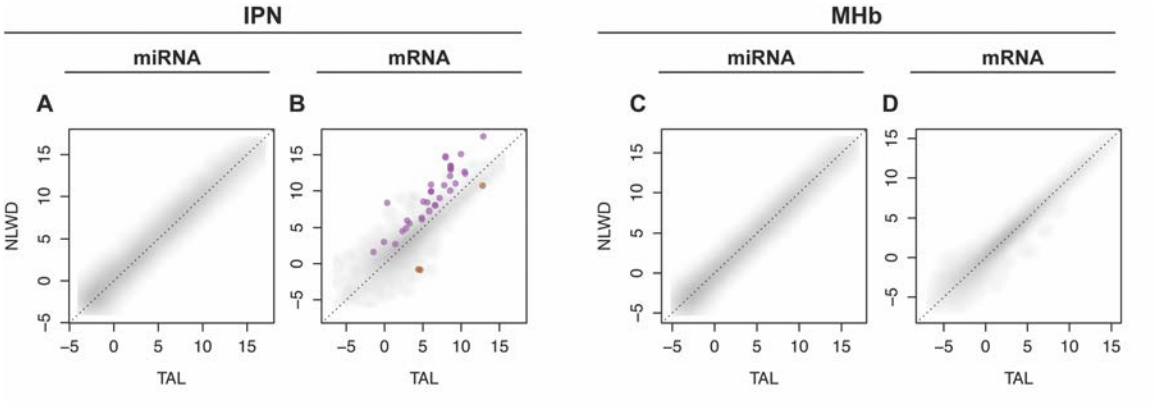

Figure 3.7. Differential expression of miRNAs and mRNAs in the IPN and MHb of NLWD- and TAL-treated mice. Scatter plots display differential expression of miRNAs or mRNAs in the IPN (A, B) and MHb (C, D) measured by deep sequencing. miRNAs (A, C) and mRNAs (B, D) isolated from mice after a long (4-week) withdrawal from nicotine (NLWD) are compared to age-matched TA-treated controls (TAL). Each dot represents an individual miRNA or mRNA plotted as $\log_2$(RPM) and $\log_2$(TPM), respectively. miRNAs (FDR < 0.01) and mRNAs (FDR < 0.01, FC >2) that are up-regulated (purple) and down-regulated (brown) in NLWD mice are highlighted. All miRNAs have RPM > 0 and all mRNAs have TPM > 0 in more than half of the replicates in each treatment group. n = 2-5, with each library synthesized using pooled RNA from 4 mice.

Gene ontology (GO) analysis of differentially expressed mRNAs in the IPN and MHb

Gene ontology analysis was performed on differentially expressed mRNAs for all treatment groups in the IPN and MHb. Comprehensive heat maps display all of the reduced terms describing the cellular compartments (CC, Figures 3.9 and 3.12), molecular functions (MF, Figures 3.10 and 3.13), and biological processes (BP, Figures 3.11 and 3.14) with significant enrichment for up- and down-regulated genes in each brain region.

To describe differential expression in the IPN and MHb during acute nicotine withdrawal, I have highlighted selected GO terms describing cellular compartments (CC, Figure 3.8A), molecular functions (MF, Figure 3.8B), and biological processes (BP, Figure 3.8C) that were significantly enriched for up- or down-regulated genes in NAWD mice compared to TA controls. CC analysis determined there was significant enrichment of genes up-regulated in the IPN and MHb related to the mitochondrion. Up-regulated genes in the IPN were also enriched for MF and BP terms related to mitochondrial structure, function, and energetics, such as electron carrier activity, NADH dehydrogenase activity, hydrogen ion transport, and regulation of metabolic processes. There was also significant enrichment of genes up-regulated in the IPN related to ribosomal terms, including structural constituent of the ribosome, rRNA binding, ribosome biogenesis, and translation. In the MHb, genes up-regulated in NAWD mice were also enriched in CC terms related to the vesicle and myelin sheath. In both the

IPN and the MHb there was significant enrichment of down-regulated genes related to neuron projection development.

As previously discussed, there are very few genes differentially expressed with fold changes > 2 in the MHb and IPN during chronic nicotine treatment compared to TA controls. However, up-regulated genes in the MHb display significant enrichment of terms related the mitochondrion, vesicle, and myelin sheath, as observed in GO analysis of genes regulated during acute nicotine withdrawal.

There are a limited number of genes that were differentially expressed in the IPN after prolonged nicotine withdrawal. However, GO analysis did not reveal any significant enrichment of CC, MF, or BP categories.

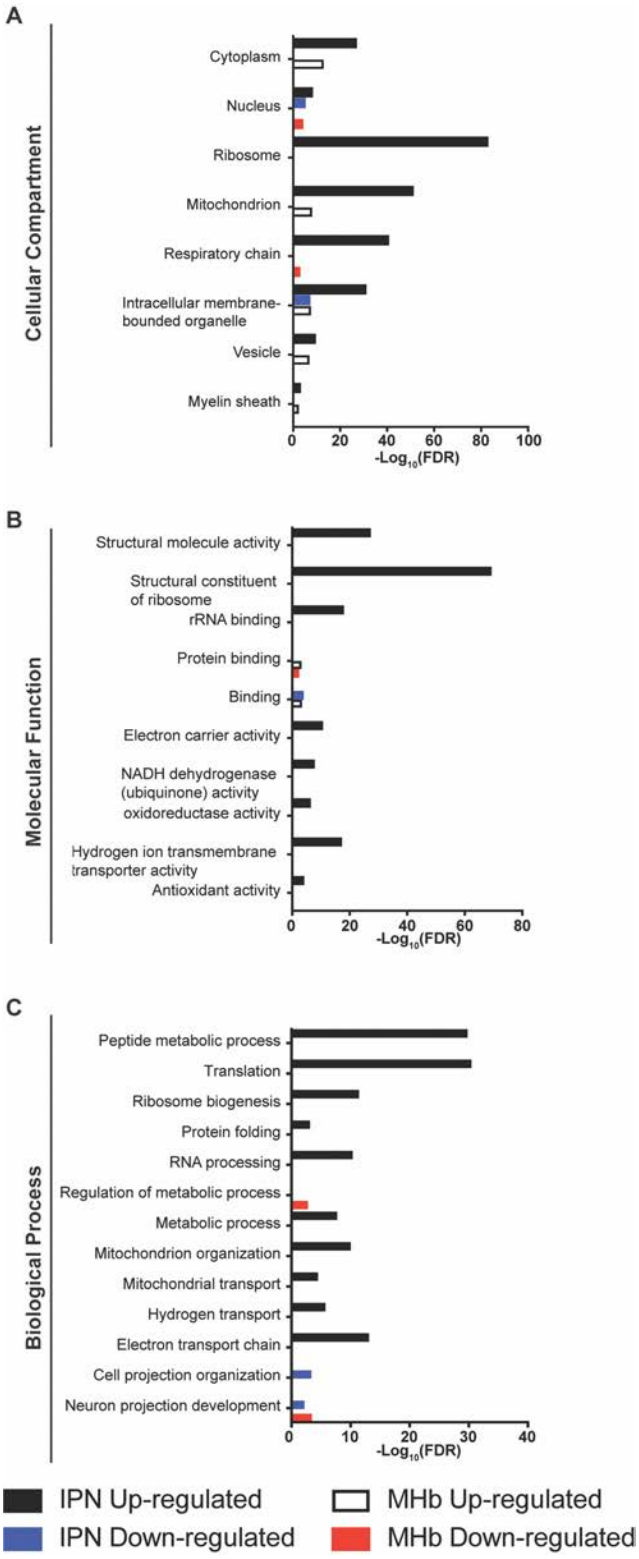

Figure 3.8. Genes differentially expressed in the IPN and MHb during acute nicotine withdrawal are overrepresented in gene ontology terms related to energetics, translation, and cell projection organization in the IPN and MHb. The vertical axes define the selected GO terms describing the cellular compartment (A), molecular function (B), or biological process (C). The number of GO terms was reduced combining similar terms using a sim_{Rel} cutoff of 0.4 as described in the Methods and Materials. The horizontal axis plots the significance of enrichment of the GO term, plotted as $-\log_{10}(\text{FDR})$.

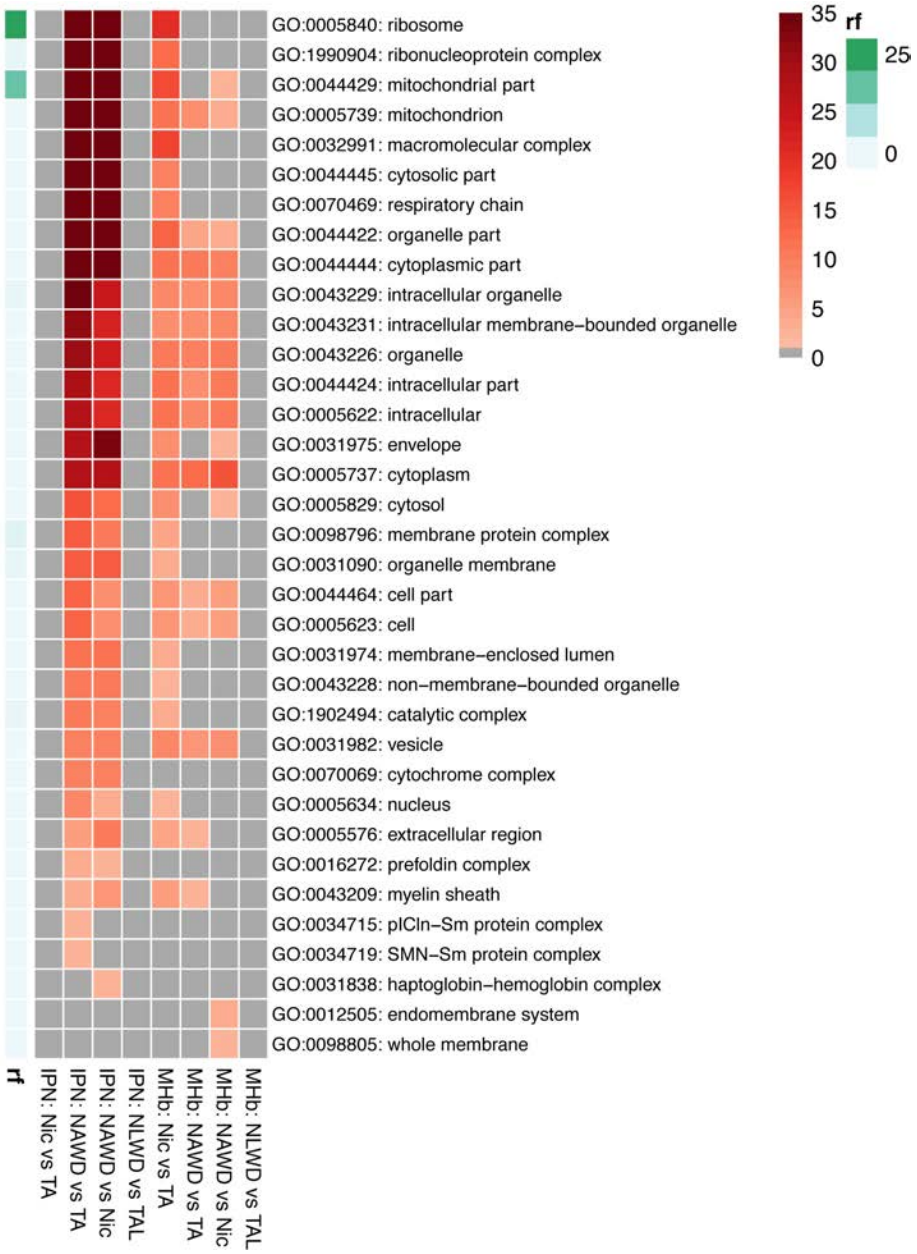

Figure 3.9. Enrichment of cellular compartments with genes up-regulated in the IPN and MHb. Heat map of the significance of enrichment of reduced GO terms describing the cellular compartment with up-regulated mRNAs in the IPN and MHb. Each column is designated a specific brain region and treatment comparison (bottom). Each row is designated a GO term (right) reduced with a sim_{Rel} cut off of 0.4 as described in the Methods and Materials. The number of terms combined within the single GO term, *rf*, is indicated by the green color gradient (left). The color gradient of the box (red) indicates the significance of enrichment as $-\log_{10}$(FDR).

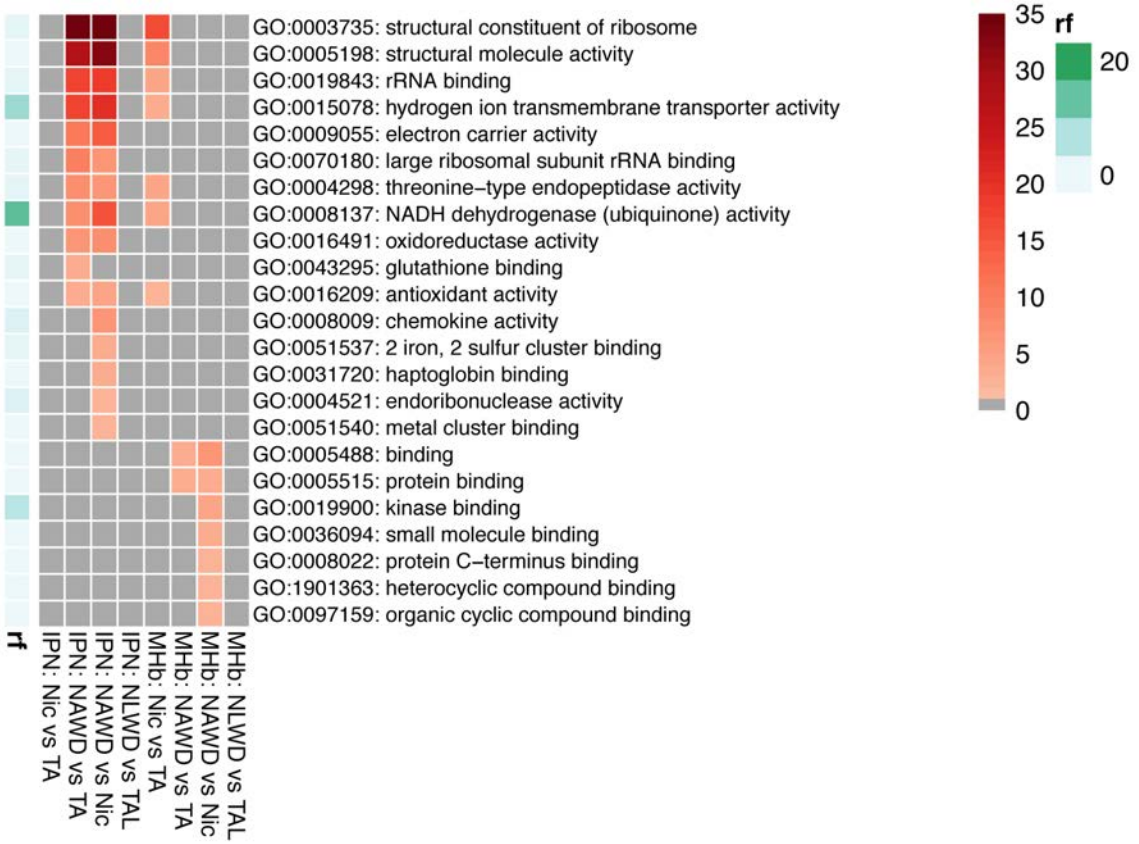

Figure 3.10. Enrichment of molecular functions with genes up-regulated in the IPN and MHb. Heat map of the significance of enrichment of reduced GO terms describing the cellular compartment with up-regulated mRNAs in the IPN and MHb. Each column is designated a specific brain region and treatment comparison (bottom). Each row is designated a GO term (right) reduced with a sim_{Rel} cut off of 0.4 as described in the Methods and Materials. The number of terms combined within the single GO term, *rf*, is indicated by the green color gradient (left). The color gradient of the box (red) indicates the significance of enrichment as $-\log_{10}$(FDR).

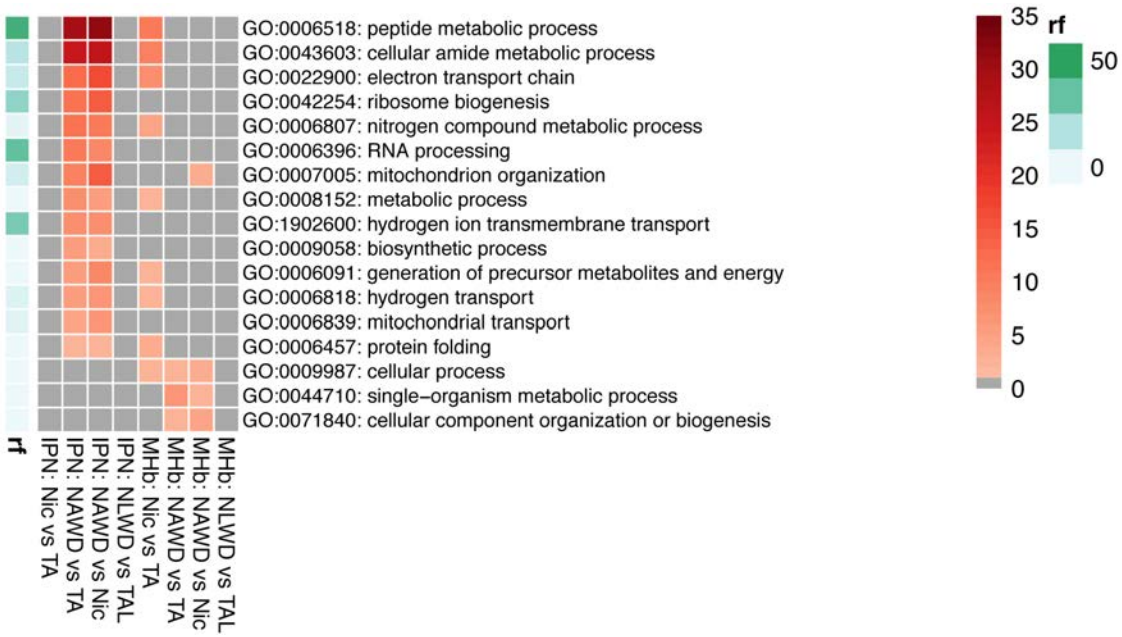

Figure 3.11. Enrichment of biological processes with genes up-regulated in the IPN and MHb. Heat map of the significance of enrichment of reduced GO terms describing the cellular compartment with up-regulated mRNAs in the IPN and MHb. Each column is designated a specific brain region and treatment comparison (bottom). Each row is designated a GO term (right) reduced with a sim_{Rel} cut off of 0.4 as described in the Methods and Materials. The number of terms combined within the single GO term, *rf*, is indicated by the green color gradient (left). The color gradient of the box (red) indicates the significance of enrichment as $-\log_{10}$(FDR).

Figure 3.12. Enrichment of cellular compartments with genes down-regulated in the IPN and MHb. Heat map of the significance of enrichment of reduced GO terms describing the cellular compartment with down-regulated mRNAs in the IPN and MHb. Each column is designated a specific brain region and treatment comparison (bottom). Each row is designated a GO term (right) reduced with a sim_{Rel} cut off of 0.4 as described in the Methods and Materials. The number of terms combined within the single GO term, *rf*, is indicated by the green color gradient (left). The color gradient of the box (red) indicates the significance of enrichment as $-\log_{10}$(FDR).

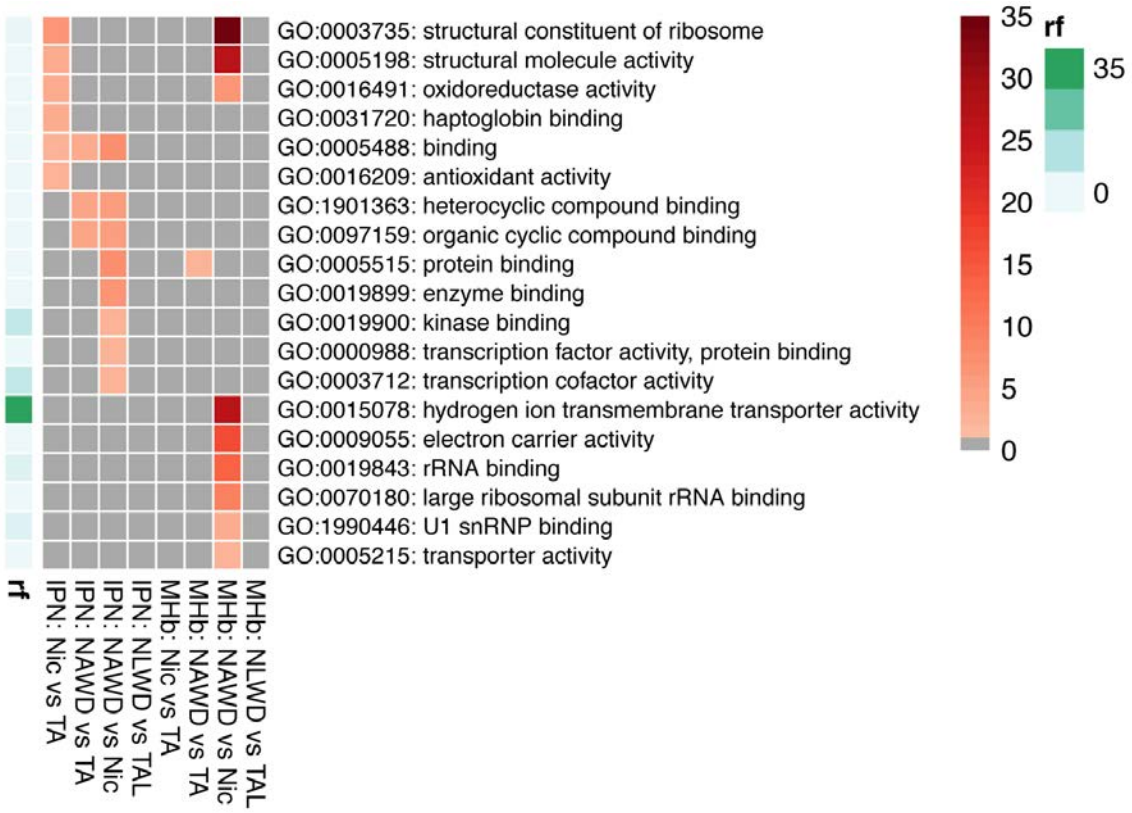

Figure 3.13. Enrichment of molecular functions with genes down-regulated in the IPN and MHb. Heat map of the significance of enrichment of reduced GO terms describing the cellular compartment with down-regulated mRNAs in the IPN and MHb. Each column is designated a specific brain region and treatment comparison (bottom). Each row is designated a GO term (right) reduced with a sim_{Rel} cut off of 0.4 as described in the Methods and Materials. The number of terms combined within the single GO term, *rf*, is indicated by the green color gradient (left). The color gradient of the box (red) indicates the significance of enrichment as $-\log_{10}$(FDR).

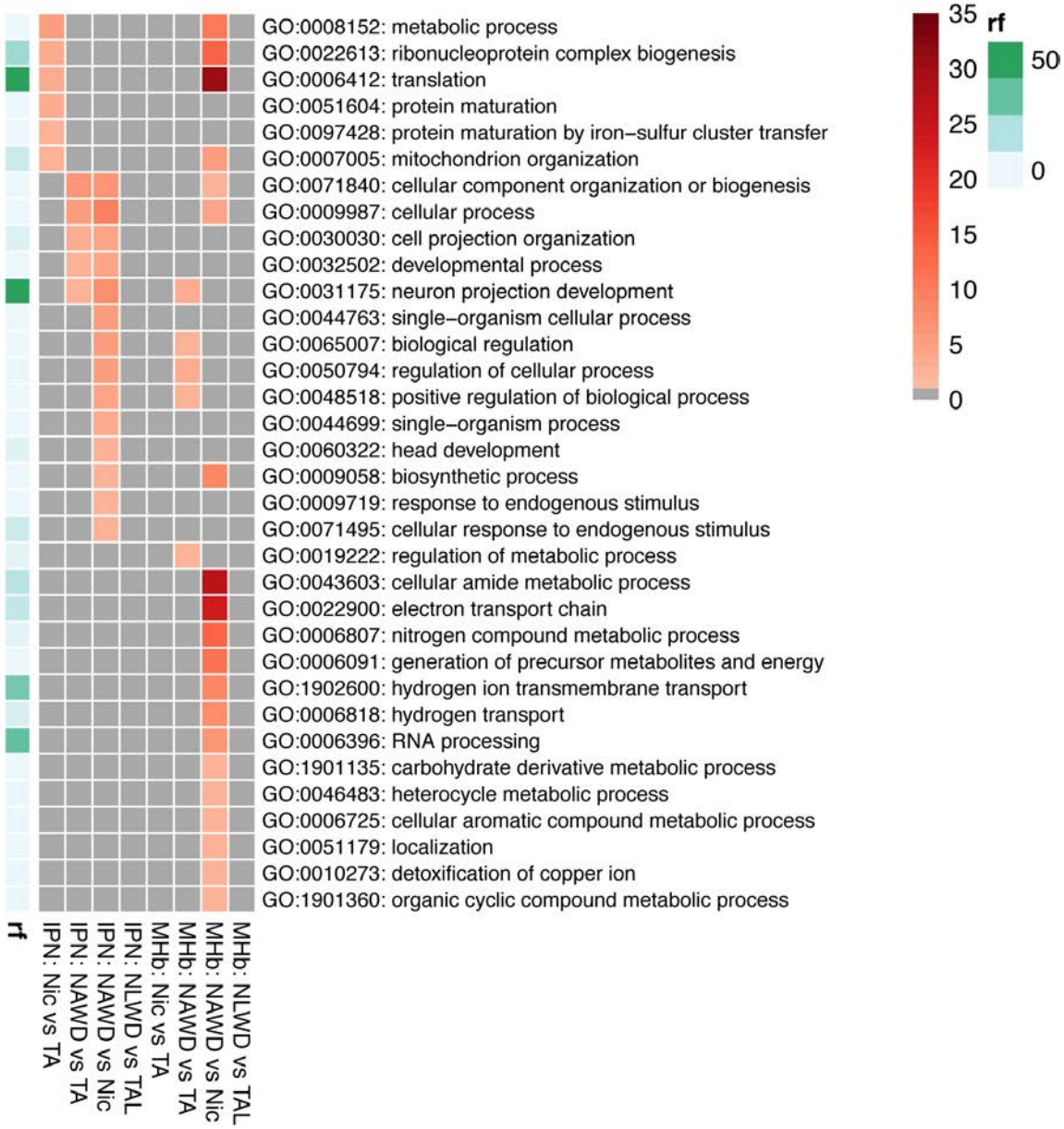

Figure 3.14. Enrichment of biological processes with genes down-regulated in the IPN and MHb. Heat map of the significance of enrichment of reduced GO terms describing the cellular compartment with down-regulated mRNAs in the IPN and MHb. Each column is designated a specific brain region and treatment comparison (bottom). Each row is designated a GO term (right) reduced with a sim_{Rel} cut off of 0.4 as described in the Methods and Materials. The number of terms combined within the single GO term, *rf*, is indicated by the green color gradient (left). The color gradient of the box (red) indicates the significance of enrichment as $-\log_{10}$(FDR).

Target prediction of miRNAs differentially expressed in the IPN

Because miRNAs are traditionally considered to be repressors of gene expression, TargetScan Mouse 7.1 was used to predict MREs within the 3′-UTR of differentially expressed mRNAs for inversely regulated miRNAs. Due to the fact that conservation of MREs increases the likelihood of biological function, only miRNAs and MREs conserved in vertebrates or mammals were considered in target prediction.

Chronic nicotine treatment induced differential expression of very few miRNAs and mRNAs in the IPN. Of the 8 miRNAs regulated by chronic nicotine treatment in the IPN, the 7 miRNAs that are down-regulated are conserved. TargetScan Mouse 7.1 predicted that only one of the 4 up-regulated mRNAs is a target of these conserved, down-regulated miRNAs. *Shank1*, a scaffolding protein enriched in post-synaptic densities (Jiang and Ehlers 2013), was up-regulated in the IPN by chronic nicotine exposure. *Shank1* was predicted to contain a conserved MRE for two different down-regulated miRNAs, miR-96-5p and miR-182-5p.

Of the 88 miRNAs differentially expressed in the IPN of NAWD mice compared to TA controls, 52 are conserved in vertebrates or mammals. Thirty-five of these miRNAs that are predicted to target at least one of 38 inversely expressed mRNAs (Table 3.2). The expression of 34 (~89%) of the predicted mRNA targets are altered only after nicotine withdrawal, being similarly regulated

in NAWD compared to either TA or Nic mice (Table 3.2, orange). Eighteen of the predicted targets contain multiple MREs for a single or different miRNAs.

In the IPN, none of the mRNAs differentially expressed after a prolonged nicotine withdrawal (NLWD) are predicted to be regulated by an inversely regulated miRNA.

Table 3.1. Target prediction of miRNAs differentially expressed in the IPN after chronic nicotine exposure (Nic) compared to TA controls.

mRNA	mRNA FC	mRNA FDR	miRNA	miRNA FC	miRNA FDR	Seed Type	Position in 3′-UTR
Shank1	2.004	1.33E-09	miR-96-5p	0.511	4.79E-11	7mer-A1	2033-2039
			miR-182-5p	0.582	1.48E-07	7mer-A1	2033-2039

Table 3.2: Target prediction of miRNAs differentially expressed in IPN during acute nicotine withdrawal (NAWD) compared to TA controls. mRNAs that are similarly up- or down-regulated in NAWD mice compared to either TA or Nic are highlighted in orange.

mRNA	mRNA FC	mRNA FDR	miRNA	miRNA FC	miRNA FDR	Seed Type	Position in 3′-UTR
Hbq1a	3.002	2.57E-07	miR-377-3p	0.592	1.08E-03	7mer-m8	252-258
Rpp21	2.852	2.35E-20	miR-136-5p	0.613	9.18E-06	8mer	3537-3544
Gchfr	2.696	9.55E-06	miR-129-1-3p	0.570	4.18E-04	7mer-m8	298-304
			miR-129-2-3p	0.590	1.62E-05	7mer-m8	298-304
Gm20390	2.669	2.25E-23	miR-429-3p	0.329	3.53E-12	7mer-m8	3377-3383
			miR-429-3p	0.329	3.53E-12	8mer	4329-4336
			miR-429-3p	0.329	3.53E-12	8mer	4714-4721
			miR-200b-3p	0.375	6.58E-08	7mer-m8	3377-3383
			miR-200b-3p	0.375	6.58E-08	8mer	4329-4336
			miR-200b-3p	0.375	6.58E-08	8mer	4714-4721
			miR-344d-3p	0.741	4.47E-03	7mer-A1	3316-3122
Gm9726	2.627	2.76E-04	miR-29b-3p	0.726	4.41E-03	8mer	326-333
Hist1h4h	2.505	1.18E-15	miR-9-5p	0.753	5.60E-03	7mer-m8	26-32
Serf2	2.421	7.81E-20	miR-200a-3p	0.381	1.24E-13	7mer-m8	213-219
			miR-141-3p	0.458	3.07E-04	7mer-m8	213-219
			let-7f-5p	0.735	8.04E-04	8mer	2110-2117
			let-7b-5p	0.741	6.40E-03	8mer	2110-2117
			let-7c-5p	0.766	9.52E-03	8mer	2110-2117
Mrps16	2.418	2.40E-15	miR-136-5p	0.613	9.18E-06	7mer-m8	86-92
Zfp46	2.409	3.91E-12	miR-129-1-3p	0.570	4.18E-04	7mer-m8	464-470
			miR-129-2-3p	0.590	1.62E-05	7mer-m8	464-470
Ndufb2	2.368	2.31E-22	miR-429-3p	0.329	3.53E-12	7mer-m8	3896-3902
			miR-200b-3p	0.375	6.58E-08	7mer-m8	3896-3902
Esrrb	2.332	7.67E-08	let-7f-5p	0.735	8.04E-04	8mer	617-624
			let-7b-5p	0.741	6.40E-03	8mer	617-624
			miR-485-5p	0.753	4.04E-03	7mer-m8	55-61
			miR-9-5p	0.753	5.60E-03	8mer	2337-2344
			let-7c-5p	0.766	9.52E-03	8mer	617-624
Polr2f	2.323	2.02E-26	miR-488-3p	0.752	8.56E-03	7mer-m8	485-491
Nme1	2.305	3.32E-21	miR-200a-3p	0.381	1.24E-13	8mer	123-130
			miR-141-3p	0.458	3.07E-04	8mer	123-130
Gm9844	2.296	1.27E-04	miR-129-5p	0.721	1.46E-03	8mer	26-33
Diras1	2.234	1.93E-12	miR-7b-5p	0.715	1.25E-03	7mer-m8	2200-2206
Myl6	2.234	8.56E-15	miR-340-5p	0.741	6.55E-03	7mer-A1	851-857
Psma2	2.174	3.46E-21	miR-132-3p	0.726	6.55E-03	7mer-A1	111-117
Mrpl14	2.172	2.53E-14	miR-340-5p	0.741	6.55E-03	7mer-A1	2823-2829
Ptrhd1	2.170	1.90E-13	miR-181d-5p	0.676	2.00E-04	7mer-m8	2022-2028
			miR-181b-5p	0.680	5.42E-05	7mer-m8	2022-2028
			miR-488-3p	0.752	8.56E-03	8mer	76-83
Dynlt1f	2.169	1.11E-08	miR-29b-3p	0.726	4.41E-03	7mer-A1	215-221

Sod1	2.162	7.65E-13	miR-377-3p	0.592	1.08E-03	7mer-m8	78-84
Cst6	2.158	6.60E-14	miR-377-3p	0.592	1.08E-03	7mer-m8	2027-2033
			miR-181d-5p	0.676	2.00E-04	7mer-m8	2023-2029
			miR-181b-5p	0.680	5.42E-05	7mer-m8	2023-2029
Rpl31	2.153	6.45E-09	miR-653-5p	0.616	4.04E-03	7mer-A1	639-645
			miR-129-5p	0.721	1.46E-03	8mer	671-678
Tmsb4x	2.126	2.94E-14	miR-183-5p	0.319	3.96E-21	7mer-m8	327-333
Ndufb9	2.104	7.81E-20	miR-200a-3p	0.381	1.24E-13	8mer	2453-2460
			miR-141-3p	0.458	3.07E-04	8mer	2453-2460
			miR-365-3p	0.654	9.94E-03	7mer-m8	2718-2724
			miR-532-5p	0.740	2.06E-03	7mer-m8	3048-3054
			miR-340-5p	0.741	6.55E-03	7mer-A1	1850-1856
			miR-379-5p	0.752	6.55E-03	7mer-m8	3186-3192
Rps12	2.097	2.19E-06	miR-96-5p	0.235	1.36E-17	7mer-m8	2285-2291
Acot13	2.097	2.94E-07	miR-429-3p	0.329	3.53E-12	7mer-m8	4417-423
			miR-200b-3p	0.375	6.58E-08	7mer-m8	4417-423
			miR-653-5p	0.616	4.04E-03	7mer-A1	5139-5145
			miR-181d-5p	0.676	2.00E-04	7mer-m8	4525-4531
			miR-181b-5p	0.680	5.42E-05	7mer-m8	4525-4532
Aamdc	2.094	9.88E-15	miR-485-5p	0.753	4.04E-03	7mer-m8	64-70
Cisd3	2.093	9.98E-20	miR-9-5p	0.753	5.60E-03	7mer-A1	358-364
Tmem151b	2.035	2.86E-07	miR-129-1-3p	0.570	4.18E-04	7mer-m8	2722-2728
			miR-129-2-3p	0.590	1.62E-05	7mer-m8	2722-2728
			miR-181d-5p	0.676	2.00E-04	7mer-m8	2226-2232
			miR-181b-5p	0.680	5.42E-05	7mer-m8	2226-2233
			miR-132-3p	0.726	6.55E-03	8mer	339-346
			miR-29b-3p	0.726	4.41E-03	7mer-m8	2452-2458
			miR-485-5p	0.753	4.04E-03	8mer	2089-2096
Erh	2.031	1.69E-09	miR-181d-5p	0.676	2.00E-04	7mer-m8	118-124
			miR-181b-5p	0.680	5.42E-05	7mer-m8	118-124
Tomm5	2.011	4.37E-19	miR-151-3p	0.770	6.36E-03	7mer-m8	383-389
Gosr2	0.374	1.22E-11	miR-27a-3p	1.421	8.66E-04	8mer	94-101
Nkx2-1	0.459	1.19E-03	miR-503-5p	1.581	1.48E-03	7mer-m8	74-80
Prkag1	0.488	8.60E-03	miR-34a-5p	1.941	7.79E-08	7mer-m8	42-48
			miR-34b-5p	1.893	1.43E-06	7mer-m8	42-48
Lurap1l	0.489	1.18E-06	miR-497a-5p	2.053	3.09E-13	8mer	60-67
			miR-503-5p	1.581	1.48E-03	7mer-A1	61-67
Pfn2	**0.496**	**8.36E-09**	**miR-106b-5p**	**1.789**	**9.32E-11**	**7mer-m8**	**452-458**
			miR-106b-5p	**1.789**	**9.32E-11**	**7mer-m8**	**1197-1203**
Zbtb9	0.496	3.34E-05	miR-497a-5p	2.053	3.09E-13	7mer-m8	42-48
			miR-497a-5p	2.053	3.09E-13	7mer-m8	45-51
			miR-106b-5p	1.789	9.32E-11	8mer	822-829

Target prediction of miRNAs differentially expressed in the MHb

As in the IPN, TargetScan Mouse 7.1 was used to identify targets of differentially expressed, conserved miRNAs that are inversely regulated by chronic nicotine treatment and withdrawal in the MHb. In a pattern similar to the IPN, very few miRNAs and mRNAs exhibit significant alterations expression level after chronic nicotine treatment. Of the 6 miRNAs differentially expressed in the MHb of Nic mice compared to TA controls, 5 are broadly conserved in vertebrates. However, there are no inversely regulated mRNAs (with FC > 2) that contain conserved MREs for these miRNAs in the IPN or MHb.

During acute nicotine withdrawal, there are 85 differentially expressed miRNAs in the MHb and 59 of these are conserved. Of these, TargetScan Mouse 7.1 predicted that 32 miRNAs target at least one of 50 different mRNAs inversely expressed (FC > 2) in NAWD mice compared to TA controls (Table 3.3). The regulation of the majority (72%) of the predicted targets is an effect solely of nicotine withdrawal, being similarly regulated in NAWD mice compared to either TA- or Nic-treated mice (Table 3.3, orange). Twenty-six (52%) of the predicted targets contain multiple MREs or are predicted to be targeted by more than one inversely expressed miRNA.

Table 3.3. Target prediction of miRNAs differentially expressed in the MHb during acute nicotine withdrawal (NAWD) compared to TA controls. mRNAs that are similarly differentially expressed during chronic nicotine treatment (Nic) compared to TA mice are highlighted in green. mRNAs are similarly up- or down-regulated in NAWD mice are compared to either TA or Nic are highlighted in orange.

mRNA	mRNA FC	mRNA FDR	miRNA	miRNA FC	miRNA FDR	Seed Type	Position in 3′-UTR
Arf5	4.543	1.01E-24	miR-29b-3p	0.650	4.95E-06	8mer	392-399
Pcolce2	4.447	9.69E-19	miR-340-5p	0.618	2.19E-10	7mer-A1	329-335
			miR-146b-5p	0.721	1.68E-04	7mer-A1	3039-3045
Tom1l1	4.011	2.74E-21	miR-340-5p	0.618	2.19E-10	7mer-A1	397-403
			miR-340-5p	0.618	2.19E-10	8mer	2622-2629
			miR-181b-5p	0.763	2.71E-03	8mer	371-378
			miR-142a-5p	0.765	8.25E-03	7mer-A1	2622-2628
			miR-181c-5p	0.770	3.26E-03	8mer	371-378
Rasd1	3.629	3.25E-11	miR-377-3p	0.558	4.71E-04	7mer-m8	572-578
			miR-30c-5p	0.710	2.01E-04	8mer	465-472
			miR-384-5p	0.735	3.14E-04	8mer	465-472
Pcna	3.195	6.07E-16	miR-137-3p	0.652	9.24E-08	8mer	420-427
Spns1	3.031	1.55E-11	miR-29b-3p	0.650	4.95E-06	8mer	266-273
Ppp2cb	3.022	5.91E-20	miR-183-5p	0.551	2.97E-06	8mer	152-159
			miR-142a-5p	0.765	8.25E-03	7mer-A1	142-148
Steap3	2.857	2.10E-06	miR-377-3p	0.558	4.71E-04	7mer-A1	704-710
Dnajc9	2.787	7.78E-14	miR-132-3p	0.710	1.32E-04	7mer-m8	1040-1046
Rpa1	2.704	2.98E-15	miR-30c-5p	0.710	2.01E-04	7mer-m8	1195-1201
			miR-384-5p	0.735	3.14E-04	7mer-m8	1195-1201
			miR-361-5p	0.762	2.72E-03	7mer-m8	591-597
			miR-361-5p	0.762	2.72E-03	7mer-A1	627-633
Net1	2.675	4.10E-07	miR-340-5p	0.618	2.19E-10	7mer-A1	31-37
			miR-135a-5p	0.631	7.96E-09	8mer	831-838
			miR-135b-5p	0.645	4.36E-05	8mer	831-838
Gpx4	2.617	1.68E-17	miR-374b-5p	0.549	2.62E-05	7mer-A1	833-839
Ogfod2	2.613	3.97E-11	miR-340-5p	0.618	2.19E-10	493-500	8mer
Sin3a	2.598	2.68E-09	miR-211-5p	0.492	7.97E-12	7mer-m8	870-876
			miR-183-5p	0.551	2.97E-06	7mer-m8	644-650
			miR-493-5p	0.699	3.98E-03	7mer-m8	724-730
			miR-493-5p	0.699	3.98E-03	8mer	840-847
Eif5a	2.561	5.52E-19	miR-495-3p	0.472	8.00E-16	7mer-A1	589-595
Gosr2	2.511	5.84E-16	miR-493-5p	0.699	3.98E-03	8mer	1649-1656
Chst15	2.455	2.63E-07	miR-342-3p	0.704	8.42E-05	8mer	1364-1371
Tmem159	2.443	1.65E-04	miR-135a-5p	0.631	7.96E-09	7mer-m8	607-613
			miR-135b-5p	0.645	4.36E-05	7mer-m8	607-613
Rab40b	2.414	3.16E-05	miR-211-5p	0.492	7.97E-12	8mer	336-343
Rabl6	2.413	2.15E-08	miR-30c-5p	0.710	2.01E-04	8mer	371-378
			miR-384-5p	0.735	3.14E-04	8mer	371-378
Id3	2.400	5.82E-11	miR-340-5p	0.618	2.19E-10	7mer-A1	489-495
Htra2	2.381	6.59E-05	miR-410-3p	0.667	4.11E-07	7mer-A1	160-166
Kctd3	2.355	2.23E-08	miR-29b-3p	0.650	4.95E-06	7mer-A1	432-438
			miR-30c-5p	0.710	2.01E-04	7mer-m8	411-417
			miR-384-5p	0.735	3.14E-04	7mer-m8	411-417
Atg16l1	2.346	3.04E-12	let-7k	0.615	1.81E-04	7mer-A1	235-241
			miR-410-3p	0.667	4.11E-07	8mer	1100-1107
			miR-142a-5p	0.765	8.25E-03	7mer-m8	872-878
Srl	2.344	8.98E-04	miR-211-5p	0.492	7.97E-12	8mer	2918-2925
			miR-136-5p	0.582	2.87E-08	8mer	818-825
			miR-136-5p	0.582	2.87E-08	8mer	4468-4475
Marcksl1	2.271	1.11E-08	miR-23b-3p	0.740	1.75E-03	8mer	576-583
			miR-23a-3p	0.755	3.09E-03	8mer	576-583
Ccdc32	2.241	2.68E-07	miR-377-3p	0.558	4.71E-04	7mer-m8	165-171

Prpf19	2.227	2.45E-17	miR-377-3p	0.558	4.71E-04	8mer	2354-2361
			miR-421-3p	0.701	6.33E-03	8mer	2841-2848
			miR-203-3p	0.732	7.63E-04	7mer-m8	120-126
Tbc1d8b	2.222	2.86E-03	miR-340-5p	0.618	2.19E-10	8mer	2336-2343
			miR-142a-5p	0.765	8.25E-03	7mer-m8	1016-1022
			miR-142a-5p	0.765	8.25E-03	7mer-A1	2336-2341
Kdelr1	2.222	7.47E-08	miR-340-5p	0.618	2.19E-10	7mer-A1	313-319
			miR-335-5p	0.637	4.58E-06	7mer-A1	715-721
Gm2a	2.184	1.22E-07	miR-6395	0.682	5.46E-03	8mer	591-598
Zfp622	2.170	1.71E-11	miR-181b-5p	0.763	2.71E-03	8mer	410-417
			miR-181c-5p	0.770	3.26E-03	8mer	410-417
Gap43	2.163	3.62E-03	miR-23b-3p	0.740	1.75E-03	7mer-m8	433-439
			miR-23a-3p	0.755	3.09E-03	7mer-m8	433-439
Grasp	2.157	9.32E-04	miR-132-3p	0.710	1.32E-04	7mer-m8	668-674
Gpr182	2.134	4.61E-03	miR-30c-5p	0.710	2.01E-04	7mer-A1	2658-2664
			miR-384-5p	0.735	3.14E-04	7mer-A1	2658-2664
Metap1	2.125	1.20E-06	miR-211-5p	0.492	7.97E-12	7mer-m8	1354-1360
			miR-382-3p	0.528	3.46E-11	7mer-m8	1373-1379
			miR-181b-5p	0.763	2.71E-03	7mer-m8	1334-1340
			miR-142a-5p	0.765	8.25E-03	7mer-m8	1221-1227
			miR-181c-5p	0.770	3.26E-03	7mer-m8	1334-1340
Chid1	2.123	5.05E-07	miR-142a-5p	0.765	8.25E-03	7mer-m8	2673-2679
Tmem184a	2.121	3.51E-03	miR-137-3p	0.652	9.24E-08	8mer	2889-2896
			miR-410-3p	0.667	4.11E-07	7mer-A1	3706-3712
			miR-493-5p	0.699	3.98E-03	7mer-m8	2883-2889
			miR-487b-3p	0.702	4.08E-04	8mer	3684-3691
Htr2c	2.106	2.43E-10	miR-382-3p	0.528	3.46E-11	8mer	1230-1237
			miR-137-3p	0.652	9.24E-08	8mer	2964-2971
			miR-23b-3p	0.740	1.75E-03	8mer	1871-1878
			miR-23a-3p	0.755	3.09E-03	8mer	1871-1878
Alpl	2.103	3.66E-06	miR-211-5p	0.492	7.97E-12	8mer	655-662
Ddah2	2.093	1.58E-08	miR-29b-3p	0.650	4.95E-06	7mer-m8	69-75
Zkscan4	2.087	1.94E-05	miR-29b-3p	0.650	4.95E-06	7mer-A1	390-396
Atg7	2.087	1.98E-05	miR-211-5p	0.492	7.97E-12	8mer	1454-1461
			miR-382-3p	0.528	3.46E-11	7mer-m8	1438-1444
			miR-142a-5p	0.765	8.25E-03	7mer-m8	879-885
Galnt18	2.083	1.04E-04	miR-340-5p	0.618	2.19E-10	7mer-A1	245-251
Thg1l	2.060	1.05E-03	miR-340-5p	0.618	2.19E-10	7mer-A1	280-286
Slc25a18	2.045	5.08E-05	let-7k	0.615	1.81E-04	8mer	106-113
Api5	2.023	3.22E-09	miR-203-3p	0.732	7.63E-04	8mer	1699-1706
Bcl2l1	2.020	8.98E-07	miR-495-3p	0.472	8.00E-16	7mer-A1	1219-1225
			miR-377	0.558	4.71E-04	7mer-m8	1242-1248
			miR-377	0.558	4.71E-04	8mer	1424-1431
			let-7k	0.615	1.81E-04	8mer	947-954
			miR-342	0.704	8.42E-05	7mer-m8	1243-1249
Cat	2.014	3.45E-06	miR-23b-3p	0.740	1.75E-03	8mer	793-800
			miR-23a-3p	0.755	3.09E-03	8mer	793-800
Ccdc80	2.011	6.43E-03	miR-29b-3p	0.650	4.95E-06	8mer	213-220
			miR-433-3p	0.673	1.45E-05	8mer	1243-1250

Validation of alterations in miRNA/mRNA expression in the IPN and MHb during acute nicotine withdrawal

To confirm the up- and down-regulation of transcripts during acute nicotine withdrawal, relative expression levels were measured by RT-qPCR. According to miRNA-Seq differential expression analysis, miR-106b-5p was up-regulated by ~80% in the IPN of mice in acute nicotine withdrawal compared to TA controls. This miRNA was similarly up-regulated when NAWD mice are compared to Nic-treated mice, indicating it is only regulated by nicotine withdrawal. According to TargetScan Mouse 7.1, miR-106b-5p is predicted to target two distinct MREs within the 3′-UTR of *Profilin 2* (*Pfn2*) (Table 3.2, bolded). *Pfn2* was significantly down-regulated by approximately 50% by acute withdrawal, when NAWD is compared to either TA or Nic mice. RT-qPCR validated that in acute withdrawal, miR-106b-5p was significantly up-regulated by a fold change of 1.773 ± 0.153 in the IPN of NAWD mice compared to nicotine-naïve controls (Figure 3.15A). Expression of *Pfn2* was significantly down-regulated with a fold change of 0.7833 ± 0.05379 (Figure 3.15B), confirming the reciprocal relationship of miR-106b-5p and its predicted target during acute nicotine withdrawal.

The differential expression of mRNAs induced by acute nicotine withdrawal in the MHb was validated using the same approach. Sequencing revealed that 122 genes, including *Arf5*, *Atg7*, *Bcl2l1*, and *Eif5a*, were differentially expressed when NAWD are compared to either TA or Nic mice. The up-regulation of these 4 genes by acute nicotine withdrawal compared to TA-

treated controls, was validated by RT-qPCR (Figure 3.16). *Arf5* was significantly up-regulated by a fold change of 1.243 ± 0.07349 (Figure 3.16A). *Atg7* was significantly up-regulated by a fold change of 1.515 ± 0.186 (Figure 3.16B). *Bcl2l1* was significantly up-regulated by a fold change of 1.542 ± 0.06557 (Figure 3.16C). *Eif5a* was significantly up-regulated by a fold change of 1.428 ± 0.1239 (Figure 3.16D).

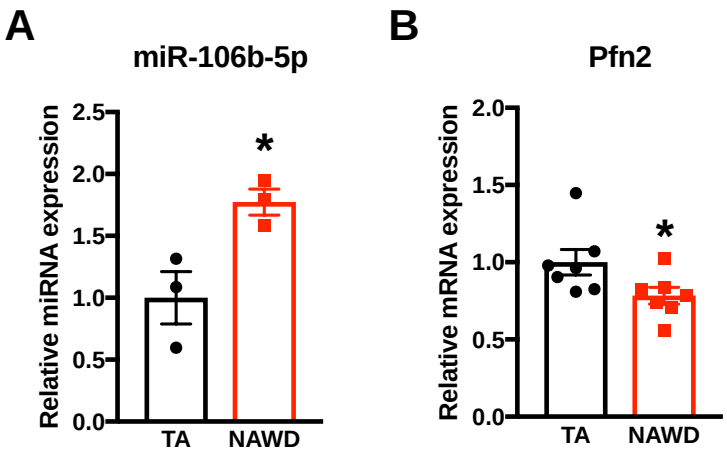

Figure 3.15. Reciprocal relationship between miR-106b-5p and *Pfn2* transcript expression in the IPN following acute withdrawal from nicotine. Total RNA was isolated from IPN tissue punches from TA (filled bars) and NAWD-treated (empty bars) mice. Relative gene expression was measured by RT-qPCR. Data are presented as mean ± SEM, normalized to TA controls. Unpaired, two-tailed *t*-test was used to compare the expression of miR-106b-5p (A, t_4 = 3.269, P = 0.0308) and *Pfn2* (B, t_{12} = 2.21, P = 0.0473) in NAWD mice compared to TA controls. (*) P < 0.05; n = 3-7, with each sample containing tissue pooled from 2 mice.

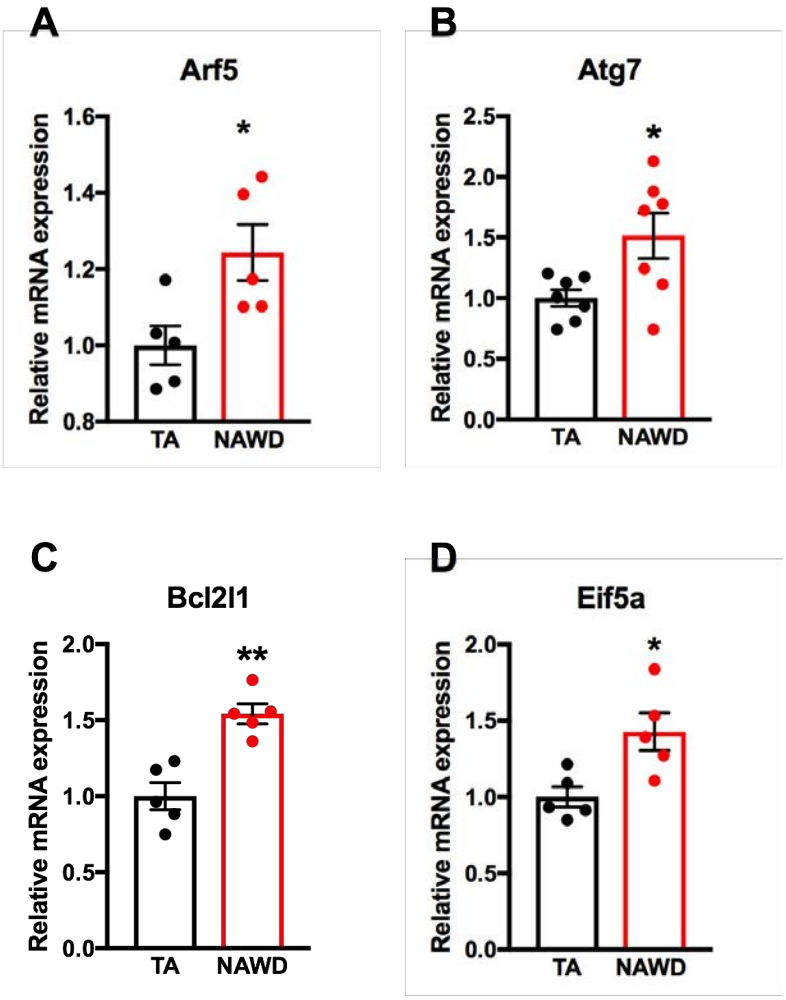

Figure 3.16. Relative quantitation of genes up-regulated in the MHb during acute nicotine withdrawal. RNA was isolated from MHb tissue punches of TA (filled bars) and NAWD-treated (empty bars) mice. Relative gene expression levels were measured by RT-qPCR. Data are presented as mean ± SEM, normalized to the TA control. Statistical analysis was performed using unpaired, two-tailed *t*-test to compare expression of *Arf5* (A, t_8 = 2.713, P = 0.0265), *Atg7* (B, t_{12} = 2.598, P = 0.0233), *Bcl2l1* (C, t_8 = 4.873, P = 0.0012), and *Eif5a* (D, t_8 = 3.041, P = 0.0160) in NAWD mice compared to TA controls. (*) P < 0.05; (**) P < 0.01; n = 5-7, with each sample containing tissue pooled from 2 mice.

3.D. Discussion

Acute nicotine withdrawal induces widespread differential expression of mRNAs in the habenulo-interpeduncular withdrawal circuit.

We employed mRNA-sequencing and differential expression analysis to measure transcriptome-wide changes in gene expression induced by chronic nicotine treatment and withdrawal in the habenulo-interpeduncular withdrawal circuit. In both the IPN and the MHb, there are very few mRNAs that are significantly altered by chronic nicotine treatment with fold changes > 2. Of the few mRNAs that are regulated by chronic nicotine exposure, the majority return expression levels to those of drug naïve animals after a 48-hour withdrawal. Specifically, only 2 mRNAs are similarly differentially expressed in both Nic and NAWD mice compared to TA controls in the MHb, indicating their regulation by chronic nicotine treatment persists for at least 48 hours after withdrawal.

After acute nicotine withdrawal, there are widespread changes in gene expression. Many of these mRNAs are similarly regulated when NAWD mice are compared to either TA- or Nic-treated mice, further suggesting that their regulation is solely the consequence of nicotine withdrawal and chronic nicotine treatment itself does not contribute to their up- or down-regulation. Gene ontology analysis identified significant enrichment of up-regulated genes in the IPN of NAWD mice related to ribosome structure and translation, further supporting the body of evidence suggesting that stable neuroadaptations

associated with drug addiction require *de novo* protein synthesis (Madsen et al. 2012). Thus, it is possible that up-regulation of ribosomes and other regulators of translation is an effort to fulfill the increased demand for protein products in the activated neurons of the IPN during nicotine withdrawal. In addition, in the MHb and IPN, there is significant enrichment of up-regulated genes related to the mitochondria. The functions of activated neurons, including maintenance of membrane resting potential, intracellular calcium buffering, and synaptic vesicle recycling, are highly energy-demanding (Harris et al. 2012, Devine and Kittler 2018). To meet the increased demand, neurons increase oxidative metabolism, but cannot up-regulate glycolysis (Magistretti and Allaman 2015). The enrichment of up-regulated genes related to mitochondria and oxidative energy production may reflect an effort to fulfill the increased energy demands of the highly active synapses of the IPN during nicotine withdrawal.

To confirm the validity of the sequencing and differential expression analysis, the relative expression of select genes was quantified by RT-qPCR. The expression of *Pfn2* in the IPN and *Arf5*, *Atg7*, *Bcl2l1*, and *Eif5a* in the MHb were significantly up- and down-regulated as observed in the differential expression analysis of sequencing data. However, in all cases, the fold changes observed in RT-qPCR experiments are lower than observed in the RNA-Seq data analysis. This is likely due to the necessity for a stably expressed endogenous control gene for normalization in calculating relative expression levels by the $2^{-\Delta\Delta Ct}$ method. Because nicotine exposure and withdrawal has widespread effects

on the expression of mRNAs, selection of a completely stable endogenous control is problematic. Using the sequencing data, *Gusb* was selected as an optimal reference gene for its stable expression across treatments and brain regions. However, there might be non-significant alterations in *Gusb* expression that explain the differences in fold changes calculated by RT-qPCR and the $2^{-\Delta\Delta Ct}$ method. Future validation of expression changes by RT-qPCR may be performed using several different endogenous controls that are stably expressed according to the RNA-Seq data analysis.

All of the genes differentially expressed in the MHb and IPN during acute nicotine withdrawal return to control expression levels after a prolonged 4-week period of abstinence. Only in the IPN were there a limited number of genes significantly and uniquely differentially expressed in NLWD mice compared to age-matched TAL controls. This suggests that,

for a subset of genes in the IPN, changes in mRNA expression induced by nicotine withdrawal are delayed and persist for at least 4 weeks. This subpopulation of genes displaying delayed/persistent dysregulation by nicotine treatment and withdrawal may contribute to the enduring anxiety behaviors observed in these mice (Figure 2.4) and the susceptibility to relapse that plagues nicotine addicts.

Differential expression of miRNAs in the habenulo-interpeduncular pathway is induced by chronic nicotine exposure and acute withdrawal.

In a pattern mirroring mRNA expression, miRNA-Seq and differential expression analysis identified many miRNAs that were differentially expressed after acute nicotine withdrawal, and relatively few miRNAs significantly differentially expressed by chronic nicotine exposure compared to TA controls. Approximately 33% and 47% of miRNAs differentially expressed in the IPN and MHb, respectively, of NAWD compared to TA mice are similarly regulated when compared to Nic mice. This suggests that these miRNAs are regulated only by withdrawal from nicotine, with no effect of the chronic nicotine treatment. In both the IPN and MHb, there are no miRNAs differentially expressed after a prolonged withdrawal from nicotine, indicating all miRNAs have returned to expression levels similar to age-matched drug naïve animals 4 weeks after cessation of nicotine treatment. Therefore, it is unlikely that alteration in miRNA expression does not play a role in the persistently anxious phenotype of mice after prolonged nicotine withdrawal. Taken together, in the MHb-IPN axis, miRNAs are regulated primarily during acute nicotine withdrawal, mirroring the effects of withdrawal on mRNA expression.

Differentially expressed miRNAs are predicted to target inversely regulated mRNAs in the IPN and MHb during acute nicotine withdrawal.

TargetScan Mouse 7.1 identified conserved MREs within the 3′-UTRs of differentially expressed mRNAs for inversely regulated miRNAs during acute nicotine withdrawal. In the IPN, 38 mRNAs differentially expressed in NAWD mice compared to TA controls were predicted contain at least one MRE for at least one of 25 inversely regulated miRNAs. In the MHb, 50 mRNAs altered in NAWD compared to nicotine-naïve controls were predicted to contain a conserved MRE for at least one of 32 conserved, inversely expressed miRNAs. In both regions, the majority of predicted targets are altered only during nicotine withdrawal. This suggests that in the MHb-IPN withdrawal axis, miRNAs may play an important role in the regulation of gene expression in response to nicotine withdrawal. This contrasts to the extremely limited number of miRNAs/mRNAs regulated and targets predicted after chronic nicotine treatment alone in these brain regions.

In many cases in the MHb and IPN, predicted mRNA targets contain multiple MREs for the same miRNA or are targeted by multiple miRNAs. For example, the 3′-UTR of *Pfn2* contains 2 predicted MREs for miR-106b-5p. In addition to the conservation of the MRE and the anti-correlation of miRNA/mRNA expression, the existence of additional MREs for a miRNA increases the probability that the miRNA is a biologically functional regulator of the predicted target. These miRNAs and their targets should be top candidates for future

studies investigating their roles in the molecular mechanisms underlying the neuroadaptations of nicotine withdrawal and withdrawal-associated anxiety.

CHAPTER 4

A Novel Role For *Profilin 2* (*Pfn2*) In Nicotine Withdrawal-Associated Anxiety

Contributions:
Cloning and luciferase assays were performed by Ciearra Smith.
Elevated plus maze and marble burying tests were performed by Rubing Zhao-Shea.
Novel object preference testing was performed by Susanna Molas.
Paul Gardner and Andrew Tapper contributed to experimental design.
I was responsible for all experimental design and data analysis. All all surgeries and experimental procedures were performed by me unless otherwise specifically noted.

4.A. Introduction

The differential expression analysis of mRNA-Seq data presented in Chapter 3 found that *Profilin 2* (*Pfn2*) was down-regulated in the IPN specifically during acute nicotine withdrawal, with no effects of chronic nicotine treatment itself. In addition, expression of miR-106b-5p, which was predicted to target 2 MREs within the 3′-UTR of *Pfn2*, was up-regulated after acute nicotine withdrawal. In light of the reciprocal expression of a predicted miRNA regulator, along with the known roles of *Pfn2* in the modulation of synaptic activity/morphology, we asked whether *Pfn2* plays a role in the induction of nicotine-withdrawal associated behaviors.

Regulation of the Synapse by Profilin 2 (Pfn2)

Pfn2 is a member of the profilin family of small, actin monomer-binding proteins (Honore et al. 1993, Witke 2004). While *Pfn1* is ubiquitously expressed throughout the body, *Pfn2* is most highly expressed in the brain (Witke et al. 2001). *Pfn2* is also the dominantly expressed profilin, representing approximately 75% of the profilin in the brains of rodents (Witke et al. 2001, Tariq et al. 2016). Importantly, the mouse *Pfn2* sequence is 94% identical to human *Pfn2* (Di Nardo et al. 2000).

Profilin’s function as a regulator of the neuronal cytoskeleton arises in part from its ability to act as a globular-actin monomer (G-actin) binding molecule. Profilin regulates actin polymerization by binding and sequestering G-actin.

Alternatively, profilins can also promote actin filament elongation by accelerating ADP-ATP nucleotide exchange on G-actin 1000-fold compared to the rates of simple diffusion (Mockrin and Korn 1980, Goldschmidt-Clermont et al. 1992), facilitating the addition of ATP-actin monomers to the growing filament (Witke 2004). In addition to its ability to bind G-actin monomers, *Pfn2* possesses a poly-L-proline binding domain which permits interaction with a plethora of other ligands whose functions contribute to synaptic morphology and function (Witke 2004) (Figure 4.1).

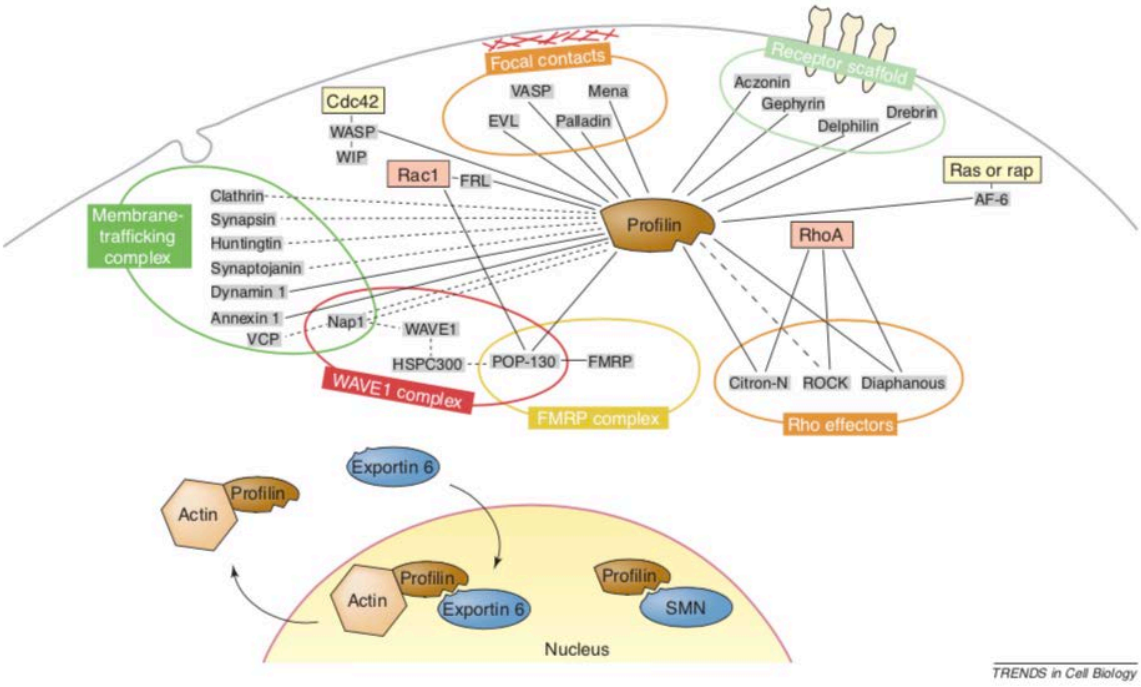

Figure 4.1. Molecular interactions of profilin. Schematic of proteins known to interact with profilins 1 and 2 grouped by cellular location and/or complexes. Direct interactions are indicated by solid lines and potential direct interactions are indicated by dashed lines. Abbreviations: AF-6: All-1 fusion partner from chromosome 6; EVL: EnaVASP-like; FMRP: Fragile X mental retardation protein; FRL: Formin-related gene in leukocytes; HSP: Heat-shock protein; Mena: Mouse homolog of Drosophila enabled; POP: Partner of profilin; SMN: Survival of motor neuron; VASP: Vasodilator-stimulated phosphoprotein; VCP: Valosine-containing protein; WASP: Wiskott-Aldrich syndrome protein; WAVE: WASP family verprolin-homologous protein; WIP: WASP-interacting protein.

In addition to binding G-actin monomers, *Pfn2* regulates actin polymerization at the synapse by direct interaction with the WAVE-complex (Pilo Boyl et al. 2007) (Figure 4.1), which in turn activates the Arp2/3 complex to promote actin nucleation. Interestingly, *Arpc3*, a component of the Arp2/3 complex, is a confirmed target of miR-29a/b, which is up-regulated in the mouse brain after acute nicotine injection, regulating dendritic spine morphology (Lippi et al. 2011). Additionally, WAVE-complexes can be activated by Arf5 GTPases (Koronakis et al. 2011). Our differential expression analysis revealed that *Arf5,* like *Pfn2,* is down-regulated in the IPN of mice in acute nicotine withdrawal, further suggesting that cytoskeletal dynamics are a key feature of the underlying mechanisms of nicotine withdrawal.

Pfn2 is expressed pre- and post-synaptically (Pilo Boyl et al. 2007). Post-synaptically, *Pfn2* accumulates in the dendritic spines of activated neurons (Ackermann and Matus 2003, Lamprecht et al. 2006), and plays a role in determining spine complexity through the regulation of cytoskeletal dynamics (Michaelsen et al. 2010, Michaelsen-Preusse et al. 2016). Changes in dendritic spine morphology are important for experience-dependent synaptic plasticity (Ottersen and Helm 2002, Trachtenberg et al. 2002). While *Pfn2* -/- mice display normal number of dendritic spines (Pilo Boyl et al. 2007), knockdown of *Pfn2* in primary hippocampal neurons decreases dendritic complexity, through pruning of already existing dendrites (Michaelsen et al. 2010). Additionally, *Pfn2*-deficient

primary hippocampal neurons exhibit abnormally motile spines, increased spine length and increased spine width (Michaelsen-Preusse et al. 2016).

Pfn2 interacts directly with ROCK, a RhoA-GTPase effector, regulating neuritogenesis in response to physiological stimuli (Da Silva et al. 2003) (Figure 4.1). Studies have shown that regulation by RhoA/ROCK contributes to the ability of *Pfn2 to* modify actin filament stability and act as a brake for neurite outgrowth (Da Silva et al. 2003, Nolle et al. 2011). Specifically, *Pfn2* -/- hippocampal neurons display increased number of highly branched neurites of increased length, while over-expression of *Pfn2* decreases neurite number and length (Da Silva et al. 2003). Interestingly, inhibition of ROCK in the mouse brain induces anxiety (Saitoh et al. 2006).

Our GO analysis revealed an enrichment of down-regulated genes related to cellular projection organization and neuron projection development in the IPN during nicotine withdrawal (Figure 3.8). In light of the known roles of *Pfn2* in the regulation of dendritic spine complexity and neuritogenesis described above, repression of *Pfn2* expression in the IPN during acute nicotine withdrawal may contribute to the molecular mechanisms underlying the biological processes related to neuron projections identified in the GO analysis.

Pre-synaptically, *Pfn2* can influence synaptic vesicle release, with *Pfn2* -/- mice displaying higher vesicle exocytosis and hyperactivation of the striatum (Pilo Boyl et al. 2007). Consistent with this, *Pfn2* has been shown to directly interact with *dynamin 1*, a GTPase involved in clathrin-mediated vesicle

formation, and other ligands regulating endocytosis and vesicle recycling (Witke et al. 1998, Gareus et al. 2006) (Figure 4.1). Regulation of the actin cytoskeleton has been linked to endocytosis, possibly by stabilizing the membrane curvature (Qualmann et al. 2000, Engqvist-Goldstein et al. 2004, Yarar et al. 2005, Gareus et al. 2006). Specifically, *Pfn2* over-expression inhibits endocytosis in HeLa cells, and cultured cortical neurons from Pfn2 -/- mice display increased endocytosis (Gareus et al. 2006).

Pfn2 can also influence the composition of neurotransmitter receptors at the post-synaptic surface (Witke 2004). For example, *Pfn2* has been shown to decrease surface localization of excitatory kainite glutamate receptors through regulation of endocytosis and membrane trafficking (Mondin et al. 2010). *Pfn2* has also been shown to interact with members of the membrane scaffold, such as gephyrin (Mammoto et al. 1997), anchoring receptors to the cytoskeleton.

The synaptic roles of *Pfn2* and its link to behaviors such as anxiety led us to hypothesize that down-regulation of *Pfn2* expression during acute nicotine contributes to the neural activation observed in the IPN during withdrawal, increasing anxiety-associated behaviors.

4.B. Materials and Methods

Animals

All experiments were conducted in accordance with the guidelines for care and use of laboratory animals provided by the National Research Council as well as with an approved animal protocol from the Institutional Animal Care and Use Committee of UMMS. WT male C57BL/6J (Jackson) were group-housed and were kept on a 12-h light/dark cycle (lights ON 7 A.M.) with food and water provided *ad libitum*.

Quantitative Reverse Transcription-PCR (RT-qPCR)

RT-qPCR for miRNAs and mRNAs was performed as previously described (Hogan et al. 2014). RNA was reverse transcribed by MMLV-reverse transcriptase (ThermoFisher Cat. # 28025013 or AM2043) using random decamers or miRNA-specific primers according to the manufacturer's instruction. Quantitative PCR was performed on a Applied Biosystems 7500 Real-Time PCR System using TaqMan miRNA and gene expression assays (ThermoFisher) for miR-106b-5p (Assay ID 000442), *Pfn2* (Assay ID Mm01289572_m1), and *Pfn1* (Assay ID Mm00726691_s1), in triplicate. Relative miRNA/gene expression was determined using the $2^{-\Delta\Delta Ct}$ method (Livak and Schmittgen 2001). miRNA and mRNA expression were normalized to snoRNA202 (Assay ID 001232) and β-

glucuronidase (Assay ID Mm01197698_m1), respectively, unless otherwise noted in figure legends.

Cloning

The 3′-UTR of *Pfn2* was amplified from mouse genomic DNA and cloned into the pMIR-REPORT Luciferase plasmid (Applied Biosystems). The WT *Pfn2* 3′-UTR was amplified using Phusion High-Fidelity DNA polymerase (NEB Cat. No. M0530) with a 1-min denaturing step at 98°C followed by 35 cycles of a 10-sec 98°C melting step, a 30-sec 57°C annealing step and a 30-sec 72°C extension step, and a final extension step at 72°C for 5 min. The PCR product was gel purified using a commercially available kit (QIAquick Gel Extraction Kit, Qiagen Cat. No. 28704). The PCR fragment and pMIR-REPORT Luciferase plasmid were digested with SpeI-HF and MluI-HF and ligated using T4 DNA ligase (NEB Cat. No. M0202) as previously described (Hogan et al. 2014). Ligation products were transformed into DH5α *Escherichia coli* (*E. coli*) (Invitrogen) and plated on LB agar plates containing 100 µg/ml ampicillin. Colonies were grown in LB medium supplemented with 100 µg/ml ampicillin and the plasmid was isolated using a commercially available kit (Plasmid Miniprep kit, Qiagen Cat. No. 27104). The WT *Pfn2* 3′-UTR luciferase expression plasmid was verified by Sanger sequencing (Genewiz).

Pfn2 3′-UTR PCR Primers:

F: 5′-ttggaggcggattgaataagaag-3′

R: 5′-ctctaccctccaagatcaacaata-3′

Site-directed Mutagenesis (SDM)

SDM was performed using a QuickChange Site-Directed Mutagenesis Kit (Agilent Cat. No. 200519) according to manufacturer's instructions. Primers substituted four nucleotides within two distinct predicted MREs*:* MRE1 and MRE2. Three mutant MRE/luciferase constructs were generated: single mutants for MRE1 or MRE2, and double mutant MRE1/2.

Briefly, the WT *Pfn2* 3′-UTR luciferase constructs were mixed with 10X reaction buffer, dNTP mix, PfuTurbo DNA polymerase, and primers. The parental DNA was digested with DpnI and transformed into XL1-Blue supercompetent *E. coli* cells (Invitrogen), grown in LB supplemented with 100 µg/ml ampicillin and isolated by Plasmid Mini Prep (Qiagen). Mutant luciferase constructs were verified by Sanger sequencing (Genewiz).

Pfn2 MRE1 SDM primers:

F: 5′-gagccaaggaaatgctccattgttttgaaaagacactgatcgagttagagac-3′

R: 5′-agtctctaactcgatcagtgtcttttcaaaacaatggagcatttccttggctc-3′.

Pfn2 MRE2 SDM primers:

F: 5′-actgtatcccagatgtaacattgtttagggaaagaaatggacaaatcagcaacaagatttg-3′

R: 5′-caaatcttgttgctgatttgtccatttctttccctaaacaatgttacatctgggatacagt-3′.

Cell Culture and Transfection

For transfection of miRNA mimics, the mouse septal cholinergic cell line SN17 (Hammond et al. 1990) was grown in Dulbecco's Modified Eagle's Medium (1X DMEM, Corning Cat. No. 10-017-CV) supplemented with 10% fetal bovine serum (FBS) and 100 U/ml penicillin/streptomycin. SN17 cells were transfected in duplicate with 10 nM miR-106b-5p mimic (ThermoFisher, mirVana Assay ID MC10067) or control scramble miRNA mimic (ThermoFisher, miRVana, Negative control #1), introduced using Lipofectamine 2000 Reagent (Invitrogen Cat. No. 11668027) in Opti-MEM reduced serum medium (Gibco, Cat. No. 31985062). After 24 hours, cells were harvested and RNA was isolated using an RNAqueous Total RNA Isolation kit (Ambion, AM1912) for RT-qPCR.

For luciferase reporter gene assays, HEK293T cells were grown in 1X DMEM supplemented with 10% FBS and 100 U/ml penicillin/streptomycin. Cells were seeded at a density of 17,000 cells per well into 96-well plates. Cells were co-transfected in duplicate with 20 ng pMIR-REPORT Luciferase construct and 20 ng pMIR-REPORT-β-galactosidase control plasmid (Applied Biosystems, AM5795), in combination with 10 nM miR-106-5p miRNA mimic or a scramble control mimic as described by Hogan et al., 2014. The plasmids and mimics were co-transfected in HEK293T cells using Opti-MEM and 0.08 µl of Lipofectamine 2000 per well. Cells were harvested and lysed using 20 µl of 1X Reporter Buffer (Promega) 24 hours post-transfection and assayed for luciferase and β-galactosidase activities.

Reporter Gene Assays

Luciferase and β-galactosidase activity were assayed in duplicate, using commercially available kits (Luciferase Assay Kit, Promega Cat. No. 6066706; Galacto-Light Plus, Invitrogen Cat. No. T1007) on an MLX Microtiter Plate Luminometer (Dynex Technologies). To correct for transfection variability, luciferase activity was normalized to β-galactosidase activity in each sample.

Knockdown of *Pfn2* in SN17 cells by Lenti-GIPZ-shRNA

To test the efficacy of shRNAs targeting *Pfn2*, SN17 cells were infected lots of commercially available lentiviral particles expressing one of three distinct shRNAs directed against *Pfn2* or a scramble shRNA control (Lenti-pGIPZ-shRNA, Dharmacon). The shRNA source clones targeted the following sequences: V3LMM_494366 5′-TTTCCTACAATCATATCTA-3′, V3LMM_494367 5′-TATCCACGTAGCTCTGCCA-3′, V3LMM_494369 5′-CTGATCACAGAACACTTCT-3′. SN17 cells (passage 5) were seeded at a density of 2.5 x 10^4 cells per well in a 24-well plate and incubated overnight. Cells were transduced with lentivirus (multiplicity of infection 0.4) in technical duplicates using 8 µg/ml polybrene in a total of 250 µl per well. After 5 hours, an additional 1 ml of complete growth medium was added to each well. Approximately 48 hours after transduction, medium was aspirated and replaced with 0.5 ml of complete growth medium containing 2.5 µg/ml puromycin to select for cells successfully transduced with lentivirus. Puromycin selection was

performed for a total of 5 days, changing medium every other day. On day 5, cells were harvested and total RNA was isolated using the RNAqueous Total RNA Isolation Kit (ThermoFisher AM1912), eluting in 60 µl RNA (125 ng) was reverse transcribed using M-MLV Reverse Transcriptase (ThermoFisher Cat No. 28025013) according to manufacturer's instructions. Relative expression of *Pfn2* was measured by RT-qPCR.

shRNA-mediated inhibition of Pfn2 in vivo

To inhibit *Pfn2* expression *in vivo*, we employed lentiviral delivery of shRNA targeting *Pfn2* (sense sequence 5′-AGAAGTGTTCTGTGATCAG-3′) to the IPN or VTA. Lenti-pGIPZ-*Pfn2*-shRNA-tGFP ($2.37x10^8$ TU/ml, V3LMM_494369, Dharmacon) or a control virus expressing a non-silencing shRNA (lenti-pGIPZ-scramble-tGFP, $9.06x10^8$ TU/ml, RHS4348, Dharmacon) were injected into IPN or VTA and expressed for 4 weeks prior to all experiments.

After behavioral testing, a subset of mice were used to confirm knockdown of *Pfn2* expression *in vivo*. Fresh frozen brains were cryosectioned (12-µm), fixed in ice-cold acetone, and dehydrated in ethanol (70%, 90%, 100%) and xylenes. Areas expressing tGFP were isolated by laser capture microdissection (LCM; Arcturus). RNA was isolated using RNAqueous-Micro Total RNA Isolation Kit (Ambion) for RT-qPCR.

Stereotaxic Lentiviral Injection

Stereotaxic injections were performed under aseptic conditions on mice aged 6 weeks as otherwise described by Molas et al. (Molas et al. 2017). Virus was injected in the IPN or VTA (unilateral) at coordinates measured from the Bregma (in mm, anterioposterior, mediolateral, dorsoventral at 0°): IPN (-3.47, ±0, -4.77), VTA (-3.45, 0.5, -4.2) using a 26s gauge 10-µl syringe (701RN, Hamilton) to deliver 300 nl of virus at a controlled rate of 60 nl/min. Unilateral VTA injections were equally distributed on the left and right within each treatment group.

Behavioral Assays

All behavioral testing was performed during the light phase in dim white light after habituation to the testing room (≥30 min). On the first test day, mice underwent the marble-burying test (MBT) followed by the elevated plus maze (EPM). Approximately 48 hours later, mice underwent object novelty preference testing. Testing was performed in two cohorts of virus-injected mice, with balanced treatment groups by an experiementer blinded to the treatment groups. Lenti-virus expression was confirmed by fluorescence microscopy of tGFP. Mice with no virus expression in the brain region of interest were excluded from analysis.

MBT. For 2 days prior to testing, mice were habituated to individual standard mouse cages, filled 5-6 cm with bedding material, for approximately 1

hour per day. On the test day, 15 sterilized 1.5-cm diameter glass marbles were placed in the cages, equally spaced in a 3 x 5 grid arrangement. Mice were placed in the test cage for 30 min. then returned to their home cage. The number of marbles buried at least 75% with bedding were counted by an experimenter blinded to treatment.

EPM. Testing was performed on a sanitized, black Plexiglas apparatus consisting of 2 open (30 x 5 x 0.25 cm) and 2 closed arms with high walls (30 x 5 x 15 cm), arranged in a perpendicular arrangement, 45 cm above the floor. Mice were placed individually in the junction (5 x 5 cm) facing the open arms and allowed to freely explore the maze for 5 min. Time spent in each arm and the number of arm entries was recorded by MED-PC IV software (MED Associates, Inc.).

Object Novelty Preference Test. Testing was performed using a protocol modified from previously established methods used in our laboratory(Molas et al. 2017). A T-shaped maze (three arms, each 9 x 30 x 20 cm, connected through a 9 x 9 cm central zone) made of white Plexiglas was used to examine interest in familiar and novel inanimate objects under dim red light conditions. First, the mouse was habituated to the apparatus for 5 min and removed. Two identical plastic objects were placed in the ends of the T-maze, one in each end. The mouse was immediately placed back into the maze for 5 min and allowed to investigate the two identical novel objects (N_1). The mouse was removed and one object was replaced by a novel object in the same location as the previous

object (counter-balanced). The mouse was immediately placed in the T-maze and allowed to investigate the familiar (F_1) and novel (N_2) objects. All sessions were video recorded from above (HDR-CX4440 camera, Sony) and mouse behavior was tracked automatically using EthoVision XT 11.5 (Noldus Apparatus). A blind experimenter manually scored the times the mouse explored the familiar and novel objects. Exploration was defined as sniffing with the nose directed at the object from a distance of less than 2 cm. Simply sitting or resting next to the object was not counted as exploration. The novel object preference ratio was calculated as: (total novel object investigation – total investigation)/(total investigation) over the third 5-min session. The apparatus and objects were cleaned with Micro-90 solution (International Products Corporation) to eliminate olfactory traces after each session.

IV. C. Results

miR-106b-5p represses the expression of Pfn2 in vitro.

To test the hypothesis that miR-106b-5p negatively regulates the expression of *Pfn2*, SN17 cells were transfected with miR-106b-5p mimic followed by measurement of *Pfn2* expression by RT-qPCR. In cells transfected with 10 nM miRNA mimic, miR-106b-5p expression was significantly up-

regulated by a fold change of 329.6 ± 107.6 compared to cells transfected with scramble control (Figure 4.1A). Transfection with miR-106b-5p mimic significantly repressed *Pfn2* (Figure 4.1B) expression by a fold change of 0.5547 ± 0.1047. Importantly, expression of *profilin1* (*Pfn1*), a *Pfn2* paralog, was not significantly altered (Figure 4.1C).

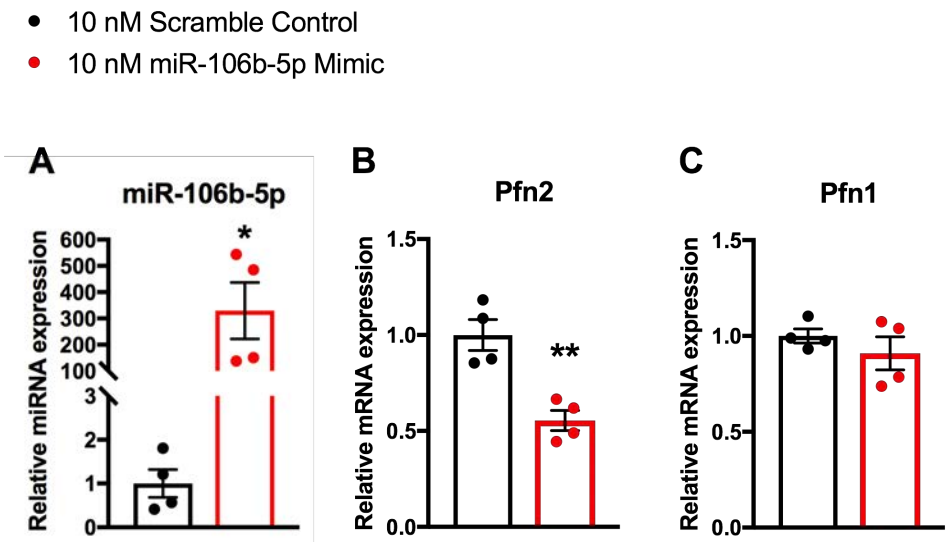

Figure 4.1. Over-expression of miR-106b-5p down-regulates *Pfn2*, but not *Pfn1*, expression in SN17 cells. SN17 cells were transfected with 10 nM miR-106b-5p mimic (empty bars) or scramble control (filled bars). Total RNA was isolated and relative gene expression was measured by RT-qPCR. Data are presented as mean ± SEM, normalized to scramble control. Unpaired, two-tailed *t*-test was used to compare relative expression of miR-106b-5p (A, $t_6 = 3.053$, P = 0.0224), *Pfn2* (B, $t_6 = 4.639$, P = 0.0035) and *Pfn1* (C, $t_6 = 0.9684$, P = 0.3702) in cells transfected with mimic compared to scramble controls. (*) P < 0.05, (**) P < 0.01; n = 4.

To test the hypothesis that one or both of the predicted MREs are required for the repression of *Pfn2* expression by miR-106b-5p, we employed a luciferase assay screen. HEK293T cells were co-transfected with miR-106b-5p mimic and a luciferase reporter containing the 3′-UTR of *Pfn2* with the WT MRE sequences, a single MRE mutant (MRE1 or MRE2), or a double mutant (MRE1/2*)* (Figure 4.2A). Co-transfection with a miR-106b-5p mimic and reporter for WT or MRE1 Mutant 3′-UTR, resulted in significant repression of luciferase activity compared to co-transfection of the WT reporter with scramble control. However, mutation of MRE2 individually or in combination with MRE1 results in de-repression of luciferase activity when co-transfected with miR-106b-5p mimic. This indicates that MRE2 at nucleotide position 1197-1203, but not MRE1, is required for repression of *Pfn2* by miR106-5p.

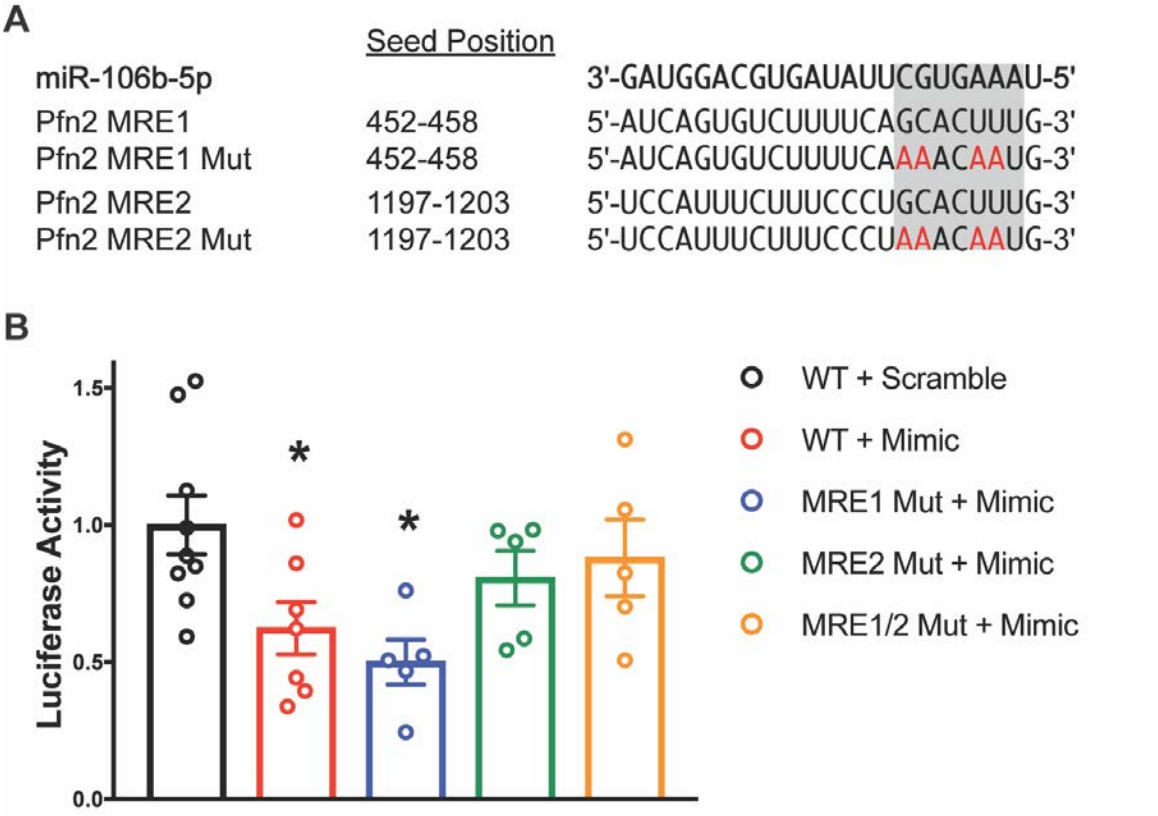

Figure 4.2. MRE2 at position 1197-1203 within the *Pfn2* 3′-UTR is required for repression of *Pfn2* by miR-106b-5p. (A) There are two predicted MREs for miR-106b-5p within the 3′-UTR of *Pfn2*. The miR-106b-5p sequence is bolded. The predicted MRE seeds are highlighted in gray, and their positions within the 3′-UTR are listed. A WT luciferase reporter containing the WT sequences at MRE1 and MRE2 is shown in black. Mutant *Pfn2* 3′-UTR reporters for each MRE individually (MRE1 Mut, MRE2 Mut) and combined (MRE1/2 Mut) were generated by site-directed mutagenesis of 4 nucleotides, indicated in red. (B) Predicted MREs were tested for miRNA-mediated repression of luciferase activity in HEK293T cells. Each bar represents normalized luciferase activity of cells co-transfected with the indicated luciferase/*Pfn2* 3′-UTR reporter and a miR-106-5p mimic, or a negative control scramble miRNA mimic. Data are presented as mean ± SEM, normalized to the WT *Pfn2* 3′-UTR reporter co-transfected with the scramble miRNA mimic. One-way ANOVA indicates there were significant differences between the mean relative luciferase activities detected in the indicated transfection groups ($F_{4,26} = 3.532$, $P = 0.0198$). Dunnett's post-test was used for statistical analysis comparing each treatment to the WT *Pfn2* 3′-UTR reporter co-transfected with the scramble miRNA mimic. (*) $P < 0.05$, n = 5-9.

Down-regulation of Pfn2 in the IPN is sufficient to induce anxiety.

Withdrawal from nicotine has been shown to induce anxiety in mice through activation of the IPN (Zhao-Shea et al. 2015). Using our treatment paradigm, WT NAWD mice displayed increased anxiety compared to nicotine- and TA-treated controls, as measured by the marble burying test and EPM (Figure 2.1). Because *Pfn2*-/- mice display increased synaptic vesicle exocytosis and hyperactivation of neurons (Pilo Boyl et al. 2007), we hypothesized that repression of *Pfn2* in the IPN is sufficient to induce anxiety, mimicking the behaviors observed in NAWD mice.

To knockdown *Pfn2* expression, the efficacies of three different commercially available shRNAs were tested in SN17 cells, a neuronal cell line derived from mice that exhibits endogenous expression of *Pfn2*. Transduction of SN17 cells with lenti-pGIPZ-Pfn2-shRNA-tGFP (Dharmacon) expressing 3 distinct shRNAs revealed shRNA494369 produced significant knockdown by 80.85% ± 0.4578 compared to cells transduced with lentivirus expressing a scramble control shRNA (Figure 4.3).

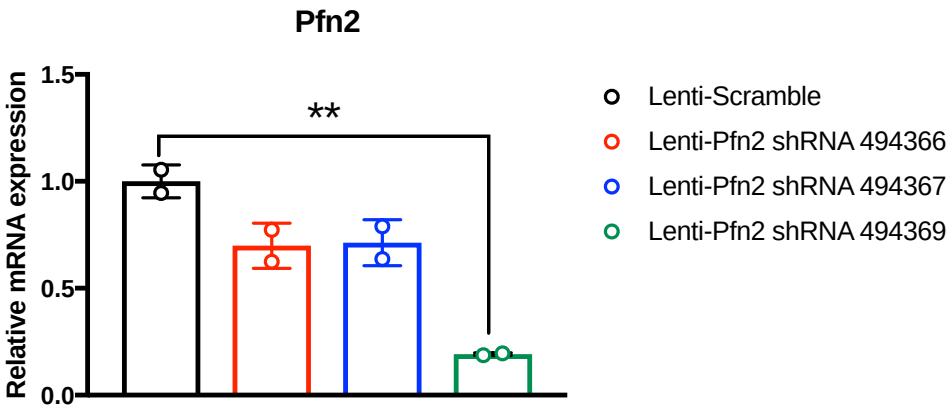

Figure 4.3. Transduction of Lenti-pGIPZ-*Pfn2*-shRNA494369-tGFP results in approximately 80% knockdown of *Pfn2* in SN17 cells. SN17 cells were transduced with the indicated lenti-pGIPZ-*Pfn2*-shRNA-tGFP or lenti-pGIPZ-Scramble-tGFP negative control as described in the Supplemental Methods and Materials. Total RNA was isolated and relative expression of *Pfn2* was determined by RT-qPCR. Data are presented as mean ± SEM, relative to lenti-scramble control. Statistical analysis was performed using a one-way ANOVA ($F_{3,4} = 31.49$, $P = 0.0031$) with Dunnett's post-test, (**) $P < 0.01$; (n = 2)

To test the hypothesis that knockdown of *Pfn2* in the IPN is sufficient to induce anxiety, the IPN of nicotine-naïve mice was injected with lenti-pGIPZ-Pfn2-shRNA494369-tGFP or control virus (Figure 4.5A). After 4 weeks of expression, mice underwent behavioral testing for anxiety and were sacrificed to confirm virus injection location and in vivo knockdown of *Pfn2*. Injection of the IPN with lenti-pGIPZ-Pfn2-shRNA494369-tGFP resulted in 54.32% ± 12.49 knockdown of *Pfn2* expression in areas of the IPN enriched in cells expressing tGFP (Figure 4.5B) compared to mice injected with control virus. Virus expression was limited to the IPN and immediately surrounding brain areas, with no spread to distant midbrain regions, as detected by fluorescence microscopy (Figure 4.6).

When *Pfn2* was knocked down in the IPN, mice spent significantly less time in the open arms of the EPM compared to controls (Figure 4.5C). Importantly, there was no significant difference in the number of total arm entries, indicating the results are not confounded by non-specific effects on locomotor activity (Figure 4.5C). To control for effects of lentiviral spread into the neighboring VTA, anxiety was measured in mice injected with lenti-pGIPZ-Pfn2-shRNA494369-tGFP in the VTA unilaterally (Figure 4.7). Any expression of lentivirus in the IPN resulted in exclusion from this control experiment. When *Pfn2* was knocked down in the VTA unilaterally, there was no significant effect on the amount of time spent in the open arms of the EPM or total number of arm

entries (Figure 4.5D). There was no significant effect of *Pfn2* KD in the IPN or VTA on the number of marbles buried in the marble bury test (Figure 4.8).

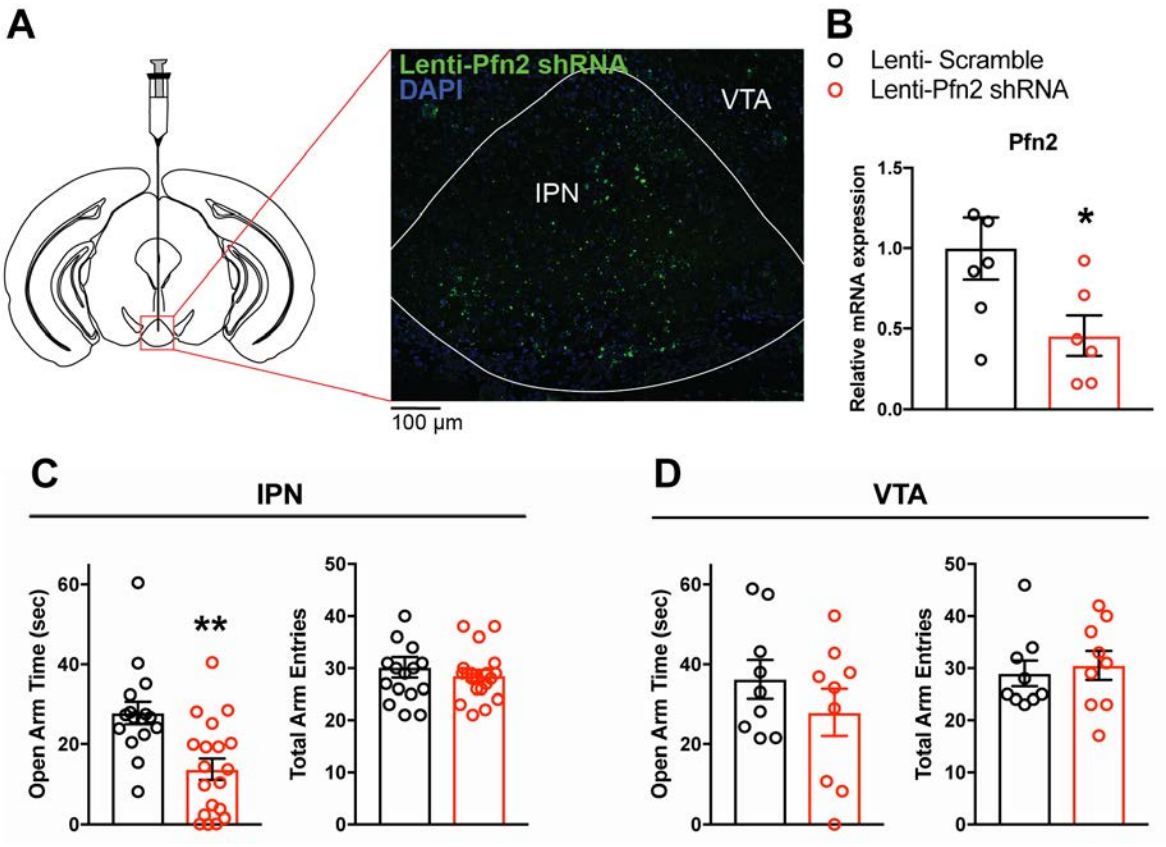

Figure 4.5. Knockdown of *Pfn2* in the IPN is sufficient to increase anxiety in the elevated plus maze. (A) Representative midbrain coronal section schematic and fluorescence microscopy image of WT mouse injected with lenti-pGIPZ-*Pfn2*-shRNA-tGFP (green) in the IPN. Nuclei were labeled with DAPI (blue). (B) Knockdown of *Pfn2* expression was measured by RT-qPCR using RNA from laser-captured IPN tissue infected with lenti-pGIPZ-*Pfn2*-shRNA-tGFP compared to lenti-pGIPZ-scramble-tGFP control. mRNA expression was normalized to β-2-microglobulin. Statistical analysis using an unpaired, two-tailed *t*-test compared lenti-*Pfn2* shRNA mice to lenti-scramble controls ($t_{11} = 2.272$, P = 0.0441). (*) P < 0.05; n = 6-7. (C) Average time spent in the open arms and total number of arm entries in the elevated plus maze of mice injected with either lenti-*Pfn2* shRNA (open bars) or lenti-scramble shRNA control (filled bars) in the IPN. Data are presented as the mean ± SEM. Statistical analysis used an unpaired two-tailed *t*-test to compare time spent in open arms ($t_{33} = 3.583$, P = 0.0011) and total number of arm entries ($t_{33} = 0.7355$, P = 0.4672) of lenti-*Pfn2* shRNA mice to lenti-scramble controls. (**) P < 0.01 n = 16-19. (D) Average time spent in the open arms and average total number of arm entries in the elevated plus maze of mice unilaterally injected with either lenti-*Pfn2* shRNA (open bars) or lenti-scramble shRNA control (filled bars) in the VTA. Data are presented as the mean

± SEM. Unpaired, two-tailed *t*-test was used for statistical analysis of time spent in open arms (t_{16} = 1.09, P = 0.2918) and total arm entries (t_{16} = 0.4153, P = 0.6835). n = 9.

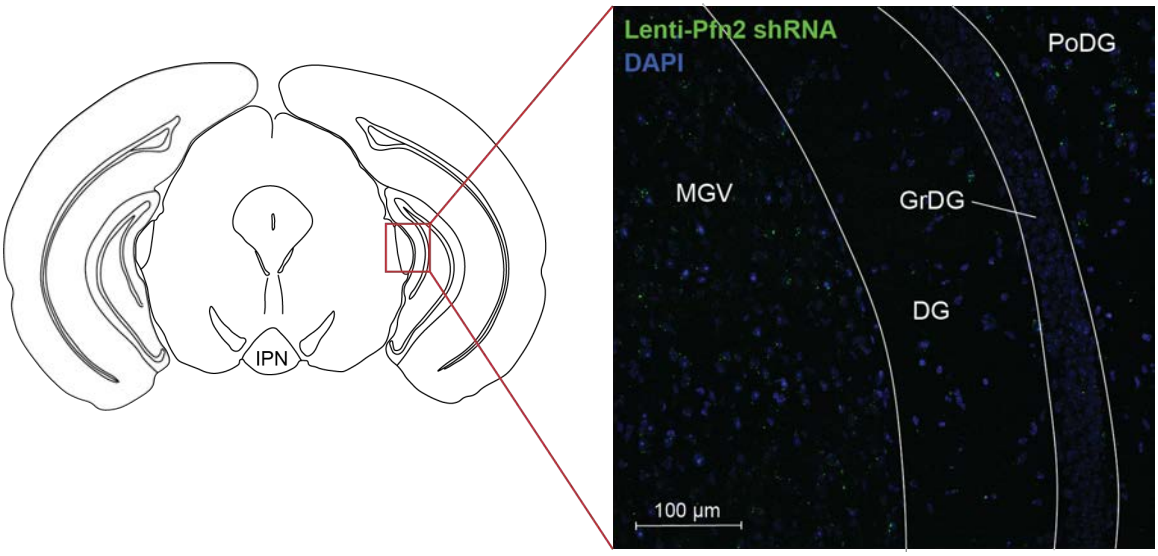

Figure 4.6. Lenti-pGIPZ-*Pfn2*-shRNA-tGFP injected in the IPN does not spread to distant brain regions within the midbrain. Representative midbrain coronal section from a WT mouse injected with lenti-pGIPz-*Pfn2*-shRNA-tGFP (green) in the IPN. There is no expression of virus above background levels in the MGV of the same slice represented in Fig. 4.5. DG: dentate gyrus; GrDG: granular layer of the dentate gyrus; MGV: medial geniculate complex, ventral part; PoDG: polymorph layer of the dentate gyrus.

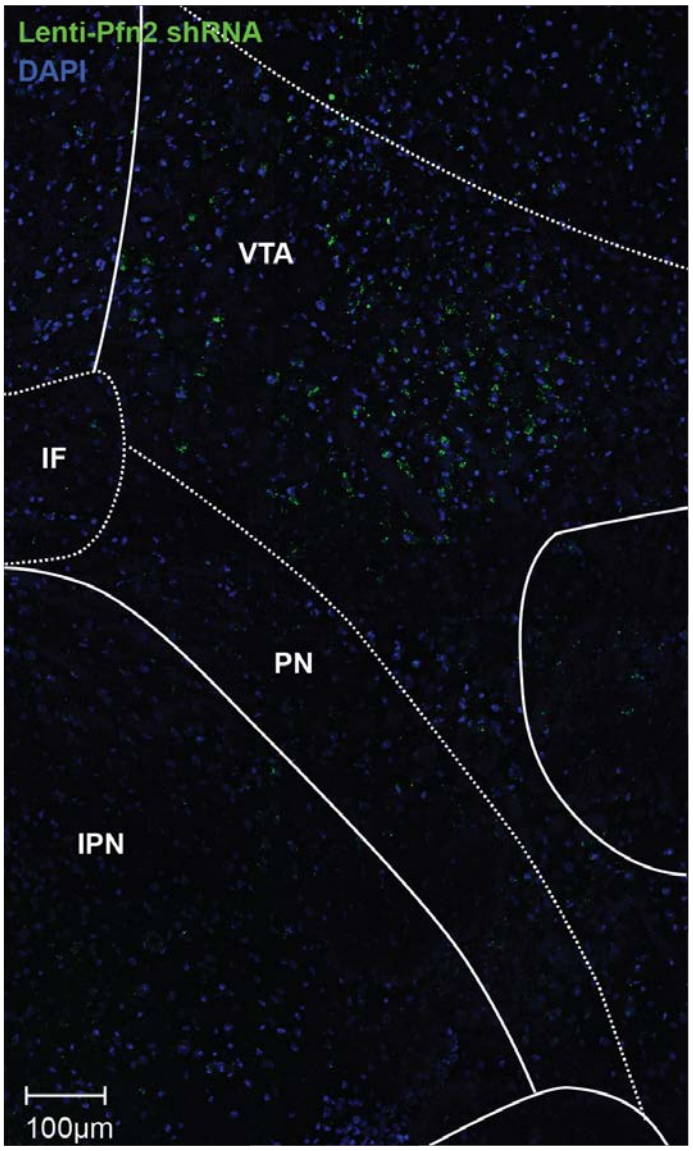

Figure 4.7. Lenti-pGIPZ-*Pfn2*-shRNA-tGFP injection of the VTA. Representative midbrain coronal section from a WT mouse infected with lenti-pGIPZ-*Pfn2*-shRNA-tGFP in the VTA (green). Nuclei were labeled with DAPI (blue). IF: interfascicular nucleus, IPN: interpeduncular nucleus; PN: paranigral nucleus; VTA: ventral tegmental area.

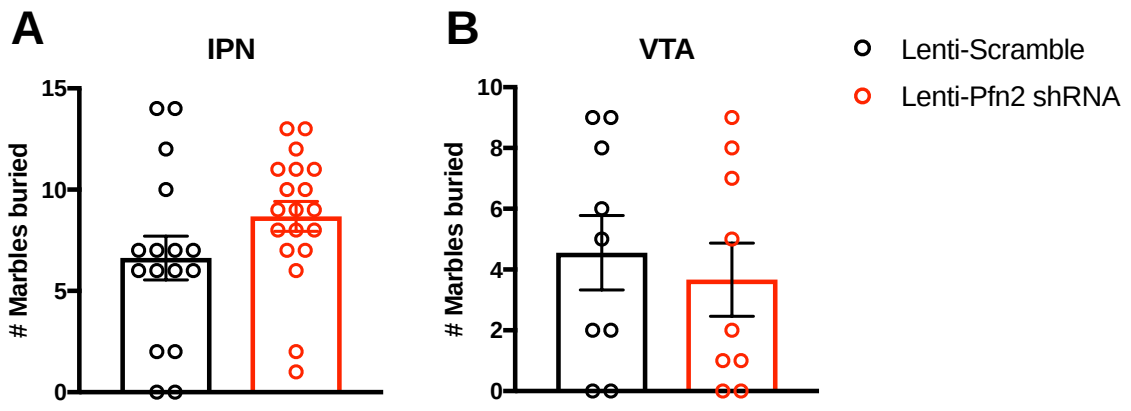

Figure 4.8. Knockdown of *Pfn2* in the IPN is not sufficient to increase anxiety in the marble burying test. Prior to testing on the EPM, WT mice injected with lenti-pGIPZ-*Pfn2*-shRNA-tGFP or lenti-scramble control were assayed in the marble burying test. Knockdown of *Pfn2* expression in the IPN (A) or VTA (unilateral; B) did not significantly alter the number of marbles buried compared to controls. Data are presented as the mean ± SEM. Statistical analysis used an unpaired, two-tailed *t*-test to compare number of marbles buried after knockdown of *Pfn2* expression in the IPN (t_{33} = 1.612, P = 0.1165, n = 16-19) or VTA (unilateral, t_{16} = 0.5177, P = 0.6117, n = 9) compared to lenti-scramble controls.

Knockdown of Pfn2 in the IPN is not sufficient to alter object novelty preference.

Because the IPN is also a prominent brain region in the circuitry underlying novelty preference (Molas et al. 2017) and novelty seeking behaviors are altered in *Pfn2* knockout mice (Pilo Boyl et al. 2007), we also tested the effect of *Pfn2* knockdown on object novelty preference. Briefly, during the test round of this assay, mice are allowed to explore a T-maze containing a novel and familiar object and the time spend actively investigating each is measured (Figure 4.9A). Expression of lenti-pGIPZ-*Pfn2*-shRNA494369-tGFP in the IPN did not significantly affect the time spent exploring the familiar or novel objects, the novel object preference ratio (calculated as described in the materials and methods), or the total time spent investigating the objects compared to controls (Figures 4.9B-D).

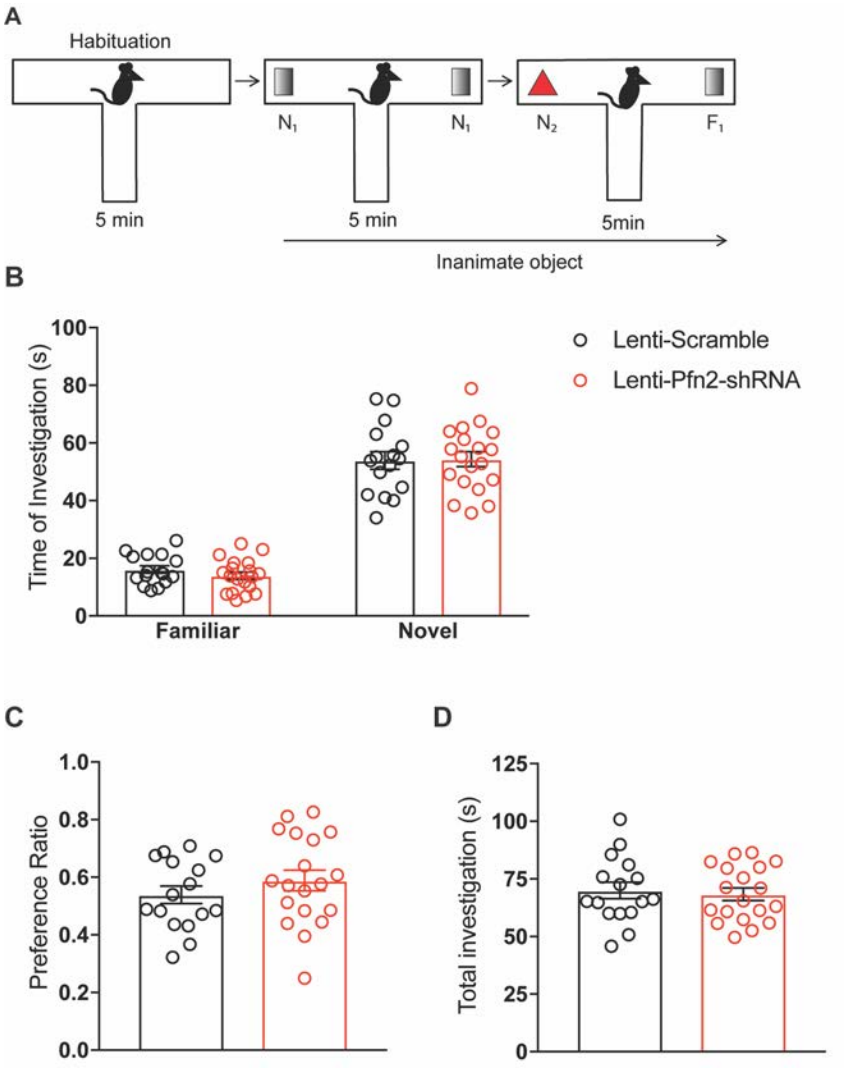

Figure 4.9. Knockdown of *Pfn2* in the IPN is not sufficient to alter object novelty preference. (A) Schematic of experimental protocol described in the Supplemental Methods and Materials. Mice expressing lenti-pGIPZ-*Pfn2*-shRNA-tGFP (open bars) in the IPN were compared to those expressing control virus (filled bars). (B) The time of investigation of the familiar (F_1) and novel (N_2) objects were manually scored by a blind experimenter for 5 minutes. Statistical testing by two-way ANOVA found there was significant effect of the row factor (object novelty) on the time of investigation ($F_{1,66}$ = 321.2, P < 0.0001). However, there is no significant effect of the column factor (virus injection) on the time of investigation ($F_{1,66}$ = 0.1425, P = 0.7071) (C) There is no difference in the novel object preference (t_{33} = 1.039, P = 0.3064, unpaired two-tailed *t*-test). (D) There is no difference in total time investigating the familiar and novel objects combined (t_{33} = 0.3692, P = 0.7143, unpaired two-tailed *t*-test). All data are presented as the mean ± SEM. n = 16-19.

4.D. Discussion

As an example of the utility of our miRNA/mRNA-Seq data analysis described in Chapters 2 and 3, we focused upon one gene regulated by acute nicotine withdrawal in the IPN, which was also predicted to be a target of an inversely expressed miRNA. Differential expression analysis of mRNA sequencing revealed *Pfn2* was down-regulated by 50.4% in the IPN of mice experiencing acute nicotine withdrawal compared to drug-naïve controls. *Pfn2* is a predicted target of miR-106b-5p, which was up-regulated by 78.9% during acute nicotine withdrawal. We demonstrated that over-expression of miR-106-5p repressed *Pfn2* expression in a cholinergic cell line. While transfection of cells with miRNA mimic increased the relative expression of miR-106b-5p to a level far beyond what is physiological or what is observed during nicotine withdrawal, the expression of *Pfn1*, a paralog that does not contain an MRE, was unaffected. This would support the hypothesis that over-expression of miR-106b-5p selectively represses its predicted targets, including *Pfn2*.

To determine if one or both of the predicted MREs within the 3′-UTR of *Pfn2* are required for repression by miR-106b-5p, we used a luciferase assay with reporters containing the 3′-UTR of WT *Pfn2*, single MRE mutants, and a double MRE mutant. This assay determined an intact MRE2 at nucleotide position 1197-1203, but not MRE1, was required for repression of *Pfn2* 3′-UTR reporter by miR-106b-5p. Further supporting MRE2 as a biologically functional target of miR-106b-5p, TargetScan mouse 7.1 ranked MRE2 with a higher

probability of conserved targeting (P_{CT}) (Friedman et al. 2009) of 0.83. Comparatively, MRE1 at position 452-458 had a P_{CT} of 0.63. Additionally, there is a strong preference for miRNAs to target MREs located in close vicinity to the stop codon and polyadenylation sites (Majoros and Ohler 2007). This further supports that MRE2, located nearer to the 3′-end of the transcript, is likely to be biologically functional.

We hypothesized that down-regulation of *Pfn2* by acute nicotine withdrawal in the IPN contributes to nicotine withdrawal-induced neuroadaptations underlying anxiety behaviors. *Pfn2* is an actin monomer-binding protein, enriched in the central nervous system, that acts a regulator of cytoskeletal dynamics (Witke et al. 2001, Witke 2004). Through an additional poly-L-proline binding domain, *Pfn2* also interacts with a variety of other ligands with functions in synaptic morphology and function (Witke 2004). For example, *Pfn2* accumulates in the dendritic spines of activated neurons (Ackermann and Matus 2003, Lamprecht et al. 2006), regulating their complexity (Da Silva et al. 2003, Michaelsen et al. 2010). Additionally, through interactions with specific effectors, *Pfn2* regulate neuritogenesis in response to physiological stimuli (Da Silva et al. 2003). Interestingly, our GO analysis (discussed in Chapter 3) revealed an enrichment of down-regulated genes related to cellular projection organization and neuron projection development in the IPN during nicotine withdrawal (Figure 3.4). We hypothesized that this enrichment may reflect changes in neuron morphology regulated by expression changes including the

repression of *Pfn2*. However, further studies are needed to determine the morphological changes of neurons in the IPN during acute nicotine withdrawal.

The IPN is activated during acute nicotine withdrawal, resulting in increased anxiety (Zhao-Shea et al. 2013, Zhao-Shea et al. 2015). *Pfn2* has also been shown to play a role in modulating synaptic activity. Through its interactions with a variety effectors involved in vesicle formation and the membrane scaffold, *Pfn2* can regulate synaptic vesicle release and the composition of receptors at the synaptic membrane (Mammoto et al. 1998, Witke et al. 1998, Witke 2004, Gareus et al. 2006, Mondin et al. 2010). In addition, *Pfn2 -/-* mice show increased vesicle exocytosis and hyperactivation of the striatum (Pilo Boyl et al. 2007). In light of this evidence, we hypothesized that down-regulation of *Pfn2* expression during acute nicotine contributes to activation of the IPN during withdrawal, increasing anxiety-associated behaviors. Supporting this hypothesis, we show that knockdown of *Pfn2* expression in the IPN of nicotine-naïve mice was sufficient to increase anxiety as measured by EPM, mimicking behaviors observed in WT mice during acute nicotine withdrawal. However, the MBT did not detect effect of Pfn2 knockdown in the IPN on anxiety. As discussed in Chapter 2, the somatic symptoms of acute, spontaneous nicotine withdrawal may contribute to increased marble burying and the MBT may have limitations in detecting anxiogenic effects of drugs (Jimenez-Gomez et al. 2011). Thus, although the EPM is the gold-standard for measuring anxiety in mice, future experiments should confirm this result using additional behavioral assays, such

as the open field test. The effect of repressing *Pfn2* expression in the IPN on behavior is specific for anxiety with no alterations in locomotor activity or object novelty preference, another behavior controlled by the IPN (Molas et al. 2017). To deepen our understanding of the functional consequences of *Pfn2* knockdown, future studies should focus on assessing the activation and morphology of neurons expressing *Pfn2* shRNA..

To control for the effects of lentiviral spread into the neighboring VTA, lenti-*Pfn2* shRNA was injected into the VTA unilaterally and anxiety was measured. Unilateral knockdown of *Pfn2* in the VTA did not significantly affect increase anxiety, but there was a trend towards a decreased time spent in the open arms in the EPM. Future studies should examine the anxiogenic effects of repressing *Pfn2* expression in the VTA bilaterally.

In addition to the knockdown of *Pfn2* using a lentiviral shRNA, future experiments may use an inducible *Pfn2* knockout mouse employing they Cre-lox system as a complementary approach. For example, generation of a mouse line with loxp sites flanking the *Pfn2* gene would allow for the conditional knockout of *Pfn2* in the IPN of adult mice via the injection of AAV expressing Cre recombinase.

Taken together, our results suggest a role for the down-regulation of *Pfn2* by miR-106b-5p in the IPN in the induction of nicotine withdrawal-associated anxiety behaviors. However, the specific mechanisms underlying the effects of *Pfn2* expression on neuronal activity and morphology in the IPN has yet to be

elucidated. Further work should focus on determining the effect of nicotine withdrawal, repression of *Pfn2,* and over-expression of miR-106b-5p on activation, organization, and morphology of the neurons and synapses of the IPN. Additionally, future experiments should investigate the effectors interacting with *Pfn2*. For example, *Pfn2* interacts directly with ROCK, a Rho GTPase effector whose inhibition in the mouse brain has been shown to induce anxiety (Da Silva et al. 2003, Saitoh et al. 2006). The role of ROCK and other ligands of *Pfn2* in nicotine withdrawal-induced behaviors must be pursued to fully understand the molecular mechanisms underlying the function of *Pfn2* and identify additional targets for pharmaceutical treatments of affective withdrawal symptoms.

CHAPTER 5

Discussion and Future Directions

5.A. Discussion and Conclusions

Nicotine addiction is a chronic relapsing disease during which many users cycle through periods of use and withdrawal when attempting to quit (Koob and Le Moal 2008). While the positive rewarding effects dominate early use of a nicotine, it is avoidance of the negative withdrawal symptoms that motivate continued use and relapse (Hughes 2007, Piper et al. 2011, Aguirre et al. 2015). Nicotine acts on nAChRs which are concentrated in the mesocorticolimbic reward and habenulo-interpeduncular withdrawal circuits in the brain (Marks et al. 1998, Dani and Bertrand 2007), mediating the two phases of the disease process of addiction. There is a great body of evidence describing the circuitry underlying behaviors associated with nicotine reward and withdrawal. However, the majority of current literature focuses on the up-regulation and activation of specific nAChR subtypes and other neurotransmitter receptors within these circuits, leaving much to be uncovered about alternative molecular mechanisms underlying the neuroadaptations of nicotine dependence. For example, miRNAs have been shown to be regulated by nicotine exposure (Lippi et al. 2011, Im and Kenny 2012, Lee et al. 2015), but their targets and functions in nicotine reward or withdrawal have not been confirmed. In an effort to identify novel mechanisms underlying the neuroadaptations of nicotine dependence, we sequenced miRNAs and mRNAs of brain regions comprising the mesocorticolimbic reward and habenulo-interpeduncular withdrawal circuits. This work presents integrated

differential expression and target prediction analyses of miRNAs/mRNAs within the NAc, midbrain, MHb and IPN during chronic nicotine treatment and withdrawal. We propose that this dataset represents a valuable resource, aiding in the identification of candidates regulated by nicotine treatment and withdrawal, such as *Pfn2*, for detailed future study.

The mesocorticolimbic transcriptome is regulated primarily by chronic nicotine exposure.

In Chapter 2, I presented differential expression analysis of miRNAs and mRNAs in the NAc and midbrain (enriched in VTA), prominent brain regions in the mesocorticolimbic DAergic reward pathway. In the NAc, chronic nicotine treatment induced limited changes in miRNA expression. However, there was widespread up- or down-regulation of mRNAs with fold changes > 2 induced by chronic nicotine treatment in the NAc. These altered mRNAs are enriched for GO categories including those related to neuron projection organization, synapse activity, binding of neurotransmitter receptors, and regulation of neurotransmitter levels. These changes in mRNA expression are likely reflective of the increased activation of the NAc in response to nicotine exposure, and these genes may contribute to the molecular mechanisms underlying the rewarding properties of nicotine, tolerance or sensitization.

After a short withdrawal of just 48 hours, approximately 97% of nicotine responsive genes in the NAc return to levels of expression observed in nicotine-

naïve animals. This would suggest that the increased anxiety behavior exhibited by mice in acute nicotine withdrawal is not due to regulation of gene expression at the transcript level in the NAc. Alternatively, it remains possible that chronic nicotine induces transient alterations in gene expression that result in persistent changes in the neuronal function beyond the level of the transcript. This may include persistent changes in protein levels, localization, and activation state, influencing neuronal and synaptic function and morphology. These possible alterations of the synapse during chronic nicotine exposure may create a new homeostatic state which is disturbed by subsequent withdrawal of nicotine, resulting in neuronal dysfunction and behavioral disturbances including anxiety.

The midbrain is similar to the NAc, in that chronic nicotine treatment induces widespread changes in mRNA expression, with very few alterations in miRNA expression. Again, the induction of transcriptional changes in the midbrain is likely reflective of the activation of the mesocorticolimbic DAergic pathway in response to nicotine treatment. However, the identity of up-or down-regulated genes in the midbrain is dissimilar to the NAc, indicating that regulation of gene expression by chronic nicotine treatment occurs in a brain-region specific manner within the reward pathway. This is also reflected in the GO analysis. For example, in the midbrain there is an overrepresentation of up-regulated mRNAs related to neuronal and synaptic activity and structure. Interestingly, these same categories are enriched in down-regulated genes in the NAc. Because both of these regions are activated by nicotine exposure (De Biasi and Dani 2011,

Pistillo et al. 2015), this inverse relationship of GO enrichment is somewhat surprising. This further supports brain-region specific molecular mechanisms underlying the nicotine-induced changes in neuronal function within the reward circuit.

Unlike the NAc, there is widespread differential expression of mRNA and miRNA expression in the midbrain during acute nicotine withdrawal. The majority of mRNA regulation in the midbrain of NAWD mice is due at least in part to the persistent effects of the initial chronic nicotine treatment. For instance, approximately 92% of the mRNAs that are up- or down-regulated during chronic nicotine treatment remain similarly altered in NAWD mice. In addition, only 2% of mRNAs regulated in NAWD mice compared to nicotine-naïve controls are regulated solely as an effect of nicotine withdrawal, being similarly differentially expressed in NAWD mice compared to either TA- or Nic-treated mice. This suggests that chronic nicotine treatment induces changes in gene expression that persist for at least 48 hours of withdrawal, possibly contributing to the induction of affective symptoms experienced during acute withdrawal, including anxiety. While traditionally thought of as a core component of the reward circuit, the VTA has been shown to project to at least a subset of neurons within the IPN, regulating nicotine withdrawal-associated anxiety (Zhao-Shea et al. 2015). The transcriptional regulation of RNAs isolated from midbrain punches enriched in VTA during acute nicotine withdrawal may reflect its interconnectedness with the traditional withdrawal circuit.

Similar to the time course of self-reported symptoms in human patients (Hughes 2007), nicotine dependent mice continue to display increased anxiety after 4 weeks of nicotine abstinence. Intriguingly, after a prolonged withdrawal period, all transcripts differentially expressed in the midbrain and NAc during acute nicotine withdrawal return to levels observed in age-matched nicotine naïve mice. This suggests that regulation of these miRNAs and mRNAs at the transcript level does not contribute to the persistent anxiety associated with nicotine withdrawal. Again, alterations in gene expression during the initial chronic nicotine treatment or withdrawal may contribute to alterations in neuronal function beyond the RNA level, including protein quantity, localization, and activation state, not detected by RNA-sequencing. There are 16 and 1 mRNAs uniquely differentially expressed in NAc and midbrain, respectively, of NLWD mice compared to age-matched controls. This suggests that this small subset of transcripts exhibit delayed regulation which persists for at least 4 weeks. This delayed response to nicotine exposure may reflect the delayed synaptic potentiation observed in the NAc (Schoffelmeer et al. 2002, Kourrich et al. 2007). The regulation of these mRNAs may contribute to the long lasting increase in anxiety associated with nicotine withdrawal and should be the focus of future studies.

In summary, Chapter 2 provides data showing chronic nicotine treatment induces extensive differential expression of mRNAs in both the NAc and midbrain. The majority of these effects are reversed by nicotine withdrawal in the NAc,

while they persist in the midbrain. This contrast in the general pattern of differential expression, as well as the specific identity of these nicotine responsive mRNAs, exemplify the brain region-specific regulation of the transcriptome within the reward circuit. These region-specific alterations in transcript expression in response to nicotine exposure may reflect changes in neural activity and neuroadaptations contributing to nicotine reward-associated behaviors, as well as a dual role for the VTA in both the reward and withdrawal circuitries. One caveat of the differential expression analysis of the mRNA-Seq is the application of a fold change threshold > 2. While we chose to focus on only robust changes in gene expression, smaller alterations in gene expression that may contribute to nicotine-invoked synaptic plasticity may be overlooked.

One major limitation of the differential expression analysis of the miRNA- and mRNA-Seq experiments is the use of tissue punches. Punches are heterogeneous tissue samples containing multiple brain sub-regions, neuron-types, as well as non-neuronal cell types like glia. Different subregions of the mesocorticolimbic DAergic circuit play distinct roles in the manifestation of reward behavior. For example, activation of the NAc shell is important for nicotine reward (Ikemoto et al. 1997, Ikemoto 2007), while the core is involved in cue-conditioned motivated behaviors (Sesack and Grace 2010). Additionally, activation of the pVTA, as opposed to the aVTA, is important for nicotine reward-associated behaviors (Ikemoto et al. 2006, Zhao-Shea et al. 2011). Tissue punches captured all sub-regions of the NAc and midbrain (enriched for VTA).

Region-specific alterations in gene expression during chronic nicotine treatment and withdrawal can not be discerned and may not be detected in RNA extracted from the heterogeneous tissue sample. Additionally, specific neuron-types contribute to the detailed microcircuitry of the mesocorticolimbic pathway underlying nicotine-reward associated behaviors, as discussed in Chapter 1. The heterogeneous population of cell types may result in the masking of important cell-type specific changes in expression. Further bioinformatic analyses may determine the relative contribution of distinct cell types to the total RNA population by evaluating the expression of cell type-specific markers. These may include neuron type-specific markers such as TH (DAergic), DAT (DAergic), GAD65/67 (GABAergic), ChAT (cholinergic), vGlut1/2 (glutamatergic), and TPH (serotonergic). Additionally, expression of glial markers such as Olig1-3 (oligodendrocytes), GFAP (astrocytes), and CD11b (microglia) should be determined to evaluate the proportion of glial cells present in tissue punches. Future sequencing experiments should use a more targeted approach, using RNA extracted from specific subregions or cell-types, or more advanced technologies may be employed to perform single-cell sequencing.

Acute nicotine withdrawal induces differential expression of miRNAs and mRNAs in the habenulo-interpeduncular circuit.

In Chapter 3, I presented differential expression analysis of miRNAs and mRNAs in the habenulo-interpeduncular withdrawal circuit during chronic nicotine

treatment and withdrawal. Interestingly, the IPN and the MHb display similar patterns of transcript regulation. Chronic nicotine treatment induces very limited alterations in miRNA expression. Additionally, there are few mRNAs up- or down-regulated with fold changes > 2 in either region. However, after acute withdrawal from nicotine, there are widespread alterations in miRNA and mRNA expression compared to drug naïve animals. Furthermore, in both regions, a large proportion of this regulation is an effect solely of nicotine withdrawal, with no significant contribution of the chronic nicotine treatment itself. For instance, 33% of miRNAs and 91% of mRNAs regulated in the IPN of mice experiencing acute nicotine withdrawal compared to drug naïve mice are similarly altered when compared to nicotine-treated mice. Likewise, 47% of miRNAs and 79% of mRNAs differentially expressed in the MHb of NAWD mice compared to TA controls are similarly regulated when compared to mice exposed to chronic nicotine.

The withdrawal-specific differential expression occurring in the MHb and IPN is reflective of the activation of the habenulo-interpeduncular circuit in acute nicotine withdrawal. This is also manifested in the GO analysis of the genes up- or down-regulated in the IPN and MHb of NAWD mice. In both regions, there is an enrichment of up-regulated genes related to the vesicle and myelin sheath. There is also an overrepresentation of down-regulated genes in the IPN and MHb in GO terms related to neuron projection development. This pattern of enrichment may represent neuroadaptations affecting synaptic transmission, signal transduction, and morphology occurring when these regions are activated

by nicotine withdrawal. In addition, there is enrichment of GO terms related to the structure and function of ribosomes and mitochondria in both the IPN and MHb. This may be indicative of the neurons responding to the increased demand for protein products and energy when activated during nicotine withdrawal. However, when comparing the specific identity of nicotine and withdrawal responsive mRNAs, there are no genes similarly regulated in both the IPN and MHb. This suggests that although there are similar alterations in the molecular functions and biological processes throughout the withdrawal circuit, the molecular mechanisms underlying these neuroadaptations during acute nicotine withdrawal are brain-region specific. One important caveat of this differential expression analysis was the application of a fold change threshold > 2. Although this allows us to focus on robust changes in gene expression, smaller fold changes which might be relevant to neuronal morphology and synaptic function may be overlooked.

Taken together, differential expression of miRNAs and mRNAs in the regions comprising the mesocorticolimbic reward and habenulo-interpeduncular withdrawal circuits during chronic nicotine treatment and withdrawal reflect the activation and known functions of each brain region. This is most striking in the MHb-IPN withdrawal axis, where the majority of robust transcript regulation occurs only when nicotine is withdrawn. In contrast, largely transient differential expression occurs in the NAc, a prominent reward center, in response to chronic nicotine treatment. The VTA, traditionally thought of as a member of the

mesocorticolimbic circuit, actually has a dual role in reward and withdrawal through its connectivity with the IPN (Zhao-Shea et al. 2015). Differential expression analysis of the sequencing results support this dual role. A multitude of transcripts are regulated in midbrain punches enriched for VTA in response to chronic nicotine treatment, as observed in the NAc. However, the persistence of these expression changes during acute nicotine withdrawal resembles the widespread alterations in gene expression observed in the IPN and MHb of NAWD mice.

As in the transcriptome analysis of NAc and midbrain in the mesocorticolimbic pathway, the use of tissue punches for miRNA- and mRNA-sequencing is a major limitation that must be considered when interpreting gene regulation of the withdrawal circuit. As discussed above, punches are heterogeneous tissue samples containing multiple brain sub-regions, neuron-types, as well as non-neuronal cell, including glia. To determine sub-region-and neuron type-specific alterations in gene expression future sequencing experiments will need to be performed using RNA isolated from subregions, cell types, or single cells. As previously discussed, the existing sequencing dataset can be used to evaluate the expression of cell type-specific markers to determine their contribution to the tissue sample.

Integrated prediction analysis identified mRNAs that are predicted targets of inversely regulated miRNAs in the reward and withdrawal circuits.

Integration of the differential expression analyses of miRNAs and mRNAs, along with TargetScan Mouse 7.1, a miRNA target prediction algorithm, was used to identify mRNAs that were predicted to be inversely regulated by miRNAs. Like differential expression analysis alone, the miRNA target prediction reflects the known activation and functions of each region within the reward and withdrawal circuits.

In the NAc, 852 mRNAs were differentially expressed during chronic nicotine exposure with fold changes > 2. The expression of only 8 conserved miRNAs was significantly altered. Although there are relatively few conserved miRNAs that are nicotine responsive, all of which are up-regulated, each of these miRNAs was predicted to target at least one of 204 down-regulated mRNAs. As in the majority of the predicted mRNA targets, the alterations in miRNA expression induced by nicotine treatment return to control levels after acute withdrawal. In light of the fact that miRNAs may have multiple targets (Lim et al. 2005), this prediction analysis suggests that even a few differentially expressed miRNAs may impart widespread regulation of gene expression in the NAc during chronic nicotine treatment, contributing to the mechanisms underlying the neuroadaptations of nicotine reward.

In contrast to the NAc, there is only one predicted mRNA target of an inversely regulated miRNA during chronic nicotine exposure in the IPN, and none

in the MHb. However, there are hundreds of mRNAs differentially expressed in the IPN and MHb of NAWD mice compared to drug-naïve controls that are predicted targets of inversely regulated miRNAs. In both regions, the majority of the mRNA targets are regulated as a sole consequence of nicotine withdrawal. Taken together, this integrated target prediction analysis suggests that miRNAs contribute to the withdrawal-induced regulation of mRNAs in the IPN and MHb, reflecting changes in neuronal function during acute nicotine withdrawal that induce behavioral dysfunction including anxiety.

Like the differential expression analysis, the target prediction analysis of miRNAs differentially expressed in the midbrain allude to the dual role of the VTA in the reward and withdrawal circuits. After chronic nicotine treatment alone, there are few conserved, differentially expressed miRNAs. Hence, out of all the mRNAs regulated in the midbrain of Nic mice compared to TA controls, only one is a predicted target of an inversely expressed miRNA. However, 45 conserved miRNAs are up- or down-regulated in acute nicotine withdrawal compared to drug naïve controls. Of these, 29 are predicted to target at least one of 380 reciprocally expressed mRNAs, most of which are up-regulated. In contrast to the regulation observed in the MHb-IPN withdrawal circuit, the initial chronic nicotine treatment contributes at least in part to the differential expression of the majority of predicted mRNA targets in the midbrain during acute withdrawal. For instance, about 28% of these mRNA targets were similarly regulated with a fold change > 2 after chronic nicotine treatment alone. In addition, only 7 (~2%) of the predicted

mRNA targets are regulated only during acute withdrawal, being similarly differentially expressed in the midbrain of NAWD- compared to either TA- or Nic-treated mice. Since none of the miRNAs themselves are significantly regulated by chronic nicotine treatment, it is possible that the induction of up- or down-regulation of miRNAs by nicotine withdrawal contributes to the propensity for nicotine responsive mRNAs to remain differentially expressed even after nicotine treatment has stopped. Hence, while contributing little to the mechanisms underlying the neuroadaptations of nicotine reward, regulation of miRNAs in the midbrain may play a role in the pathophysiology of nicotine withdrawal and the associated symptoms, including anxiety.

One limitation of the integrated target prediction analysis is the inability to detect differential expression of specific isoforms of mRNAs in the current analyses. Interestingly, GO analysis identified a significant enrichment of up-regulated genes related to RNA processing in the IPN during nicotine withdrawal. If nicotine treatment and withdrawal promotes alternative splicing, differential expression of individual gene isoforms would not have been detected by the analyses performed in this study. Additionally, most genes contain multiple functional polyadenylation sites, and alternative polyadenylation events have been shown to cause widespread lengthening of 3'-UTRs in the mammalian brain (Miura et al. 2013). Lengthening of 3'-UTRs may in brain may contain additional MREs that were not included in the integrated target prediction analysis. Future

bioinformatic analysis should determine the differential expression of splice and polyadenylation variants for target prediction.

Many genes differentially expressed in the NAc, midbrain, MHb, and IPN during chronic nicotine treatment and withdrawal were not predicted to be targets of inversely expressed miRNAs. Therefore, alternative mechanisms contributing to the regulation of these genes, and also those that are predicted targets of miRNAs, should be considered. Possible alternative mechanisms include the induction of transcription factors, epigenetic mechanisms, and neurotoxicity.

Transcription factors bind to specific DNA sequences and regulate transcription of RNA through interactions with RNA polymerase II (Mitchell and Tjian 1989). Transcription factors are induced or repressed by environmental stimuli, including nicotine (Madsen et al. 2012). In particular, nicotine and withdrawal has been shown to alter the expression and phosphorylation of CREB (Pandey et al. 2001, Brunzell et al. 2003, Brunzell et al. 2009), as well as the Fos family of early immediate genes (Marttila et al. 2006). The RNA-Seq data presented here may be used to perform a transcription factor binding enrichment analysis to determine if there is an over-representation of differentially expressed genes containing known motifs associated with transcription factor binding sites.

In addition to the regulation of transcription factors, other epigenetic mechanisms of gene regulation by nicotine treatment and withdrawal should be considered. Regulation of histone modifications, such as acetylation, methylation, phosphorylation, ubiquitination and sumoylation, signal the recruitment of

transcription factors and determine the accessibility of DNA to the transcription complex (Madsen et al. 2012). Nicotine has been shown to increases histone acetylation (Levine et al. 2011) and methylation (Jung et al. 2016) at specific transcription factor binding sites. The effect of nicotine treatment and withdrawal on the regulation of epigenetic mechanisms and their role in the widespread alterations of gene expression in the mesocorticolimbic and habenulo-interpeduncular circuits should be examined in future studies.

Finally, the neurotoxic effects of nicotine should be considered as a possible mechanism underlying the alterations in gene expression and behaviors during chronic nicotine treatment and withdrawal. Specifically, nicotine treatment induces selective degeneration of the Fr, composed of axons projecting from the MHb to the IPN (Carlson et al. 2000). The toxic effects of nicotine on the habenular axons in the withdrawal circuit may contribute to the altered neural activation, gene regulation, and behaviors during acute nicotine withdrawal.

Repression of Pfn2 expression in the IPN is sufficient to induce anxiety.

In Chapter 4, we demonstrate the utility of this sequencing screen by focusing on a single differentially expressed gene for detailed study. *Pfn2,* a regulator of cytoskeletal dynamics and synaptic activity (Witke 2004), was identified as an ideal candidate. Selection of *Pfn2* was based on its conservation, robust overall expression level, known functions, and differential expression in the IPN during nicotine withdrawal. Based on sequencing data, acute nicotine

withdrawal induced a ~50% down-regulation of *Pfn2* expression in NAWD mice compared to both nicotine-naïve and nicotine-treated mice. Integrated target analysis identified 2 conserved MREs for miR-106b-5p, which was up-regulated by approximately 80% in the IPN during acute nicotine withdrawal. Results of *in vitro* miRNA over-expression and luciferase assay experiments suggest that miR-106b-5p is a negative regulator of *Pfn2* expression through at least one of the predicted MREs located at nucleotide position 1197-1203.

Pfn2 is a regulator of cytoskeletal dynamics enriched in the brain (Witke et al. 2001, Tariq et al. 2016). *Pfn2* has been shown to play a role in neuronal morphology and function, being involved in the regulation of dendritic spines, neuritogenesis, synaptic receptor composition, and synaptic vesicle exocytosis (Witke 2004). These neuronal functions of *Pfn2* align with the findings of the GO analysis, identifying enrichment of down-regulated genes related to neuron projection organization. Whole-body *Pfn2* knockout mice exhibit increased synaptic vesicle exocytosis, as well as hyperactivation of the striatum (Pilo Boyl et al. 2007). Importantly, the neurons in the IPN are activated during acute nicotine withdrawal, inducing anxiety (Zhao-Shea et al. 2015, Molas et al. 2017). Thus, we hypothesized that down-regulation of *Pfn2* contributes to the activation of the IPN during acute nicotine withdrawal, resulting in anxiety. To test the hypothesis that down-regulation of *Pfn2* in the IPN plays a role in the molecular mechanisms underlying the pathophysiology of withdrawal-associated anxiety, we used lentiviral delivery of a shRNA to knock down *Pfn2* expression in the IPN

and assayed anxiety behavior. We found that repression of *Pfn2* expression in the IPN was sufficient to increase anxiety behavior in the EPM. However, unlike NAWD mice, KD of *Pfn2* in the IPN was not sufficient to increase anxiety in the MBT. Future experiments may use additional behavioral assays, such as the open field test, to confirm the anxiogenic effect of *Pfn2* KD in the IPN. Additionally, *Pfn2* KD did not affect object novelty preference, another behavior controlled by the IPN (Molas et al. 2017). This suggests that the role of *Pfn2* in the IPN is specific to influencing anxiety. Further work is needed to determine the specific effects of *Pfn2* expression on neuronal activation and morphology in the IPN during nicotine withdrawal-induced anxiety. These results presented in Chapter 4 illustrate how the integration of differential expression and target prediction analyses in the reward and withdrawal circuits can be used to identify novel roles for genes and their miRNA regulators in the neuroadaptations underlying the pathophysiology of nicotine addiction.

5.B. Future Directions

We used integrated miRNA-/mRNA-sequencing to determine transcriptome-wide expression changes in the mesocorticolimbic reward and habenulo-interpeduncular withdrawal pathways during chronic nicotine treatment and withdrawal. However, all of these experiments were performed on male mice.

Currently, men smoke tobacco at higher rates than women (Sieminska and Jassem 2014). However, women have a harder time quitting than men (Smith et al. 2015), reporting higher levels of craving and negative affect during nicotine abstinence and in response to stress and other environmental smoking cues (Xu et al. 2008, Doran 2014, Wray et al. 2015). Neuroimaging studies have revealed gender differences in activation of the mesolimbic dopamine system while smoking (Cosgrove et al. 2014). Gender differences in brain activity may underlie the differences in susceptibility to relapse between men and women. Understanding the gender-specific neuroadaptations of nicotine exposure and withdrawal is essential to designing optimal smoking cessation aids. Hence, the sequencing studies presented in Chapters 2 and 3 should be repeated using female mice.

We found that there are widespread alterations in miRNA and mRNA expression in the NAc, VTA, MHb, and IPN during nicotine treatment or acute withdrawal, in a brain region-specific manner. However, it is still unknown whether this effect is mediated through nAChR signaling or some other mechanism, including the neurotoxic effects of nicotine. To investigate this, studies employing mecamylamine, a non-selective nAChR antagonist, and other receptor subtype antagonists should be performed. For example, differential expression of miRNAs/mRNAs may be determined by sequencing or RT-qPCR in Nic and NAWD mice being administered nAChR antagonists through osmotic minipumps during nicotine treatment and withdrawal. If regulation of a transcript

is the result of nAChR signaling, one would hypothesize that nAChR antagonists would prevent the differential expression of that transcript when compared to controls.

Future studies should determine if the miRNA/mRNA regulation in the NAc, midbrain, MHb and IPN is a specific effect of nicotine or are a common effect of all drugs of abuse. Addictive drugs commonly result in increased extracellular DA in the NAc, promoting positive and rewarding emotions (Di Chiara and Imperato 1988, Pontieri et al. 1996). In addition, increased anxiety is a common feature of acute withdrawal in all major drugs of abuse (Koob and Volkow 2010). Nicotine has also been shown to act as a "gateway drug," with nicotine pretreatment increasing behavioral and synaptic responses to cocaine (Levine et al. 2011). Future work should employ mRNA- and miRNA-sequencing to measure differential expression in the mesocorticolimbic circuit and MHb-IPN axis of mice treated chronically and withdrawn from other drugs of abuse, such as cocaine, amphetamine, opioids, and ethanol. The induction of similar miRNA/mRNA regulation in response to other drugs may contribute to molecular mechanisms underlying co-abuse with nicotine and nicotine's role as a "gateway drug."

All of the studies presented used RNA extracted from whole tissue punches. As described in Chapter 1, each brain region is composed of different sub-regions and neuronal cell types. To improve our understanding of the microcircuitry underlying responses to nicotine treatment and withdrawal, the sequencing experiments should be repeated in a sub-region- and neuron-type-

specific manner. To achieve this, laser capture microdissection can be employed to isolate specific sub-regions or neuron types, identified by immune-labeling or using mouse lines expressing fluorescent reporter fusion proteins. Alternatively, 10X Genomics technology is a high-throughput technology to achieve single cell gene expression analysis. However, the low overall level of transcripts detected is a limitation of any single-cell sequencing experiment.

Brain circuits other than the classical mesocorticolimbic reward pathway and the MHb-IPN withdrawal axis underlie nicotine dependence and symptoms of nicotine withdrawal. For example, the amygdala, within the arousal-stress system, and the hypothalamic-pituitary-adrenal axis are activated by the withdrawal of all drugs of abuse and these effects are mediated by the stress hormone, CRF (Koob and Volkow 2010). Activation of the hypothalamic-pituitary-adrenal axis during nicotine withdrawal contributes to somatic signs such as alterations in appetite, as well as affective symptoms, such as depression (Miyata et al. 1999, Semba et al. 2004). These broader hypothalamic effects may contribute to withdrawal signs that confound the behavioral assays we used to measure anxiety. Future studies should monitor body weight and other physical signs, such as body temperature, heart rate and other somatic withdrawal signs. In addition to anxiety tests, a more comprehensive analysis of behaviors, including depression and locomotor activity assays, may be used to assess behaviors during various stages of nicotine withdrawal and to characterize the effects of candidate gene regulation. To better understand these broader effects

of withdrawal, future studies may use sequencing to perform transcriptome-wide differential expression analysis in additional brain regions including the amygdala and hypothalamus.

In the NAc and midbrain of the mesocorticolimbic limbic reward pathway, mRNA-Seq identified a plethora of genes regulated my chronic nicotine treatment. Using the differential expression and GO analyses, candidate genes that are differentially expressed in the NAc and midbrain of Nic mice should be identified for validation by RT-qPCR and other further lines of investigation. Priority should be given to candidates that are conserved, robustly expressed overall, more highly up- or down-regulated, and related to enriched GO terms. GO terms of highest interest relate to regulation of neuron projections, regulation synaptic structure or activity, regulation of neurotransmitter levels and binding of receptors/ion channels. Although there are only a few miRNAs regulated after chronic nicotine treatment, many anti-correlated mRNAs are predicted to be targets of these miRNAs in the NAc. When ranking candidates for further studies, priority should also be given to mRNA candidates predicted to be targets of inversely expressed miRNAs. In light of the known function of the reward circuitry and identification of a multitude of nicotine responsive transcripts in the NAc and midbrain, the effects of each candidate genes' expression level on nicotine reward and sensitization behaviors should be determined. Behavioral testing may include nicotine self-administration, conditioned place preference, and nicotine-induced locomotor activity assays.

Although classically thought of as a member of the reward circuitry, the VTA is also interconnected to the MHb-IPN withdrawal axis, as previously discussed. The majority of mRNAs differentially expressed during chronic nicotine treatment remain similarly up- or down-regulated during acute nicotine withdrawal. Therefore, the effect of mRNA regulation in the midbrain of Nic- and NAWD-treated mice on MHb-IPN axis' neuronal activity and withdrawal-induced anxiety should be determined. Candidates should be identified and prioritized as described above. Based on the GO analysis, focus should again largely be on genes related to the regulation of neuron projections, regulation of synaptic structure or activity, regulation of neurotransmitter levels and binding of receptors/ion channels. During acute withdrawal, many miRNAs are inversely regulated to their predicted targets. Again, priority should be given to genes that are predicted targets of differentially expressed miRNAs.

In Chapter 3, sequencing and differential expression analysis identified a multitude of changes in miRNA/mRNA expression during acute nicotine withdrawal. As discussed for the analysis of the mesocorticolimbic reward pathway, mRNA and miRNA candidates should be identified and prioritized for validation and future studies. We had chosen to focus on mRNAs that were regulated solely as an effect of nicotine withdrawal, validating the differential expression of selected genes in the IPN and MHb. However, future experiments may also choose to focus on other genes whose differential expression is due at least in part to the effect of the initial chronic nicotine treatment itself. Chapter 4

serves as an example of the initial follow-up experiments that should be pursued with each candidate. In addition to conservation, overall expression level, and fold change, GO analysis can be used to prioritize candidates for further investigation and determine the specific experimental plan. For example, in the IPN, up-regulated mRNAs are enriched in GO terms describing the mitochondria and energetics. Future experiments might include observing the effect of acute nicotine withdrawal on mitochondrial morphology, number or membrane potential in neurons of the IPN. Then, to test the hypothesis that up-regulation of candidate mRNAs contributes to these effects, genes can be over-expressed in the IPN of WT mice via lentiviral delivery and the effects on mitochondria and anxiety behaviors can be measured. Additionally, in the IPN and MHb there is an overrepresentation of down-regulated genes related to cell/neuron projection organization and development. An example of a down-regulated candidate gene in the IPN that has functions related to cytoskeletal dynamics and synaptic morphology was described in Chapter 4, and similar experimental strategies can be applied to other candidates identified in the sequencing data analyses.

In Chapter 4, we present evidence that *Pfn2* expression in the IPN plays a role in the modulation of nicotine withdrawal-induced anxiety. Relative quantification of expression by sequencing and RT-qPCR, shows that *Pfn2* is down-regulated in the IPN of NAWD mice compared to drug-naïve controls. Further, we show that knockdown of *Pfn2* in the IPN is sufficient to induce anxiety as measured by the EPM, mimicking the behavioral effects of nicotine

withdrawal. To strengthen this result, a *Pfn2* rescue experiment should be performed, over-expressing *Pfn2* in the IPN via lentiviral delivery during nicotine treatment and acute withdrawal. The amelioration of nicotine withdrawal-associated anxiety behavior by the over-expression of *Pfn2* in the IPN would add further support to the conclusion that down-regulation of *Pfn2* in the IPN during nicotine withdrawal plays in important role in the mechanisms underlying nicotine withdrawal-associated anxiety.

The effect of *Pfn2* knockdown on neural activity and morphology in the IPN are as yet unknown. Future studies should employ electrophysiology to make measurements including action potential frequency and frequency/amplitude of excitatory postsynaptic potentials to asses neuronal activity and neurotransmitter release in IPN neurons infected with lenti-GIPZ-*Pfn2*-shRNA-tGFP. Neurons in whole animal *Pfn2* -/- mice exhibit increased synaptic vesicle release and hyperactivation (Pilo Boyl et al. 2007). Thus, I would hypothesize that neurons expressing *Pfn2* shRNA would display similar features. Because previous studies have shown that *Pfn2* contributes to regulation of dendritic spines (Ackermann and Matus 2003) and neuritogenesis (Da Silva et al. 2003), microscopy should be used to observe changes in synaptic morphology.

Differential expression analysis of miRNA-sequencing data revealed down-regulation of miR-106b-5p in the IPN, which was confirmed by RT-qPCR. TargetScan Mouse 7.1 predicted that miR-106b-5p targets anti-correlated mRNAs, including *Pfn2* which possesses two MREs within its 3′-UTR. In Chapter

4, I presented data suggesting that miR-106b-5p targets at least one MRE within the 3′-UTR of *Pfn2*, repressing its expression *in vitro*. However, the repression of *Pfn2* expression by miR-106b-5p must be confirmed *in vivo*. To do this, miR-106b-5p should be over-expressed and inhibited in the IPN using lentiviral or AAV delivery of miRNA mimics and anti-miRs. *Pfn2* expression can then be measured at the transcript and protein level. To confirm the regulation of *Pfn2* by miR-106b-5p through interaction with MRE2 at nucleotide position 1197-1203, CRISPR-Cas9 gene editing technology could be used to introduce mutations to the predicted MREs, in a similar fashion to our luciferase screen. The failure of miR-106b-5p over-expression to repress *Pfn2* expression in mutant MRE mice would further support our conclusions that miR-106b-5p is a negative regulator of *Pfn2*.

In addition to expanding on our understanding of the regulation of *Pfn2* by miR-106b-5p, future work should determine the upstream role of miR-106b-5p on neural function and nicotine withdrawal-associated behaviors. Similar to the studies described using lentiviral delivery of shRNA to inhibit expression of *Pfn2*, miR-106b-5p should be over-expressed in the IPN of WT mice using viral delivery of miRNA mimic. Because KD of *Pfn2* in the IPN increases anxiety in WT mice, I hypothesize that over-expression of miR-106b-5p is also sufficient to induce anxiety in nicotine-naïve mice, mimicking the effects of nicotine withdrawal. Conversely, I would hypothesize that inhibition of miR-106b-5p in the IPN by viral delivery of anti-miR or tough decoy would ameliorate the increase in

anxiety of mice in acute nicotine withdrawal. Effects on neuronal activity and morphology should also be determined as described for KD and overexpression of *Pfn2*.

Pfn2 is expressed in all regions of the brain (Witke et al. 2001, Pilo Boyl et al. 2007). However, studies exploring the effects of *Pfn2* down-regulation in specific sub-regions or neuron cell-types within the IPN will further our understanding of its function as a regulator of habenulo-interpeduncular withdrawal circuit activity and nicotine withdrawal-induced anxiety. First, patterns in *Pfn2* expression should be identified using FISH and/or immunohistochemistry. A Cre-lox expression system can then be used to determine the cell-type specific effects of *Pfn2* KD on neural activity, cell morphology, and anxiety behaviors.

As discussed here, the results of the sequencing screens described in Chapters 2 and 3 may inspire seemingly endless lines of future investigation. Individualized pursuit of nicotine and withdrawal responsive genes in the reward and withdrawal circuits, as proposed for *Pfn2*, are certain to lead to discovery of novel molecular mechanisms underlying nicotine dependence and associated behaviors.

REFERENCES

Ackermann, M. and A. Matus (2003). "Activity-induced targeting of profilin and stabilization of dendritic spine morphology." Nat Neurosci **6**(11): 1194-1200.

Agarwal, V., G. W. Bell, J. W. Nam and D. P. Bartel (2015). "Predicting effective microRNA target sites in mammalian mRNAs." Elife **4**.

Aguirre, C. G., J. Madrid and A. M. Leventhal (2015). "Tobacco withdrawal symptoms mediate motivation to reinstate smoking during abstinence." J Abnorm Psychol **124**(3): 623-634.

Albuquerque, E. X., E. F. Pereira, M. Alkondon and S. W. Rogers (2009). "Mammalian nicotinic acetylcholine receptors: from structure to function." Physiol Rev **89**(1): 73-120.

Allen, S. S., T. Bade, D. Hatsukami and B. Center (2008). "Craving, withdrawal, and smoking urges on days immediately prior to smoking relapse." Nicotine Tob Res **10**(1): 35-45.

Ambroggi, F., A. Ishikawa, H. L. Fields and S. M. Nicola (2008). "Basolateral amygdala neurons facilitate reward-seeking behavior by exciting nucleus accumbens neurons." Neuron **59**(4): 648-661.

Ameres, S. L. and P. D. Zamore (2013). "Diversifying microRNA sequence and function." Nat Rev Mol Cell Biol **14**(8): 475-488.

Antolin-Fontes, B., J. L. Ables, A. Gorlich and I. Ibanez-Tallon (2015). "The habenulo-interpeduncular pathway in nicotine aversion and withdrawal." Neuropharmacology **96**(Pt B): 213-222.

Azam, L., U. Maskos, J. P. Changeux, C. D. Dowell, S. Christensen, M. De Biasi and J. M. McIntosh (2010). "alpha-Conotoxin BuIA[T5A;P6O]: a novel ligand that discriminates between alpha6ss4 and alpha6ss2 nicotinic acetylcholine receptors and blocks nicotine-stimulated norepinephrine release." FASEB J **24**(12): 5113-5123.

Babb, S., A. Malarcher, G. Schauer, K. Asman and A. Jamal (2017). "Quitting Smoking Among Adults - United States, 2000-2015." MMWR Morb Mortal Wkly Rep **65**(52): 1457-1464.

Bak, M., A. Silahtaroglu, M. Moller, M. Christensen, M. F. Rath, B. Skryabin, N. Tommerup and S. Kauppinen (2008). "MicroRNA expression in the adult mouse central nervous system." RNA **14**(3): 432-444.

Balaraman, S., U. H. Winzer-Serhan and R. C. Miranda (2012). "Opposing actions of ethanol and nicotine on microRNAs are mediated by nicotinic acetylcholine receptors in fetal cerebral cortical-derived neural progenitor cells." Alcohol Clin Exp Res **36**(10): 1669-1677.

Barrot, M., S. R. Sesack, F. Georges, M. Pistis, S. Hong and T. C. Jhou (2012). "Braking dopamine systems: a new GABA master structure for mesolimbic and nigrostriatal functions." J Neurosci **32**(41): 14094-14101.

Bartel, D. P. (2009). "MicroRNAs: target recognition and regulatory functions." Cell **136**(2): 215-233.

Bartel, D. P. (2018). "Metazoan MicroRNAs." Cell **173**(1): 20-51.

Bennett, B. L., Y. Satoh and A. J. Lewis (2003). "JNK: a new therapeutic target for diabetes." Curr Opin Pharmacol **3**(4): 420-425.

Benowitz, N. L. (1999). "Nicotine addiction." Prim Care **26**(3): 611-631.

Benowitz, N. L. (2009). "Pharmacology of nicotine: addiction, smoking-induced disease, and therapeutics." Annu Rev Pharmacol Toxicol **49**: 57-71.

Benowitz, N. L. (2010). "Nicotine addiction." N Engl J Med **362**(24): 2295-2303.

Benwell, M. E., D. J. Balfour and J. M. Anderson (1988). "Evidence that tobacco smoking increases the density of (-)-[3H]nicotine binding sites in human brain." J Neurochem **50**(4): 1243-1247.

Braun, J. E., E. Huntzinger, M. Fauser and E. Izaurralde (2011). "GW182 proteins directly recruit cytoplasmic deadenylase complexes to miRNA targets." Mol Cell **44**(1): 120-133.

Britt, J. P. and A. Bonci (2013). "Optogenetic interrogations of the neural circuits underlying addiction." Curr Opin Neurobiol **23**(4): 539-545.

Brunzell, D. H., Y. S. Mineur, R. L. Neve and M. R. Picciotto (2009). "Nucleus accumbens CREB activity is necessary for nicotine conditioned place preference." Neuropsychopharmacology **34**(8): 1993-2001.

Brunzell, D. H., D. S. Russell and M. R. Picciotto (2003). "In vivo nicotine treatment regulates mesocorticolimbic CREB and ERK signaling in C57Bl/6J mice." J Neurochem **84**(6): 1431-1441.

Cachope, R., Y. Mateo, B. N. Mathur, J. Irving, H. L. Wang, M. Morales, D. M. Lovinger and J. F. Cheer (2012). "Selective activation of cholinergic interneurons

enhances accumbal phasic dopamine release: setting the tone for reward processing." Cell Rep **2**(1): 33-41.

Carlson, J., B. Armstrong, R. C. Switzer, 3rd and G. Ellison (2000). "Selective neurotoxic effects of nicotine on axons in fasciculus retroflexus further support evidence that this a weak link in brain across multiple drugs of abuse." Neuropharmacology **39**(13): 2792-2798.

Carr, D. B. and S. R. Sesack (2000). "GABA-containing neurons in the rat ventral tegmental area project to the prefrontal cortex." Synapse **38**(2): 114-123.

CDC (2013). Notes from the field: electronic cigarette use among middle and high school students - United States, 2011-2012. MMWR Morb Mortal Wkly Rep. US, Centers for Disease Control and Prevention. **62(35):** 729-730.

Champtiaux, N., C. Gotti, M. Cordero-Erausquin, D. J. David, C. Przybylski, C. Lena, F. Clementi, M. Moretti, F. M. Rossi, N. Le Novere, J. M. McIntosh, A. M. Gardier and J. P. Changeux (2003). "Subunit composition of functional nicotinic receptors in dopaminergic neurons investigated with knock-out mice." J Neurosci **23**(21): 7820-7829.

Chekulaeva, M., H. Mathys, J. T. Zipprich, J. Attig, M. Colic, R. Parker and W. Filipowicz (2011). "miRNA repression involves GW182-mediated recruitment of CCR4-NOT through conserved W-containing motifs." Nat Struct Mol Biol **18**(11): 1218-1226.

Chen, X., Y. Che, L. Zhang, A. H. Putman, I. Damaj, B. R. Martin, K. S. Kendler and M. F. Miles (2007). "RhoA, encoding a Rho GTPase, is associated with smoking initiation." Genes Brain Behav **6**(8): 689-697.

Chuhma, N., H. Zhang, J. Masson, X. Zhuang, D. Sulzer, R. Hen and S. Rayport (2004). "Dopamine neurons mediate a fast excitatory signal via their glutamatergic synapses." J Neurosci **24**(4): 972-981.

Cinciripini, P. M., J. D. Robinson, M. Karam-Hage, J. A. Minnix, C. Lam, F. Versace, V. L. Brown, J. M. Engelmann and D. W. Wetter (2013). "Effects of varenicline and bupropion sustained-release use plus intensive smoking cessation counseling on prolonged abstinence from smoking and on depression, negative affect, and other symptoms of nicotine withdrawal." JAMA Psychiatry **70**(5): 522-533.

Collins, A. C., E. Romm and J. M. Wehner (1988). "Nicotine tolerance: an analysis of the time course of its development and loss in the rat." Psychopharmacology (Berl) **96**(1): 7-14.

Contestabile, A. and B. A. Flumerfelt (1981). "Afferent connections of the interpeduncular nucleus and the topographic organization of the habenulo-interpeduncular pathway: an HRP study in the rat." J Comp Neurol **196**(2): 253-270.

Cooper, E., S. Couturier and M. Ballivet (1991). "Pentameric structure and subunit stoichiometry of a neuronal nicotinic acetylcholine receptor." Nature **350**(6315): 235-238.

Cornwall, J., J. D. Cooper and O. T. Phillipson (1990). "Afferent and efferent connections of the laterodorsal tegmental nucleus in the rat." Brain Res Bull **25**(2): 271-284.

Corrigall, W. A. and K. M. Coen (1989). "Nicotine maintains robust self-administration in rats on a limited-access schedule." Psychopharmacology (Berl) **99**(4): 473-478.

Corrigall, W. A., K. M. Coen and K. L. Adamson (1994). "Self-administered nicotine activates the mesolimbic dopamine system through the ventral tegmental area." Brain Res **653**(1-2): 278-284.

Corrigall, W. A., K. B. Franklin, K. M. Coen and P. B. Clarke (1992). "The mesolimbic dopaminergic system is implicated in the reinforcing effects of nicotine." Psychopharmacology (Berl) **107**(2-3): 285-289.

Cosgrove, K. P., S. Wang, S. J. Kim, E. McGovern, N. Nabulsi, H. Gao, D. Labaree, H. D. Tagare, J. M. Sullivan and E. D. Morris (2014). "Sex differences in the brain's dopamine signature of cigarette smoking." J Neurosci **34**(50): 16851-16855.

Cross, S. J., S. Lotfipour and F. M. Leslie (2017). "Mechanisms and genetic factors underlying co-use of nicotine and alcohol or other drugs of abuse." Am J Drug Alcohol Abuse **43**(2): 171-185.

Da Silva, J. S., M. Medina, C. Zuliani, A. Di Nardo, W. Witke and C. G. Dotti (2003). "RhoA/ROCK regulation of neuritogenesis via profilin IIa-mediated control of actin stability." J Cell Biol **162**(7): 1267-1279.

Damaj, M. I., W. Kao and B. R. Martin (2003). "Characterization of spontaneous and precipitated nicotine withdrawal in the mouse." J Pharmacol Exp Ther **307**(2): 526-534.

Dani, J. A. and D. J. Balfour (2011). "Historical and current perspective on tobacco use and nicotine addiction." Trends Neurosci **34**(7): 383-392.

Dani, J. A. and D. Bertrand (2007). "Nicotinic acetylcholine receptors and nicotinic cholinergic mechanisms of the central nervous system." Annu Rev Pharmacol Toxicol **47**: 699-729.

Dani, J. A. and M. De Biasi (2001). "Cellular mechanisms of nicotine addiction." Pharmacol Biochem Behav **70**(4): 439-446.

Dani, J. A. and M. De Biasi (2013). "Mesolimbic dopamine and habenulo-interpeduncular pathways in nicotine withdrawal." Cold Spring Harb Perspect Med **3**(6): 1-13.

De Biasi, M. and J. A. Dani (2011). "Reward, addiction, withdrawal to nicotine." Annu Rev Neurosci **34**: 105-130.

Devine, M. J. and J. T. Kittler (2018). "Mitochondria at the neuronal presynapse in health and disease." Nat Rev Neurosci **19**(2): 63-80.

Di Chiara, G. and A. Imperato (1988). "Drugs abused by humans preferentially increase synaptic dopamine concentrations in the mesolimbic system of freely moving rats." Proc Natl Acad Sci U S A **85**(14): 5274-5278.

Di Nardo, A., R. Gareus, D. Kwiatkowski and W. Witke (2000). "Alternative splicing of the mouse profilin II gene generates functionally different profilin isoforms." J Cell Sci **113 Pt 21**: 3795-3803.

Dobi, A., G. K. Seabold, C. H. Christensen, R. Bock and V. A. Alvarez (2011). "Cocaine-induced plasticity in the nucleus accumbens is cell specific and develops without prolonged withdrawal." J Neurosci **31**(5): 1895-1904.

Doran, N. (2014). "Sex differences in smoking cue reactivity: craving, negative affect, and preference for immediate smoking." Am J Addict **23**(3): 211-217.

Eacker, S. M., M. J. Keuss, E. Berezikov, V. L. Dawson and T. M. Dawson (2011). "Neuronal activity regulates hippocampal miRNA expression." PLoS One **6**(10): e25068.

Eichhorn, S. W., H. Guo, S. E. McGeary, R. A. Rodriguez-Mias, C. Shin, D. Baek, S. H. Hsu, K. Ghoshal, J. Villen and D. P. Bartel (2014). "mRNA destabilization is the dominant effect of mammalian microRNAs by the time substantial repression ensues." Mol Cell **56**(1): 104-115.

Ekpu, V. U. and A. K. Brown (2015). "The Economic Impact of Smoking and of Reducing Smoking Prevalence: Review of Evidence." Tob Use Insights **8**: 1-35.

Engqvist-Goldstein, A. E., C. X. Zhang, S. Carreno, C. Barroso, J. E. Heuser and D. G. Drubin (2004). "RNAi-mediated Hip1R silencing results in stable association between the endocytic machinery and the actin assembly machinery." Mol Biol Cell **15**(4): 1666-1679.

Ericson, M., E. Lof, R. Stomberg, P. Chau and B. Soderpalm (2008). "Nicotinic acetylcholine receptors in the anterior, but not posterior, ventral tegmental area mediate ethanol-induced elevation of accumbal dopamine levels." J Pharmacol Exp Ther **326**(1): 76-82.

Fabian, M. R., M. K. Cieplak, F. Frank, M. Morita, J. Green, T. Srikumar, B. Nagar, T. Yamamoto, B. Raught, T. F. Duchaine and N. Sonenberg (2011). "miRNA-mediated deadenylation is orchestrated by GW182 through two conserved motifs that interact with CCR4-NOT." Nat Struct Mol Biol **18**(11): 1211-1217.

Falk, D. E., H. Y. Yi and S. Hiller-Sturmhofel (2006). "An epidemiologic analysis of co-occurring alcohol and tobacco use and disorders: findings from the National Epidemiologic Survey on Alcohol and Related Conditions." Alcohol Res Health **29**(3): 162-171.

Fenu, S., L. Spina, E. Rivas, R. Longoni and G. Di Chiara (2006). "Morphine-conditioned single-trial place preference: role of nucleus accumbens shell dopamine receptors in acquisition, but not expression." Psychopharmacology (Berl) **187**(2): 143-153.

Fiore, M. C., S. S. Smith, D. E. Jorenby and T. B. Baker (1994). "The effectiveness of the nicotine patch for smoking cessation. A meta-analysis." JAMA **271**(24): 1940-1947.

Flores, C. M., M. I. Davila-Garcia, Y. M. Ulrich and K. J. Kellar (1997). "Differential regulation of neuronal nicotinic receptor binding sites following chronic nicotine administration." J Neurochem **69**(5): 2216-2219.

Fowler, C. D., M. A. Arends and P. J. Kenny (2008). "Subtypes of nicotinic acetylcholine receptors in nicotine reward, dependence, and withdrawal: evidence from genetically modified mice." Behav Pharmacol **19**(5-6): 461-484.

Fowler, C. D. and P. J. Kenny (2011). "Intravenous nicotine self-administration and cue-induced reinstatement in mice: effects of nicotine dose, rate of drug infusion and prior instrumental training." Neuropharmacology **61**(4): 687-698.

Fowler, C. D., Q. Lu, P. M. Johnson, M. J. Marks and P. J. Kenny (2011). "Habenular alpha5 nicotinic receptor subunit signalling controls nicotine intake." Nature **471**(7340): 597-601.

Friedman, R. C., K. K. Farh, C. B. Burge and D. P. Bartel (2009). "Most mammalian mRNAs are conserved targets of microRNAs." Genome Res **19**(1): 92-105.

Fukaya, T., H. O. Iwakawa and Y. Tomari (2014). "MicroRNAs block assembly of eIF4F translation initiation complex in Drosophila." Mol Cell **56**(1): 67-78.

Galzi, J. L., A. Devillers-Thiery, N. Hussy, S. Bertrand, J. P. Changeux and D. Bertrand (1992). "Mutations in the channel domain of a neuronal nicotinic receptor convert ion selectivity from cationic to anionic." Nature **359**(6395): 500-505.

Garduno, J., L. Galindo-Charles, J. Jimenez-Rodriguez, E. Galarraga, D. Tapia, S. Mihailescu and S. Hernandez-Lopez (2012). "Presynaptic alpha4beta2 nicotinic acetylcholine receptors increase glutamate release and serotonin neuron excitability in the dorsal raphe nucleus." J Neurosci **32**(43): 15148-15157.

Gareus, R., A. Di Nardo, V. Rybin and W. Witke (2006). "Mouse profilin 2 regulates endocytosis and competes with SH3 ligand binding to dynamin 1." J Biol Chem **281**(5): 2803-2811.

Geisler, S., C. Derst, R. W. Veh and D. S. Zahm (2007). "Glutamatergic afferents of the ventral tegmental area in the rat." J Neurosci **27**(21): 5730-5743.

Gerdeman, G. L., J. G. Partridge, C. R. Lupica and D. M. Lovinger (2003). "It could be habit forming: drugs of abuse and striatal synaptic plasticity." Trends Neurosci **26**(4): 184-192.

Goldschmidt-Clermont, P. J., M. I. Furman, D. Wachsstock, D. Safer, V. T. Nachmias and T. D. Pollard (1992). "The control of actin nucleotide exchange by thymosin beta 4 and profilin. A potential regulatory mechanism for actin polymerization in cells." Mol Biol Cell **3**(9): 1015-1024.

Gorelova, N., P. J. Mulholland, L. J. Chandler and J. K. Seamans (2012). "The glutamatergic component of the mesocortical pathway emanating from different subregions of the ventral midbrain." Cereb Cortex **22**(2): 327-336.

Gotti, C., S. Guiducci, V. Tedesco, S. Corbioli, L. Zanetti, M. Moretti, A. Zanardi, R. Rimondini, M. Mugnaini, F. Clementi, C. Chiamulera and M. Zoli (2010). "Nicotinic acetylcholine receptors in the mesolimbic pathway: primary role of ventral tegmental area alpha6beta2* receptors in mediating systemic nicotine effects on dopamine release, locomotion, and reinforcement." J Neurosci **30**(15): 5311-5325.

Govind, A. P., P. Vezina and W. N. Green (2009). "Nicotine-induced upregulation of nicotinic receptors: underlying mechanisms and relevance to nicotine addiction." Biochem Pharmacol **78**(7): 756-765.

Grabus, S. D., B. R. Martin, A. M. Batman, R. F. Tyndale, E. Sellers and M. I. Damaj (2005). "Nicotine physical dependence and tolerance in the mouse following chronic oral administration." Psychopharmacology (Berl) **178**(2-3): 183-192.

Grabus, S. D., B. R. Martin, S. E. Brown and M. I. Damaj (2006). "Nicotine place preference in the mouse: influences of prior handling, dose and strain and attenuation by nicotinic receptor antagonists." Psychopharmacology (Berl) **184**(3-4): 456-463.

Grieder, T. E., M. A. Herman, C. Contet, L. A. Tan, H. Vargas-Perez, A. Cohen, M. Chwalek, G. Maal-Bared, J. Freiling, J. E. Schlosburg, L. Clarke, E. Crawford, P. Koebel, V. Repunte-Canonigo, P. P. Sanna, A. R. Tapper, M. Roberto, B. L. Kieffer, P. E. Sawchenko, G. F. Koob, D. van der Kooy and O. George (2014). "VTA CRF neurons mediate the aversive effects of nicotine withdrawal and promote intake escalation." Nat Neurosci **17**(12): 1751-1758.

Grilli, M., S. Zappettini, L. Raiteri and M. Marchi (2009). "Nicotinic and muscarinic cholinergic receptors coexist on GABAergic nerve endings in the mouse striatum and interact in modulating GABA release." Neuropharmacology **56**(3): 610-614.

Grimson, A., K. K. Farh, W. K. Johnston, P. Garrett-Engele, L. P. Lim and D. P. Bartel (2007). "MicroRNA targeting specificity in mammals: determinants beyond seed pairing." Mol Cell **27**(1): 91-105.

Groenewegen, H. J., S. Ahlenius, S. N. Haber, N. W. Kowall and W. J. Nauta (1986). "Cytoarchitecture, fiber connections, and some histochemical aspects of the interpeduncular nucleus in the rat." J Comp Neurol **249**(1): 65-102.

Gruber, A. J., R. J. Hussain and P. O'Donnell (2009). "The nucleus accumbens: a switchboard for goal-directed behaviors." PLoS One **4**(4): e5062.

Guo, H., N. T. Ingolia, J. S. Weissman and D. P. Bartel (2010). "Mammalian microRNAs predominantly act to decrease target mRNA levels." Nature **466**(7308): 835-840.

Guo, J. Z., T. L. Tredway and V. A. Chiappinelli (1998). "Glutamate and GABA release are enhanced by different subtypes of presynaptic nicotinic receptors in the lateral geniculate nucleus." J Neurosci **18**(6): 1963-1969.

Ha, M. and V. N. Kim (2014). "Regulation of microRNA biogenesis." Nat Rev Mol Cell Biol **15**(8): 509-524.

Hamill, G. S. and D. M. Jacobowitz (1984). "A study of afferent projections to the rat interpeduncular nucleus." Brain Res Bull **13**(4): 527-539.

Hamill, G. S. and N. J. Lenn (1984). "The subnuclear organization of the rat interpeduncular nucleus: a light and electron microscopic study." J Comp Neurol **222**(3): 396-408.

Hammond, D. N., H. J. Lee, J. H. Tonsgard and B. H. Wainer (1990). "Development and characterization of clonal cell lines derived from septal cholinergic neurons." Brain Res **512**(2): 190-200.

Han, J., Y. Lee, K. H. Yeom, Y. K. Kim, H. Jin and V. N. Kim (2004). "The Drosha-DGCR8 complex in primary microRNA processing." Genes Dev **18**(24): 3016-3027.

Han, J., Y. Lee, K. H. Yeom, J. W. Nam, I. Heo, J. K. Rhee, S. Y. Sohn, Y. Cho, B. T. Zhang and V. N. Kim (2006). "Molecular basis for the recognition of primary microRNAs by the Drosha-DGCR8 complex." Cell **125**(5): 887-901.

Harris, J. J., R. Jolivet and D. Attwell (2012). "Synaptic energy use and supply." Neuron **75**(5): 762-777.

He, M., Y. Liu, X. Wang, M. Q. Zhang, G. J. Hannon and Z. J. Huang (2012). "Cell-type-based analysis of microRNA profiles in the mouse brain." Neuron **73**(1): 35-48.

Henley, B. M., B. A. Williams, R. Srinivasan, B. N. Cohen, C. Xiao, E. D. Mackey, B. J. Wold and H. A. Lester (2013). "Transcriptional regulation by nicotine in dopaminergic neurons." Biochem Pharmacol **86**(8): 1074-1083.

Hikosaka, O. (2010). "The habenula: from stress evasion to value-based decision-making." Nat Rev Neurosci **11**(7): 503-513.

Hilario, M. R., J. R. Turner and J. A. Blendy (2012). "Reward sensitization: effects of repeated nicotine exposure and withdrawal in mice." Neuropsychopharmacology **37**(12): 2661-2670.

Hogan, E. M., A. P. Casserly, M. D. Scofield, Z. Mou, R. Zhao-Shea, C. W. Johnson, A. R. Tapper and P. D. Gardner (2014). "miRNAome analysis of the mammalian neuronal nicotinic acetylcholine receptor gene family." RNA **20**(12): 1890-1899.

Hollander, J. A., H. I. Im, A. L. Amelio, J. Kocerha, P. Bali, Q. Lu, D. Willoughby, C. Wahlestedt, M. D. Conkright and P. J. Kenny (2010). "Striatal microRNA controls cocaine intake through CREB signalling." Nature **466**(7303): 197-202.

Honore, B., P. Madsen, A. H. Andersen and H. Leffers (1993). "Cloning and expression of a novel human profilin variant, profilin II." FEBS Lett **330**(2): 151-155.

Hu, H. Y., Z. Yan, Y. Xu, H. Hu, C. Menzel, Y. H. Zhou, W. Chen and P. Khaitovich (2009). "Sequence features associated with microRNA strand selection in humans and flies." BMC Genomics **10**: 413.

Huang, W. and M. D. Li (2009). "Nicotine modulates expression of miR-140*, which targets the 3'-untranslated region of dynamin 1 gene (Dnm1)." Int J Neuropsychopharmacol **12**(4): 537-546.

Hughes, J. R. (2007). "Effects of abstinence from tobacco: valid symptoms and time course." Nicotine Tob Res **9**(3): 315-327.

Hurst, R., H. Rollema and D. Bertrand (2013). "Nicotinic acetylcholine receptors: from basic science to therapeutics." Pharmacol Ther **137**(1): 22-54.

Hurt, R. D., D. P. Sachs, E. D. Glover, K. P. Offord, J. A. Johnston, L. C. Dale, M. A. Khayrallah, D. R. Schroeder, P. N. Glover, C. R. Sullivan, I. T. Croghan and P. M. Sullivan (1997). "A comparison of sustained-release bupropion and placebo for smoking cessation." N Engl J Med **337**(17): 1195-1202.

Ikemoto, S. (2007). "Dopamine reward circuitry: two projection systems from the ventral midbrain to the nucleus accumbens-olfactory tubercle complex." Brain Res Rev **56**(1): 27-78.

Ikemoto, S., B. S. Glazier, J. M. Murphy and W. J. McBride (1997). "Role of dopamine D1 and D2 receptors in the nucleus accumbens in mediating reward." J Neurosci **17**(21): 8580-8587.

Ikemoto, S., M. Qin and Z. H. Liu (2006). "Primary reinforcing effects of nicotine are triggered from multiple regions both inside and outside the ventral tegmental area." J Neurosci **26**(3): 723-730.

Im, H. I. and P. J. Kenny (2012). "MicroRNAs in neuronal function and dysfunction." Trends Neurosci **35**(5): 325-334.

Izzotti, A., G. A. Calin, P. Arrigo, V. E. Steele, C. M. Croce and S. De Flora (2009). "Downregulation of microRNA expression in the lungs of rats exposed to cigarette smoke." FASEB J **23**(3): 806-812.

Izzotti, A., P. Larghero, M. Longobardi, C. Cartiglia, A. Camoirano, V. E. Steele and S. De Flora (2011). "Dose-responsiveness and persistence of microRNA expression alterations induced by cigarette smoke in mouse lung." Mutat Res **717**(1-2): 9-16.

Jackson, K. J., B. R. Martin, J. P. Changeux and M. I. Damaj (2008). "Differential role of nicotinic acetylcholine receptor subunits in physical and affective nicotine withdrawal signs." J Pharmacol Exp Ther **325**(1): 302-312.

Jackson, K. J., P. P. Muldoon, M. De Biasi and M. I. Damaj (2015). "New mechanisms and perspectives in nicotine withdrawal." Neuropharmacology **96**(Pt B): 223-234.

Jacobs, M., A. M. Alonso, K. M. Sherin, Y. Koh, A. Dhamija, A. L. Lowe and A. P. P. Committee (2013). "Policies to restrict secondhand smoke exposure: American College of Preventive Medicine Position Statement." Am J Prev Med **45**(3): 360-367.

Jennes, L. (1987). "Sites of origin of gonadotropin releasing hormone containing projections to the amygdala and the interpeduncular nucleus." Brain Res **404**(1-2): 339-344.

Jha, P. (2009). "Avoidable global cancer deaths and total deaths from smoking." Nat Rev Cancer **9**(9): 655-664.

Jha, P., C. Ramasundarahettige, V. Landsman, B. Rostron, M. Thun, R. N. Anderson, T. McAfee and R. Peto (2013). "21st-century hazards of smoking and benefits of cessation in the United States." N Engl J Med **368**(4): 341-350.

Jhou, T. C., H. L. Fields, M. G. Baxter, C. B. Saper and P. C. Holland (2009). "The rostromedial tegmental nucleus (RMTg), a GABAergic afferent to midbrain dopamine neurons, encodes aversive stimuli and inhibits motor responses." Neuron **61**(5): 786-800.

Jhou, T. C., S. Geisler, M. Marinelli, B. A. Degarmo and D. S. Zahm (2009). "The mesopontine rostromedial tegmental nucleus: A structure targeted by the lateral habenula that projects to the ventral tegmental area of Tsai and substantia nigra compacta." J Comp Neurol **513**(6): 566-596.

Jiang, Y. H. and M. D. Ehlers (2013). "Modeling autism by SHANK gene mutations in mice." Neuron **78**(1): 8-27.

Jimenez-Gomez, C., A. Osentoski and J. H. Woods (2011). "Pharmacological evaluation of the adequacy of marble burying as an animal model of compulsion and/or anxiety." Behav Pharmacol **22**(7): 711-713.

Jonas, S. and E. Izaurralde (2015). "Towards a molecular understanding of microRNA-mediated gene silencing." Nat Rev Genet **16**(7): 421-433.

Jorenby, D. E., J. T. Hays, N. A. Rigotti, S. Azoulay, E. J. Watsky, K. E. Williams, C. B. Billing, J. Gong, K. R. Reeves and G. Varenicline Phase 3 Study (2006). "Efficacy of varenicline, an alpha4beta2 nicotinic acetylcholine receptor partial agonist, vs placebo or sustained-release bupropion for smoking cessation: a randomized controlled trial." JAMA **296**(1): 56-63.

Jung, Y., L. S. Hsieh, A. M. Lee, Z. Zhou, D. Coman, C. J. Heath, F. Hyder, Y. S. Mineur, Q. Yuan, D. Goldman, A. Bordey and M. R. Picciotto (2016). "An epigenetic mechanism mediates developmental nicotine effects on neuronal structure and behavior." Nat Neurosci **19**(7): 905-914.

Kalivas, P. W., N. Volkow and J. Seamans (2005). "Unmanageable motivation in addiction: a pathology in prefrontal-accumbens glutamate transmission." Neuron **45**(5): 647-650.

Kawaja, M. D., B. A. Flumerfelt and A. W. Hrycyshyn (1989). "Glutamate decarboxylase immunoreactivity in the rat interpeduncular nucleus: a light and electron microscope investigation." Neuroscience **30**(3): 741-753.

Kawamata, T. and Y. Tomari (2010). "Making RISC." Trends Biochem Sci **35**(7): 368-376.

Kawano, M., A. Kawasaki, H. Sakata-Haga, Y. Fukui, H. Kawano, H. Nogami and S. Hisano (2006). "Particular subpopulations of midbrain and hypothalamic dopamine neurons express vesicular glutamate transporter 2 in the rat brain." J Comp Neurol **498**(5): 581-592.

Kim, U. and S. Y. Chang (2005). "Dendritic morphology, local circuitry, and intrinsic electrophysiology of neurons in the rat medial and lateral habenular nuclei of the epithalamus." J Comp Neurol **483**(2): 236-250.

Klemm, W. R. (2004). "Habenular and interpeduncularis nuclei: shared components in multiple-function networks." Med Sci Monit **10**(11): RA261-273.

Klink, R., A. de Kerchove d'Exaerde, M. Zoli and J. P. Changeux (2001). "Molecular and physiological diversity of nicotinic acetylcholine receptors in the midbrain dopaminergic nuclei." J Neurosci **21**(5): 1452-1463.

Koegelenberg, C. F., F. Noor, E. D. Bateman, R. N. van Zyl-Smit, A. Bruning, J. A. O'Brien, C. Smith, M. S. Abdool-Gaffar, S. Emanuel, T. M. Esterhuizen and E. M. Irusen (2014). "Efficacy of varenicline combined with nicotine replacement

therapy vs varenicline alone for smoking cessation: a randomized clinical trial." JAMA **312**(2): 155-161.

Konu, O., J. K. Kane, T. Barrett, M. P. Vawter, R. Chang, J. Z. Ma, D. M. Donovan, B. Sharp, K. G. Becker and M. D. Li (2001). "Region-specific transcriptional response to chronic nicotine in rat brain." Brain Res **909**(1-2): 194-203.

Koob, G. F. and M. Le Moal (2008). "Review. Neurobiological mechanisms for opponent motivational processes in addiction." Philos Trans R Soc Lond B Biol Sci **363**(1507): 3113-3123.

Koob, G. F. and N. D. Volkow (2010). "Neurocircuitry of addiction." Neuropsychopharmacology **35**(1): 217-238.

Koronakis, V., P. J. Hume, D. Humphreys, T. Liu, O. Horning, O. N. Jensen and E. J. McGhie (2011). "WAVE regulatory complex activation by cooperating GTPases Arf and Rac1." Proc Natl Acad Sci U S A **108**(35): 14449-14454.

Korpi, E. R., B. den Hollander, U. Farooq, E. Vashchinkina, R. Rajkumar, D. J. Nutt, P. Hyytia and G. S. Dawe (2015). "Mechanisms of Action and Persistent Neuroplasticity by Drugs of Abuse." Pharmacol Rev **67**(4): 872-1004.

Kotz, D., J. Brown and R. West (2014). "'Real-world' effectiveness of smoking cessation treatments: a population study." Addiction **109**(3): 491-499.

Kourrich, S., P. E. Rothwell, J. R. Klug and M. J. Thomas (2007). "Cocaine experience controls bidirectional synaptic plasticity in the nucleus accumbens." J Neurosci **27**(30): 7921-7928.

Krichevsky, A. M., K. S. King, C. P. Donahue, K. Khrapko and K. S. Kosik (2003). "A microRNA array reveals extensive regulation of microRNAs during brain development." RNA **9**(10): 1274-1281.

Krol, J., I. Loedige and W. Filipowicz (2010). "The widespread regulation of microRNA biogenesis, function and decay." Nat Rev Genet **11**(9): 597-610.

Lammel, S., B. K. Lim and R. C. Malenka (2014). "Reward and aversion in a heterogeneous midbrain dopamine system." Neuropharmacology **76 Pt B**: 351-359.

Lamprecht, R., C. R. Farb, S. M. Rodrigues and J. E. LeDoux (2006). "Fear conditioning drives profilin into amygdala dendritic spines." Nat Neurosci **9**(4): 481-483.

Landgraf, P., M. Rusu, R. Sheridan, A. Sewer, N. Iovino, A. Aravin, S. Pfeffer, A. Rice, A. O. Kamphorst, M. Landthaler, C. Lin, N. D. Socci, L. Hermida, V. Fulci, S. Chiaretti, R. Foa, J. Schliwka, U. Fuchs, A. Novosel, R. U. Muller, B. Schermer, U. Bissels, J. Inman, Q. Phan, M. Chien, D. B. Weir, R. Choksi, G. De Vita, D. Frezzetti, H. I. Trompeter, V. Hornung, G. Teng, G. Hartmann, M. Palkovits, R. Di Lauro, P. Wernet, G. Macino, C. E. Rogler, J. W. Nagle, J. Ju, F. N. Papavasiliou, T. Benzing, P. Lichter, W. Tam, M. J. Brownstein, A. Bosio, A. Borkhardt, J. J. Russo, C. Sander, M. Zavolan and T. Tuschl (2007). "A mammalian microRNA expression atlas based on small RNA library sequencing." Cell **129**(7): 1401-1414.

Lassi, G., A. E. Taylor, N. J. Timpson, P. J. Kenny, R. J. Mather, T. Eisen and M. R. Munafo (2016). "The CHRNA5-A3-B4 Gene Cluster and Smoking: From Discovery to Therapeutics." Trends Neurosci **39**(12): 851-861.

Laviolette, S. R. and D. van der Kooy (2004). "The neurobiology of nicotine addiction: bridging the gap from molecules to behaviour." Nat Rev Neurosci **5**(1): 55-65.

Lawson, G. M., R. D. Hurt, L. C. Dale, K. P. Offord, I. T. Croghan, D. R. Schroeder and N. S. Jiang (1998). "Application of serum nicotine and plasma cotinine concentrations to assessment of nicotine replacement in light, moderate, and heavy smokers undergoing transdermal therapy." J Clin Pharmacol **38**(6): 502-509.

Le Foll, B. and S. R. Goldberg (2005). "Nicotine induces conditioned place preferences over a large range of doses in rats." Psychopharmacology (Berl) **178**(4): 481-492.

Lee, S., J. Woo, Y. S. Kim and H. I. Im (2015). "Integrated miRNA-mRNA analysis in the habenula nuclei of mice intravenously self-administering nicotine." Sci Rep **5**: 12909.

Lee, Y., C. Ahn, J. Han, H. Choi, J. Kim, J. Yim, J. Lee, P. Provost, O. Radmark, S. Kim and V. N. Kim (2003). "The nuclear RNase III Drosha initiates microRNA processing." Nature **425**(6956): 415-419.

Lee, Y., M. Kim, J. Han, K. H. Yeom, S. Lee, S. H. Baek and V. N. Kim (2004). "MicroRNA genes are transcribed by RNA polymerase II." EMBO J **23**(20): 4051-4060.

Lena, C. and J. P. Changeux (1997). "Role of Ca2+ ions in nicotinic facilitation of GABA release in mouse thalamus." J Neurosci **17**(2): 576-585.

Levine, A., Y. Huang, B. Drisaldi, E. A. Griffin, Jr., D. D. Pollak, S. Xu, D. Yin, C. Schaffran, D. B. Kandel and E. R. Kandel (2011). "Molecular mechanism for a gateway drug: epigenetic changes initiated by nicotine prime gene expression by cocaine." Sci Transl Med **3**(107): 107ra109.

Lewis, B. P., I. H. Shih, M. W. Jones-Rhoades, D. P. Bartel and C. B. Burge (2003). "Prediction of mammalian microRNA targets." Cell **115**(7): 787-798.

Lewohl, J. M., Y. O. Nunez, P. R. Dodd, G. R. Tiwari, R. A. Harris and R. D. Mayfield (2011). "Up-regulation of microRNAs in brain of human alcoholics." Alcohol Clin Exp Res **35**(11): 1928-1937.

Li, M. D., J. K. Kane, J. Wang and J. Z. Ma (2004). "Time-dependent changes in transcriptional profiles within five rat brain regions in response to nicotine treatment." Brain Res Mol Brain Res **132**(2): 168-180.

Lim, L. P., N. C. Lau, P. Garrett-Engele, A. Grimson, J. M. Schelter, J. Castle, D. P. Bartel, P. S. Linsley and J. M. Johnson (2005). "Microarray analysis shows that some microRNAs downregulate large numbers of target mRNAs." Nature **433**(7027): 769-773.

Lim, S. S., T. Vos, A. D. Flaxman, G. Danaei, K. Shibuya, H. Adair-Rohani, M. Amann, H. R. Anderson, K. G. Andrews, M. Aryee, C. Atkinson, L. J. Bacchus, A. N. Bahalim, K. Balakrishnan, J. Balmes, S. Barker-Collo, A. Baxter, M. L. Bell, J. D. Blore, F. Blyth, C. Bonner, G. Borges, R. Bourne, M. Boussinesq, M. Brauer, P. Brooks, N. G. Bruce, B. Brunekreef, C. Bryan-Hancock, C. Bucello, R. Buchbinder, F. Bull, R. T. Burnett, T. E. Byers, B. Calabria, J. Carapetis, E. Carnahan, Z. Chafe, F. Charlson, H. Chen, J. S. Chen, A. T. Cheng, J. C. Child, A. Cohen, K. E. Colson, B. C. Cowie, S. Darby, S. Darling, A. Davis, L. Degenhardt, F. Dentener, D. C. Des Jarlais, K. Devries, M. Dherani, E. L. Ding, E. R. Dorsey, T. Driscoll, K. Edmond, S. E. Ali, R. E. Engell, P. J. Erwin, S. Fahimi, G. Falder, F. Farzadfar, A. Ferrari, M. M. Finucane, S. Flaxman, F. G. Fowkes, G. Freedman, M. K. Freeman, E. Gakidou, S. Ghosh, E. Giovannucci, G. Gmel, K. Graham, R. Grainger, B. Grant, D. Gunnell, H. R. Gutierrez, W. Hall, H. W. Hoek, A. Hogan, H. D. Hosgood, 3rd, D. Hoy, H. Hu, B. J. Hubbell, S. J. Hutchings, S. E. Ibeanusi, G. L. Jacklyn, R. Jasrasaria, J. B. Jonas, H. Kan, J. A. Kanis, N. Kassebaum, N. Kawakami, Y. H. Khang, S. Khatibzadeh, J. P. Khoo, C. Kok, F. Laden, R. Lalloo, Q. Lan, T. Lathlean, J. L. Leasher, J. Leigh, Y. Li, J. K. Lin, S. E. Lipshultz, S. London, R. Lozano, Y. Lu, J. Mak, R. Malekzadeh, L. Mallinger, W. Marcenes, L. March, R. Marks, R. Martin, P. McGale, J. McGrath, S. Mehta, G. A. Mensah, T. R. Merriman, R. Micha, C. Michaud, V. Mishra, K. Mohd Hanafiah, A. A. Mokdad, L. Morawska, D. Mozaffarian, T. Murphy, M. Naghavi, B. Neal, P. K. Nelson, J. M. Nolla, R. Norman, C. Olives, S. B. Omer, J. Orchard, R. Osborne, B. Ostro, A. Page, K. D. Pandey, C. D. Parry, E. Passmore, J. Patra, N. Pearce, P. M. Pelizzari, M. Petzold, M. R. Phillips, D. Pope, C. A. Pope, 3rd, J. Powles, M.

Rao, H. Razavi, E. A. Rehfuess, J. T. Rehm, B. Ritz, F. P. Rivara, T. Roberts, C. Robinson, J. A. Rodriguez-Portales, I. Romieu, R. Room, L. C. Rosenfeld, A. Roy, L. Rushton, J. A. Salomon, U. Sampson, L. Sanchez-Riera, E. Sanman, A. Sapkota, S. Seedat, P. Shi, K. Shield, R. Shivakoti, G. M. Singh, D. A. Sleet, E. Smith, K. R. Smith, N. J. Stapelberg, K. Steenland, H. Stockl, L. J. Stovner, K. Straif, L. Straney, G. D. Thurston, J. H. Tran, R. Van Dingenen, A. van Donkelaar, J. L. Veerman, L. Vijayakumar, R. Weintraub, M. M. Weissman, R. A. White, H. Whiteford, S. T. Wiersma, J. D. Wilkinson, H. C. Williams, W. Williams, N. Wilson, A. D. Woolf, P. Yip, J. M. Zielinski, A. D. Lopez, C. J. Murray, M. Ezzati, M. A. AlMazroa and Z. A. Memish (2012). "A comparative risk assessment of burden of disease and injury attributable to 67 risk factors and risk factor clusters in 21 regions, 1990-2010: a systematic analysis for the Global Burden of Disease Study 2010." Lancet **380**(9859): 2224-2260.

Lippi, G., J. R. Steinert, E. L. Marczylo, S. D'Oro, R. Fiore, I. D. Forsythe, G. Schratt, M. Zoli, P. Nicotera and K. W. Young (2011). "Targeting of the Arpc3 actin nucleation factor by miR-29a/b regulates dendritic spine morphology." J Cell Biol **194**(6): 889-904.

Livak, K. J. and T. D. Schmittgen (2001). "Analysis of relative gene expression data using real-time quantitative PCR and the 2(-Delta Delta C(T)) Method." Methods **25**(4): 402-408.

Love, M. I., W. Huber and S. Anders (2014). "Moderated estimation of fold change and dispersion for RNA-seq data with DESeq2." Genome Biol **15**(12): 550.

Lovinger, D. M. (2010). "Neurotransmitter roles in synaptic modulation, plasticity and learning in the dorsal striatum." Neuropharmacology **58**(7): 951-961.

Lugli, G., V. I. Torvik, J. Larson and N. R. Smalheiser (2008). "Expression of microRNAs and their precursors in synaptic fractions of adult mouse forebrain." J Neurochem **106**(2): 650-661.

Macrae, I. J., K. Zhou, F. Li, A. Repic, A. N. Brooks, W. Z. Cande, P. D. Adams and J. A. Doudna (2006). "Structural basis for double-stranded RNA processing by Dicer." Science **311**(5758): 195-198.

Madsen, H. B., R. M. Brown and A. J. Lawrence (2012). "Neuroplasticity in addiction: cellular and transcriptional perspectives." Front Mol Neurosci **5**: 99.

Magistretti, P. J. and I. Allaman (2015). "A cellular perspective on brain energy metabolism and functional imaging." Neuron **86**(4): 883-901.

Majoros, W. H. and U. Ohler (2007). "Spatial preferences of microRNA targets in 3' untranslated regions." BMC Genomics **8**: 152.

Malas, M., J. van der Tempel, R. Schwartz, A. Minichiello, C. Lightfoot, A. Noormohamed, J. Andrews, L. Zawertailo and R. Ferrence (2016). "Electronic Cigarettes for Smoking Cessation: A Systematic Review." Nicotine Tob Res **18**(10): 1926-1936.

Malek, A. M., M. Cushman, D. T. Lackland, G. Howard and L. A. McClure (2015). "Secondhand Smoke Exposure and Stroke: The Reasons for Geographic and Racial Differences in Stroke (REGARDS) Study." Am J Prev Med **49**(6): e89-97.

Mammoto, A., T. Sasaki, T. Asakura, I. Hotta, H. Imamura, K. Takahashi, Y. Matsuura, T. Shirao and Y. Takai (1998). "Interactions of drebrin and gephyrin with profilin." Biochem Biophys Res Commun **243**(1): 86-89.

Mammoto, T., Y. Yamamoto, K. Kagawa, Y. Hayashi, T. Mashimo, I. Yoshiya and A. Yamatodani (1997). "Interactions between neuronal histamine and halothane anesthesia in rats." J Neurochem **69**(1): 406-411.

Mansvelder, H. D., J. R. Keath and D. S. McGehee (2002). "Synaptic mechanisms underlie nicotine-induced excitability of brain reward areas." Neuron **33**(6): 905-919.

Marks, M. J., J. R. Pauly, S. D. Gross, E. S. Deneris, I. Hermans-Borgmeyer, S. F. Heinemann and A. C. Collins (1992). "Nicotine binding and nicotinic receptor subunit RNA after chronic nicotine treatment." J Neurosci **12**(7): 2765-2784.

Marks, M. J., K. W. Smith and A. C. Collins (1998). "Differential agonist inhibition identifies multiple epibatidine binding sites in mouse brain." J Pharmacol Exp Ther **285**(1): 377-386.

Marttila, K., H. Raattamaa and L. Ahtee (2006). "Effects of chronic nicotine administration and its withdrawal on striatal FosB/DeltaFosB and c-Fos expression in rats and mice." Neuropharmacology **51**(1): 44-51.

Mathonnet, G., M. R. Fabian, Y. V. Svitkin, A. Parsyan, L. Huck, T. Murata, S. Biffo, W. C. Merrick, E. Darzynkiewicz, R. S. Pillai, W. Filipowicz, T. F. Duchaine and N. Sonenberg (2007). "MicroRNA inhibition of translation initiation in vitro by targeting the cap-binding complex eIF4F." Science **317**(5845): 1764-1767.

Mathys, H., J. Basquin, S. Ozgur, M. Czarnocki-Cieciura, F. Bonneau, A. Aartse, A. Dziembowski, M. Nowotny, E. Conti and W. Filipowicz (2014). "Structural and biochemical insights to the role of the CCR4-NOT complex and DDX6 ATPase in microRNA repression." Mol Cell **54**(5): 751-765.

Meijer, H. A., E. M. Smith and M. Bushell (2014). "Regulation of miRNA strand selection: follow the leader?" Biochem Soc Trans **42**(4): 1135-1140.

Michaelsen, K., K. Murk, M. Zagrebelsky, A. Dreznjak, B. M. Jockusch, M. Rothkegel and M. Korte (2010). "Fine-tuning of neuronal architecture requires two profilin isoforms." Proc Natl Acad Sci U S A **107**(36): 15780-15785.

Michaelsen-Preusse, K., S. Zessin, G. Grigoryan, F. Scharkowski, J. Feuge, A. Remus and M. Korte (2016). "Neuronal profilins in health and disease: Relevance for spine plasticity and Fragile X syndrome." Proc Natl Acad Sci U S A **113**(12): 3365-3370.

Mihalak, K. B., F. I. Carroll and C. W. Luetje (2006). "Varenicline is a partial agonist at alpha4beta2 and a full agonist at alpha7 neuronal nicotinic receptors." Mol Pharmacol **70**(3): 801-805.

Mitchell, P. J. and R. Tjian (1989). "Transcriptional regulation in mammalian cells by sequence-specific DNA binding proteins." Science **245**(4916): 371-378.

Miura, P., S. Shenker, C. Andreu-Agullo, J. O. Westholm and E. C. Lai (2013). "Widespread and extensive lengthening of 3' UTRs in the mammalian brain." Genome Res **23**(5): 812-825.

Miyata, G., M. M. Meguid, S. O. Fetissov, G. F. Torelli and H. J. Kim (1999). "Nicotine's effect on hypothalamic neurotransmitters and appetite regulation." Surgery **126**(2): 255-263.

Mockrin, S. C. and E. D. Korn (1980). "Acanthamoeba profilin interacts with G-actin to increase the rate of exchange of actin-bound adenosine 5'-triphosphate." Biochemistry **19**(23): 5359-5362.

Molas, S., S. R. DeGroot, R. Zhao-Shea and A. R. Tapper (2017). "Anxiety and Nicotine Dependence: Emerging Role of the Habenulo-Interpeduncular Axis." Trends Pharmacol Sci **38**(2): 169-180.

Molas, S., R. Zhao-Shea, L. Liu, S. R. DeGroot, P. D. Gardner and A. R. Tapper (2017). "A circuit-based mechanism underlying familiarity signaling and the preference for novelty." Nat Neurosci **20**(9): 1260-1268.

Mondin, M., M. Carta, E. Normand, C. Mulle and F. Coussen (2010). "Profilin II regulates the exocytosis of kainate glutamate receptors." J Biol Chem **285**(51): 40060-40071.

Moore, R. Y., R. Weis and M. M. Moga (2000). "Efferent projections of the intergeniculate leaflet and the ventral lateral geniculate nucleus in the rat." J Comp Neurol **420**(3): 398-418.

Nair-Roberts, R. G., S. D. Chatelain-Badie, E. Benson, H. White-Cooper, J. P. Bolam and M. A. Ungless (2008). "Stereological estimates of dopaminergic, GABAergic and glutamatergic neurons in the ventral tegmental area, substantia nigra and retrorubral field in the rat." Neuroscience **152**(4): 1024-1031.

Nashmi, R. and H. Lester (2007). "Cell autonomy, receptor autonomy, and thermodynamics in nicotine receptor up-regulation." Biochem Pharmacol **74**(8): 1145-1154.

Natera-Naranjo, O., A. Aschrafi, A. E. Gioio and B. B. Kaplan (2010). "Identification and quantitative analyses of microRNAs located in the distal axons of sympathetic neurons." RNA **16**(8): 1516-1529.

Ngolab, J., L. Liu, R. Zhao-Shea, G. Gao, P. D. Gardner and A. R. Tapper (2015). "Functional Upregulation of alpha4* Nicotinic Acetylcholine Receptors in VTA GABAergic Neurons Increases Sensitivity to Nicotine Reward." J Neurosci **35**(22): 8570-8578.

Nguyen, H. N., B. A. Rasmussen and D. C. Perry (2003). "Subtype-selective up-regulation by chronic nicotine of high-affinity nicotinic receptors in rat brain demonstrated by receptor autoradiography." J Pharmacol Exp Ther **307**(3): 1090-1097.

Nguyen, T. A., M. H. Jo, Y. G. Choi, J. Park, S. C. Kwon, S. Hohng, V. N. Kim and J. S. Woo (2015). "Functional Anatomy of the Human Microprocessor." Cell **161**(6): 1374-1387.

Nolle, A., A. Zeug, J. van Bergeijk, L. Tonges, R. Gerhard, H. Brinkmann, S. Al Rayes, N. Hensel, Y. Schill, D. Apkhazava, S. Jablonka, J. O'Mer, R. K. Srivastav, A. Baasner, P. Lingor, B. Wirth, E. Ponimaskin, R. Niedenthal, C. Grothe and P. Claus (2011). "The spinal muscular atrophy disease protein SMN is linked to the Rho-kinase pathway via profilin." Hum Mol Genet **20**(24): 4865-4878.

Novak, G., P. Seeman and B. Le Foll (2010). "Exposure to nicotine produces an increase in dopamine D2(High) receptors: a possible mechanism for dopamine hypersensitivity." Int J Neurosci **120**(11): 691-697.

O'Carroll, D. and A. Schaefer (2013). "General principals of miRNA biogenesis and regulation in the brain." Neuropsychopharmacology **38**(1): 39-54.

Oakman, S. A., P. L. Faris, P. E. Kerr, C. Cozzari and B. K. Hartman (1995). "Distribution of pontomesencephalic cholinergic neurons projecting to substantia nigra differs significantly from those projecting to ventral tegmental area." J Neurosci **15**(9): 5859-5869.

Omelchenko, N. and S. R. Sesack (2006). "Cholinergic axons in the rat ventral tegmental area synapse preferentially onto mesoaccumbens dopamine neurons." J Comp Neurol **494**(6): 863-875.

Ottersen, O. P. and P. J. Helm (2002). "How hardwired is the brain?" Nature **420**(6917): 751-752.

Ozsolak, F., L. L. Poling, Z. Wang, H. Liu, X. S. Liu, R. G. Roeder, X. Zhang, J. S. Song and D. E. Fisher (2008). "Chromatin structure analyses identify miRNA promoters." Genes Dev **22**(22): 3172-3183.

Pandey, S. C., A. Roy and N. Mittal (2001). "Effects of chronic ethanol intake and its withdrawal on the expression and phosphorylation of the creb gene transcription factor in rat cortex." J Pharmacol Exp Ther **296**(3): 857-868.

Pandey, S. C., A. Roy, T. Xu and N. Mittal (2001). "Effects of protracted nicotine exposure and withdrawal on the expression and phosphorylation of the CREB gene transcription factor in rat brain." J Neurochem **77**(3): 943-952.

Pang, X., L. Liu, J. Ngolab, R. Zhao-Shea, J. M. McIntosh, P. D. Gardner and A. R. Tapper (2016). "Habenula cholinergic neurons regulate anxiety during nicotine withdrawal via nicotinic acetylcholine receptors." Neuropharmacology **107**: 294-304.

Park, J. E., I. Heo, Y. Tian, D. K. Simanshu, H. Chang, D. Jee, D. J. Patel and V. N. Kim (2011). "Dicer recognizes the 5' end of RNA for efficient and accurate processing." Nature **475**(7355): 201-205.

Partridge, J. G., S. Apparsundaram, G. A. Gerhardt, J. Ronesi and D. M. Lovinger (2002). "Nicotinic acetylcholine receptors interact with dopamine in induction of striatal long-term depression." J Neurosci **22**(7): 2541-2549.

Peacock, A., J. Leung, S. Larney, S. Colledge, M. Hickman, J. Rehm, G. A. Giovino, R. West, W. Hall, P. Griffiths, R. Ali, L. Gowing, J. Marsden, A. J. Ferrari, J. Grebely, M. Farrell and L. Degenhardt (2018). "Global statistics on alcohol, tobacco and illicit drug use: 2017 status report." Addiction.

Peacock, A., A. Pennay, N. Droste, R. Bruno and D. I. Lubman (2014). "'High' risk? A systematic review of the acute outcomes of mixing alcohol with energy drinks." Addiction **109**(10): 1612-1633.

Peter, M. E. (2010). "Targeting of mRNAs by multiple miRNAs: the next step." Oncogene **29**(15): 2161-2164.

Picciotto, M. R. and P. J. Kenny (2013). "Molecular mechanisms underlying behaviors related to nicotine addiction." Cold Spring Harb Perspect Med **3**(1): a012112.

Picciotto, M. R. and Y. S. Mineur (2014). "Molecules and circuits involved in nicotine addiction: The many faces of smoking." Neuropharmacology **76 Pt B**: 545-553.

Pichardo-Casas, I., L. A. Goff, M. R. Swerdel, A. Athie, J. Davila, M. Ramos-Brossier, M. Lapid-Volosin, W. J. Friedman, R. P. Hart and L. Vaca (2012). "Expression profiling of synaptic microRNAs from the adult rat brain identifies regional differences and seizure-induced dynamic modulation." Brain Res **1436**: 20-33.

Pignatelli, M. and A. Bonci (2015). "Role of Dopamine Neurons in Reward and Aversion: A Synaptic Plasticity Perspective." Neuron **86**(5): 1145-1157.

Pillai, R. S., S. N. Bhattacharyya, C. G. Artus, T. Zoller, N. Cougot, E. Basyuk, E. Bertrand and W. Filipowicz (2005). "Inhibition of translational initiation by Let-7 MicroRNA in human cells." Science **309**(5740): 1573-1576.

Pilo Boyl, P., A. Di Nardo, C. Mulle, M. Sassoe-Pognetto, P. Panzanelli, A. Mele, M. Kneussel, V. Costantini, E. Perlas, M. Massimi, H. Vara, M. Giustetto and W. Witke (2007). "Profilin2 contributes to synaptic vesicle exocytosis, neuronal excitability, and novelty-seeking behavior." EMBO J **26**(12): 2991-3002.

Piper, M. E., T. R. Schlam, J. W. Cook, M. A. Sheffer, S. S. Smith, W. Y. Loh, D. M. Bolt, S. Y. Kim, J. T. Kaye, K. R. Hefner and T. B. Baker (2011). "Tobacco withdrawal components and their relations with cessation success." Psychopharmacology (Berl) **216**(4): 569-578.

Pirkle, J. L., J. T. Bernert, S. P. Caudill, C. S. Sosnoff and T. F. Pechacek (2006). "Trends in the exposure of nonsmokers in the U.S. population to secondhand smoke: 1988-2002." Environ Health Perspect **114**(6): 853-858.

Pisani, A., G. Bernardi, J. Ding and D. J. Surmeier (2007). "Re-emergence of striatal cholinergic interneurons in movement disorders." Trends Neurosci **30**(10): 545-553.

Pistillo, F., F. Clementi, M. Zoli and C. Gotti (2015). "Nicotinic, glutamatergic and dopaminergic synaptic transmission and plasticity in the mesocorticolimbic system: focus on nicotine effects." Prog Neurobiol **124**: 1-27.

Pistillo, F., F. Fasoli, M. Moretti, T. McClure-Begley, M. Zoli, M. J. Marks and C. Gotti (2016). "Chronic nicotine and withdrawal affect glutamatergic but not nicotinic receptor expression in the mesocorticolimbic pathway in a region-specific manner." Pharmacol Res **103**: 167-176.

Pons, S., L. Fattore, G. Cossu, S. Tolu, E. Porcu, J. M. McIntosh, J. P. Changeux, U. Maskos and W. Fratta (2008). "Crucial role of alpha4 and alpha6 nicotinic acetylcholine receptor subunits from ventral tegmental area in systemic nicotine self-administration." J Neurosci **28**(47): 12318-12327.

Pontieri, F. E., G. Tanda, F. Orzi and G. Di Chiara (1996). "Effects of nicotine on the nucleus accumbens and similarity to those of addictive drugs." Nature **382**(6588): 255-257.

Prochaska, J. J. (2015). "Nicotine Replacement Therapy as a Maintenance Treatment." JAMA **314**(7): 718-719.

Prut, L. and C. Belzung (2003). "The open field as a paradigm to measure the effects of drugs on anxiety-like behaviors: a review." Eur J Pharmacol **463**(1-3): 3-33.

Qin, C. and M. Luo (2009). "Neurochemical phenotypes of the afferent and efferent projections of the mouse medial habenula." Neuroscience **161**(3): 827-837.

Qualmann, B., M. M. Kessels and R. B. Kelly (2000). "Molecular links between endocytosis and the actin cytoskeleton." J Cell Biol **150**(5): F111-116.

Rezvani, K., Y. Teng, D. Shim and M. De Biasi (2007). "Nicotine regulates multiple synaptic proteins by inhibiting proteasomal activity." J Neurosci **27**(39): 10508-10519.

Risinger, F. O. and R. A. Oakes (1995). "Nicotine-induced conditioned place preference and conditioned place aversion in mice." Pharmacol Biochem Behav **51**(2-3): 457-461.

Risso, D., J. Ngai, T. P. Speed and S. Dudoit (2014). "Normalization of RNA-seq data using factor analysis of control genes or samples." Nat Biotechnol **32**(9): 896-902.

Robison, A. J. and E. J. Nestler (2011). "Transcriptional and epigenetic mechanisms of addiction." Nat Rev Neurosci **12**(11): 623-637.

Russell, M. A. (1971). "Cigarette smoking: natural history of a dependence disorder." Br J Med Psychol **44**(1): 1-16.

Saccone, S. F., A. L. Hinrichs, N. L. Saccone, G. A. Chase, K. Konvicka, P. A. Madden, N. Breslau, E. O. Johnson, D. Hatsukami, O. Pomerleau, G. E. Swan, A. M. Goate, J. Rutter, S. Bertelsen, L. Fox, D. Fugman, N. G. Martin, G. W. Montgomery, J. C. Wang, D. G. Ballinger, J. P. Rice and L. J. Bierut (2007). "Cholinergic nicotinic receptor genes implicated in a nicotine dependence association study targeting 348 candidate genes with 3713 SNPs." Hum Mol Genet **16**(1): 36-49.

Saitoh, A., M. Yamada, M. Yamada, S. Kobayashi, N. Hirose, K. Honda and J. Kamei (2006). "ROCK inhibition produces anxiety-related behaviors in mice." Psychopharmacology (Berl) **188**(1): 1-11.

Salas, R., F. Pieri and M. De Biasi (2004). "Decreased signs of nicotine withdrawal in mice null for the beta4 nicotinic acetylcholine receptor subunit." J Neurosci **24**(45): 10035-10039.

Salas, R., R. Sturm, J. Boulter and M. De Biasi (2009). "Nicotinic receptors in the habenulo-interpeduncular system are necessary for nicotine withdrawal in mice." J Neurosci **29**(10): 3014-3018.

Salgado, S. and M. G. Kaplitt (2015). "The Nucleus Accumbens: A Comprehensive Review." Stereotact Funct Neurosurg **93**(2): 75-93.

Salminen, O., K. L. Murphy, J. M. McIntosh, J. Drago, M. J. Marks, A. C. Collins and S. R. Grady (2004). "Subunit composition and pharmacology of two classes of striatal presynaptic nicotinic acetylcholine receptors mediating dopamine release in mice." Mol Pharmacol **65**(6): 1526-1535.

Satoh, K. and H. C. Fibiger (1986). "Cholinergic neurons of the laterodorsal tegmental nucleus: efferent and afferent connections." J Comp Neurol **253**(3): 277-302.

Schlicker, A., F. S. Domingues, J. Rahnenfuhrer and T. Lengauer (2006). "A new measure for functional similarity of gene products based on Gene Ontology." BMC Bioinformatics **7**: 302.

Schoffelmeer, A. N., T. J. De Vries, G. Wardeh, H. W. van de Ven and L. J. Vanderschuren (2002). "Psychostimulant-induced behavioral sensitization depends on nicotinic receptor activation." J Neurosci **22**(8): 3269-3276.

Schultz, W. (1986). "Responses of midbrain dopamine neurons to behavioral trigger stimuli in the monkey." J Neurophysiol **56**(5): 1439-1461.

Schwartz, R. D. and K. J. Kellar (1983). "Nicotinic cholinergic receptor binding sites in the brain: regulation in vivo." Science **220**(4593): 214-216.

Schwarz, D. S., G. Hutvagner, T. Du, Z. Xu, N. Aronin and P. D. Zamore (2003). "Asymmetry in the assembly of the RNAi enzyme complex." Cell **115**(2): 199-208.

Selbach, M., B. Schwanhausser, N. Thierfelder, Z. Fang, R. Khanin and N. Rajewsky (2008). "Widespread changes in protein synthesis induced by microRNAs." Nature **455**(7209): 58-63.

Sellings, L. H. and P. B. Clarke (2003). "Segregation of amphetamine reward and locomotor stimulation between nucleus accumbens medial shell and core." J Neurosci **23**(15): 6295-6303.

Semba, J., M. Wakuta, J. Maeda and T. Suhara (2004). "Nicotine withdrawal induces subsensitivity of hypothalamic-pituitary-adrenal axis to stress in rats: implications for precipitation of depression during smoking cessation." Psychoneuroendocrinology **29**(2): 215-226.

Sesack, S. R. and A. A. Grace (2010). "Cortico-Basal Ganglia reward network: microcircuitry." Neuropsychopharmacology **35**(1): 27-47.

Shabat-Simon, M., D. Levy, A. Amir, M. Rehavi and A. Zangen (2008). "Dissociation between rewarding and psychomotor effects of opiates: differential roles for glutamate receptors within anterior and posterior portions of the ventral tegmental area." J Neurosci **28**(34): 8406-8416.

Shan, H., Y. Zhang, Y. Lu, Y. Zhang, Z. Pan, B. Cai, N. Wang, X. Li, T. Feng, Y. Hong and B. Yang (2009). "Downregulation of miR-133 and miR-590 contributes to nicotine-induced atrial remodelling in canines." Cardiovasc Res **83**(3): 465-472.

Sheffield, E. B., M. W. Quick and R. A. Lester (2000). "Nicotinic acetylcholine receptor subunit mRNA expression and channel function in medial habenula neurons." Neuropharmacology **39**(13): 2591-2603.

Shih, P. Y., J. M. McIntosh and R. M. Drenan (2015). "Nicotine Dependence Reveals Distinct Responses from Neurons and Their Resident Nicotinic Receptors in Medial Habenula." Mol Pharmacol **88**(6): 1035-1044.

Siegel, G., R. Saba and G. Schratt (2011). "microRNAs in neurons: manifold regulatory roles at the synapse." Curr Opin Genet Dev **21**(4): 491-497.

Sieminska, A. and E. Jassem (2014). "The many faces of tobacco use among women." Med Sci Monit **20**: 153-162.

Slemmer, J. E., B. R. Martin and M. I. Damaj (2000). "Bupropion is a nicotinic antagonist." J Pharmacol Exp Ther **295**(1): 321-327.

Smith, P. H., K. A. Kasza, A. Hyland, G. T. Fong, R. Borland, K. Brady, M. J. Carpenter, K. Hartwell, K. M. Cummings and S. A. McKee (2015). "Gender differences in medication use and cigarette smoking cessation: results from the International Tobacco Control Four Country Survey." Nicotine Tob Res **17**(4): 463-472.

Smith, Y., D. V. Raju, J. F. Pare and M. Sidibe (2004). "The thalamostriatal system: a highly specific network of the basal ganglia circuitry." Trends Neurosci **27**(9): 520-527.

Sombers, L. A., M. Beyene, R. M. Carelli and R. M. Wightman (2009). "Synaptic overflow of dopamine in the nucleus accumbens arises from neuronal activity in the ventral tegmental area." J Neurosci **29**(6): 1735-1742.

Spina, L., S. Fenu, R. Longoni, E. Rivas and G. Di Chiara (2006). "Nicotine-conditioned single-trial place preference: selective role of nucleus accumbens shell dopamine D1 receptors in acquisition." Psychopharmacology (Berl) **184**(3-4): 447-455.

Stahl, S. M., J. F. Pradko, B. R. Haight, J. G. Modell, C. B. Rockett and S. Learned-Coughlin (2004). "A Review of the Neuropharmacology of Bupropion, a Dual Norepinephrine and Dopamine Reuptake Inhibitor." Prim Care Companion J Clin Psychiatry **6**(4): 159-166.

Supek, F., M. Bosnjak, N. Skunca and T. Smuc (2011). "REVIGO summarizes and visualizes long lists of gene ontology terms." PLoS One **6**(7): e21800.

Sutherland, R. J. (1982). "The dorsal diencephalic conduction system: a review of the anatomy and functions of the habenular complex." Neurosci Biobehav Rev **6**(1): 1-13.

Swan, G. E., T. McAfee, S. J. Curry, L. M. Jack, H. Javitz, S. Dacey and K. Bergman (2003). "Effectiveness of bupropion sustained release for smoking cessation in a health care setting: a randomized trial." Arch Intern Med **163**(19): 2337-2344.

Takahashi, K., S. Yokota, N. Tatsumi, T. Fukami, T. Yokoi and M. Nakajima (2013). "Cigarette smoking substantially alters plasma microRNA profiles in healthy subjects." Toxicol Appl Pharmacol **272**(1): 154-160.

Tan, K. R., C. Yvon, M. Turiault, J. J. Mirzabekov, J. Doehner, G. Labouebe, K. Deisseroth, K. M. Tye and C. Luscher (2012). "GABA neurons of the VTA drive conditioned place aversion." Neuron **73**(6): 1173-1183.

Tapper, A. R., S. L. McKinney, R. Nashmi, J. Schwarz, P. Deshpande, C. Labarca, P. Whiteaker, M. J. Marks, A. C. Collins and H. A. Lester (2004). "Nicotine activation of alpha4* receptors: sufficient for reward, tolerance, and sensitization." Science **306**(5698): 1029-1032.

Tariq, N., Z. Basharat, S. Butt and D. N. Baig (2016). "Distribution analysis of profilin isoforms at transcript resolution with mRNA-seq and secondary structure in various organs of Rattus norvegicus." Gene **589**(1): 49-55.

Taylor, S. R., S. Badurek, R. J. Dileone, R. Nashmi, L. Minichiello and M. R. Picciotto (2014). "GABAergic and glutamatergic efferents of the mouse ventral tegmental area." J Comp Neurol **522**(14): 3308-3334.

Tepper, J. M. and J. P. Bolam (2004). "Functional diversity and specificity of neostriatal interneurons." Curr Opin Neurobiol **14**(6): 685-692.

Thorgeirsson, T. E., F. Geller, P. Sulem, T. Rafnar, A. Wiste, K. P. Magnusson, A. Manolescu, G. Thorleifsson, H. Stefansson, A. Ingason, S. N. Stacey, J. T. Bergthorsson, S. Thorlacius, J. Gudmundsson, T. Jonsson, M. Jakobsdottir, J. Saemundsdottir, O. Olafsdottir, L. J. Gudmundsson, G. Bjornsdottir, K. Kristjansson, H. Skuladottir, H. J. Isaksson, T. Gudbjartsson, G. T. Jones, T. Mueller, A. Gottsater, A. Flex, K. K. H. Aben, F. de Vegt, P. F. A. Mulders, D. Isla, M. J. Vidal, L. Asin, B. Saez, L. Murillo, T. Blondal, H. Kolbeinsson, J. G. Stefansson, I. Hansdottir, V. Runarsdottir, R. Pola, B. Lindblad, A. M. van Rij, B. Dieplinger, M. Haltmayer, J. I. Mayordomo, L. A. Kiemeney, S. E. Matthiasson, H. Oskarsson, T. Tyrfingsson, D. F. Gudbjartsson, J. R. Gulcher, S. Jonsson, U. Thorsteinsdottir, A. Kong and K. Stefansson (2008). "A variant associated with nicotine dependence, lung cancer and peripheral arterial disease." Nature **452**(7187): 638-642.

Threlfell, S., T. Lalic, N. J. Platt, K. A. Jennings, K. Deisseroth and S. J. Cragg (2012). "Striatal dopamine release is triggered by synchronized activity in cholinergic interneurons." Neuron **75**(1): 58-64.

Tolu, S., R. Eddine, F. Marti, V. David, M. Graupner, S. Pons, M. Baudonnat, M. Husson, M. Besson, C. Reperant, J. Zemdegs, C. Pages, Y. A. Hay, B. Lambolez, J. Caboche, B. Gutkin, A. M. Gardier, J. P. Changeux, P. Faure and U. Maskos (2013). "Co-activation of VTA DA and GABA neurons mediates nicotine reinforcement." Mol Psychiatry **18**(3): 382-393.

Trachtenberg, J. T., B. E. Chen, G. W. Knott, G. Feng, J. R. Sanes, E. Welker and K. Svoboda (2002). "Long-term in vivo imaging of experience-dependent synaptic plasticity in adult cortex." Nature **420**(6917): 788-794.

Tredway, T. L., J. Z. Guo and V. A. Chiappinelli (1999). "N-type voltage-dependent calcium channels mediate the nicotinic enhancement of GABA release in chick brain." J Neurophysiol **81**(2): 447-454.

Tsai, H. C., F. Zhang, A. Adamantidis, G. D. Stuber, A. Bonci, L. de Lecea and K. Deisseroth (2009). "Phasic firing in dopaminergic neurons is sufficient for behavioral conditioning." Science **324**(5930): 1080-1084.

USDHHS (2006). The Health Consequences of Involuntary Exposure to Tobacco Smoke: A Report of the Surgeon General US, United States Department of Health and Human Services, Centers for Disease Control.

USDHHS (2014). The Health Consequences of Smoking - 50 years of Progress. A Report of the Surgeon General. US, United States Department of Health and Human Services, Centers for Diease Control and Prevention.

van Zessen, R., J. L. Phillips, E. A. Budygin and G. D. Stuber (2012). "Activation of VTA GABA neurons disrupts reward consumption." Neuron **73**(6): 1184-1194.

Vertes, R. P. and B. Fass (1988). "Projections between the interpeduncular nucleus and basal forebrain in the rat as demonstrated by the anterograde and retrograde transport of WGA-HRP." Exp Brain Res **73**(1): 23-31.

Villalobos, J. and A. Ferssiwi (1987). "The differential ascending projections from the anterior, central and posterior regions of the lateral hypothalamic area: an autoradiographic study." Neurosci Lett **81**(1-2): 89-94.

Walters, C. L., S. Brown, J. P. Changeux, B. Martin and M. I. Damaj (2006). "The beta2 but not alpha7 subunit of the nicotinic acetylcholine receptor is required for nicotine-conditioned place preference in mice." Psychopharmacology (Berl) **184**(3-4): 339-344.

Wang, J., R. Gutala, Y. Y. Hwang, J. M. Kim, O. Konu, J. Z. Ma and M. D. Li (2008). "Strain- and region-specific gene expression profiles in mouse brain in response to chronic nicotine treatment." Genes Brain Behav **7**(1): 78-87.

Wang, Y., J. W. Lee, G. Oh, S. R. Grady, J. M. McIntosh, D. H. Brunzell, J. R. Cannon and R. M. Drenan (2014). "Enhanced synthesis and release of dopamine in transgenic mice with gain-of-function alpha6* nAChRs." J Neurochem **129**(2): 315-327.

Watabe-Uchida, M., L. Zhu, S. K. Ogawa, A. Vamanrao and N. Uchida (2012). "Whole-brain mapping of direct inputs to midbrain dopamine neurons." Neuron **74**(5): 858-873.

Watkins, S. L., S. A. Glantz and B. W. Chaffee (2018). "Association of Noncigarette Tobacco Product Use With Future Cigarette Smoking Among Youth in the Population Assessment of Tobacco and Health (PATH) Study, 2013-2015." JAMA Pediatr **172**(2): 181-187.

Weinberger, A. H., J. Platt, H. Esan, S. Galea, D. Erlich and R. D. Goodwin (2017). "Cigarette Smoking Is Associated With Increased Risk of Substance Use Disorder Relapse: A Nationally Representative, Prospective Longitudinal Investigation." J Clin Psychiatry **78**(2): e152-e160.

West, R., A. McEwen, K. Bolling and L. Owen (2001). "Smoking cessation and smoking patterns in the general population: a 1-year follow-up." Addiction **96**(6): 891-902.

WHO (2012). WHO global report: mortality attributable to tobacco. Geneva, Switzerland, World Health Organization

Wilczynska, A. and M. Bushell (2015). "The complexity of miRNA-mediated repression." Cell Death Differ **22**(1): 22-33.

Witke, W. (2004). "The role of profilin complexes in cell motility and other cellular processes." Trends Cell Biol **14**(8): 461-469.

Witke, W., A. V. Podtelejnikov, A. Di Nardo, J. D. Sutherland, C. B. Gurniak, C. Dotti and M. Mann (1998). "In mouse brain profilin I and profilin II associate with regulators of the endocytic pathway and actin assembly." EMBO J **17**(4): 967-976.

Witke, W., J. D. Sutherland, A. Sharpe, M. Arai and D. J. Kwiatkowski (2001). "Profilin I is essential for cell survival and cell division in early mouse development." Proc Natl Acad Sci U S A **98**(7): 3832-3836.

Wray, J. M., K. M. Gray, E. A. McClure, M. J. Carpenter, S. T. Tiffany and M. E. Saladin (2015). "Gender differences in responses to cues presented in the natural environment of cigarette smokers." Nicotine Tob Res **17**(4): 438-442.

Xu, J., A. Azizian, J. Monterosso, C. P. Domier, A. L. Brody, T. W. Fong and E. D. London (2008). "Gender effects on mood and cigarette craving during early abstinence and resumption of smoking." Nicotine Tob Res **10**(11): 1653-1661.

Xu, X., E. E. Bishop, S. M. Kennedy, S. A. Simpson and T. F. Pechacek (2015). "Annual healthcare spending attributable to cigarette smoking: an update." Am J Prev Med **48**(3): 326-333.

Yamaguchi, T., T. Danjo, I. Pastan, T. Hikida and S. Nakanishi (2013). "Distinct roles of segregated transmission of the septo-habenular pathway in anxiety and fear." Neuron **78**(3): 537-544.

Yang, J., A. Y. Liu, B. Tang, D. Luo, Y. J. Lai, B. L. Zhu, X. F. Wang, Z. Yan and G. J. Chen (2017). "Chronic nicotine differentially affects murine transcriptome profiling in isolated cortical interneurons and pyramidal neurons." BMC Genomics **18**(1): 194.

Yarar, D., C. M. Waterman-Storer and S. L. Schmid (2005). "A dynamic actin cytoskeleton functions at multiple stages of clathrin-mediated endocytosis." Mol Biol Cell **16**(2): 964-975.

Yates, S. L., M. Bencherif, E. N. Fluhler and P. M. Lippiello (1995). "Up-regulation of nicotinic acetylcholine receptors following chronic exposure of rats to mainstream cigarette smoke or alpha 4 beta 2 receptors to nicotine." Biochem Pharmacol **50**(12): 2001-2008.

Yi, R., Y. Qin, I. G. Macara and B. R. Cullen (2003). "Exportin-5 mediates the nuclear export of pre-microRNAs and short hairpin RNAs." Genes Dev **17**(24): 3011-3016.

Young, M. D., M. J. Wakefield, G. K. Smyth and A. Oshlack (2010). "Gene ontology analysis for RNA-seq: accounting for selection bias." Genome Biol **11**(2): R14.

Zahm, D. S. and J. S. Brog (1992). "On the significance of subterritories in the "accumbens" part of the rat ventral striatum." Neuroscience **50**(4): 751-767.

Zhang, Y., T. Pan, X. Zhong and C. Cheng (2014). "Nicotine upregulates microRNA-21 and promotes TGF-beta-dependent epithelial-mesenchymal transition of esophageal cancer cells." Tumour Biol **35**(7): 7063-7072.

Zhao-Shea, R., S. R. DeGroot, L. Liu, M. Vallaster, X. Pang, Q. Su, G. Gao, O. J. Rando, G. E. Martin, O. George, P. D. Gardner and A. R. Tapper (2015). "Increased CRF signalling in a ventral tegmental area-interpeduncular nucleus-medial habenula circuit induces anxiety during nicotine withdrawal." Nat Commun **6**: 6770.

Zhao-Shea, R., L. Liu, X. Pang, P. D. Gardner and A. R. Tapper (2013). "Activation of GABAergic neurons in the interpeduncular nucleus triggers physical nicotine withdrawal symptoms." Curr Biol **23**(23): 2327-2335.

Zhao-Shea, R., L. Liu, L. G. Soll, M. R. Improgo, E. E. Meyers, J. M. McIntosh, S. R. Grady, M. J. Marks, P. D. Gardner and A. R. Tapper (2011). "Nicotine-

mediated activation of dopaminergic neurons in distinct regions of the ventral tegmental area." Neuropsychopharmacology **36**(5): 1021-1032.

Zheng, H., Y. Zeng, X. Zhang, J. Chu, H. H. Loh and P. Y. Law (2010). "mu-Opioid receptor agonists differentially regulate the expression of miR-190 and NeuroD." Mol Pharmacol **77**(1): 102-109.